UNIVERSITÄT ZU LÜBECK

From the Institute for Systemic Inflammation Research
of the University of Lübeck
Director: Prof. Dr. med. Jörg Köhl

"The role of the anaphylatoxin receptors C3aR, C5aR1 and C5aR2 on alveolar macrophages in experimental allergic asthma"

Dissertation
for Fulfillment of
Requirements
for the Doctoral Degree
of the University of Lübeck

from the Department of Natural Sciences

Submitted by

Katharina Maria Quell
from Hünfeld

Lübeck 2019

First referee:	Dr. rer. nat. Yves Laumonnier
Second referee:	Prof. Dr. rer. nat. Hauke Busch
Date of oral examination:	12.11.2019
Approved for printing.	Lübeck, 14.11.2019

List of contents

Abstract

Allergic asthma is a global disease that represents a major public health problem, with both prevalence and incidence increasing worldwide. Right now, allergic asthma is affecting 339 million people, with an increasing prevalence in developing countries. Allergic asthma is clinically characterized by a chronic airway inflammation with reversible airflow obstruction, bronchial hyperreactivity, allergen-specific IgE in the serum, mucosal hyperplasia and airway remodeling. These pathological changes lead to typical asthma symptoms such as wheezing, coughing, chest tightness, breathlessness and mucus overproduction. The underlying mechanism is an overreaction of the immune system against innocuous environmental allergens leading to a T helper (Th2)/Th17 immune response associated with intense recruitment of immune cells including eosinophils and mast cells to the lung and a marked increase of pro-inflammatory cytokines such as interleukin (IL)-4, IL-5 and IL-13. Although the general immunological mechanisms involved in asthma are already well known, details are not yet understood. Hence, a huge necessity is needed to investigate these unknown aspects, in order to develop new therapeutic strategies for the treatment and/or prevention of the disease.

The complement system, as part of the innate immune response, has been shown to play an important role regarding the development and severity of allergic asthma. In particular, the anaphylatoxins C3a and C5a, which arise by proteolytic cleavage of complement factors C3 and C5 after canonical and non-canonical complement activation, are generated both during the sensitization and the effector phase. The role of the C5a/C5aR1 axis has been extensively investigated. Köhl et al. have shown the dual role of C5a during allergen sensitization and the effector phase. Indeed, C5aR1 has a protective effect during the development of a type 2 immune response after initial allergen exposure whereas it features a pro-allergic effect with enhanced airway inflammation and airway hyperresponsiveness in an established allergic asthma. In addition, C5aR1 participates to the aggravation of the allergic asthma phenotype through the regulation of Th17 cells. In contrast, although the C3a/C3aR axis has been reported to be a critical driver of bronchoconstriction during the effector phase of allergic asthma, and to trigger a strong increased airway hyperresponsiveness and Th2 associated inflammation, this could be observed only in some, but not all studies, depending on the allergen, the species and/or the method that has been used for immunization. In addition, mechanistically, nearly all studies investigating the role and functions of C3aR have concentrated on the DC/T cell interface, excluding the impact of C3a on other immune cells like eosinophils and alveolar macrophages. Therefore, the role of the C3a/C3aR axis requires further investigation.

C3aR expression on human cell types is relatively well defined. At steady state, it is expressed on several cell types of the myeloid lineage such as neutrophils, eosinophils, mast cells, monocytes, and basophils and several human cell lines. Whether C3aR expression on murine cells is identical, remains

unclear and conflicting. The expression of C3aR has been reported in normal bronchial epithelial and smooth muscle cells as well as under ovalbumin (OVA)-induced allergic asthma conditions. Furthermore, some studies have shown *C3ar1* mRNA expression of resting, flow-sorted $CD4^+$ and $CD4^+Foxp3^+$ nTreg cells and upon T cell activation by anti-CD3/CD28 stimulation. However, analyses of C3aR expression have frequently used western blot, flow cytometry and immunohistochemistry approaches using polyclonal or monoclonal antibodies which have been recognized to give false positive results due to unspecific antibody binding. Therefore, the expression, function, and regulation of murine C3aR at steady-state conditions and during the development of allergic asthma require more investigation and enlightenment.

Using a newly developed *tdTomato-C3ar1*$^{flox/flox}$ reporter knock-in mouse, I investigated C3aR expression in various pulmonary cells at steady-state and under allergic asthma conditions. C3aR expression was detected in eosinophils and in pulmonary $CD11b^+$ conventional dendritic cells (cDCs) and monocyte-derived DCs. Intriguingly, $SiglecF^+F4/80^-$ alveolar macrophages (AMs) expressing high levels of C5aR1 and C5aR2 at steady-state, expressed C3aR neither on the protein nor on mRNA level. This was in sharp contrast to all other $SiglecF^-F4/80^+$ macrophage populations from visceral adipose tissue, brain, lamina propria of the small intestine and peritoneal cavity, which expressed C3aR either on their surface and/or intracellularly. Furthermore, inducing a house dust mite-mediated effector phase of allergic asthma in WT and *C3ar1*$^{-/-}$ mice, I could demonstrate that absence of C3aR was dampen the airway hyperresponsiveness while it was dispensable for the pulmonary recruitment and the composition of immune cells during the effector phase. Interestingly, under these conditions, both airway and tissue-associated AMs showed elevated levels of C3aR in comparison to other pulmonary leukocytes. They developed a $C3aR^{hi}MHCII^+$ and a $C3aR^{low}MHCII^-$ AM subpopulation. In addition, AMs showed reciprocal regulation of C5aR1 and C3aR upon allergic asthma conditions, since C5aR1 was completely downregulated after multiple allergen exposure. Moreover, using pro-inflammatory cytokine models and appropriate knockout strains, I evidenced that the expression of C3aR and C5aR1 is regulated by the pro-inflammatory cytokines IL-33 and IL-13, which are released during a Th2 immune response. Furthermore, *in vitro* stimulation of AMs with GM-CSF, a growth factor known to be also secreted by epithelial cells upon allergen exposure, recapitulated the upregulation of C3aR on AMs. Further, flow cytometric assessment of specific macrophage surface markers and using *Ccr2*$^{-/-}$ mice, revealed that this mechanism is independent of blood-recruited monocytes.

Finally, I identified multinucleated macrophages, cells frequently observed in pulmonary granulomatous diseases, in the $C3aR^{hi}MHCII^+$ subpopulation of tissue-associated AMs upon experimental allergic asthma. These macrophages were found *ex vivo* and *in vivo*, and their formation could be recapitulated by *in vitro* stimulation of naïve AMs with GM-CSF. Further, *in vitro* assays suggested that multinucleated macrophages were formed by cell-to-cell fusion and cytokinesis failure.

Interestingly, *in vitro,* C3aR seemed to participate to the GM-CSF triggered multinucleated macrophage formation. Finally, my data suggested that multinucleated macrophages display a better phagocytic capacity to mononucleated cells, leading to the assumption that they may play a role in the resolution of airway inflammation, however, this remains to be further investigated.

Altogether, my data suggest that C3aR activation in tissue-associated alveolar macrophages plays an underestimated role in allergic asthma severity via their involvement in multinucleated macrophage formation. In addition, these finding open new therapeutic strategies for the treatment and prevention of allergic asthma and other pulmonary diseases.

Zusammenfassung

Das allergische Asthma ist eine globale Erkrankung, die mit steigender Prävalenz und Inzidenz weltweit ein großes öffentliches Gesundheitsproblem darstellt. Derzeit sind 339 Millionen Menschen vom allergischen Asthma betroffen, mit steigender Prävalenz in den Entwicklungsländern. Das allergische Asthma ist klinisch charakterisiert durch eine chronische Atemwegsentzündung mit reversibler Atemwegsobstruktion, bronchialer Hyperreagibilität, Allergen-spezifischem IgE im Serum, Schleimhauthyperplasie und struktureller Umbildung der Atemwege, dem sogenannten *airway remodeling*. Diese pathologischen Veränderungen führen zu den typisch asthmatischen Symptomen wie Pfeifatmung, Husten, Engegefühl in der Brust und Schleimüberproduktion. Der dabei zugrunde liegende Mechanismus ist eine Überreaktion des Immunsystems gegen harmlose Antigene in der Umgebung, die zu einer T-Helfer (TH2)/ TH17 Immunantwort führt, die mit einer heftigen Rekrutierung von Immunzellen, darunter eosinophile Granulozyten und Mastzellen, in die Lunge und einem starkem Anstieg pro-inflammatorischer Zytokine wie Interleukin (IL)-4, IL-5 und IL-13 einhergeht. Obwohl der allgemeine immunologische Mechanismus, der in Asthma involviert ist, schon bekannt ist, sind Details noch nicht verstanden. Daher besteht die große Notwendigkeit die noch unbekannten Aspekte zu untersuchen, um neue therapeutische Strategien für die Behandlung und/oder Prävention dieser Erkrankung zu entwickeln.

Das Komplementsystem als Teil der angeborenen Immunantwort wurde aufgezeigt, dass es eine wichtige Rolle im Bezug auf die Entwicklung und Schwere des allergischen Asthmas spielt. Im Speziellen, die Anaphylatoxine C3a und C5a, die durch eine proteolytische Spaltung der Komplementfaktoren C3 und C5 nach Komplementaktivierung entstehen, werden in der Sensibilisierung und der Effektorphase generiert. Die Rolle der C5a/C5aR1 Achse wurde umfangreich untersucht. Köhl et al. haben gezeigt, dass C5a eine duale Rolle während der Sensibilisierung und der Effektorphase spielt. Tatsächlich hat C5aR1 einen protektiven Effekt während der Entwicklung einer Typ 2 Immunantwort nach initialer Allergenexposition, wohingegen es eine pro-allergischen Effekt mit verstärkter Atemwegsentzündung und Atemwegshyperreagibilität im etablierten Asthma aufweist. Des Weiteren ist der C5aR1 an der Verschlimmerung des allergisch asthmatischen Phenotyps durch die Regulierung von TH17 Zellen beteiligt. Im Gegenteil dazu, obwohl die C3a/C3aR Achse als ein kritischer Treiber der Bronchokonstriktion während der Effektorphase des allergischen Asthmas berichtet worden ist und einen starken Anstieg der Atemwegshyperreagibilität und eine TH2-assoziierte Entzündung auslöst, wurde dies nur in einigen, aber nicht allen Studien, abhängig vom Allergen, der Spezies und/oder der Methode, die für die Immunisierung benutzt wurde, beobachtet. Des Weiteren haben sich mechanistisch fast alle Studien auf die Rolle und Funktion von C3aR auf die DC/T Zell Schnittstelle konzentriert, dabei jedoch den Einfluss von C3a auf andere Immunzellen wie

Eosinophile und Alveolar Makrophagen ausgeschlossen. Deshalb erfordert die C3a/C3aR Achse weitere Untersuchung.

C3aR Expression auf humanen Zelltypen ist relativ gut definiert. Unter Steady-State Bedingungen ist der Rezeptor auf verschiedenen Zelltypen der myeoliden Abstammungslinie wie Neutrophilen, Eosinophilen, Mastzellen, Monozyten und Basophilen, als auch auf verschiedenen humanen Zelllinien exprimiert. Ob die C3aR Expression auf murinen Zellen identisch ist, verbleibt unklar und widersprüchlich. Die Expression wurde berichtet in normalen bronchialen Epithel- und glatten Muskelzellen, wie auch unter Ovalbumin (OVA)-induziertem allergischen Asthma. Weiterhin haben einige Studien C3ar1 mRNA Expression auf ruhenden, FACS-sortierten $CD4^+$ and $CD4^+Foxp3^+$ nTreg Zellen und in durch anti-CD3/CD28 Stimulation aktivierten T Zellen beschrieben. Allerdings wurden zur Analyse der C3aR Expression vielfach polyklonale und monoklonale Antikörper verwendet, von denen aufgezeigt wurde, dass sie im Western Blot, der Durchflusszytometrie und Immunohistochemie durch unspezifische Antikörperbindung falsch positive Ergebnisse ergeben. Deshalb erfordert die Expression, Funktion und Regulierung des murinen C3aR unter Steady-State Bedingungen und während der Entwicklung des allergischen Asthmas erfordert weitere Untersuchung und Aufklärung.

Unter Benutzung einer neu entwickelten *tdTomato-C3aR*$^{flox/flox}$ Reportermaus untersuchte ich die C3aR Expression in verschienden pulmonaren Zellen unter Steady-State und allergischen Asthma-bedingungen. C3aR Expression wurde entdeckt in Eosinophilen und pulmonaren $CD11b^+$ konventionellen dendritischen Zellen (cDCs) sowie monozytären DCs. Interessanterweise exprimierten $SiglecF^+F4/80^-$ Alveolar Makrophagen (AMs) ein hohes Level an C5aR1 und C5aR2 unter Steady-State Bedingungen, aber C3aR weder auf Protein noch mRNA Ebene. Dies war im deutlichen Kontrast zu allen anderen $SiglecF^-F4/80^+$ Makrophagen Populationen vom viszeralen Fettgewebe, dem Gehirn, der Lamina Propria des Dünndarms und der Bauchhöhle, welche C3aR entweder auf der Oberfläche und/oder intrazellulär exprimierten. Zudem konnte ich durch die Induktion einer Hausstaubmilben-vermittelten Effektorphase des allergischen Asthmas in WT und *C3ar1*$^{-/-}$ Mäusen aufzeigen, dass die Abwesenheit von C3aR die Atemwegshyperreagibilität schwächte, während C3aR unwichtig für die pulmonare Rekrutierung und Zusammensetzung der Immunzellen während der Effektorphase zu sein scheint. Interessanterweise zeigten unter diesen Bedingungen sowohl Atemwegs- als auch Gewebe-assozierte Alveolar Makrophagen erhöhte Level von C3aR im Vergleich mit anderen pulmonaren Immunzellen. Sie entwickelten eine $C3aR^{hi}MHCII^+$ und eine $C3aR^{low}MHCII^-$ AM Subpopulation. Des Weiteren zeigten AMs eine reziproke Regulation von C5aR1 und C3aR unter allergischen Asthmabedingungen, da C5aR1 nach mehrfacher Allergen-Exposition komplett herunterreguliert wurde. Überdies konnte ich durch Benutzung pro-inflammatorischer Zytokin-Modelle und geeigneter Gen-defizienter Mäuse beweisen, dass die Expression von C3aR und C5aR1 durch die pro-inflammatorischen Zytokine IL-13 und IL-33, welche während der TH2 Immunantwort freigesetzt

werden, reguliert wird. Zudem rekapitulierte die *in vitro* Stimualtion von AMs mit GM-CSF, ein Wachstumsfaktor der bekannt ist, dass er unter Allergen-Exposition von Epithelzellen sekritiert wird, die Hochregulierung von C3aR. Des Weiteren zeigte die Beurteilung Makrophagen-spezifischer Oberflächenmarker bei Durchflusszytometrie und die Benutzung von *Ccr2*$^{-/-}$ Mäusen, dass der Mechanismus unabhängig von rekrutierten Monozyten des Blutes ist. Abschließend indentifizierte ich mehrkernige Makrophagen, Zellen die regelmäßig in pulmonaren granulomatösen Erkrankungen beobachtet werden, in meiner C3aR^{hi}MHCII^{+} Subpopulation der Gewebe-assoziierten AMs im experimentell allergischen Asthma. Diese Makrophagen wurden auch *ex vivo* und *in vivo* gefunden, und ihre Bildung wurde rekapituliert durch *in vitro* Stimulation naiver AMs mit GM-CSF. Außerdem legten *in vitro* Analysen nahe, dass die mehrkernigen Makrophagen sich durch Zell-zu-Zell Fusion und Defekte in Zytokinese bildeten. Interessanterweise scheinte C3aR *in vitro,* in der durch GM-CSF ausgelösten Bildung mehrkerniger Makrophagen, beteiligt zu sein. Abschließend deuten meine Daten darauf hin, dass mehrkernige Makrophagen eine bessere phagozytäre Leistung im Vergleich zu einkernigen Zellen aufweisen. Allerdings erfordert dies weitere Untersuchungen.

Zusammenfassend zeigen meine Daten, dass die Aktivierung von C3aR in Gewebe-assoziierten Alveolar Makrophagen eine unterschätzte Rolle in der Schwere des allergischen Asthmas durch ihre Beteiligung in der Bildung mehrkerniger Makrophagen spielt. Zudem eröffnen diese Ergebnisse neue therapeutische Strategien für die Behandlung und Prävention des allergischen Asthmas und anderer pulmonarer Erkrankungen.

1 Introduction

The aim of the following dissertation was to improve the comprehension of the complex roles of the anaphylatoxin receptors C3aR, C5aR1 and C5aR2 in the development and severity of allergic asthma using different experimental mouse models. Thereby, the main focus was to investigate the expression, regulation and role of the anaphylatoxin receptors in particular in alveolar macrophages. For a better understanding of my work, I will briefly introduce the immune system, and will then describe in more detail the origin, development and function of macrophages with particular emphasis on alveolar macrophages. Moreover, in the following paragraphs I will picture the function of the complement system in general, and in anaphylatoxins and their receptors in particular. Finally, I will place the roles of alveolar macrophages and the complement system in the context of asthma.

1.1 The immune system

The immune system developed as an interactive network of humoral factors, specialized cells and lymphoid organs, to defend the host's own body against disease-causing microorganisms and environmental substances, to prevent infection as well as to protect against endogenous danger caused by apoptotic or necrotic bodies, and abnormal cells (1). To shelter the host from such threats, the immune system has evolved various effector mechanisms providing an appropriate immune response. These mechanisms underlie a strict regulation, since the immune system has to discriminate self from non-self to maintain physiologic homeostasis, prevent overreaction against host's own healthy cells and harmless antigens, but combat pathogens by an inflammatory response (1). In case of autoimmune disorders or allergies, this regulation is disturbed (2).

The defense system can, basically, be pictured as consisting of three levels: (i) anatomical and physiological barriers; (ii) innate immunity; and (iii) adaptive immunity (3). If one of these systems fails, it will massively increase the susceptibility to infection.

The first lines of defense against pathogens are anatomic and physiological barriers. Indeed, intact skin comprising epidermal surfaces, sweat glands and sebaceous glands, but also mucosal surfaces with secreted mucus, ciliated epithelial cells with mucociliary clearance mechanisms, low stomach pH and bacteriolytic lysozyme in tears and saliva, trap pathogens and debris, not only prevent the invasion of internal tissues by danger molecules, but also facilitate their removal (1, 3). Furthermore, epithelial cells from skin, gastrointestinal and respiratory tract and various body cavities produce a wide range of antimicrobial enzymes and proteins such as lysozyme, pepsin, α-defensins (cryptins and cathelicidins), ß-defensins, histatins, and pulmonary surfactant (1) in order to inhibit microbial growth or to directly kill pathogens. However, these barriers can be overcome, and the innate and adaptive

(or acquired) immunities are necessary stepping in. As an immediate and relatively unspecific defense, the innate immunity stands against dangers. It includes humoral components like natural antibodies (NAbs), complement and coagulation cascades (4, 5) as well as cellular components such as macrophages, neutrophils and dendritic cells (1, 3). To a later timepoint, a danger-specific reaction follows, as adaptive immunity, composed of the T and B cell responses. In contrast to the innate immunity, the adaptive immunity is highly antigen-specific and generates an immunological memory, which will lead to an accelerated and enhanced immune response after renewed antigen contact (1). However, although the innate and adaptive immunity differ in the involved cell types and factors, both systems should never be pictured separately but rather as an interactive network where cellular cross-talk and mutual stimulation act in concert to effectively protect the host's body against exogenous and endogenous threats (1).

1.1.1 Innate Immunity: The first line of defense

Innate immunity is evolutionarily the most ancient component of host defense and is present in all multicellular organisms while adaptive immunity evolved much later and is only found in higher vertebrates (6). The current model of innate immunity dates back to 1884, when Élie Metchnikoff made fundamental observations by studying starfish larvae, and discovered phagocytes, an immune cell type that protects organisms from dangers by ingesting foreign particles or microorganisms, thus serving as host's own defense (7).

As infection starts, i.e. when a microorganism pervades the host's anatomic and physiological barriers, then the innate immune mechanisms start acting immediately. They encompass humoral and cellular components. Firstly, the complement system, as a major component of the humoral innate immunity, immediately gets activated and will label pathogens both for lysis and phagocytosis by innate immune cells, in particular the macrophages. Complement is a collection of over 50 different plasma proteins that act together as one of the most important effector mechanisms in serum and interstitial tissues (1) and will be examined in greater detail in a devoted chapter (1.4.2). In addition to the complement system, plasma contains components of a second proteolytic cascade, the coagulation system, which maintain vascular integrity as well as protect the vascular system from injury and invading pathogens (5). Moreover, the humoral immune response includes NAbs, which are produced primarily by B1 B-lymphocytes (8). They are encoded by unmutated germ-line genes with restricted epitope specificities and are produced in the absence of external antigen stimulation. NAbs are usually of the Immunoglobulin (Ig)M isotype but may also include IgG and IgA isotypes (9) and participate in the host defense in three main ways: (i) they can directly bind and neutralize bacterial toxins, leading to the ingestions and clearance by phagocytes, (ii) they can opsonize bacterial surfaces in the extracellular space causing the ingestion and destruction of pathogens, and (iii) they can coat bacterial cells in

plasma resulting in the activation of the complement system, leading to lysis and ingestion of the pathogen (1). In addition to NAbs, pentraxins, a family of multimeric pattern recognition proteins, provide a humoral immune response. Pentraxins are acute phase proteins that are rapidly synthesized and serve as markers for infection, inflammation and tissue damage (4). The family is divided into short pentraxins like C reactive protein (CRP) and serum amyloid P protein (SAP) which are produced by the liver (10) and long pentraxins such as pentraxin 3 (PTX3) synthesized by various cell types (11). Similar to NAbs, they recognize and bind pathogens and endogenous ligands leading to pathogen clearance via Fcγ receptors on macrophages and other innate immune cells and through the activation of the complement cascade (11-13).

Besides engulfing and digesting tagged pathogens, phagocytic cells that lie beneath the epithelial barriers, initiate the next phase of innate immune response. Indeed, macrophages, neutrophils and dendritic cells act as sensor cells that detect pathogen-driven inflammatory response and orchestrate downstream inflammatory effector mechanisms. These cells express a number of germline-encoded recognition receptors, the so-called pattern recognition receptors (PRRs), that recognize microbial-conserved molecular structures that are expressed by a large variety of microbes but not by the host's own cells. These simple but evolutionary conserved molecules are known as pathogen-associated molecular patterns (PAMPs) like the lipopolysaccharides (LPS) and the mannose-rich oligosaccharides. Furthermore, the innate immune system can detect self-derived host molecules related to cellular infection, damage, or stress via innate receptors recognizing such proteins and mediating cellular responses. Such indicator molecules have been termed damage-associated molecular patterns (DAMPs). Well characterized DAMPs include extracellular proteins such as biglycan and tenascin C, intracellular or nuclear proteins such as high mobility group box 1 protein (HMGB-1), S100 proteins, histones, heat-shock proteins (HSPs) and uric acid as well as plasma proteins like fibrinogen and serum amyloid A (SAA) (3, 14). The recognition of both PAMPS and DAMPs via Toll-like receptors (TLRs), nucleotide oligomerization domain (NOD)-like receptors (NLRs) and others, activates phagocytes as part of the cellular innate immune response. Activated cells respond by releasing toxic agents such as superoxide, hydrogen peroxide, nitric oxide (NO) and antimicrobial peptides and enzymes such a cathelicidin, defensins, elastase and lysozyme that directly lead to the destruction of pathogens. Further, activation of innate cells propagates the immune response through the secretion of cytokines, such as IL-1ß, and chemokines that trigger the recruitment of other innate immune cells like eosinophils and initiate the adaptive immune response (1).

1.1.2 Adaptive Immunity: The highly specialized part of the immune system

Although the innate immune system has evolved to rapidly sense and promote the elimination of a wide range of dangers, the spectrum of common pathogenic molecular patterns it can recognize is limited and it is incapable to generate an immunological memory to prevent reinfection. The need of an immune memory, the high variability of antigenic structures, as well as the ability of pathogens to mutate to avoid host detection, have driven the evolution of the adaptive immune system (6).

In contrast to the PRRs of the innate immune system, which are entirely encoded in the germline genome, adaptive immune responses depend on receptors that are highly antigen-specific and selected through a process of somatic recombination (1). After initial pathogen encounter, cells expressing these immune receptors can persist in the host for life, providing an immunological memory for rapid, accelerated and enhanced immune responses in case of re-exposure. This process of adaptive immunity is the basis for vaccination (1).

The adaptive immune system is composed of a cellular immune response provided by T and B lymphocytes and the humoral immunity by antibodies (1). Both lymphocytes are highly mobile and mainly inactive. After developing in the central / primary lymphoid organs, they traffic to peripheral / secondary lymphoid organs where they get presented a specific antigen which binds to the appropriate specific T cell receptor (TCR) on their cell surface. As a result, they become activated, proliferate, and differentiate into fully functional lymphocytes, known as effector lymphocytes. They rise by clonal expansion and egress from secondary lymphoid organs to many sites in the body to exert effector functions.

T lymphocytes are characterized by their T cell receptor (TCR) and the expression of specific surface molecules. The TCRs recognize short peptidic sequences, originating from degraded proteins, presented by an antigen-presenting cell (APC) via a specialized cell-surface glycoprotein named major histocompatibility complex (MHC)-I or -II. Moreover, two main classes of T cells, characterized by their cell-surface protein cluster of differentiation (CD)4 or CD8, could be distinguished. These co-receptors provide functional differences between $CD4^+$ and $CD8^+$ T cells, since $CD4^+$ T cells recognize antigens presented by MHC class II, while $CD8^+$ T cells recognize the peptide via MHC class I (1). Binding of the MHC/antigen complex leads to proliferation and differentiation into one of the three broad classes of effector T cells. $CD8^+$ T cells differentiate into cytotoxic T cells that kill other cells that are infected with viruses or intracellular pathogens, while $CD4^+$ T cells can differentiate into regulatory T (Treg) cells or helper T cells. Such T helper (Th) cells can be divided into Th1, Th2, Th17, and T follicular helper (Tfh) cells, defined on the different combinations of cytokines they secrete (1, 15). Besides of effector T cell development, also memory T cells develop to induce a rapid immune response in case of re-exposure (1).

In contrast, B lymphocytes perform different tasks. Firstly, B cells are professional antigen-presenting cells. They express at their surface a receptor known as B cell receptor (BCR) that is specific for an antigen. Binding of a microbial antigen by the BCR leads to its receptor internalization, antigen processing, and presentation of antigen-derived peptide by MHC class II molecules to already differentiated antigen-specific Th cells. These effector T cells help the B cell to proliferate and to differentiate into antibody-secreting plasma cells and memory B cells (1). The antibodies released by B cells are the highly specific soluble form of the BCR, and provide a protection against extracellular pathogens and their toxic products. Indeed, they can opsonize pathogens, neutralize toxins and trigger the complement activation through the formation of immune complexes (1). However, the Th subset of cells present determines which type of Ig subtype is produced. As an example, binding of an antigen-specific Th2 cell to the same antigen presented by MHCII of a B cell, triggers the secretion of the cytokines IL-4 and IL-13, leading to a class switch in B cells from IgM to IgE production.

1.2 The macrophage

Macrophages were first described by Élie Metchnikoff late in the 19th century when he performed experiments with simple marine invertebrates. He recognized them as phagocytes able to respond to foreign particles and infection by a process analog to inflammation in higher organisms (16, 17). These professional phagocytic cells were named “macrophages” (from the Greek "$\mu\alpha\kappa\rho\acute{o}$" macro = large and "*ἔφαγον*" éphagon= devouring, hence large devouring cells).

Nowadays, macrophages are recognized as the main effector cells of innate immunity. They are distributed in tissues throughout the body and are present throughout evolution, from lower (invertebrates) to highly complex organisms (vertebrates) (18, 19). They are involved in both homeostasis and disease, by responding to internal and external changes within the body, not only as phagocytes involved in defense against pathogens and clearance of apoptotic cells, but also through regulatory, inflammatory and repair functions. Thus, tissue-resident macrophages represent an attractive target for modern medicine to treat a wide spectrum of diseases in which they have been implicated, including asthma, atherosclerosis, autoimmune diseases, neurodegenerative, metabolic disorders, and tumor growth (20-24). Understanding the origin and developmental pathways of macrophages will help to design novel intervention strategies targeting these cells in tissue-specific sites.

1.2.1 Origin

In 1968, van Furth proposed that all tissue macrophages originate from blood circulating monocytes through adult hematopoiesis, which terminally differentiate in the tissue and were unable to proliferate (25). This has been the prevailing view for the last decades. However, few years ago the biology of tissue macrophages has drastically revised our understanding of macrophage origin. Various publications have shown that, although monocytes may give rise to subsets of macrophages upon inflammatory signals, many tissue-resident macrophages in fact differentiate and colonize organs already during embryonic development and self-renew during adulthood independently of circulating monocytes (26-29).

1.2.1.1 Adult hematopoiesis gives rise to monocytes and monocyte-derived macrophages

Macrophages are a part of the mononuclear phagocyte system (MPS), which also includes circulating monocytes and dendritic cells (30). Since monocytes and dendritic cells (DCs) have their progenitors in the bone marrow (BM), van Furth proposed the early dogma that all resident macrophages originate from circulating adult blood monocytes and are constantly replenished from bone marrow-derived monocytes as a continuum of differentiation (25) (Figure 1.1). In such model, Ly6C^{hi} and Ly6C^{low} monocytes (31, 32) are released in the bloodstream can be recruited into the tissue where they differentiate into macrophages or monocyte-derived DCs (33, 34).

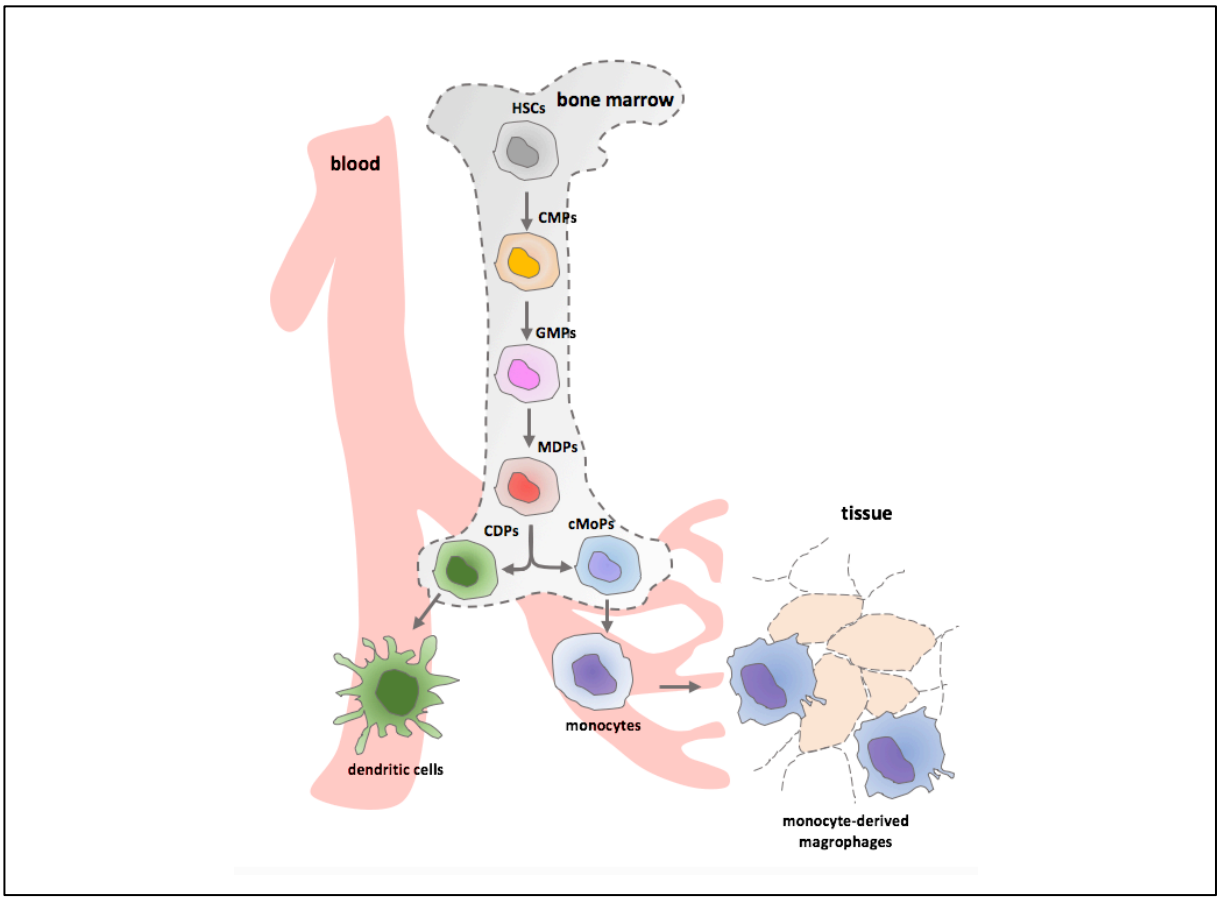

Figure 1.1 Adult hematopoiesis. Circulating monocytes and monocyte-derived macrophages are generated in the bone marrow by differentiation of hematopoietic stem cells (HSCs). High levels of the transcription factor c-Myc induce the differentiation of HSCs towards a more committed progenitor, the common myeloid progenitor (CMP). Such CMPs further differentiate into the granulocyte-macrophage progenitors (GMP) and subsequently give rise to the macrophage/dendritic cell (DC) progenitors (MDP). The MDPs develop either to common DC progenitors (CDP) which differentiate later to conventional (c) and plasmacytoid (p)DCs in the tissue (35, 36), or they give rise to a common monocyte precursor (cMoP) (37) that can further differentiate to Ly6C^{hi} and Ly6C^{low} monocytes (31, 32). Adapted from (31).

1.2.1.2 Embryonic hematopoiesis gives rise to most tissue-resident macrophages

Besides monocytic-derived macrophages, tissue-resident macrophages including alveolar macrophages, microglia, Kupffer cells and peritoneal macrophages (PM) are mainly established during embryonic hematopoiesis. Mammalian embryonic hematopoiesis is a complex process (Figure 1.2). In the mouse, embryonic hematopoiesis is characterized by distinct waves, occurring in different compartments of the embryo and in a sequential way. These sequential waves of hematopoiesis overlap in time and space and remain difficult to separate clearly (38).

While the embryonic origin of certain tissue macrophages is now accepted, the exact identity of progenitors, the exact pathway of differentiation to mature cells, and which precursor give rise to the majority of tissue-resident macrophages remains still a matter of debate (31, 38).

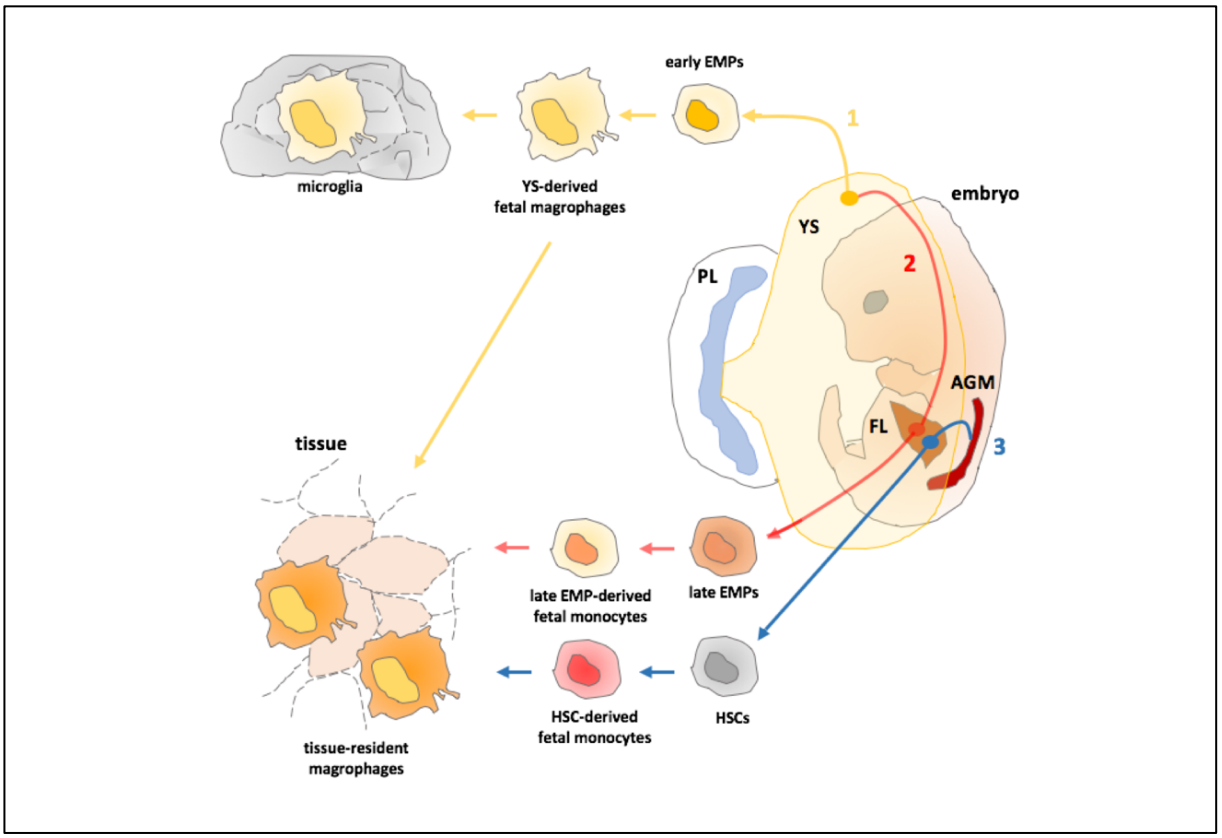

Figure 1.2 Embryonic hematopoiesis. (**1**) The Primitive (myb-independent) hematopoiesis. The first wave of hematopoiesis appears in the yolk sac (YS) blood island and gives rise to early erythro-myeloid progenitors (EMPs) that generate YS-derived fetal macrophages without going through a monocytic progenitor intermediate. These fetal macrophages appear at embryonic day (E)9 with a unique pattern of differentiation, spread into the embryo through the blood as soon as the circulatory system is fully established (from E8.5 to E10), and colonize various tissues, including the brain. Importantly, this occurs before the onset of fetal monocyte production by the fetal liver (FL), which starts around E11.5/E12.5 (26, 39-41). (**2**-**3**) The Definitive (myb-dependent) hematopoiesis comprises a transient definitive stage, generating late EMPs, and a definitive stage characterized by the production of HSCs in the aorta-gonad-mesonephros (AGM). The transient definitive stage (2) takes place simultaneously to the establishment of the blood circulation. Late EMPs expressing c-Myb are generated by the YS hemogenic endothelium (HE). At approximately E9.5-10.5 these late EMPs are able to colonize the FL, where they expand and generate fetal monocytes and give rise to probably the majority of adult macrophages (39, 41-44). Concomitant at E8.5-E10.5, the definitive stage (3) leads to the emergence of hematopoietic stem cells (HSCs) from the AGM and give rise to fetal monocytes and all other immune lineages. At E10.5, HSCs migrate to the fetal liver, where they serve from E12.5 onward as the major hematopoietic organ during the remainder of embryonic development until the perinatal period (P1) where the bone marrow (BM) HSCs become the primary site of hematopoiesis (45-49). Adapted from (31).

1.2.2 Heterogeneity and function

Tissue macrophages consist in a heterogeneous cell population found in all tissues of adult mammals. Hence, according to their tissue localization, macrophages bear different names, such as osteoclasts (bone), alveolar macrophages (lung), microglia (brain), Kupffer cells (liver) or Langerhans cells (LC) (skin). Further, it is increasingly recognized that in addition to their ontological origin, environmental factors play a critical role in defining functionally tissue-resident macrophages and determining their fate and persistence in tissues (50-52). In consequence, while tissue macrophages acquire specific morphological and functional phenotypes according to their surrounding microenvironment, they share characteristic functions in all tissues, such as maintenance of tissue homeostasis (recognizing

and removing abnormal and apoptotic cells), and protective functions (reaction to infections and tissue damage by initiating, developing and resolving an inflammatory response).

Brain

The brain contains various distinct resident microglia and other macrophage populations. Recent fate-mapping studies have established that microglia are of embryonic origin (29), persist in the brain during adulthood, and sustain independently from BM-derived monocytes by a self-renewal capacity (53). Microglia exclusively originate from YS fetal macrophages and patrol the neuropil continuously. Further, they monitor the surrounding to sense and resolve any disturbance. Moreover, microglia are important for normal CNS development and function, including developmentally regulated neuronal apoptosis, neurogenesis, myelogenesis, and synaptic pruning (31, 54). In contrast, non-parenchymal central nervous system (CNS) macrophages are composed of FL monocytes. Finally, among the CNS macrophages, choroid plexus macrophages are the only population consisting of substantial bone marrow progenitors (54), although, during an experimental autoimmune encephalomyelitis (EAE), monocyte-derived macrophages are massively recruited into the brain, although they do not contribute to the replenishment of microglia once homeostasis is restored (55).

Intestine

Fate-mapping and parabiotic mouse models have demonstrated that the intestinal mucosa is colonized by embryonic macrophage precursors during embryonic development, but they do not persist into adulthood (56). In contrast, because of the continual exposure to environmental stimuli, there is a constant necessity for the replenishment by blood monocytes, which differentiate *in situ* into mature anti-inflammatory macrophages contributing to the integrity of the epithelium (57). To ensure a symbiotic relationship and tolerogenic environment, gut macrophages are essential for the tight crosstalk with microbiota (56). In general, it is possible to distinguish between tissue-resident macrophages and monocyte-derived macrophages, however, in the gut, one should rather draw a distinction between resident monocyte-derived macrophages and newly recruited monocytes. At steady-state, monocytes recruited from the blood differentiate locally into anti-inflammatory monocyte-derived macrophages. They are located directly beneath the epithelial cell barrier, where they favor constantly its renewal and perform tissue remodeling. These macrophages are able to inspect the tissue by sensing and sampling the luminal content. Furthermore, they can cross-talk with $CD103^+$ DCs and transfer antigen (58, 59). In addition, through IL-10 production, they enforce the expansion of regulatory T cells (60). In the mouse, monocytes that are immediately recruited upon inflammation from the blood to the intestine trigger an inflammatory reaction, whereas resident monocyte-derived macrophages keep their anti-inflammatory signature (31, 61).

Liver

Kupffer cells (KCs) are the resident macrophages of the liver. They arise from YS fetal macrophages and fetal liver monocytes during embryonic hematopoiesis (62) and, at steady state, they maintain their cell number through self-renewal throughout adulthood with minimal contribution of blood monocytes (28). A major function of KCs is the support of the tolerogenic milieu within the liver and the prevention of a generalized inflammation by eliminating circulating pathogen-specific cytotoxic T cells (63-65). As $F4/80^{+}$ phagocytes, they have functions in innate recognition. Furthermore, they express the complement receptor of the immunoglobulin superfamily (CRIg), a tissue-specific complement receptor, that KCs need for their efficient binding and phagocytosis of complement C3-opsonized particles (66). When infection occurs, KCs ensure the protection of the host by rapid clearance of bacteria from the blood stream (67) and by the complex interaction with microbicidal neutrophils, which are rapidly recruited in response to infection (68, 69). Moreover, they play a critical role in eliminating activated neutrophils, thereby suppressing their production of toxic metabolic compounds and degradative enzymes (70, 71). Furthermore, KCs produce cytokines such as IL-6, which activates hepatocytes leading to the release of acute phase plasma proteins including complement, to provide an early response to infection (72). Upon microbial infection, embryonic-derived Kupffer cells necrotize, which is a key signal to orchestrate a type 1 antimicrobial inflammation and a type 2 mediated responses for liver repair (73). Since the liver is the best organ capable of regeneration, the dead embryonic-derived Kupffer cells will be replenished by newly recruited bone marrow-derived monocytes which fully differentiate into KCs (74). Finally, KCs also provide lipid ligands and iron for hepatocyte biosynthesis and secretion into blood (75, 76).

Peritoneum: The prototypical macrophage

Much of our knowledge about tissue-resident macrophages and their role in molecular biology derives from *ex vivo* studies of murine macrophages from the peritoneal cavity (PerC). Peritoneal macrophages (PMs) are easily to obtain by wash-out of the PerC and purification by adhesion and cultivation *in vitro* (80). They can be obtained in different functional states as unstimulated or as inflammatory exudate, the so-called elicited macrophages, after peritoneal injection of unsterile agents such as thioglycolate or bacterial LPS (77). Although PMs are one of the best-studied macrophage populations, only recently the co-existence of two subsets of macrophages in mouse PerC with distinct phenotypes, functions, and origins, has been demonstrated under homeostatic conditions (78). According to their morphology, these macrophage subsets have been classified as large peritoneal macrophages (LPMs) and small peritoneal macrophages (SPMs). LPMs are the most abundant subset under steady state conditions. They develop during embryogenic hematopoiesis from fetal liver monocytes and maintain throughout adult life by self-renewal. LPMs express high levels of F4/80 and low levels of MHC class II

and appear to be responsible for phagocytosis of apoptotic cells and tissue repair. Conversely, SPMs, a minor subset in unstimulated PerC, originate from bone marrow-derived circulating monocytes. They express low levels of F4/80 and high levels of MHCII. However, upon infectious or inflammatory stimuli, the myeloid compartment is modified dramatically, SPMs becoming the predominant population while LPMs disappear (78, 79).

Adipose tissue

Adipose tissue is mainly composed of adipocytes. However, it also comprises immune cells to maintain tissue homeostasis. With 5% of the adipose tissue in lean and up to 50% in obese humans (80), the most abundant leukocyte population is the adipose tissue macrophage population (ATM) (81). In contrast to other macrophages, little is known about their origin and their maintenance. However, at steady-state, ATMs are characterized by their expression of F4/80, CD206 and CD11b, whereas they do not express monocytic markers such as Ly6C and CCR2 (81, 82), suggesting that steady-state ATMs were established during embryonic hematopoiesis. Their main function is the regulation of tissue homeostasis, through clearance of dead adipocytes and cellular debris, and participation to tissue immune surveillance (81, 82). Besides of their key role as phagocytes, ATMs facilitate acute metabolic tasks (79). However, during obesity the number of ATMs increases significantly through the recruitment of circulating monocytes via a CCL2/CCR2 pathway and are associated with systemic insulin resistance (83, 84).

1.2.3 Pulmonary macrophages

In the lung environment, pulmonary macrophages are the most abundant immune cell under homeostasis. They participate, together with other immune cells, in the preservation of an appropriate balance between maintenance of physiologic homeostasis and orchestration of pulmonary host defense (85, 86). However, lung macrophages are a heterogeneous cell population with remarkable plasticity depending on their origin, tissue localization and environmental stimuli (87, 88). High diversity and plasticity help to efficiently respond to a wide spectrum of stimuli, including various pathogenic antigens, immune complexes, apoptotic or necrotic cells and several mediators released by other immune cells to direct an appropriate immune response. However, lung macrophages play also a central role in pulmonary diseases and therefore are a feasible target for new therapeutic strategies.

At least two distinct macrophage populations are present in the lung at steady-state, the alveolar macrophages (AMs) and the interstitial macrophages (IM), that can be distinguished by their localization in the lung, their functional properties as well as their expression of characteristic surface molecules. Indeed, while the IMs, which reside in the lung parenchyma, express low levels of the

integrin CD11c and Siglec-F, but high levels of CD11b, the AMs, located in the airway lumen or attached to the epithelial surface show high expression of CD11c and Siglec-F, but lack CD11b (89).

Several studies have shown that IMs represent a heterogeneous population in the steady-state lung (90-92). Further, IM ontogeny is complex and poorly known although they seem to have a mixed origin, deriving both from embryonic YS macrophages and from postnatal bone marrow-derived precursors (96). However, at least in part, IMs can be replenished through blood monocytes differentiation, both for their maintenance in adults and in a microbe-rich environment (93, 94). Due to their location in the interstitium, between adjacent alveoli, and their expression of MHCII (92, 94), IMs have been thought to interact with DCs and to promote immunity by antigen presentation to T lymphocytes. However, mouse and human IMs express the immunosuppressive cytokine IL-10 at steady state (95, 96), which increases in response to environmental stimuli such as LPS, CpG-DNA, or house dust mite (HDM) (94-96). Moreover, in a co-culture system between freshly isolated IMs and OVA-LPS-pulsed bone marrow-derived DCs (BMDCs), IMs impaired the ability of BMDCs to migrate to the draining lymph node (LN) and inhibited DCs to promote a Th2-mediated airway allergy once reinjected in the trachea of recipient mice (97). All these data suggest rather that IMs are critical in maintaining immune homeostasis in the respiratory tract and play a more regulatory function.

In contrast to IMs, AMs, based on their unique position at the interface between pulmonary mucosa and external environment, not only play a role in maintenance of physiological homeostasis and immune tolerance, but also play a major role in host defense. In a subsequent paragraph (1.3), I will concentrate more specifically on the characterization and functions of AMs, since they were of main importance for my project.

1.2.4 Plasticity and polarization

Since macrophages have an immune surveillance role, they have to respond to a wide spectrum of stimuli, including various pathogens, apoptotic or necrotic cells and several mediators released by other immune cells. Therefore, cells of the monocyte-macrophage lineage display a considerable high diversity and plasticity, meaning they have to adequately change their functional phenotype in response to the local environment and/or to the pathogenic microorganism.

The concept of macrophage polarization was introduced by Charlie Mills in 2000 and pictures the complex mechanisms driving macrophage towards two opposite states of activation, the M1 or classical, and the M2 or alternative activation (98). This M1/M2 macrophage polarization paradigm was inspired by the Th1/Th2 concept introduced earlier by Mosmann and Coffman (99). The M1 activation is driven by viruses, bacterial cell components like LPS and lipoteichoic acid (LTA) and other TLR ligands (100). Furthermore, cytokines such as interferon (IFN)-γ and tumor necrosis factor (TNF)-α are also potent inducers of the M1 activation (100, 101). Upon such activation, M1 macrophages

secrete inflammatory cytokines such as IL-12, IL-6, TNF-α, IL-1 and produce massive amounts of nitric oxide (NO) via the expression of the Nitric Oxide synthase (NOS)2 (also known as inducible (i)NOS), resulting in an effective pathogen killing mechanism (102, 103). In addition, the M1 macrophage phenotype is characterized by the expression of co-stimulatory molecules CD80, CD86 and MHCII (100, 104, 105). In contrast, the M2 activation is triggered as a response to fungi, helminths and the cytokines IL-4 and IL-13 (106, 107). Conversely to M1 macrophages, M2 macrophages secrete anti-inflammatory cytokines such as IL-10 and TGF-ß, have a high phagocytic capacity, are involved in pathogen defense, and in tissue integrity (101). Therefore, they are widely described as macrophages responsible for resolution, wound healing, tissue repair, and immunoregulation. However, stimuli such as immune complexes (IC), IL-1R ligands, IL-10, M-CSF and glucocorticoids induce M2 activation (100). In response to activation, M2 macrophages are thought to participate to allergic inflammation, growth of tumor tissues, tissue remodeling and provide housing for pathogens (100, 106, 107). Depending on the nature of the stimuli, M2 macrophages undergo different transcriptional changes leading to their subdivision into the M2a, M2b, and M2c subtypes. The M2a subtype, also known as alternative activated macrophage, responds to allergy, fungal and helminth infections as well as to IL- 4 and IL-13 cytokines. Such macrophages are characterized by high expression of Arginase-1 (Arg1), MHC class II, mannose receptor (CD206), chitinase-3-like protein 3 (YM1) and are producers of anti-inflammatory mediators as IL-10, TGF-ß and IL-1 receptor antagonist (IL-1ra) (100, 107). The M2b subtype, also defined as type 2 macrophage, is activated through immune complexes (IC) and bacterial LPS. Furthermore, M2b macrophages are characterized by the expression of CD86, MHCII and by the release of IL-1, IL-6, IL-10 and TNFα (100, 107). Finally, the M2c subtype, also called deactivated macrophage, is activated by IL-10, glucocorticoids, and TGF-ß leading to the expression of CD206, CD163 and the production of IL-10, TGF-ß and extracellular matrix (ECM) (100, 107). This "deactivated" terminology refers to their ability *in vitro* to switch from an M1 to an M2 phenotype, thus deactivating the M1 gene transcription program (108).

However, M1 and M2 signatures often coexist in the same microenvironment resulting in a mixed phenotype that depends on the balance of activatory and inhibitory signals and the nature of the tissue environment (100). Such phenomenon happens in allergic inflammation, when increased production of cytokines IL-4 and IL-13 leads to an M2 phenotype switch (109). However, in the area of allergic inflammation, not only the M2 but also the M1 macrophages can be found (110). In general, such tissues rather seem to contain mixed macrophage populations with a wide spectrum of activation states.

Although the M1/M2 concept provides a useful framework, especially for selected immune responses, one should mention that the M1/M2 concept has been established using extensively *in vitro* cultures that relies on well-defined sets of factors. However, macrophages that have been taken out of their

native environment and have been placed in culture, change dramatically their tissue-specific gene expression programs (50). Therefore, it is misleading to conclude roles and functions of macrophages *in vivo* using *in vitro* settings. In consequence, the M1/M2 polarization paradigm picture is now considered to be a rather old and oversimplified concept of the role of macrophages *in vivo*, and the macrophage research field recently demanded that the M1/M2 classification requires reassessment or should be abandon (100, 104, 105, 111). Therefore, defining macrophage functions in the context of their origin (adult- vs. embryonic-hematopoiesis), their environmental stimuli (tissue localization, steady-state vs. inflammation) and the time (development, stages of inflammation, aging) they occur (105) may be more beneficial to understand which role and functions they play and to establish mechanisms and possible therapeutic targets to improve treatment strategies of human diseases where macrophages are involved.

1.2.5 Atypical functions of macrophages: Multinucleated giant cells formation

One unique feature of monocytes and macrophages is their ability to form multinucleated giant cells (MNGCs) in particular upon Th2-related inflammation (112-114). These MNGCs are thought to be responsible for engulfing large particles like foreign material, intracellular bacteria and other pathogens like parasites and fungi (115). Further, MNGCs are important for the generation of osteoclasts, which are involved in resorption of bone tissue, for the formation of foreign body giant cells, which are involved in degradation/resorption of foreign material or for the formation of granulomas important for phagocytosis and antigen-presentation of pathogens (116, 117). In addition, MNGCs can exert pro- or anti-inflammatory functions, and participate in tissue repair and tissue remodeling (118). Further, their polarization is likely to promote the progression/resolution of various diseases (119).

In the past, MNGCs have been shown to form by cell-to-cell fusion (120). However, a recent study has also demonstrated that persistent DNA damage signaling can lead to macrophage polyploidy by cytokinesis failure/endoreplication (121) (Figure 1.3).

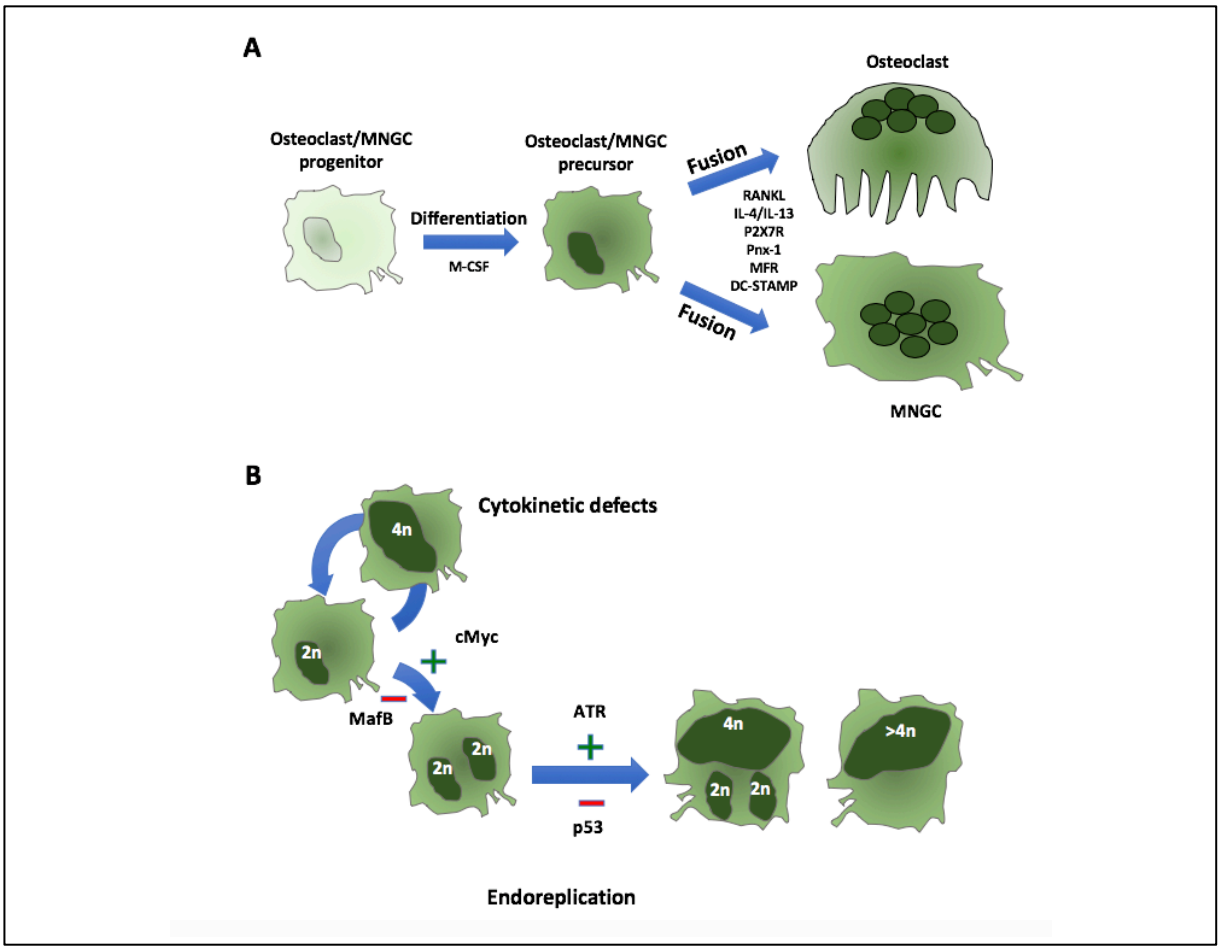

Figure 1.3 Multinucleated (giant) cell formation. (**A**) Cell-to-cell fusion. Engagement of osteoclast/MNGC progenitors to form MNGCs by exogenous stimuli and endogenous signaling pathways. (**B**) Cytokinesis failure. Multinucleated macrophage development through cytokinetic defects and/or endoreplication in response to persistent DNA damage.

Cell-to-cell fusion

To engage fusion, macrophages should firstly become fusion competent. This competence is acquired through the enhanced transcription and expression of essential fusogens, which are induced by exogenous stimuli and endogenous signaling pathways (Figure 1.3). Signals that contribute to the pre-fusion programming of macrophages are induced by M-CSF, RANKL or IL-4/IL-13. M-CSF leads to the differentiation of both osteoclast and MNGC progenitors to their precursors. Subsequently, in osteoclast precursors, binding of RANKL to its receptor RANK induces a fusion-competent status through activation of the transcription factor nuclear factor of activated T-Cells 1 (NFATc1) leading to osteoclast formation. In macrophages, IL-4 and IL-13 bind to their cognate receptors, which share the same IL-4 receptor beta subunit, and induce a fusion-competent status through the activation of the transcription factor STAT6, giving rise to MNGCs (122). Finally, both in osteoclasts and MNGCs, membrane receptors such as dendritic cell-specific transmembrane protein (DC-STAMP), P2X7 receptor (P2X7R), Pannexin-1 (Pnx-1) and macrophage fusion receptor (MFR) are expressed and required for cell-to-cell fusion (123-125).

Cytokinesis failure

Multinucleated macrophages can develop in response to persistent DNA damage signaling induced by genotoxic stress, including replication stress, which promotes multinucleation via endoreplication and cytokinesis failure or recurrent cytokinesis failure. Thereby macrophages re-enter the cell cycle by cMyc and overcome p53-dependent barriers to their proliferation (see Figure 1.3).

1.3 Alveolar macrophages: An extraordinary macrophage population

1.3.1 Origin of AMs

Fate-mapping strategies have shown that, at steady-state, alveolar macrophages originate mainly from embryonic progenitors and independently from circulating monocytes (126) (Figure 1.2). They either develop from fetal macrophages of the yolk sac during primitive hematopoiesis and are characterized by their F4/80^{hi}CD11b^{int} expression pattern, or they arise from fetal liver monocytes during definitive hematopoiesis with the expression pattern of F4/80^{int}CD11b^{hi}Ly6C^{+} (127). However, after birth, lung macrophages change dramatically their expression of surface markers. They increase their expression of CD11c, Siglec-F and CD64 and concurrently downregulate their expression of Ly6C and CD11b until they reach a mature stage with a characteristic surface molecule pattern consisting in CD11c^{hi}SiglecF^{hi}CD64^{hi}CD11b^{lo}Ly6C^{lo} (127). In contrast to more "classical" macrophages, the level of F4/80 expression in mature alveolar macrophages is low (128-130). In addition, it has been shown that after depletion of alveolar macrophages, the majority of the population renewed by cellular proliferation by M-CSF and GM-CSF (28). However, besides of the embryonic origin at steady-state, it has been demonstrated that alveolar macrophages in BAL fluid of mice can also originate from blood monocytes after a triple-allergen (dust mite, ragweed, and *Aspergillus* sp (DRA))-induced allergic asthma model and in human subjects in a model of allergic airway inflammation. Such newly recruited alveolar macrophages have been identified in mice as CD11c^{-}CD11b^{+}CD14^{+} cells with less granules than resident macrophages and as CD163^{+}CD11b^{+}CD14^{+} cells in human subjects (131). The increase in AMs was concomitant to a marked increase in monocyte chemotactic proteins (MCPs) MCP-1 (CCL2) and MCP-3 in the BAL released by bronchial epithelial cells. In addition, MCP-1 receptor (CCR2), MCP-1, MCP-3, and MCP-4 were also increased in post-allergen challenged AMs, suggesting that, in addition to the bronchial epithelial secretion of MCP-1, an autocrine macrophage activation further amplified monocyte recruitment and macrophage differentiation in the airways (131).

1.3.2 AMs under steady-state conditions

Besides their major role in maintaining physiological homeostasis and phagocytosis, alveolar macrophages display regulatory and tolerogenic functions at steady-state. They have been shown to

suppress immune responses through the inhibition of DC-mediated antigen presentation to T cells (132) as well as through their intrinsic ability to promote the generation of forkhead box P3-positive ($Foxp3^+$) inducible Treg (iTreg) cells. Indeed, AMs are able to take up inhaled innocuous antigens and to present the antigen to antigen-specific $CD4^+$ T cells which results in the generation of $Foxp3^+$ iTreg cells (133). This process is dependent on the expression of both tumor growth factor (TGF)-ß and retinal dehydrogenases 1 and 2 (RALDH1 and RALDH2) by AMs. Interestingly, this process occurs in lung tissue and not in the draining lymph nodes and is dependent on antigen presentation by AMs, but not by DCs (133). TGF-ß-induced $Foxp3^+$ Treg cells inhibit themselves spontaneous and antigen-induced Th2-type airway inflammation, and therefore promote airway tolerance (134, 135).

Furthermore, tissue-associated AMs are able to form gap junctions with alveolar epithelial cells (AECs) through the use of connexin (Cnx)43 hemichannels. This allows syncicial communication between AMs and AECs and suppresses the secretion of proinflammatory chemokines, such as macrophage inflammatory protein (MIP)-1a (CCL3) and CXCL1/5 by AMs and AECs, leading to a diminished recruitment of pro-inflammatory neutrophils (136). In addition, AMs express the receptor for CD200 (CD200R), which interaction with its ligand CD200L on AECs suppresses TLR-induced responses and dampens airway inflammation (137).

1.3.3 AMs in defense

On the other hand, AMs, because of their localization, are the first line of defense in the lower respiratory tract against bacterial, fungal and viral pathogens. Their phagocytic ability is essential for the clearance of pulmonary infections by *Streptococcus pneumonia*, *Pseudomonas aeruginosa, Pneumocystis carinii* and *Haemophilus influenzae* (138-141).

The important role of AMs in defending the lung against various pathogens and in regulating inflammatory reactions has been shown in various studies in which AMs were depleted. Indeed, depletion of AMs during influenza virus led to severe impairment of the innate, but not adaptive, immune responses and critically affected the progression of the disease (142, 143). Furthermore, AM-ablated mice showed increased viral load in the lungs, leading to severe airway inflammation, pulmonary edema, vascular leakage, impaired gas exchange and fatal hypoxia associated with severe morbidity (142). Further, selective reconstitution of AMs by neonatal transfer of wild-type AM progenitors prevented severe morbidity and mortality (143).

In addition, AMs are able to initiate an inflammatory response and are able to recruit other immune cells into the alveolar space once they are confronted with large numbers of pathogens or more virulent microbes. To do so, they synthesize and secrete various cytokines, chemokines, including pyrogenic cytokines such as IL-1ß, TNF-α, IL-6, and IL-8, and oxygen metabolites such as reactive oxygen species (ROS), reactive nitrogen species (RNS) and NO (144-146). In this context, IL-1ß

stimulates the production of acute phase proteins and is a chemoattractant for granulocytes, enhances the expansion and differentiation of $CD4^+$ T cells, and increases the expression of cell adhesion molecules on leukocytes and endothelial cells (146, 147). Moreover, TNF-α leads to an enhanced production of other pro-inflammatory/chemotactic mediators, the upregulation of adhesion molecules, and reinforced migration of eosinophils and neutrophils (144, 148). Moreover, both IL-1ß and TNF-α lead to the induction of airway smooth muscle cell contraction (149). While IL-6 signaling leads to the recruitment of monocytes to the site of inflammation and inhibits T cell apoptosis and development of Tregs (150, 151), IL-8 secretion causes the recruitment and activation of neutrophils (152). Finally, the secretion of high levels of ROS, RNS, and NO fosters a highly microbicidal environment, and has a role in mediating the destruction of pathogens (146). All of these mediators together induce a pro-inflammatory response with increased vascular permeability and recruitment of inflammatory cells to facilitate an adequate defense of the host.

1.3.4 AMs in resolution

Clearance of inflammatory leukocytes and the restoration of the epithelial barrier integrity and functions are essential processes terminating an inflammatory phase. Thereby, apoptosis of granulocytes, is an important mechanism that requires subsequent efferocytosis by AMs (153).

Not only apoptotic neutrophils or eosinophils are generating apoptotic debris like any other cells, but in addition they retain their potentially injurious granule contents. Therefore, without clearance by phagocytic AMs, apoptotic granulocytes undergo secondary necrosis, release their granule contents into the alveolar space and tissue, and lead to further tissue injury and prolonged inflammation (154). Usually, apoptotic granulocytes change surface markers, including the exposure of phosphatidylserine and loss of sialic acid residues, as well as the expression of Fas receptor and Fas ligand (155, 156). Such early apoptotic events potently trigger alveolar macrophages for efficient phagocytosis and clearance. Further, phagocytosis of granulocytes reduces macrophage secretion of pro-inflammatory cytokines and also stimulates production of anti-inflammatory cytokines, such as TGF-ß, IL-10, prostaglandin E2 (PGE_2), and platelet-activating factor (PAF) (157). Besides of neutrophils and eosinophils, type II AEC also undergo apoptosis during inflammation and are target for AMs efferocytosis. However, this event has been shown to initiate lung fibrosis in a model of murine lung injury (158). The importance of AMs in the resolution phase of an infection has been shown by a study of experimental pneumococcal pneumonia. In this model, depletion of alveolar macrophages resulted in higher levels of inflammatory cytokines IL-1ß, TNF-α and greater levels of apoptotic and dead neutrophils indicating a reduced clearance of apoptotic neutrophils, lower levels of anti-inflammatory IL-10, resulting in prolonged inflammation, necrosis and parenchymal destruction of lung tissue (159).

1.4 The complement system

The complement system was discovered by Jules Bordet and Paul Ehrlich at the end of the 19th century and was described as a system of heat-labile serum-circulating components that could complement the antibody-mediated bactericidal activity of immune sera (1). Part of this process leads to coating of pathogens with antibodies and/or complement proteins, the so-called opsonization, so that phagocytic cells can easily recognize pathogens, take them up and eliminate them. Although the complement system has been discovered in the context of antibody response, it is, on its own, a part of the innate immune system (1).

The complement consists in a system encompassing 50 soluble proteins, found in the blood, lymph and interstitial fluids, together with cell membrane-bound and intracellular proteins (160, 161). It plays a key role in the initial antimicrobial defense through the recognition and elimination of invading pathogens and/or self-derived danger such as apoptotic cells. Further, it regulates and supports innate and adaptive immune responses, and initiates general inflammatory reactions. Therefore, it has been shown to be crucial for tissue homeostasis, angiogenesis, elimination of immune complexes, lipid metabolism, mobilization of hematopoietic precursors and participation in neurological processes (162-164).

The fluid-phase proteins are principally synthesized in the liver and are mainly present as inactive zymogens widely distributed throughout body fluids and tissues, whereas the membrane-bound proteins are composed of receptors and regulators of activated complement fragments (1, 161). Once a pathogen has breached the host anatomic barriers, serum-circulating complement components label it, which results in the activation of the complement cascade and subsequent clearance of the microbe. Three pathways can lead to the activation of the complement cascade: the classical, the lectin and the alternative pathway (see Figure 1.4).

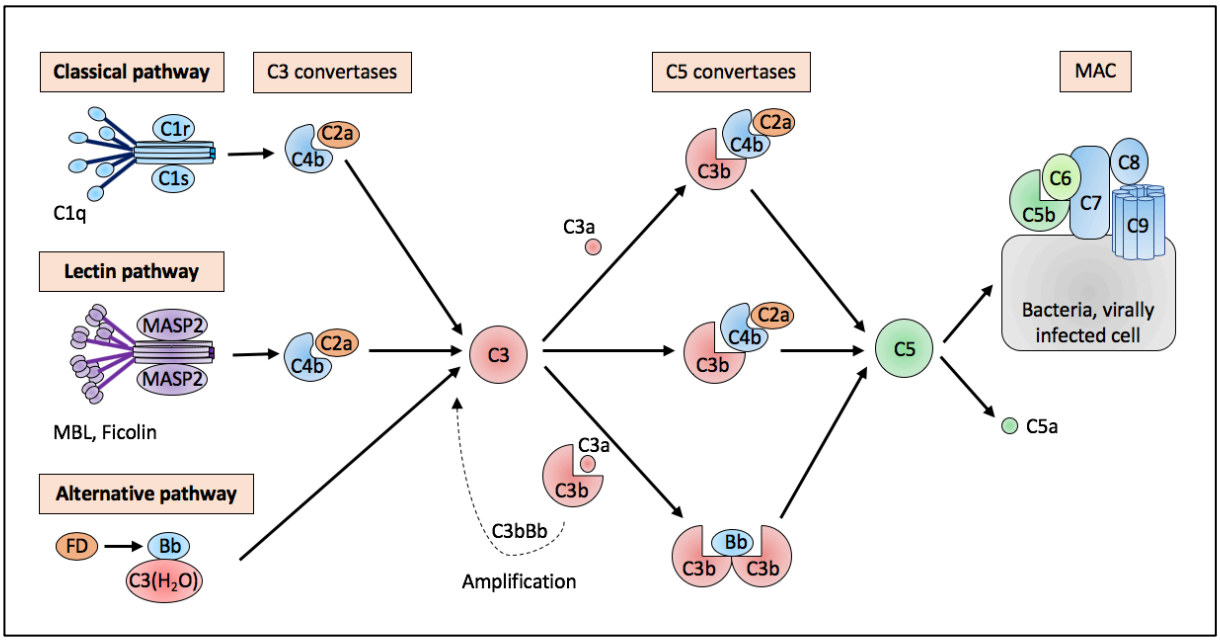

Figure 1.4 Activation of the complement system.
(1) The classical pathway. The classical pathway is initiated when the C1 complex, consisting of a recognition protein C1q and associated inactive proteases (C1s and C1r), recognizes a microbial surface directly or binds to antibodies that have already bound to a pathogen. C1q is a homohexamer each of them consisting in a globular head and a long collagen-like tail. The tails bind to two C1r and C1s molecules forming the C1 complex C1q:$C1r_2$:$C1s_2$. When two or more heads of C1q bind to a pathogen surface or constant region of an antibody, the $C1r_2$:$C1s_2$ complex undergoes a conformational change which causes the activation of C1r, which in turn activates the serine protease C1s. Activated C1s is able cleave complement component C4 into C4b and C4b-bounded C2 into C2a resulting in the formation of the C3 convertase enzyme complex C4b2a of the classical complement pathway which then activates and cleaves the central molecule C3 (1).
(2) The lectin pathway. The lectin pathway is initiated by soluble pattern recognition receptors – mannose-binding lectin (MBL) and ficolins – that circulate in blood and extracellular fluids and recognize carbohydrate structures on pathogenic surfaces. MBL and ficolins show a structure similar to C1q and by analogy to the C1 complex. Then MBL and ficolins form with MBL-associated serine proteases (MASP)-1, MASP-2, and MASP-3 a MBL-MASP complex. With binding of MBL or ficolins to carbohydrates on microbial surfaces, MASP-1 undergoes a conformational change that activates a MASP-2 molecule. Likewise activated C1s in the classical pathway, activated MASP-2 cleaves C4 into C4b and C4b-bounded C2 into C2a and thus generating the C3 convertase C4b2a that is also generated during the classical complement activation (1).
(3) The alternative pathway. The third way to activate complement, probably the most ancient way, is the alternative pathway. It can be, either initiated by spontaneous hydrolysis and activation of the complement component C3, independently from binding to pathogen surfaces beforehand, or by the action of the classical and lectin pathways. Hydrolysis of the thioester bond in C3 forms C3(H_20). Then, C3(H_20) can bind factor B which in turn is cleaved by a plasma protease factor D into C3b(H_2O)Bb. This complex is a fluid-phase C3 convertase and activates further C3 molecules through their cleavage. The formed C3b molecules are usually rapidly inactivated unless they bind to cell surfaces of microbes. Covalently bound to the cell surface, C3b binds factor B which in turn again is cleaved by factor D to Bb which forms together with C3b the alternative pathway C3 convertase – C3bBb. C3b is also generated by the lectin or classical pathways and can covalently bind to the microbial surface. In the same way as C3b produced by the fluid-phase by C3 convertase does, it can bind factor B which leads to its cleavage into Ba and Bb by factor D. Finally, Bb remains associated with C3b forming the C3 convertase C3bBb (1). This convertase functions in the same way as the C4b2a convertases of the lectin and classical pathways does leading to the formation of MAC. However, since the C3 convertase is composed of C3b itself, it has a special role in complement activation. By producing C3b, it can generate more of itself and with that, leading to an amplification loop to rapidly increase C3b production (1)**.** Adapted from (161).

Although they differ in the initiation of the cascade, all pathways converge at a central step in complement activation – the formation of the C3 and C5 convertase enzyme complexes that cleave complement component C3 into the anaphylatoxin C3a and the opsonin C3b, and C5 into the anaphylatoxin C5a and into C5b, respectively (1, 161). Further, the release of C5b initiates the terminal way of complement activation, via the assembly, into the cell membrane of the microbe, of the

membrane attack complex (MAC) consisting in C5b together with the later complement components C6, C7, C8 and the 10-16 molecules of C9 forming a pore and disrupting the microbial cell membrane that can lead to the killing of the pathogen (1, 161). However, the importance of the MAC in host defense is debatable, since the effect of killing seems to be important for only few pathogens, mainly gram-negative bacteria (165, 166). Therefore, the importance of the MAC formation is under debate (167).

1.4.1 Effector functions of the complement system

Although the damaging effect of the membrane attack complex appears to be very dramatic, this effector complex is quite limited in host defense (1). Therefore, the MAC may not represent the main effector function of the complement system. Instead the main functions are opsonization of pathogens and the generation of small cleavage fragments like C3a and C5a. Indeed, the opsonin and anaphylatoxins, early cleavage products of the complement cascade, promote the recruitment of scavenger cells involved in phagocytosis of the pathogens, and activate macrophages, granulocytes, mast cells, and lymphocytes to produce local inflammatory responses (1, 161).

Opsonization occurs through the binding of C3b and its degradation products iC3b and C3dg to the microbial surface and exerts effective signaling functions for phagocytosis. In addition, iC3b, gains high affinity for the integrin receptors, complement receptor (CR)3 (CD11b/CD18) and CR4 (CD11c/CD18), thereby largely enhancing the complement-mediated phagocytosis (168). Besides of the role of C3b in the complement response via opsonization, it additionally acts directly on the innate and adaptive immune response. Indeed, through binding to CR1 on immune cells, C3b induces immune adherence and leads to the transport of opsonized cells to the spleen and liver. Furthermore, binding of C3b to human membrane cofactor protein (MCP/CD46) has been shown to influence T-cell responses particularly in human subjects. However, since mice do not express CD46, the validity of such mechanism in such model is unclear. In addition, the conversion of C3b to iC3b enables the interaction with CR2, a receptor that is expressed on B cells and follicular dendritic cells (FDCs), which lowers the threshold for B cell activation, directs antigen handling by FDCs and contributes to the maintenance of B cell tolerance and memory (161, 168). In conclusion, C3b is involved in various effector functions ranging from immune adherence and transport to phagocytosis and adaptive immune modulation.

Another function of the complement system is to recruit immune cells in particular neutrophils, eosinophils and mast cells. This is mediated by the cleavage fragments of the complement cascade, namely the anaphylatoxins C3a and C5a. The role and functions of these molecules as well as their corresponding receptors will be described in more detail in chapter 1.4.4.

1.4.2 Complement regulators

The complement system with its powerful effector functions, its distribution throughout the body, its pronounced autocrine amplification loop, and its impact on innate and adaptive immunity, is a nearly perfect system to handle danger, but is potentially very harmful for the host. Activation of the classical and lectin pathway is usually dependent on pathogens. However, under certain conditions, both pathways can be activated and result in autologous damage. Considerably more hazardous can be the randomly deposition of C3b on pathogens and nearby surfaces of the host via the alternative activation pathway, since its nondiscriminatory amplification loop, if not properly regulated, can injure the host. Thus, the system requires a tight regulation. On the one hand, its activity needs to be down-regulated on host cells while, on the other hand an efficient activation should be permitted on foreign targets. Therefore, humans and other mammals have developed various inhibitory proteins, present in the plasma or on the cell surface of host cells, which regulate the location and activity of the complement system.

Of note, properdin, a plasma glycoprotein, is the only known positive regulator of the complement cascade (169). Properdin binds to and stabilizes the alternative pathway C3 convertase C3bBb (170), and in some cases, may also serve as a platform to form new C3bBb convertases on the cell surface (171). In addition, properdin is well known to promote the alternative pathway of complement activation in the context of host defense. Its deficiency has been shown to increase the risk, in humans, of *Neisseria meningitidis* infection (172). In contrast, the activation of the classical and lectin pathway is controlled by a serpin molecule, C1 Inhibitor (C1Inh), which binds irreversibly and inactivates C1r and C1s of the classical pathway as well as MASP-1 and MASP-2 from the lectin pathway, leading to the inhibition of the initial steps of these pathways (162, 168, 173). On the other hand, the alternative pathway is regulated by Factor I and Factor H. Indeed, Factor I is a plasmatic serine protease that inactivates, together with Factor H as a cofactor, the conversion of C3b into iC3b. Furthermore, Factor I is also able to cleave the C4b component of the C3 convertase C4b2a in the presence of the plasma cofactor C4b-binding protein (C4BP) (1, 162). In addition, Factor H competes with Factor B for the binding to C3b and thereby decreases the stability of the C3bBb convertase complex, leading to the dissociation into C3b and Bb, and limiting the C5 convertase formation. Besides plasmatic regulators, membrane-bound complement regulators exist. In humans, the membrane cofactor protein (MCP, CD46) acts as a cofactor for Factor I-mediated cleavage of C3b and C4b. In contrast, decay-accelerating factor (DAF, CD55) accelerates the dissociation of the C3 convertases C3bBb and C4b2a. Finally, CR1 (CD35) acts as a cofactor for Factor I to cleave C3b to iC3b, and thereafter to C3c and C3dg. In addition, CR1 also displaces Bb from C3b and C2a from C4b (1, 162). Finally, there are also soluble inhibitors of the MAC formation such as vitronectin, also known as protein S, and Clusterin (1, 174). Vitronectin binds preferentially to the C5b-7 complex whereas Clusterin not only binds to C7, but also to C8 and

to C9, inhibiting the polymerization of C9 (174, 175). Finally, Protectin (CD59) is a membrane-bound regulator of the MAC formation, binding to C8 and therefore inhibiting C5b-9 formation (1, 174).

1.4.3 Novel aspects of complement activation

Local or systemic complement activation

Components of the classical, alternative and terminal pathways of the complement system are all present in plasma. In the late 1960s, hepatocytes in the liver, have been identified as the main source of plasma complement (176, 177), and for a long time it was assumed that complement components were synthesized solely there. However, already in the 1980s evidences pointed toward an extrahepatic production of complement factors. Firstly, BM-derived and tissue macrophages from guinea pigs were reported to synthesize C2 and C4 components of complement (178). Then, local extrahepatic expression of complement genes C3, Factor B, C2, and C4 was shown to be increased in murine lupus nephritis (179). Finally, in the late 1990, the first indication that the liver is the main but not only source of complement was provided in studies with human subjects where bone marrow and extrahepatic C3 and C7 production were quantified in bone marrow transplant (BMT) and liver transplant (LT) recipients of C3 and C7 allotypes (180, 181). Today, the paradigm is that almost all cells in the human body can produce complement proteins including macrophages, T and B lymphocytes, epithelial cells and neutrophils and that local complement synthesis occurs in various tissues and organs including the lung, intestine, kidney, heart, skin and synovial tissues (182). Furthermore, in some immune-privileged organs, such as the brain, local production is the main source of complement (182). In addition, while some local complement components are synthesized constitutively, others can be increased or downregulated by cytokines and growth factors. In turn, increases in local complement can modulate cytokine production by immune cells, indicating the existence of a bi-directional feedback loop (183, 184). These findings also suggest that extrahepatic complement production may have evolved to respond to environmental stimuli that require a local immune response without inducing systemic complement activation (161, 185).

1.4.4 The anaphylatoxins

Besides of the large cleavage products that are generated during the complement activation cascade and are involved in the MAC formation, small cleavage fragments from C3 and C5 are generated, the so-called anaphylatoxins (ATs) C3a and C5a. Their name originates from the shock like syndrome, termed anaphylactic shock, similar to that seen in a systemic allergic reaction, they induce when produced in large amounts or injected systemically (1).

Non-Canonical generation of anaphylatoxins

ATs are generated either during systemic activation of serum complement (see Figure 1.4) or by local non-canonical activation of complement (see 1.4.3). Originally, it has been assumed that C3 and C5 are activated only by serum-derived convertases of the fluid phase and/or of the cell surface. However, recent studies have demonstrated that in humans, activated T cells produce in addition to C3 and C5 upon interaction with APCs together with Factor B and Factor D, thereby, providing the complete activation machinery for local C3 and C5 convertase formation. In such case, once local complement is activated by a cell-activating signal, such as TCR stimulation, secretion of C3, C5, Factor B and Factor D is initiated and leads to C3 and C5 convertase formation in the extracellular space and/or on the cell surface. Moreover, the newly generated complement cleavage fragments C3a, C3b, C5a and C5b, bind autocrinally to their cognate receptors on the T cell / APC and mediate cellular effector responses such as APC maturation, secretion of pro-inflammatory cytokines and an induction of a Th1 or Th17 immune response (161). Similarly, in mice, a surface protease is cleaving C5 and generates C5a at the surface of pulmonary (186) or elicited peritoneal macrophages (187).

Intracellular anaphylatoxin generation - the complosome

Both systemic and local complement activations were thought to be restricted to the extracellular space either by serum-derived convertases or surface bound convertase components. However, this position has been challenged by the recent discovery that complement activation also occurs intracellularly (188), a concept now called the complosome. Indeed, in humans, resting $CD4^+$ T cells were shown to contain intracellular stores of C3. In addition, they expressed the protease cathepsin L (CTSL) in endosomal and lysosomal compartments that cleaves C3 into its active fragments C3a and C3b. Interestingly, this tonic C3a generation was essential for homeostatic T cell survival through basal activation of mammalian target of rapamycin (mTOR). Moreover, shuttling of this intracellular C3-activation-system to the cell surface upon T cell stimulation induced autocrine proinflammatory cytokine production (188). Moreover, the activation of intracellular C3 and its signaling via CD46 in human $CD4^+$ T cells regulates other key metabolic events, including glycolysis, nutrient influx and mitochondrial oxidative phosphorylation (OXPHOS) (160, 189). Besides of C3, it has also been shown that T cells constantly generate intracellular C5a from internal C5 sources (190). Once more, upon TCR activation, intracellular C5a acts on intracellular C5aR1 and induces oxygen metabolism through increased production of ROS that supports cell activation (190). However, intracellular complement is not limited to T cells but has also been mentioned in a wide range of immune and non-immune cells including B cells, monocytes, neutrophils, and fibroblasts (188). Furthermore, the importance of intracellular C3 has been shown within gut epithelial cells that drive intestinal tissue damage during mesenteric ischemia. There, epithelial cells exposed to LPS or to hypoxic conditions, expressed higher

levels of *C3* mRNA as well as increased amount of C3a fragment. In addition, these cells produced cathepsins B and L, and inhibition of cathepsins suppressed the release of C3a. Finally, treatment with a cathepsin inhibitor and cathepsin B-deficient mice showed limited intestinal injury during the ischemic phase (191). Interestingly, intracellular complement activation has also been shown for tumor cells. Tumor cell-derived C3 was activated intracellularly resulting in the generation of C3a. Then, C3a, via C3aR-PI3Kγ signaling, modulated the functions of tumor-associated macrophages, thereby repressing antitumor immunity (192). Since intracellular complement is widely distributed and is important for the regulation of metabolism, nutrient influx and antitumor immunity, it suggests that intracellular complement activation could be of broad physiological significance.

Immunological effects of anaphylatoxins

The ATs are small polypeptides consisting of 77 for C3a and 74 amino acids for C5a. Both ATs contain highly conserved C-terminal pentapeptide sequences that are essential for activation of their cognate G-protein coupled receptors. The ATs are generally potent inflammatory mediators targeting a wide spectrum of non-immune and immune cells. They induce smooth muscle cell contraction, regulate vasodilatation and increase the permeability of blood vessels (193). Moreover, in neutrophils, macrophages and eosinophils ATs trigger oxidative burst by ROS production (194-196), and in basophils and mast cells C3a and C5a stimulation leads to degranulation and histamine release (197, 198). Further, C3a induces aggregation and serotonin release from platelets, regulates secretion of IL-6 and TNF-α from B-cells and monocytes and leads to the production of IL-8 by the ECV 304 epithelial cell line (199-202). In contrast, C5a acts as a powerful chemoattractant for macrophages, neutrophils, basophils as well as activated B- and T-lymphocytes (203-207). Besides of their pro-inflammatory characteristics, ATs were shown to regulate tissue regeneration, to have immunoregulatory properties in hepatic homeostasis, to be involved in liver fibrosis and to have a neuroprotective effect for the brain (208-211).

Since ATs are powerful bioactive molecules, control mechanisms have coevolved for effective protection and regulation of their activity. The tight regulation is controlled by carboxypeptidases, which rapidly cleave off the C-terminal arginine residue of the ATs in the circulation and in tissues, leading to the formation of C3a-desArg and C5a-desArg (212, 213). The resulting C5a-desArg retains 1-10% of the inflammatory activity of C5a, while C3a-desArg is devoid of any pro-inflammatory activity (193).

Anaphylatoxin receptors

C3a and C5a exert their multiple effector and regulatory functions through binding and activation of their cognate immune receptors, the anaphylatoxin receptors (ATRs). The three ATRs belong to the

large superfamily of seven transmembrane guanine nucleotide-binding (G)-protein-coupled receptors (GPCRs) and comprise the C3a receptor (C3aR), C5a receptor 1 (C5aR1, CD88) and C5a receptor 2 (C5aR2, C5L2, GPR77). They show close similarities in their sequence, and cluster with other chemoattractant receptors including the formyl peptide receptor family, bradykinin receptors, ChemR23, chemokine receptors CXCR1 and CXCR2 and several orphan receptors (193, 214-217). However, despite their high homology, they differ in ligand specificity and signal transduction.

C3aR

C3a exerts its pro- and anti-inflammatory functions through binding to its cognate GPCR C3aR. The ligand of C3aR is exclusively C3a, since neither its degradation product C3a-desArg (also named Acylation-Stimulating Protein) nor C5a are binding to it. C3aR is a 54 kilodalton (kDa) molecule consisting of 482 amino acids, two predicted extracellular asparagine (N)-linked glycosylation sites at amino acid positions 9 and 194, and a sulfation site at the tyrosine 174. In comparison to the other ATRs, C3aR comprises a large second extracellular loop which constitutes nearly a third of its size and is, together with the sulfated tyrosine, essential for C3a binding (217-219). The murine C3a receptor structural gene is a single copy gene of approximately 8 kilobase pair (kb) comprised of 2 exons which are separated by a large intron spanning 4724 base pair (bp). The first exon encodes 97 bp of 5'-untranslated sequence, while the exon 2 encodes the remaining 8 bp of 5'-untranslated sequence and the entire coding and 3'-untranslated sequences (220). This genomic construct is typical for chemoattractant receptor genes, which contain their entire coding sequence on a single exon (220). The binding of C3a to C3aR activates intracellular signal transduction pathways via pertussis-toxin-sensitive or pertussis-toxin-insensitive G-proteins, respectively. Downstream signaling events include intracellular Ca^{2+} mobilization and phosphorylation of the extracellular signal-regulated kinases (ERK)1 and ERK2 and the serine/threonine-specific protein kinase Akt (221-228). In addition, ligand binding triggers a very rapid internalization of C3aR (223, 225).

In humans, flow cytometric and western immunoblot analysis, as well as binding and functional assays revealed that C3aR is expressed in human innate and adaptive immune cells including neutrophils, eosinophils, basophils, dendritic cells, monocytes, mast cells and activated B- and T-lymphocytes (188, 197, 206, 221, 229-232), as well as in non-immune cells (233, 234). However, the murine C3aR expression pattern was until recently ill defined, partly because only a limited number of cell types have been tested for mRNA or protein expression and are not always providing information about intracellular or cell surface protein localization. In addition, tissue and cell expression analyses of C3aR have often been performed by western blot, flow cytometry and immunohistochemistry using polyclonal or monoclonal antibodies which showed false positive results due to unspecific antibody binding (227). Despite such limitations, C3aR expression has been shown on platelets where it

regulates distinct steps of thrombus formation such as platelet adhesion, spreading, and Ca^{2+} influx on platelets, and *in vivo* hemostasis (235, 236). Notably, *C3ar1*$^{-/-}$ mice were less prone to experimental stroke and myocardial infarction (235, 236). Finally, C3aR has been demonstrated to drive pro-tumorigenic neutrophil activities during small intestinal tumorigenesis. This process occurs through increased circulating LPS that induce upregulation of C3aR on neutrophils isolated from $APC^{Min/+}$ mice, activation of the complement cascade, NETosis, induction of coagulation and N2 polarization, which prompt tumorigenesis (237).

C5aR1 (CD88)

In contrast to C3aR, C5aR1 recognizes both C5a and its degradation product C5a-desArg (238, 239). Indeed, physiological levels of C5a-desArg have been shown to induce significant levels of cell activation that were even higher than those with analogous concentrations of C5a (240). In addition, the ribosomal protein S19 (RP S19) can bind to C5aR1 (241). C5aR1 is a 42 kDa protein comprising 350 amino acids with a glycosylation at the N-terminus and sulfated tyrosines, the latter being critical for ligand binding (242). Two binding motifs are involved in the interaction between C5a and C5aR1. First, the acidic N-terminal extracellular domain of C5aR1 and second the C-terminus of C5a which interacts with a binding pocket located in the second extracellular loop of C5aR1 (243). The second step is essential for receptor activation. Like C3aR, binding of C5a to C5aR1 leads to intracellular signal transduction via pertussis-toxin-sensitive and pertussis-toxin-insensitive G proteins. Albeit, a unique feature of C5aR1 is pre-coupling to G-proteins in the absence of C5a, thereby lacking a lower affinity state found in other GPCRs (244). Binding of C5a leads to phosphorylation of C5aR1 by associated kinases, which in turn leads to the binding of β-arrestins 1 and 2, targeting C5aR1 for receptor internalization via clathrin coated pits (245). C5aR1 activation leads to downstream activation of several components of different signaling pathways like phosphatidylinositol 3-kinase gamma (PI3K-γ), phospholipase C (PLC) and phospholipase D (PLD) (246-248). Further, downstream signaling results in intracellular Ca^{2+} mobilization and phosphorylation of ERK1/2, p38-mitogen activated protein kinase (MAPK) and Akt (249-252).

In humans and rodents, C5aR1 is expressed in various cell types, but predominantly on cells originating from the myeloid lineage like neutrophils, basophils, eosinophils, macrophages, monocytes, mast cells and DCs (196, 232, 249, 253-259). Several reports have shown C5aR1 expression in human T cells and its involvement in Th1 effector functions (161, 163, 179). In contrast, data about the expression of C5aR1 in murine T cells are controversial (260). While some studies have shown that locally produced C5a binds to T cell-expressed C5aR1 to enhance effector T-cell expansion by limiting antigen-induced apoptosis (160, 190, 207, 261), two independent studies using GFP-C5aR1 reporter mice found no C5aR1 expression in naïve or activated $CD4^+$ T cells (249, 258). One reason could be that the widely

used C5aR1-specific antibody 20/70 shows cross-reactivity with a subpopulation of apoptotic T cells (249), at least questioning C5aR1-expression data obtained with this antibody. Besides immune cells, keratinocytes, epithelial, endothelial, smooth muscle and neuronal cells such as astrocytes were reported to express C5aR1 in mice (262-267).

C5aR2 (C5L2, GPR77)

The second receptor for C5a, C5aR2, was discovered in 2000 as a putative orphan receptor (268). It is a 37kDa protein consisting of 337 amino acids that shares 58% sequence homology with C5aR1 and 55% with C3aR. C5aR2 is bound by both C5a and its cleavage product C5a-desArg. Notably, C5a-desArg binds C5aR2 with a much higher affinity compared to C5aR1. Further, some studies have considered C3a-desArg, as a ligand for C5aR2 (269, 270). However, if this is a true binding or an unspecific binding to plastic surfaces due to the highly cationic nature of the ligands C3a and C3a-desArg is still under debate (193, 271). Similar to C5aR1, C5aR2 is a seven transmembrane GPCR, but is uncoupled from heterotrimeric G proteins, due to an amino acid alteration in the so-called DRY sequence at the end of the third intracellular segment (272). Because of this property, C5aR2 was initially considered as a decoy-receptor only regulating the functions of C5aR1 by limiting the amount of free C5a (272). In line with that hypothesis, intracellular Ca^{2+} mobilization occurs neither in C5aR2 transfected cells after AT administration (272, 273), nor in C5aR1-deficient C5aR2^{+} neutrophils (274). However, more recent studies showed that C5aR2 binds β-arrestins and inhibits C5aR1-driven ERK1/2 phosphorylation (275), suggesting that C5aR2 is a negative modulator of signal transduction. Moreover, additional studies have shown that C5aR2 promotes either pro- or anti-inflammatory properties (276-278).

Frequently, the cellular and tissue expression of C5aR2 is similar to that observed for C5aR1 (279). However, C5aR2 is often expressed at a much lower level than C5aR1 (268, 275, 277). Further, in humans, C5aR2 expression was shown in cells of the myeloid lineage like neutrophils, eosinophils, macrophages, monocytes and dendritic cells (190, 268, 275, 277, 278). Using a newly developed tdTomato-C5aR2 reporter mouse, our lab confirmed this broad expression of C5aR2 (280). Similar to the ongoing debate regarding C5aR1 expression in murine T and B cells (249, 258, 281), data about C5aR2 expression are controversial. In humans, C5aR2 has been shown to be expressed in naïve and central memory T cells as well as in γδ T cells (190, 275). Albeit, only one study showed C5aR2 mRNA expression in murine T cells (281), the characterization of the tdTomato-C5aR2 reporter mouse did not confirm C5aR2 expression in either naïve or activated T cells (280). These findings suggest that differences observed for C5aR1 expression in human and mouse T cells may also apply to C5aR2.

1.5 Macrophages, complement and their role in pulmonary diseases

Macrophages are distributed overall tissues in the body. Besides their collective role in maintenance tissue homeostasis and protection of the host against microbes, molecular analysis, murine disease models and genome-wide sequencing technologies have shown that macrophages also play a key role in human diseases. It has now become clear that macrophages are associated with chronic inflammatory diseases such as atherosclerosis, obesity, diabetes, cancer, skin diseases, and neurodegenerative diseases (20-22, 24, 105). However, lung macrophages have also been shown to play a central role in pulmonary diseases. Moreover, in these pulmonary diseases very often the complement system, in particular C3 and the C3a/C3aR axis have been shown to be involved.

1.5.1 Chronic Obstructive Lung Disease

In patients suffering from chronic obstructive lung disease (COPD), the most common chronical lung disease, increased numbers of macrophages, macrophage chemoattractants and their released mediators, TNF-α and IL-6, have been found (282-284). Additionally, AMs in COPD show an impaired innate immune response to respiratory pathogens, mediated by impaired TLR responses, underlying a propensity for exacerbations in COPD (285). Furthermore, AMs from subjects with COPD are deficient in their ability to phagocyte apoptotic epithelial cells, eosinophils and bacteria leading to progression of airflow obstruction requiring hospitalizations (286-288). Lung parenchymal destruction is a key feature of COPD. Macrophages have been shown to directly contribute to this process by the secretion of MMP-12, which is a potent elastin-degrading enzyme that causes tissue destruction, and which has been linked to emphysema (289). Intriguingly, maintenance of an M2-phenotype of AMs during COPD fails to resolve inflammation and contributing to airway remodeling (85).

Moreover, patients with COPD have been shown to exhibit lower serum levels of complement components C3 and C4 (290, 291), but higher C3a and C5a levels in sputum of patients compared to healthy subjects (292, 293) which correlated with respiratory tract infections, the degree of emphysema and the forced expiratory flow rate in patients with chronic bronchitis (290). The fact of higher levels of C3a in sputum, suggest that C3aR in AMs may play a role in the disease.

1.5.2 Cystic Fibrosis

Cystic Fibrosis (CF), is a genetic disorder in the CF transmembrane conductance regulator (CFTR) gene, characterized by a salty-tasting skin, poor growth, and poor weight gain, accumulation of thick, sticky mucus, and coughing or shortness of breath. One major problem of CF is a failure to clear infections with gram-negative bacteria such as *Pseudomonas (P.) aeruginosa*, *Staphylococcus aureus*, *Burkholderia cepacia* and *Haemophilus influenza*. The switch from IL-10 to inflammatory cytokine

production by macrophages has been shown to play a key role in the development of CF lung disease. In addition, high levels of cytokines released by macrophages, such as TNF-α, IL-1β, IL-6 and IL-8, are elevated in the lungs of patients with chronic CF compared with healthy controls promoting a destructive inflammatory process in the lung (294). Moreover, changes in macrophage functions during the course of CF have been described. Dysfunctional CFTR alters the bactericidal activity of human and murine macrophages against bacteria, which leads to persistent bacterial infections and may also lead to continual stimulation of macrophages contributing to chronic inflammation (295, 296).

Besides macrophages, the anaphylatoxins, C5a and C3a, have been shown to play a significant role in cystic fibrosis. There, C5a and C3a in lung fluid correlated with disease severity. Interestingly, increased C5a was associated with increased inflammation and poorer clinical measures, whereas increased C3a appeared to be associated with less inflammation and improved clinical measures (297). As mentioned before, one major problem in CF patients is a failure to clear infections with *P. aeruginosa*. It has been shown that the alternative activation pathway and complement component C3 are critical for a protective immune response against *P. aeruginosa* in a murine model. In this study, the alternative pathway was critical for the survival of mice and the protection provided by complement was in part due to C3-mediated opsonization and phagocytosis of *P. aeruginosa* (298). So far, no studies investigated the putative role of C3aR in AMs in the outcome of CF.

1.5.3 Lung cancer

The role of AMs in lung cancer has been shown to be multifaceted and divers. On the one hand, the secretion of proinflammatory cytokines such as TNF-α, IL-1ß and IL-6, by AMs has been demonstrated to enhance anti-tumor functions, to inhibit tumor growth, and cytotoxicity (299-301). On the other hand, pro-tumor functions of AMs in lung cancer have also been reported, since the inhibition of anti-tumor function, via the secretion of the anti-inflammatory cytokines like IL-10 and TGF-ß, may contribute to lung cancer progression and metastasis (302, 303). In addition, AMs have also been found to contribute to angiogenesis and tumor growth via the secretion of IL-8 and vascular endothelial growth factor (VEGF) (304, 305).

Various reports have demonstrated a role for complement in lung cancer. Interestingly, the activation of the C3aR pathway has been shown to alter $CD4^+$ T lymphocytes and to mediate lung cancer progression (306). In addition, C3aR contributes to melanoma tumorigenesis by inhibiting neutrophil and $CD4^+$ T cell responses (307). Since alveolar macrophages play a vital role in lung cancer, one could question the role of C3aR in AMs in disease pro- or regression.

1.5.4 Respiratory Tract Infections (RTIs)

Macrophages have been demonstrated to play a central role in the pathogenesis of several respiratory tract infections (RTIs) including *Mycobacterium tuberculosis* (Mtb) and *Streptococcus pneumoniae*. In Mtb, macrophages play a complex role in the infection. On the one hand they control the infection, but on the other hand they promote disease progression. At the early stage of Mtb infection, macrophages have been shown to express iNOS, IL-1ß, TNF-α and IL-12 to control infection (145). In contrast, a recent study revealed that early, productive Mtb infection occurs almost exclusively within airway-resident AMs and enabling infected cells to disseminate from the alveoli to the lung interstitium (308). Mtb is recognized via interactions with complement receptors, mannose receptors and Fc receptors and quickly phagocytized by AMs leading to the killing of bacteria. However, bacilli may survive and then disseminate to the interstitium or remain latent through their ability to block phagolysosome maturation and their resistance against ROS and reactive nitrogen species (RNS). Indeed, although Mtb infection promotes NO production in human macrophages, it results in increased viability and growth of mycobacteria (309). Finally, infected AMs trigger the recruitment of neutrophils, lymphocytes and other immune cells to the site of infection forming a cellular infiltrate that later builds the typical structure of a macrophage-rich granuloma (310). Actually, this tissue response is designed to control infection, however, in immunocompromised patients latent tuberculosis infection is activated leading to active bacterial replication, persistent inflammation, and collateral tissue damage (310).

Further, AMs play a major role in *S. pneumonia* infection, the major common cause of pneumonia. Alveolar macrophages are able to phagocyte *S. pneumonia* up to a defined threshold without developing features of pneumonia. However, when AMs fail to control the infection other inflammatory immune cells, in particular neutrophils, are recruited to the lung to control infection (159). Transcriptome analysis demonstrated that *S. pyogenes* induces an atypical activation program in murine macrophages. On the one hand, infection leads to the upregulation of proinflammatory cytokines in macrophages such us TNF-α, IL-1ß and IL-6, on the other hand macrophages upregulate anti-inflammatory mediators, such as IL-1 decoy receptor and IL-10, maybe indicating that AMs participate in the inflammation but also resolution of the infection (311). Efferocytosis of cells by AMs triggers the release of molecules such as TGF-ß, IL-10, NO, and prostaglandin E_2 (PGE_2), surprisingly leading to impaired phagocytosis and bacterial killing thus dampening the clearance of *S. pneumoniae* (312). In concert, it has been shown that administration of glucocorticoids during active murine pneumonia infection augments efferocytosis hindering AMs to kill bacteria via inhibition of inflammatory cytokine production (313). This explains the complexity of glucocorticoid treatment in patients with COPD and the role of AMs in increased risk for pneumonia and exacerbation in these patients.

The role of complement in RTIs has not been intensively investigated so far. However, one study of Mtb infection in *C3ar1*$^{-/-}$*/C5ar1*$^{-/-}$ mice found a decreased bacterial burden in these mice indicating a better control of mycobacterial growth than WT mice (314). Another study has demonstrated that C3aR is critical in defense against *Chlamydia psittaci* in mouse lung infection and is required for antibody and optimal T cell response (315). Since AMs play a role in RITs and complement seems also to be involved in these infections, studies of C3aR in alveolar macrophages in RITs could to be a new interesting and promising research field.

1.5.5 Fibrotic lung disease

Fibrotic lung disease is characterized by excessed deposition of ECM in the lung, the destruction of the lung architecture, and therefore compromised gas exchange. Today, there are strong evidences that a fibroproliferative and dysregulated wound healing cascade, maybe driven by macrophages, causes the fibrosis (316). Pro-inflammatory mediators such as TNF-α and IL-1ß released by AMs lead to continuous inflammation. In addition, profibrotic mediators like IL-10, CCL-18 and Chitinase 3-like 1 (Chi3l1) contribute to fibrotic processes in the lung with fibroblast proliferation, and lung matrix deposition (89).

In addition, it has been shown that the anaphylatoxin receptors, C3aR and C5aR1, contribute to the pathogenesis of pulmonary fibrosis. The study showed that bleomycin-injured mice with fibrotic lungs, showed elevated local C3a and C5a levels, and overexpressed their receptors and when they blocked C3aR and C5aR1, it arrested the progression of fibrosis by attenuating local complement activation and TGF-ß signaling (317).

1.5.6 Acute lung injury

Acute lung injury (ALI) is a respiratory disorder characterized by hypoxemia, pulmonary infiltration, pulmonary edema, a decrease in pulmonary compliance, and a decrease in the functional residual capacity leading to mortality in patients in intensive care units (318). There is increasing evidence that macrophages, including AMs and blood-recruited monocytes, are key factors in the pathogenesis of ALI (319, 320). Macrophages have both pro- and anti-inflammatory functions in the disease based on the microenvironment in different pathological stages (318). In response to infection-induced activation of TLRs or other PRRs, AMs act as the first line of defense against pathogenic microorganisms, such as endotoxin and ventilator-induced lung injury through the release of various potent pro-inflammatory mediators including IL- 1β, IL-6, and IL-18 (321-323). Therefore, macrophages serve as a promoter in the process of lung tissue damage in ALI. Once the pathogen has been eliminated, resident and recruited macrophages shift from a pro-inflammatory to an anti-inflammatory phenotype. They initiate lung tissue repair by limiting the levels of pro-inflammatory

cytokines in the cellular space, release anti-inflammatory cytokines including IL-10, IL-1Ra and TGF-ß, and clear apoptotic neutrophils from inflammatory sites (318). However, pulmonary fibrosis, a late complication of ALI, develops through the persistence of these anti-inflammatory macrophages at the injury sites promoting fibroblast proliferation, excessive deposition of ECM and collagen (324).
Several studies have reported an association between ALI and the complement system. Indeed, H5N1-driven ALI in mice was caused by excessive complement activation, as shown by the deposition of C3 in lung tissue, and the upregulation of C3aR and C5aR1. Further, when H5N1-infected mice were treated with a C3aR antagonist, it led to significantly reduced inflammation in lungs, alleviating ALI (325).
In the past, immunocomplex deposition in $C3^{-/-}$ mice led to the conclusion that this form of ALI was independent of complement activation (326). However, it was later recognized that $C3^{-/-}$ mice undergoing immunocomplex deposition had high levels of C5a in their BAL fluids and that neutralization of C5a in these mice markedly attenuated ALI (186). Recently, activated clotting and fibrinolytic factors have been shown to generate C5a from C5 (327), suggesting that in the absence of C3, mice may compensate the production of anaphylatoxin C5a through supernormal levels of thrombin in liver, allowing formation of C5a in various tissues.

To conclude, both AMs and the complement system seem to play an important role in the development and severity of various pulmonary diseases. Therefore, it is predictable that they also may play an important role in the development and severity of allergic asthma. Indeed, decades of research have shown the complement system, in particular the anaphylatoxins, playing a key role in allergic asthma. However, studies examining the role and functions of the anaphylatoxins on alveolar macrophages in the development and severity of allergic asthma remain elusive.

1.6 Allergic Asthma

Asthma is a chronic inflammatory disorder of the airways, which causes persistent bronchial hyperreactivity leading to paroxysmal dyspnea. It is associated with high disability and mortality and the total cost of the disease, both in direct medical costs and indirect costs caused by loss of productivity, reached $81.9 billion in the United States in 2013 (328, 329).

1.6.1 Asthma prevalence and symptoms

Asthma is a major public health problem affecting the lives of up to 339 million people worldwide, with an increasing prevalence in developing countries. Particularly comprising children, almost 1 in 10 children and 1 in 12 adults are affected. The burden of asthma is greatest in children between 10-14

years and in elderly people in the age of 75-79. Asthma is the 14th most important disorder in the world in terms of the extent and duration of disability (330, 331).

Physiologically, the constant inflammation of the airways leads to mucus overproduction, airway wall remodeling, airway narrowing and airway hyperresponsiveness (AHR) causing repeated periods of coughing, shortness of breath, wheezing and chest tightness. In many patients, the disease can be controlled by short- and/or long-acting $ß_2$-adrenergic agonists (which lead to bronchodilatation) alone or in combination with an inhaled corticosteroid (which suppresses the inflammation). However, 5–10% of patients are refractory to corticosteroid treatment, which often leads to increased disease severity and hospitalization due to secondary respiratory viral infection (332).

In general, as mentioned before, pathophysiological changes of the respiratory tract have been linked to a dysregulation of a Th2/Th17 immune response in the lung, which will be described in more detail in chapter 1.6.5.

1.6.2 Allergic and non-allergic asthma

Traditionally, asthma has been divided into two forms in the clinic, the non-allergic (intrinsic, non-atopic), and the allergic (extrinsic, atopic) asthma, which are displaying similar symptoms. However, non-allergic patients neither show IgE reactivity to allergens nor the involvement of the adaptive Th2 immune cells. Non-atopic asthma often develops during later lifetime and is more common in women. It is associated with chronic rhinosinusitis, nasal polyps, obesity, and often require long-term therapy with systemic corticosteroids (332). In contrast, allergic asthma individuals have become sensitized to innocuous environmental antigens present in allergen such as house dust mite (HDM) feces, animal danders, fungal spores, pollen, or peanuts. The allergic feature can be assessed by a positive skin-prick test to the proteins of common allergens and/or the presence of specific serum immunoglobulin E (IgE). While the disease often starts with allergic sensitization during childhood, it is often associated with eczema and can later develop into allergic rhinitis and progress to asthma (332), and, children with multiple allergies during the early years of life have a higher risk to develop allergic asthma (333). However, clinical research including genome-wide expression studies as well as first biological therapies and animal models have challenged this traditional concept of dividing asthma into atopic and non-atopic forms, by exposing a much more complex and heterogeneous disease. In more recent studies, asthma phenotypes have been shown to be stratified into various asthma endotypes characterized by distinct immunopathology, genetic susceptibility, environmental risk factors, age, clinical presentation, prognosis and response to therapies that can offer new therapeutic opportunities for specific patient endotypes (332, 334-336).

1.6.3 Genetic, environmental and other risk factors

Asthma development is associated with strong genetic and environmental components. The progress in asthma genetics led to the identification of several susceptibility genes. However, the phenotypic impact of each of these genes is mild, although larger effects may occur when multiple variants interact with environmental factors. Asthma susceptibility genes can be categorized in four main groups: genes associated with innate immunity and immunoregulation, genes associated with Th2 cell differentiation and effector functions, genes associated with epithelial biology and mucosal immunity, and genes associated with lung function, airway remodeling and disease severity (337). As an example, allergic inflammation and IgE regulation were shown to be influenced by polymorphisms in the gene encoding Toll-like receptor (TLR)4, in genes that regulate Th2 differentiation and effector functions such as *GATA3, IL4,* and *IL13*, in genes that are expressed in epithelial cells such as *defensin beta 1*, and variants in genes that are associated with lung function, airway remodeling and disease severity including *TNF* and *TGFB1* (338-344).

Although genetic predisposition has an obvious impact, gene/environment interactions can explain more of the diversity in prevalence rates for allergy and asthma worldwide. In the past, a concept of 'hygiene hypothesis' (345) has been postulated to explain such variability. That hypothesis claimed that the decrease of the infectious burden in early childhood in western countries leads to an increased susceptibility for allergic diseases (345). However, nowadays it is clear that the term 'hygiene hypothesis' is incorrect and misleading and therefore should be modified (346-348). Rather, it is now well accepted that allergic diseases are not caused by improved hygiene including personal cleanliness, washing hands, keeping food clean and fresh, sanitizing the home, but more because the gut microbiome has changed considerably in developed countries e.g. due to increased use of antibiotics and reduced contact to pets. Instead of owning a great diversity of commensal bacteria, people from western countries start to show a reduced bacterial diversity, suggesting that early childhood microbial exposure provide a protection against allergic diseases (348). Moreover, a growing number of studies showed that children living in environments with a lot of traffic have increased risks of new-onset asthma, asthma symptoms, exacerbations, and asthma-related hospitalizations (349, 350) pointing toward detrimental effects of outdoor air pollutants, including ozone, nitrogen oxides, and respirable particulate matters on asthma (349, 351).

Finally, besides of genetic and environmental factors, prenatal risk factors, such as maternal smoking, diet and nutrition, stress, use of antibiotics and delivery by cesarean section may also affect the early development of allergic asthma (352-357). Risk factors for asthma in childhood or adulthood, may include infant feeding, allergic sensitization, tobacco smoke, exposure to animals, family size and structure, socio-economic status, antibiotics and infections (358-364).

In summary, rather than a unifying concept, various events ranging from the host's immune response, the level and variety of the environmental exposure, and the interactions between a genetic background and a range of exposures, act in concert eventually leading to the clinical manifestation of the complex syndrome of allergic asthma.

1.6.4 The anatomy and functions of the lung

The lung is the central organ for gas exchange. It provides oxygen to the blood and eliminates carbon dioxide from the blood into the surrounding to ensure an effective oxidative gain of energy. The function of the lung is reflected by its anatomy, which provides a maximal gas exchange, through a great number of bifurcations in the airways. The lung consists in lobes containing an interlobular septum (a wall, composed of connective tissue, which separates lobules from one another), a bronchiole and affiliated branches, and clusters of alveoli where the gas exchange takes place. In total, the lung comprises about 300-400 million alveoli with a total surface of 100 m^2. To ensure a fluent gas exchange, the blood circulation encages the lung, via a dense network of capillaries. Besides that crucial function, the lung displays also non-respiratory functions. In particular, it maintains an appropriate acid-base balance by regulating the respiratory frequency to keep a constant blood pH of 7.4, releases vasoactive substances in the blood, and produces substances used in the alveoli. Finally, it ensures an appropriate 'air-conditioning' of the airways by heating the inhaled air up to body temperature and humidifying it to prevent excessive dryness of the tissues and the mucus (365). Furthermore, lung establishes its own defense against inhaled foreign materials (particulate matter, pollen, carbon black or asbestos) or pathogens, via humoral (e.g. pulmonary surfactant) and cellular defense mechanisms (e.g. AMs, AECs).

Pulmonary surfactant is a complex lipid/protein interface lining the alveolar surface exerting two essential roles in respiratory functions. On the one hand, it plays a biophysical role by reducing surface tension at the air/liquid interface, facilitating gas exchange and alveolar stability, and, on the other hand, plays a role in the pulmonary immune system by maintaining sterility and balancing immune reactions in the distal airways (366). Pulmonary surfactant comprises 90% lipids and 10% proteins, the later encompass four surfactant proteins: (SP)-A, SP-B, SP-C, and SP-D. Besides of their role in surface tension, SP-A and SP-D bind to carbohydrate-structures on bacteria, fungi, and viruses, trigger their agglutination and promote their elimination by neutrophils and macrophages driven phagocytosis (367-374). Of note, abnormal surfactant levels and composition in human subjects or genetic variation/deletion of surfactant protein genes have been associated with respiratory dysfunction and inflammation (375-379).

1.6.5 The immunology of allergic asthma

The actual concept of allergic asthma development involves the activation of airway epithelial cells by environmental physical or molecular stimuli. The epithelial mucosa responds by producing alarmins and various other chemokine and growth factors. However, although that is a part of the normal response of the lung mucosa, in susceptible individuals it initiates a pathogenic cascade of events leading to airway inflammation. Susceptible individuals may have preexisting atopy, specific genetic risk factors or other less well-understood vulnerabilities. Furthermore, allergic asthma-driven inflammation can be subdivided into three phases: allergen sensitization, the effector phase and resolution of allergic airway inflammation (see Figure 1.5).

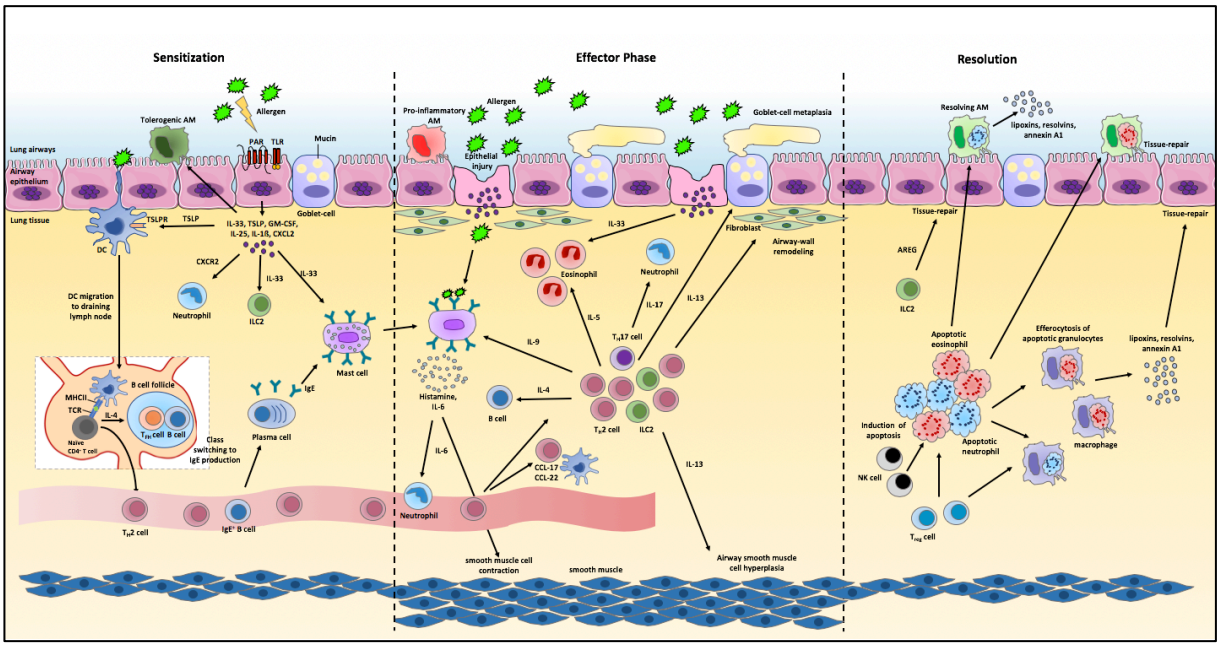

Figure 1.5 Three phases of allergic asthma. Sensitization. Immunological reaction to the first allergen contact. **Effector phase.** Immunological response to prolonged or repetitive exposure to allergens. **Resolution.** Resolution of airway inflammation.

Allergen sensitization

The airway epithelial cell layer is a physical barrier and make up the first line of defense against inhaled pathogens and other environmental stimuli. However, epithelial cells express also PRRs such as TLRs and protease-activated receptors (PARs), which recognize microbial patterns and allergens (380-383). Allergen contact activates non-ciliated epithelial cells through in particular TLR4, and PARs, both inducing nuclear factor κB (NF-κB) stabilization, nuclear translocation and finally pro-inflammatory response (383-385). In addition, physical damages and/or insults of the mucosal epithelium trigger the release of alarmins such as IL-33, IL-25, IL-1ß, thymic stromal lymphopoietin (TSLP). Further, activated airway epithelial cells secrete growth factors such as GM-CSF, chemokines as CCL-17, CCL-20, CXCL2, and endogenous danger molecules (i.e. high-mobility group box 1, uric acid, adenosine triphosphate)

(383, 386, 387). This cascade of events leads to the recruitment and activation of neutrophils, macrophages, mast cells, type 2 innate lymphoid cells (ILC2s), and pulmonary dendritic cells (DCs) in the airways (332, 388).

In this context, ILC2s play a critical role in priming a local type 2 immune response to allergens, including the recruitment of eosinophils, Th2 cytokine production and serum IgE levels (389). Moreover, recruitment of activated neutrophils facilitates allergic sensitization and airway inflammation through ROS generation, by induction of proinflammatory cytokines, matrix metalloproteinase 9 (MMP-9), and MUC5AC (390-394). Pulmonary mucosal DCs comprise 4 different lung DC populations, $CD103^+$ conventional (c)DCs, $CD11b^+$ cDCs, few monocyte-derived (mo)DCs and plasmacytoid DCs (pDCs). They are located in the basolateral space, only separated from the inhaled air by the epithelium tight-junction barrier. Those DCs, mostly the $CD11b^+$ subset, can extend their dendrites between epithelial cells directly into the airway lumen (395), although their 'periscope' function does not enable them to capture fluorescently labeled antigens after antigen administration to the airways in the steady state (396). Alternatively, the allergen can penetrate the underlying lamina propria of the mucosal surface through allergen-induced cleavage of tight junctions (387). Release of TSLP by epithelial cells leads to the maturation of pulmonary $CD11b^+$ DCs, induces their expression of OX40 ligand (OX40L) and promotes their mobilization to the local draining lymph nodes where they present processed antigen via MHCII and co-stimulatory molecules to naïve $CD4^+$ T cells and activate them to an IL-4-competent state (397-399). Then, the presence of IL-4 mediates the activation and nuclear translocation of the signal transducer and activator of transcription 6 (STAT6) factor. Following, STAT6 induces the expression of GATA3, a key transcription factor for Th2 differentiation, and therefore accelerate the maturation of T cells toward the Th2 phenotype (400-404). In addition, IL-4-competent T cells migrate to the B cell zones of the lymph node, where they differentiate into Tfh cells. In the parafollicular B cell areas, the Tfh-dependent IL-4 causes class-switching of the B cells into IgE producing B cells (1, 388). Subsequently, IgE^+ B cells migrate via the blood to the peripheral tissue where they transform into IgE-producing plasma cells, secreting antigen-specific IgE antibodies and sensitizing mast cells and other effector cells through binding to Fcε receptor I (FcεRI) present on their surface. In addition, besides of the development of a Th2 immune response, it has been shown that the development of Th17 cells is associated with severe forms of allergic asthma (405-407). Such Th17 cells arise when instead of IL-4, cytokines such as IL-6, IL-1ß, TGF-β and IL-23 are present. The development toward a Th17 phenotype involves the production of IL-21 by the T cell itself, which acts in an autocrine manner to activate STAT3. Furthermore, the signature transcription factor expressed by differentiated Th17 cells is RORγT, which drives the expression of characteristic Th17 cell-derived cytokines of the IL-17 family (1).

Effector phase of allergic asthma

Upon re-exposure to the original or a cross-reactive antigen, the allergen causes crosslinking of adjacent FcεRI-bound IgE at the surface of sensitized mast cells leading to the aggregation of surface FcεRI. Within minutes of antigen exposure, mast cells secrete biologically active products from their cytoplasmic granules, like histamine and serotonin, proteases such as tryptase and chymase and proteoglycans, as well as newly formed lipid-derived mediators such as PGD2, LTB_4, LTC_4, LTD_4 and LTE_4 and additional cytokines (408, 409). These mediators induce an immediate hypersensitivity reaction, characterized by increased vascular permeability, contraction of the airway smooth muscle and enhanced secretion of mucus, resulting in an acute breathlessness and wheezing (410-414).

Parallel to that immediate mast cell-driven immune response, repeated allergen exposure enforces an inappropriate Th2/Th17-adaptive immune response (415-418). Indeed, allergen exposure disrupts the epithelial cell barrier, in turn leading to the release of alarmins, among which IL-33, which recruit eosinophils to the site of inflammation and trigger ILC2s and Th2 cells to release the characteristic Th2-derived cytokines IL-4, IL-5, and IL-13 (388, 419, 420). Whereas IL-4 is important for class-switching of B cells, IL-13 contributes to airway remodeling via airway smooth muscle cell hyperplasia and to goblet-cell metaplasia (421). Moreover, the release of IL-5 by Th2 cells and ILC2s mediates the recruitment and accumulation of eosinophils (422). Recruited eosinophils carry a range of highly toxic granule proteins (i.e., major basic protein, eosinophil cationic protein, eosinophil-derived neurotoxin) and free radicals (423, 424), thus are well equipped to kill microorganisms and parasites. Furthermore, activated eosinophils release lipid mediators (i.e., prostaglandins, leukotrienes) and cytokines (i.e., IL-3, IL-5, CSF-2), amplifying the inflammatory response by activating epithelial cells and driving a positive feedback loop in recruitment and activation of additional leukocytes. Moreover, eosinophils secrete proteins involved in airway tissue remodeling (i.e., eosinophil collagenase, matrix metalloproteinase-9) (422, 425, 426). In addition to eosinophils, mast cells, in humans, play also a role in the chronic allergic inflammation through the secretion of diverse cytokines, chemokines and growth factors that lead to the recruitment of immune cells (e.g. TNF-α, LTB_4, IL-8, IL-6, CCL2). In addition, IL-4, IL-5, IL-13 and TGF-ß have the potential to influence airway remodeling (420, 427-429). Finally, upon allergen exposure $CD11c^+$ DCs secrete large amounts of chemokines CCL17 and CCL22, which attract additional effector T cells to the site of inflammation and lead to their accumulation (430).

Besides of the Th2 immune response, in severe asthma phenotypes, Th17 cells have been shown to play a major role, increasing neutrophil recruitment and release of Th17 cytokines such as IL-17A, IL-17F, and IL-22. Binding of IL-17A to the IL-17 receptor (IL-17R) complex on airway epithelial cells, leads to an increased NF-κB activation and the secretion of neutrophil chemokines, including CXCL8 (431). In addition, Th17 cytokines also induce mucus cell hyperplasia and have pleotropic effects on airway smooth muscle cells resulting in airway narrowing (432).

Finally, chronic airway inflammation including all immunological processes described above, lead to changes in the epithelium, including an increased number of goblet cells, increased production of cytokines and chemokines as well as epithelial cell injury. This in turn causes inflammation of the submucosa, including the development of increased deposition of extracellular matrix (ECM) molecules in the lamina reticularis (beneath the epithelial basement membrane), changes in fibroblasts, increased development of myofibroblasts and increased vascularity (420).

In summary, induced prolonged or repetitive exposure to specific allergens causes persistent airway inflammation which is typically characterized by the presence of large numbers of innate and adaptive immune cells at the affected site and also by substantial changes in the ECM and alterations in the number, phenotype and function of structural cells in the affected tissue causing the typical asthmatic symptoms like coughing, wheezing, bronchial hyperreactivity and breathlessness.

Resolution of airway inflammation

Resolution of acute inflammation consists, in the lung, to promote the clearance of inflammatory leukocytes, the restoration of the epithelial barrier integrity and function as well as to dampen the bronchial hyperreactivity. Until recently, it was thought to be a passive process, but recent compiling evidences showed that resolution of inflammation involves active biochemical programs that enable inflamed tissues to return to homeostasis.

To dampen the inflammatory response, the synthesis of pro-inflammatory mediators is terminated. This process is regulated by class switching of granulocytes that produce pro-inflammatory arachidonic acid-derived eicosanoids from prostaglandins and leukotrienes during inflammation to the production of lipoxins that prevent pro-inflammatory cytokine release (433). Further, to limit granulocytes accumulation, chemokine gradients are normalized (434), and local granulocytes undergo programmed cell death (apoptosis) leading to their clearance by phagocytic macrophages. This process, named efferocytosis, is of particular importance for the clearance of eosinophils in the airways, and a substantial cellular mechanism of airway resolution in asthmatic patients. Indeed, delayed eosinophilic clearance induces secondary necrosis and subsequent release of toxic cellular contents resulting in tissue damage and persisting inflammation (435, 436). Mechanistically, the granulocyte apoptosis is triggered either by humoral factors such as Fas ligand (Fas-L), TNF-α and TNF-related apoptosis-inducing ligand (TRAIL) (155) or cellular factors like natural killer (NK) and Treg cells. Indeed, NK cells have been shown to play a role in resolution of inflammation by directly interacting with eosinophils and triggering their apoptosis (437, 438). Similarly, Treg cells stimulate the apoptosis of neutrophils and enhance the efferocytosis capacity of macrophages (439). In response, macrophages release anti-inflammatory cytokines like TGF-β and IL-10 and different growth factors during efferocytosis of granulocytes (440, 441).

Besides efferocytosis, pro-resolving mediators are produced and released by macrophages, ILC2s and Treg cells in order to restrain inflammation (434, 440, 442). Thus, various pro-resolving mediators have been identified including specialized lipid mediators (SPMs) (like lipoxins, resolvins, protectins, maresins) and proteins (like annexin A1). In contrast to anti-inflammatory mediators like IL-10 and TGF-ß, pro-resolving mediators are not immunosuppressive but rather tissue protective and reparative. They promote key cellular steps of resolution by the recruitment of monocytes, induction of granulocyte apoptosis and enhancement of macrophage efferocytosis. Moreover, they induce a switch of macrophages from a pro-inflammatory M1 towards a pro-resolving M2 phenotype. Finally, resolvins promote the return of non-apoptotic cells to the lymphatics and blood vessels, and stimulate tissue regeneration to restore epithelial barrier integrity (434, 443, 444).

Nowadays, there is increasing evidence that chronic, uncontrolled inflammation and airway remodeling in asthma does not only result from an increased or repetitive exposure of allergens but in addition from an uncontrolled, insufficient resolution of airway inflammation. Indeed, it has been shown that asthmatic patients with severe and uncontrolled asthma showed decreased levels of counter-regulatory and pro-resolving lipid mediators together with a defect in the expression of the related biosynthetic genes and receptors in relation to patients with moderate asthma (445-447). Furthermore, pathological changes of chronic asthma have been associated with a disruption of leukocyte apoptosis, in particular eosinophils, together with an insufficient efferocytosis of airway macrophages, which correlated with asthma severity (448-451). Defects in apoptotic cell phagocytosis results in the persistence of inflammation in asthmatic patients not just through secondary cell necrosis, but also through a diminished release of pro-resolving, counter-regulatory mediators that are usually released during efferocytosis by alveolar macrophages (452). Moreover, gene expression studies of bronchial epithelial cells in individuals with asthma showed a marked decrease in genes linked to epithelial growth and repair in patients with severe asthma (453).

Therefore, investigating the mechanisms of resolution of airway inflammation is a new and important research area, since it opens new windows to understand disease pathogenesis and enables the design of new therapeutic approaches for the treatment of asthma patients (434).

1.6.6 Role of complement system in allergic asthma

The complement system provides a key role in linking innate and adaptive immunity. In addition, allergic asthma development is a complex interplay between innate and adaptive immune cells. Many symptoms of asthma exacerbations such as smooth muscle contraction, mucus hypersecretion, and recruitment of inflammatory cells are consistent with reported effects of the anaphylatoxins C3a and C5a (1). In particular, C3a stimulates the release of histamine and leukotrienes from mast cells, and both C3a and C5a have been shown to induce the degranulation of eosinophils (454, 455). Therefore,

their strong biologic activity, early generation, and their overall pattern of action suggest that C3a and C5a, could play an important role in the pathophysiology of allergic asthma. In addition, various publications have shown that complement components, in particular C3a and C5a, are increased in BAL and serum of asthma patients and are associated with asthma severity (456-460), while several allergens triggering asthma are also able to induce complement activation (461-464).

However, besides of the anaphylatoxins, other components of the complement system such as MBL from the lectin pathway, C1q from the classical pathway, and Factor B and H from the alternative pathway, have been shown to be involved in allergic asthma. Indeed, serum MBL levels were significantly higher in a study of asthmatic children than in healthy controls (465). Furthermore, high MBL levels in serum of asthmatic children positively correlated with peripheral blood eosinophils (465, 466). Moreover, MBL levels in both adults and children have been associated with allergic asthma severity (467). In addition, polymorphisms of MBL have been shown to contribute to elevated plasma MBL levels and activity, and increased susceptibility to asthma (466, 468). Besides of the lectin pathway, massive local alternative pathway activation by both Factor B and Factor H have been demonstrated to play a critical role in the development of an allergen-induced AHR and airway inflammation during the sensitization and effector phase of allergic asthma (469, 470). In contrast, C1q has been shown to be a potent inhibitor of allergic inflammation. Released by regulatory dendritic cells, C1q can mediate a potent direct anti-inflammatory activity, independently of the capacity of DCs to expand Treg cells. Interestingly, C1q was as potent as dexamethasone in reducing AHR, eosinophil, and ILC2 infiltrates in BAL, as well as allergen-specific Th2 cells in the lungs (471).

As described above, the complement system is usually activated via three canonical pathways (Figure 1.4). However, anaphylatoxin generation in the airways can occur via multiple mechanisms (472). Carbohydrate structures on allergens can be recognized by PRRs and activates the mannose-binding lectin pathway of the complement cascade. Similar, macromolecular structures from the dust mite, fungii, or ragweed allergen may be recognized by the alternative pathway and activate complement directly. In addition, anaphylatoxins can be generated besides of the three pathways of complement activation. C3 and C5 can be cleaved by proteases (like trypsin, thrombin, elastase) that are released from mast cells and other inflammatory cells in the lung as a consequence of IgE-mediated degranulation (472). Furthermore, probably the most important mechanism of anaphylatoxin production comes from exogenous proteases derived from allergens (such as *Der p3* and *Der f3* from *Dermatophagoides* ssp.) that have been shown to directly cleave C3 and C5 into their active fragments C3a and C5a (473). Moreover, Th2-derived IL-4 has been shown to increase the production of C3 by alveolar epithelial cells (474). Finally, besides of the allergen-derived proteases, properdin (Complement Factor P, CFP), a positive alternative pathway complement regulator (see 1.4.2), has been shown to contribute to allergic airway inflammation through the local production of C3a. It has

been demonstrated that allergen challenge caused properdin release into the airways of asthmatic patients, and properdin levels correlated positively with proinflammatory cytokines in human BAL and OVA-sensitized and challenged mice. In addition, Properdin-deficient mice showed markedly reduced total and eosinophil cell counts in BAL and reduced AHR to methacholine compared to WT mice (475).

Role of anaphylatoxins and their receptors in allergic asthma

To enroll the influence of the anaphylatoxins on the development and severity of allergic asthma, the role of C3a and C5a and their cognate receptors during the sensitization and the effector phase has to be evaluated independently.

Various studies have shown the protective effect of the C5a/C5aR1 signaling axis during allergen sensitization using C5- and C5aR1-deficient *in vivo* models or by direct pharmacological targeting of C5aR1 during initial allergen exposure. Thereby, ablation of C5 or C5aR1 led to excessive airway inflammation and Th2/Th17 immune responses associated with an increased allergic phenotype regarding AHR, airway inflammation and mucus production (259, 407, 456, 476, 477). The increased allergic phenotype was linked to an increased frequency of pro-inflammatory $CD11b^+$ conventional (c)DCs and a decreased frequency of tolerogenic plasmacytoid (p)DCs (259). In addition, pulmonary DCs from C5aR1-targeted mice produced increased levels of the chemokines CCL17 and CCL22 *ex vivo*, suggesting a negative impact of C5aR1 signaling on pulmonary homing of Th2 cells (259). Moreover, it has been shown that the protective role of C5a during sensitization was mediated by the modulation of the co-stimulatory molecules programmed death ligand 1 (PD-L1, B7-H1) and PD-L2 (B7-DC) on pDCs (478). In contrast, local targeting of C5aR1 in an established allergic asthma environment revealed a pro-allergic role of the C5a/C5aR1 signaling axis. Further, C5aR1 targeting was associated with a reduced airway inflammation and AHR although still associated with an increased production of Th2 effector cytokines (259). Altogether, these data show the protective effect of C5a/C5aR1 during allergen sensitization and its pro-allergic effect during the effector phase of allergic asthma.

Intriguingly, in a study where C5a/C5aR1 function in DCs on the allergic asthma development was specifically addressed, intratracheal (i.t.) adoptive transfer of *in vitro* generated and allergen-pulsed C5aR1-deficient bone marrow-derived (BM)DCs into WT recipient mice, rechallenge failed to reproduce the protective effect of the C5a/C5aR1 axis during early asthma development. Indeed, the disease phenotype showed a reduced Th2/Th17 maladaptive immunity associated with reduced airway hyperresponsiveness, mucus production, and airway inflammation (479-481). Such conflicting results may derive from the use of a BMDC culture, which is recognized to be a heterogeneous population comprising not only DCs, but in addition macrophages as well as MDSCs (481, 482). Moreover, BMDCs do not mirror the pulmonary DC compartment, which consist of the complex interplay between $CD11b^+$, $CD103^+$ cDCs, pDCs, and moDCs. Consequently, the regulatory impact of

C5a on BMDCs is now thought to be different of the pulmonary dendritic cells. In contrast to the C5a/C5aR1 signaling axis, the effects of C3a and C3aR on the asthma pathophysiology remain controversial. Indeed, while studies using C3 and C3aR-deficient animals revealed a strong pro-inflammatory effect on established allergic asthma by reduction of AHR and bronchoconstriction in these animals (407, 460, 478, 483-485), a potential role of the C3a/C3aR signaling axis during allergen sensitization has not been evaluated due to the lack of a reliable C3aR antagonist. Furthermore, intriguingly, only some, but not all studies showed the development of a Th2 immune response together with the induction of airway inflammation, mucus production, and IgE secretion. These effects may depend on the allergen, the species/strain and/or the method that has been used for immunization (478). In addition, similar to C5aR1, studies have shown a critical role of C3aR-mediated regulation of dendritic cells on antigen uptake, T-cell stimulation and driving Th2 cell proliferation (486, 487). Interestingly, targeting C5aR1 in C3aR-deficient mice during allergen sensitization reversed the protective effect leading to an enhanced Th2 cytokine production, airway inflammation, and airway responsiveness, suggesting that the reduced allergic phenotype in C3aR-deficient mice results from protective C5aR1 signaling (478). In contrast to the *in vivo* models, the adoptive transfer of *C3ar1*$^{-/-}$ BMDCs promoted a strong asthmatic phenotype associated with a marked airway resistance, strong Th2 cytokine and mucus production, as well as mixed eosinophilic and neutrophilic airway inflammation (480). Again, the conflicting result may derive from the use of a BMDC culture.

In contrast to the extensively investigated dual role of the C5a/C5aR1 axis, the functional role of C5aR2 *in vivo* remains enigmatic. Due to the uncoupling from G-proteins, C5aR2 was thought to be a non-signaling, decoy-receptor. However, first experiments with C5aR2-deficient mice in a model of immune complex injury of the lung exhibited both in histologic analysis of the BAL and tissue sections enhanced inflammation (488). In contrast, using C5L2-deficient mice in experimental allergic asthma models, showed a protection from the development of airway hyperresponsiveness, Th2 cytokine production, eosinophilic airway inflammation, serum IgE, and mucus production (277, 278). Interestingly, HDM-induced experimental asthma in these mice was associated with increased pulmonary IL-17A production and increased airway neutrophil numbers. However, in line with C3a/C3aR these results did not distinguish between the role in allergen sensitization and effector phase since an appropriate C5aR2 antagonist was missing. In addition and in contrast to the *in vivo* models, adoptive transfer of HDM-pulsed C5L2-deficient BMDCs into wild-type recipient mice induced strong Th2 cytokine production associated with marked IFN-ɣ and IL-17A production, decreased eosinophil numbers, and reduced IgE secretion as compared with HDM-pulsed BMDCs from wild-type mice (278). These finding suggest a complex role for C5L2 in the development of experimental allergic asthma.

1.6.7 Role of alveolar macrophages during asthma development

The role of alveolar macrophages in allergic asthma is diverse and complex. Alveolar macrophages have been described as tolerogenic, pro-inflammatory or pro-resolving AMs or as macrophages with an M1, M2, M2a or M2c phenotype (110, 489). However, to classify AMs just into one group or phenotype would be misleading. Therefore, it is important to regard their function and role in the three different phases of allergic asthma – allergen sensitization, effector phase and resolution – in order to characterize them properly (see Figure 1.6).

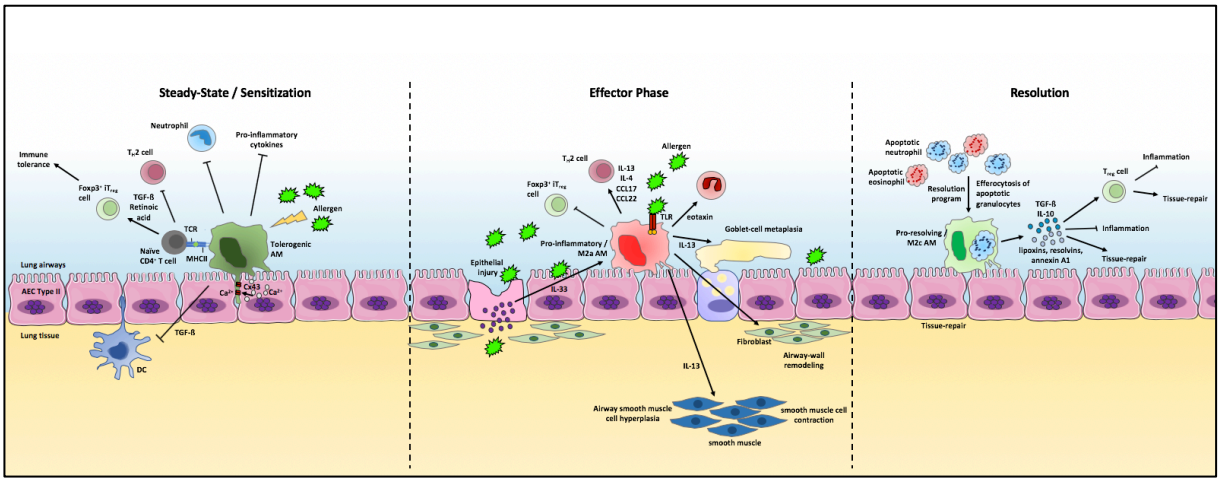

Figure 1.6 Role and function of alveolar macrophages in the three different phases of allergic asthma.

At steady-state, AMs maintain physiological homeostasis, phagocyte airborne pathogens and stimuli to keep environmental threats at bay. In addition, they play a key role in preserving tolerance. AMs produce TGF-ß which downregulates the antigen presenting cell function of pulmonary DCs and inhibits T cells activation (132). Moreover, they sample harmless airborne antigens, present them to antigen-specific $CD4^+$ T cells in the lung tissue and release TGF-ß and retinoic acid, which on the one hand inhibits a Th2 immune response and on the other hand leads to the generation of $Foxp3^+$ iTreg cells from naive $CD4^+$ T cells (133). In addition, it has been shown that a subset of AMs attached to the alveolar wall form connexin 43 (Cx43)-containing gap junction channels with the epithelium. Once inflammation occurs, these AMs establish a syncytial communication through synchronized Ca^{2+} waves, using the epithelium as the conducting pathway. This results in immune-suppression associated with inhibition of alveolar neutrophil recruitment and prevention of proinflammatory cytokine secretion (136).

However, once alveolar macrophages come in contact with harmless antigens that are mixed with allergens containing proteases and that are known to trigger TLR4 signaling (i.e., feces from house dust mites or *Aspergillus fumigatus*), AMs switch from a tolerogenic mode to an inflammatory mode

accompanied by a secretion of IL-1ß, IL-6 and TNFα (133). Moreover, antigen persistence leads to the release of the pro-inflammatory cytokine IL-33 by activated and disrupted epithelial cells (383). In addition, it is well appreciated that allergen leads to a Th2 immune response with production of IL-4 and IL-13 by Th2 cells and ILC2s. Both, IL-33 and Th2 cytokines leads to the activation of AMs and to a switch of their phenotype from a tolerogenic to a pro-inflammatory, M2a-phenotype (110, 489, 490). These activated AMs have been shown to secrete pro-inflammatory cytokines like IL-4, IL-13 and chemokines like CCL17, CCL22 and eotaxin (489, 490). Therefore, they promote persistent Th2 immune response, tissue remodeling, mucus hypersecretion, smooth muscle cell hyperplasia and mobilization and recruitment of inflammatory eosinophils to the lung. However, mouse models of HDM-mediated allergic inflammation and human asthmatics, have shown a mix in macrophage subtypes (491, 492), leading to an "unexpected" phenotype where typical type 1 cytokines (IFN-γ, TNF-α, and IL-12) coexist with a type 2 cytokines released by the M2a-phenotype during allergic asthma (493).

Nevertheless, once the active resolution program has been started, apoptotic granulocytes, in particular apoptotic eosinophils, leads to a switch in AMs from their pro-inflammatory phenotype back to their phagocytic function. Efferocytosis of apoptotic granulocytes leads to a pro-resolving, M2c-phenotype in AMs with the release of pro-resolving mediators like lipoxins, resolvins and annexin A1 and secretion of anti-inflammatory cytokines like TGF-ß and IL-10 that dampens inflammation, induces Treg cell proliferation, and inhibits Th2 differentiation. Of note, pro-resolving mediators interact with specific receptors on leukocytes and structural cells to blunt further inflammation, promote tissue repair and generally diminishes the disease (110, 434, 443, 444, 489).

In conclusion, AMs play a key role in the development, severity, but also resolution of allergic airway disease.

1.7 Aims

Despite the fact that AMs are the most important immune cells capable of taking up environmental stimuli and that they are a key player in either promoting or suppressing inflammatory responses in the airways, their roles in allergic asthma has been underestimated in the past and many gaps in knowledge about AMs remain to be filled by additional studies. In addition, although a lot of seminal work has been done studying functions of ATs and their cognate receptors in dendritic cells during sensitization and established asthma, no study so far investigated extensively their expression and their functions in AMs. Further insights in these topics will open opportunity for new therapeutic strategies of allergic asthma and may also be applicable to other allergic and pulmonary diseases (493).

Central Hypothesis

"Changes in anaphylatoxin receptors expression levels impact alveolar macrophages functions during the severity of allergic asthma"

- Evaluating the steady state anaphylatoxin receptors expression profiles in various pulmonary leukocytes populations.
    - Defining the expression level of C3a receptor, C5a receptor 1 and C5a receptor 2 in alveolar macrophages.
    - Defining the expression level of C3a receptor in alveolar macrophages in comparison to other innate and adaptive immune cells of the lung.
    - Comparing the C3a receptor expression level in different macrophage populations.

- Delineating the role and functions of anaphylatoxin receptors, in particular C3aR, in alveolar macrophages during the development of experimental allergic asthma.
    - Defining the expression level of C3a receptor in relation to C5a receptor 1 in alveolar macrophages upon house dust mite-mediated allergic asthma.
    - Investigating of the C3a receptor expression profile in alveolar macrophages in comparison to other murine leukocytes upon allergic asthma development.
    - Determining the molecular mechanisms involved in the anaphylatoxin receptors expression in alveolar macrophages with special attention to C3a receptor.

- Identifying multinucleated pulmonary macrophages in experimental allergic asthma and delineating the role and function of C3aR in their formation
    - Identifying a multinucleated population of AMs in allergic asthma lungs
    - Developing an *in vitro* assay to study the molecular mechanisms involved in the formation of multinucleated macrophages
    - Evaluating the role of C3aR in multinucleation processes

2 Material, Equipment and Methods

2.1 Material

2.1.1 Chemicals

Table 2.1 Used chemicals.

Substance	Manufacturer
Acetyl-β-Methyl-Choline (Methacholine)	Sigma-Aldrich Chemie GmbH, Steinheim
Agarose, low melting point	Bio-Rad Laboratories GmbH, Munich
Aluminum potassium sulfate ($KAl(SO_4)_2$)	Merck, KGaA, Darmstadt
Alzane® 5% (Atipamezole hydrochloride)	Zoetis Deutschland GmbH, Berlin
Amersham ECL Prime Western Blotting Detection Reagent	GE Healthcare Life Science
Ammonium chloride (NH_4Cl)	Sigma-Aldrich Chemie GmbH, Steinheim
Aqua ad injectabilia	B. Braun Melsungen AG, Melsungen
BD FACS Flow Sheath Fluid	BD Biosciences Europe, Erembodegem, Belgium
β-Mercaptoethanol	Sigma-Aldrich Chemie GmbH, Steinheim
BLOTTO low-fat dry milk	Rockland Immunochemicals, Pennsylvania, USA
Bovine serum albumin (BSA)	Sigma-Aldrich Chemie GmbH, Steinheim
C3a, human, recombinant	Hycult Biotech, Uden, Netherlands
C5a, human, recombinant	Hycult Biotech, Uden, Netherlands
Chloroform	Fisher Scientific BP1145-1
Citric acid, crystalline	Merck, KGaA, Darmstadt
Compensation beads (anti rat/hamster)	BD Biosciences Europe, Erembodegem, Belgium
CSF-2 (GM-CSF), recombinant murine	Peprotech Corporation, Rocky Hill, USA
Deoxynucleotide triphosphate (dNTP) mix	Life technologies Corporation, Carlsbad, USA
Dimethyl sulfoxide (DMSO)	Sigma-Aldrich Chemie GmbH, Steinheim
Dithiothreitol (DTT)	Life technologies Corporation, Carlsbad, USA
DNase I from bovine pancreas	Sigma-Aldrich Chemie GmbH, Steinheim
Dorbene vet® 1% (Medetomidine hydrochloride)	Zoetis Deutschland GmbH, Berlin
Dulbecco's Phosphate Buffered Saline (D-PBS)	Life technologies Corporation, Carlsbad, USA
D(+)-saccharose	Carl Roth GmbH & Co. KG, Karlsruhe
Entellan®	Merck Millipore, Darmstadt
Eosin	Chroma Technology Corporation, Bellow Falls, USA
Esmeron® (Rocuronium bromide)	Organon, Oss, Niederlande
Ethanol, absolute	J. T. Baker, Deventer, Netherlands
Ethanol, 70% denaturated	Carl Roth GmbH & Co. KG, Karlsruhe

Ethanol, 96% denaturated	Carl Roth GmbH & Co. KG, Karlsruhe
Ethylenediaminetetraacetic acid (EDTA)	Sigma-Aldrich Chemie GmbH, Steinheim
Fetal calf serum (FCS) (Lot A04304-0413)	PAA Laboratories GmbH, Pasching, Östereich
5x First Strand Buffer	Life technologies Corporation, Carlsbad, USA
Formaldehyde solution, 37%	Sigma-Aldrich Chemie GmbH, Steinheim
Fluoroshield™ histology mounting medium	Sigma-Aldrich Chemie GmbH, Steinheim
Fluo-4, AM, cell permeant	Invitrogen, Paisley, UK
Giemsa solution	Sigma-Aldrich Chemie GmbH, Steinheim
Glycogen	Life technologies Corporation, Carlsbad, USA
Glycine	Merck Millipore, Darmstadt
Hydrochloric acid, 25%	Merck KGaA, Darmstadt
Hank's Balanced Salt Solution (HBSS) with $CaCl_2$ and $MgCl_2$ / without $CaCl_2$ and $MgCl_2$	Life technologies Corporation, Carlsbad, USA
HEPES 1M	Life technologies Corporation, Carlsbad, USA
Hematoxylin	Chroma Technology Corporation, Bellow Falls, USA
Heparin natrium 25000	Ratiopharm GmbH, Ulm
House dust mite extract (lot 262538)	Greerlabs Laboratories Inc., Lenoir, USA
Interleukin 33 (IL-33), mouse, recombinant	eBioscience, Vienna, Austria
Interleukin 13 (IL-13), mouse, recombinant	eBioscience, Vienna, Austria
Interleukin 5 (IL-5), mouse, recombinant	Peprotech Corporation, Rocky Hill, USA
Isopropanol	Otto Fishar GmbH & Ko. KG, Saarbrücken
Kaleidoscope™ Prestained Standards	Bio-Rad Laboratories GmbH, Munich
Ketamine hydrochloride	Sigma-Aldrich Chemie GmbH, Steinheim
Ketavet 2% (Ketamin hydrochloride)	Pfizer Deutschland GmbH, Berlin
4x Laemmli Sample Buffer	Bio-Rad Laboratories GmbH, Munich
L-glutamine (200 mM concentrate)	Life technologies Corporation, Carlsbad, USA
Liberase™ TL Research Grade	Roche Diagnostics International AG, Rotkreuz, Switzerland
Macs® BSA stock solution	Milteny Biotec GmbH, Bergisch Gladbach
May-Grünwald solution	Sigma-Aldrich Chemie GmbH, Steinheim
Mini-PROTEAN®TGX™ Precast Protein Gel 4-15%	Bio-Rad Laboratories GmbH, Munich
Mowiol 4-88	Hoechst AG, Frankfurt
Nuclease-free water	Qiagen, Venlo, Netherlands
Penicillin-Streptomycin, 100x Liquid	Life technologies Corporation, Carlsbad, USA
Potassium bicarbonate ($KHCO_3$)	Sigma-Aldrich Chemie GmbH, Steinheim
RNAse inhibitor	New England Biolabs, Ipswich, USA
Rompun vet. (Xylazine hydrochloride 10%)	Bayer AG, Leverkusen
RPMI 1640	Life technologies Corporation, Carlsbad, USA
Sodium chloride	Sigma-Aldrich Chemie GmbH, Steinheim

Sodium chloride, 0.9%	Berlin-Chemie AG, Berlin
Sodium dihydrogen phosphate (Na_2H2PO_4)	Sigma-Aldrich Chemie GmbH, Steinheim
Sodium dodecyl sulfate	Sigma-Aldrich Chemie GmbH, Steinheim
Sodium hydrogen phosphate (Na_2HPO_4)	Sigma-Aldrich Chemie GmbH, Steinheim
Sodium iodate ($NaIO_3$)	Merck KGaA, Darmstadt
Sodium pyruvate	Life technologies Corporation, Carlsbad, USA
SYBR Green I	Bio-Rad Laboratories GmbH, Munich
SuperScript™ II RT	Life technologies Corporation, Carlsbad, USA
Trizma® base (Tris)	Sigma-Aldrich Chemie GmbH, Steinheim
Thioglycolate	Sigma-Aldrich Chemie GmbH, Steinheim
Trizol reagent®	Life technologies Corporation, Carlsbad, USA
Trypan blue	Life technologies Corporation, Carlsbad, USA
Tween 20	Sigma-Aldrich Chemie GmbH, Steinheim
VectaMount™	Vector Laboratories, Burlingame, USA
Xylazine	Sigma-Aldrich Chemie GmbH, Steinheim

2.1.2 Antibodies and compounds for flow cytometry, immunofluorescence staining and western immunoblot

Table 2.2 Antibodies used for flow cytometry, immunofluorescence staining and western immunoblot. APC = Allophycocyanin, AF = Alexa Fluor, BV = Brilliant Violet, Cy = Cyanin dye, eF = eFlour, FC = flow cytometry, FITC = Fluoresceinisothiocyanat, HRP = Horseradish peroxidase, IHC = Immunohistochemistry, PE = Phycoerythrin, PerCP = Peridinin chlorophyll protein, V = Violet, WB = Western blot.

Antibody	Clone	Label	Manufacturer	Isotype	Conc. mg/ml	Application	Dilution
anti-mouse B220	RA3-6B2	PE-Cy7	BD Biosciences Belgium	Rat IgG2a	0.2	FC	1:400
anti-mouse C3aR	14D4	–	Hycult Biotech, Netherlands	Rat IgG2a	0.1	FC, IHC	1:400
anti-mouse C3aR BSA free	14D4	–	Hycult Biotech, Netherlands	Rat IgG2a	1.89	FC, IHC	1:400
anti-mouse C3aR	H-300	–	Santa Cruz, USA	Rabbit IgG	0.2	WB	1:2000
anti-mouse C3aR	D-12	–	SantaCruz, USA	Mouse IgG2a	0.2	FC, WB	1:1000
anti-mouse C3aR	D-20	–	SantaCruz, USA	Goat IgG	0.2	FC, WB	1:1000
anti-mouse CCR2	47530	APC	R&D Systems	Rat IgG2b	100 Tests	FC	1:200
anti-mouse CD3	17A2	AF488	BioLegend, UK	Rat IgG2b	0.5	FC	1:400
anti-mouse CD3e	145-2C11	eF450	eBioscience, Austria	Hamster IgG	0.2	FC	1:300
anti-mouse CD4	RM4-5	PE-Cy7	eBioscience, Austria	Rat IgG2a	0.2	FC	1:400
anti-mouse CD4	RM4-5	V450	BD Biosciences Belgium	Rat IgG2a	0.2	FC	1:400

anti-mouse CD11b	M1/70	BV510	BioLegend, UK	Rat IgG2b	0.2	FC	1:800
anti-mouse CD11b	M1/70	AF700	eBioscience, Austria	Rat IgG2b	0.2	FC	1:800
anti-mouse CD11c	N418	APC	eBioscience, Austria	Hamster IgG	0.2	FC, IHC	1:800
anti-mouse CD11c	N418	FITC	eBioscience, Austria	Hamster IgG	0.5	FC, IHC	1:800
anti-mouse CD11c	N418	APC-Cy7	eBioscience, Austria	Hamster IgG	0.2	FC	1:800
anti-mouse CD16/32	93	–	eBioscience, Austria	Rat IgG2a	0.1	FC	1:100
anti-mouse CD19	ID3	eF450	eBioscience, Austria	Rat IgG2a	0.2	FC	1:300
anti-mouse CD25	PC61.5	PE-Cy7	BioLegend, UK	Rat IgG1	0.2	FC	1:400
anti-mouse CD45	30-F11	APC	BioLegend, UK	Rat IgG2b	0.2	FC	1:400
anti-mouse CD49b	DX5	eF450	eBioscience, Austria	Rat IgM	0.2	FC	1:300
anti-mouse CD64	X54-5/7.1	PE	BioLegend, UK	Mouse IgG1	0.2	FC	1:800
anti-mouse CD64	X54-5/7.1	BV711	BioLegend, UK	Mouse IgG1	0.5	FC	1:800
anti-mouse CD64	X54-5/7.1	FITC	BioLegend, UK	Mouse IgG1	0.5	FC	1:800
anti-mouse CD88	20/70	APC	BioLegend, UK	Rat IgG2b	0.2	FC	1:800
anti-mouse CD88	20/70	PE-Cy7	BioLegend, UK	Rat IgG2b	0.2	FC	1:400
anti-mouse CD90.2	30-H12	FITC	BD Biosciences Belgium	Rat LOU	0.5	FC	1:400
anti-mouse CD103	2E7	PerCP-Cy5.5	BioLegend, UK	Hamster IgG	0.2	FC	1:800
anti-mouse CD115	AFS98	BV711	BioLegend, UK	Rat IgG2a	0.2	FC	1:400
anti-mouse CD127	A7R34	PE-Cy5	eBioscience, Austria	Rat IgG2a	0.2	FC	1:400
anti-mouse F4/80	BM8	BV510	BioLegend, UK	Rat IgG2a	0.2	FC	1:400
anti-mouse F4/80	BM8	BV421	BioLegend, UK	Rat IgG2a	0.2	FC	1:400
anti-mouse IgG	–	HRP	JacksonImmuno Research, UK	IgG	–	WB	1:2500
anti-mouse Ly6C	AL-21	PE-Cy7	BD Biosciences Belgium	Rat IgM	0.2	FC	1:800
anti-mouse Ly6G	1A8	V450	BD Biosciences, Belgium	Rat IgG2a	0.2	FC	1:300
anti-mouse Ly6G	1A8	PE	BD Biosciences, Belgium	Rat IgG2a	0.2	FC	1:400
anti-mouse Ly6G	1A8	FITC	BD Biosciences Belgium	Rat IgG2a	0.5	FC	1:400
anti-mouse MerTK	DS5MMER	PE-Cy7	eBioscience, Austria	Rat IgG2a	0.2	FC	1:400
anti-mouse MHCII	M5/114.15.2	FITC	BioLegend, UK	Rat IgG2b	0.5	FC	1:1500
anti-mouse MHCII	M5/114.15.2	APC-eF780	eBioscience, Austria	Rat IgG2b	0.2	FC, IHC	1:1500
anti-mouse NKp46	29A1.4	FITC	eBioscience, Austria	Rat IgG2a	0.5	FC	1:400

anti-mouse pERK1/2	20A	AF647	BD Biosciences Belgium	Mouse IgG1	5 µl /Test	FC	–
anti-mouse SiglecF	E50-2440	BV421	BD Biosciences Belgium	Rat IgG2a	0.2	FC	1:300
anti-rabbit IgG-HRP	–	HRP	JacksonImmuno Research, UK	IgG	–	WB	1:2500
anti-rat $F(ab')_2$	ab150151	AF647	Abcam, Berlin	Rat IgG	2.0	FC, IHC	1:1500
DsRed	–	–	Takara Biotech, USA	–	–	WB	1:1000

Table 2.3 Compounds used for flow cytometry, immunofluorescence staining and western immunoblot. AF = Alexa Fluor, Conc. = concentration, DAPI=4',6-diamidino-2-phenylindole, eF = eFlour, FC = flow cytometry, Fix= fixable, IHC = Immunohistochemistry, WB = Western blot, WGA= Wheat Germ Agglutinin.

Compound	Label	Manufacturer	Conc. mg/ml	Application	Dilution
DAPI	–	Invitrogen, Paisley, UK	5.0	IHC	1:500
Fixable Viability Dye	APC-eF780	eBioscience, Vienna, Austria	–	FC	1:1500
Fixable Viability Dye	eF506	eBioscience, Vienna, Austria	–	FC	1:1000
WGA	AF488	Invitrogen, Paisley, UK	1.0	IHC	1:100

2.1.3 Primer

Table 2.4 Used primers with the appropriate annealing temperature. All primers were manufactured by Eurofins Product Service GmbH, Reichenwalde. Declared are the sequences of forward and reverse primers as well as their used annealing temperatures.

Gene	Sequence	Annealing temperature
Arg1	5'-CATGAGCTCCAAGCCAAAGT-3' 5'-TTTTTCCAGCAGACCAGCTT-3'	55°C
C3ar1	5'-TCGATGCTGACACCAATTCAA-3' 5'-TCCCAATAGACAAGTGAGACCAA-3'	60°C
C5ar1	5'-TTCCTGCTGGTGTTCAAG-3' 5'-CTGAGTAGAAGTCCTTATATGC-3'	55°C
Ccr2	5'-ATCCACGGCATACTATCAACATC-3' 5'-CAAGGCTCACCATCATCGTAG-3'	64°C
Nos2	5'-AGCCAAGCCCTCACCTAC-3' 5'-AATCTCTGCCTATCCGTC-3'	54°C
S14	5'-GAGGAGTCTGGAGACGACGA-3' 5'-TGGCAGACACCAAACACATT-3'	60°C

2.1.4 Consumables

Table 2.5 Consumables.

Material	Manufacturer
BD Microtainer tube	BD Biosciences Europe, Erembodegem, Belgium
Falcon® cell strainer 40 µm, 100 µm	Corning Incorporated, New York, USA
ELISA-reservoir 25 ml	VWR International GmbH, Darmstadt
FACS tube 75x12mm	Sarstedt AD & Co., Nümbrecht
FACS polystyrene round-bottom tube 75x12mm	Corning Incorporated, New York, USA
Filtertip 10 µl, 100 µl, 1000 µl	Sarstedt AD & Co., Nümbrecht
gentleMACS™ tube	Milteny Biotec GmbH, Bergisch Gladbach
Microscope slide76x26 mm	Gerhard Menzel GmbH, Braunschweig
MACS Separation LS Column	Milteny Biotec GmbH, Bergisch Gladbach
Micro tube 0.5 ml; 1.5 ml; 2 ml	Sarstedt AD & Co., Nümbrecht
Microseal® 'B' PCR plate sealing film	Bio-Rad Laboratories GmbH, Munich
Multiplate™ 96-well PCR plate, low profile	Bio-Rad Laboratories GmbH, Munich
Needle BD Microlance™ 3 26G 0.45x13 mm	BD Biosciences Europe, Erembodegem, Belgium
Needle BD Blunt Fill Needle 18G 1.2x40 mm	BD Biosciences Europe, Erembodegem, Belgium
Nitrile Powder-Free Examination Gloves	Ansell Healthcare GmbH, Munich
Petri dish 60x15 mm	Greiner Bio-One GmbH, Frickenhausen
Permanox slide sterile 8-well with cover	Thermo Fisher Scientific, Waltham, USA
Pipette tip 10 µl, 100 µl, 1000 µl	Sarstedt AD & Co., Nümbrecht
Pipette with tip 5 ml, 10 ml, 25 ml	Greiner Bio-One GmbH, Frickenhausen
Plate 6 well	Sarstedt AD & Co., Nümbrecht
Plate 24 well	Sarstedt AD & Co., Nümbrecht
Plate 96 well (U bottom)	Greiner Bio-One GmbH, Frickenhausen
Protein LoBind Tube 1.5 ml	Eppendorf AG, Hamburg
Protran® Nitrocellulose transfer membrane, 0.45 µm	Schleicher & Schnell GmbH, Dassel
Pur-Zellin swab	Greiner Bio-One GmbH, Frickenhausen
Spatula	VWR International GmbH, Darmstadt
Single-use syringe 1 ml	B. Braun Melsungen AG, Melsungen
Syringe BD Discardit™ II 5 ml, 10 ml	BD Biosciences Europe, Erembodegem, Belgium
Tracheal cannula for mouse 1.2x45 mm	Hugo Sachs, March-Hugstetten
Tubes 5 ml, 15 ml, 50 ml	Sarstedt AD & Co., Nümbrecht
Tube stripe 0.2 ml	Bio-Rad Laboratories GmbH, Munich
Vasofix® Safety 18G 1.3x45 mm	B. Braun Melsungen AG, Melsungen
Weighing dish	Greiner Bio-One GmbH, Frickenhausen

2.1.5 Kits

Table 2.6 Kits.

Kit	Manufacturer
Foxp3 Intracellular staining kit	eBioscience, Vienna, Austria
LP dissociation kit	Milteny Biotec GmbH, Bergisch Gladbach
CD4+ T cell isolation kit, mouse	Milteny Biotec GmbH, Bergisch Gladbach
CellTrace™ CFSE Cell Proliferation Kit	Thermo Fisher Scientific, Waltham, USA
PKH26 Fluorescent Cell Linker Kit	Sigma-Aldrich Chemie GmbH, Steinheim
AF647™ antibody labeling kit	Invitrogen Corporation, Carlsbad, USA

2.1.6 Buffers and Solutions

Table 2.7 Buffers and solutions.

Buffer/Solution	Substance
Anesthetic 10x (BALB/c)	2% Xylazin 50 mg/ml Ketamin
Anesthetic 1x (BALB/c)	PBS 10% 10x anesthetic (Balb/c)
Anesthetic 1x (C57BL/6)	Sodium chloride, 0.9% 37.5 mg/kg Ketamin 0.375 mg/kg Meditomidine
Antagonist (C57BL/6)	Sodium chloride, 0.9% 18,75 mg/kg Atipamezole
Complete medium (lung cell isolation)	RPMI 1640 10% FCS, heat inactivated 100 Units/ml Penicillin 100 µg/ml Streptomycin 2mM L-Glutamine
Digestion solution (lamina propria dissociation)	HBSS (w) 5% FCS
DNAse I reconstitution	Sodium chloride, 0.9% 100 mg/ml DNAse I
Enzyme mix (lamina propria dissociation)	2.35 mL pre-heated digestion solution 100 µL Enzyme D 50 µL of Enzyme R 12.5 µL of Enzyme A
Fc-block buffer	anti-mouse CD16/32 antibody 1:100 dilution in flow buffer

Flow buffer/MACS buffer	PBS 0,5% MACS® BSA stock solution
Formalin solution, phosphate-buffered	900 ml dH_20 7.8 g Na_2HPO_4 1.87 g NaH_2PO_4 100 ml Formaldehyde stock solution (37%)
HBSS (w/o)	HBSS without $CaCl_2$ and $MgCl_2$ 10 mM HEPES
HBSS (w)	HBSS with $CaCl_2$ and $MgCl_2$ 10 mM HEPES
HDM reconstitution	Ampuwa® (Aqua ad injectabilia) 10 mg/ml protein
HDM (i.t. application)	PBS sterile 20% HDM reconstituted
HEPES-Ringer buffer	10 mM HEPES 136.4 mM NaCl 5.6 mM KCl 1 mM $MgCl_2$ 2.2 mM $CaCl_2$ 11 mM glucose pH 7.4
PBS20	PBS 20% FCS
Predigestion solution (lamina propria dissociation)	HBSS (w/o) 5mM EDTA 5% FCS 1 mM ß-Mercaptoethanol
Red blood cell lysis (RBCL) buffer	dH_20 155 mM NH_4Cl 10 mM $KHCO_3$ 0.1 mM EDTA pH 7.2 sterile
Re-stimulation medium	RPMI 1640 10% FBS, heat inactivated 100 Units/ml Penicillin 100 µg/ml Streptomycin 2 mM L-Glutamine 1 mM Sodium-Pyrovate 0.05 mM ß-mercaptoethanol
Saponin-based permeabilization buffer	PBS 20% FCS 0.2% Saponin

10x SDS running buffer	dH_20 0.25 M Tris 1.92 M glycine 0.1% SDS pH 8.3
1x SDS running buffer	dH_20 10% 10x SDS running buffer
5x Stimulation mix	PMA 250 ng/ml Ionomycin 2500 ng/ml Brefeldin 5x Monensin 5x
10x Transfer buffer	dH_20 0.25 M Tris 1.92 M glycine pH 8.3
1x Transfer buffer	dH_20 10% 10x Transfer buffer
Tris-buffered Saline (TBS)	dH_20 50mM Tris 150 mM NaCl adjust pH 7.6 with 1M HCl
TTBS	TBS 0.1 % Tween 20
TTBS-milk (western blot blocking buffer)	TTBS 5% BLOTTO
Wash medium (lung cell isolation)	RPMI 1640 10% FBS, heat-inactivated 100 Units/ml Penicillin 100 µg/ml Streptomycin 2 mM L-Glutamine 0.5 mg/ml DNAse I

2.1.7 Mouse strains

Table 2.8 Specification of used mouse strains.

Name	Strain	Official name (symbol)	Breeder
C5aR1$^{-/-}$	BALB/c	C5ar1^{tm1Cge}	Internal breeding, ISEF, AG Köhl, Lübeck, Germany
C3ar1$^{-/-}$	BALB/c	C3ar1^{tm1Cge}	Internal breeding, ISEF, AG Köhl, Lübeck, Germany
Ccr2$^{-/-}$	C57BL/6	Ccr2^{tm1Ifc}	Internal breeding, UC, Deepe Lab, Cincinnati, US

tdTomato-C3ar1$^{fl/fl}$	BALB/c	C3ar1^{tm1Jko}	Internal breeding, ISEF, AG Köhl, Lübeck, Germany
tdTomato-C5ar2$^{fl/+}$	C57BL/6	C5ar2^{tm1Jko}	Internal breeding, ISEF, AG Köhl, Lübeck, Germany
IL-13Ra1$^{-/-}$	BALB/c	Il13ra1^{tm1Twy}	Internal breeding, CCHMC, Lewkowich Lab, Cincinnati, USA
ST2$^{-/-}$	BALB/c	Il1rl1^{tm1Anjm}	Internal breeding, CCHMC, Rothenberg Lab, Cincinnati, USA
Wildtype (WT)	BALB/c	BALB/cAnNCrl	Charles River, Breeding Laboratories, Sulzfeld, Germany
Wildtype (WT)	BALB/c	BALB/cAnNRj	Internal breeding, ISEF, AG Köhl, Lübeck, Germany
Wildtype (WT)	C57BL/6	C57BL/6J	The Jackson Laboratory, Bar Harbor, USA
Wildtype (WT)	C57BL/6	C57BL/6JRj breeder	Internal breeding, ISEF, AG Köhl, Lübeck, Germany

2.2 Equipment and Software

2.2.1 Equipment

Table 2.9 Used equipment.

Equipment	Manufacturer
Biological Safety Cabinets	Nuaire Inc., Plymouth, USA
Cell analyzer BD™ LSR II	BD Bioscience, San Jose, USA
Cell analyzer BD LSRFortessa™	BD Bioscience, San Jose, USA
Cell Sorter BD FACSAria™ III	BD Bioscience, San Jose, USA
Cell Sorter BD FACSAria™ II	BD Bioscience, San Jose, USA
Cell Sorter MoFlo Legacy	Beckman Coulter GmbH, Krefeld
Centrifuge 5424	Eppendorf AG, Hamburg
Centrifuge 5424R	Eppendorf AG, Hamburg
Centrifuge 5810R	Eppendorf AG, Hamburg
Chemical hood	Waldner Laboreinrichtungen GmbH & Co KG, Wangen
Confocal laser scanning microscope LSM710	Carl Zeiss, Oberkochen
Confocal laser scanning microscope FV1000	Olympus Corporation, Tokyo, Japan
Cytospin centrifuge Cellspin I	Tharmac GmbH, Walsolms
Dissecting scissors	WPI Deutschland GmbH, Berlin

FlexiVent	SCIREQ Scientific Respiratory Equipment Inc., Montreal, Canada
Forceps	WPI Deutschland GmbH, Berlin
Fridge, 4 °C and -20 °C combined	Liebherr-International Deutschland GmbH, Biberach an der Riß
Fusion SL Chemiluminescence Imaging	Vilbert Lourmat, Collegién, France
Hot-air cabinet	Memmert, Schwabach
gentleMACS Dissociator™	Milteny Biotec GmbH, Bergisch Gladbach
Incubator	Heraeus, Hanau
IR Direct Heat CO_2 Incubator	Nuaire Inc., Plymouth, USA
Magnetic Cell Separator QuadroMACS™	Milteny Biotec GmbH, Bergisch Gladbach
Microscope Fluovert FS	Leica Mikrosysteme Vertrieb GmbH, Wetzlar
Microscope Leica DM IL LED	Leica Mikrosysteme Vertrieb GmbH, Wetzlar
Microscope camera Leica EC3	Leica Mikrosysteme Vertrieb GmbH, Wetzlar
Multichannel pipette Biohit M300	Sartorius Biohit Liquid Handling Oy, Helsinki, Finnland
Multiphoton microscope Trim Scope II	LaVision, Goettingen
Neubauer counting chamber, improved	VWR International GmbH, Darmstadt
PCR, Cycler Mastercycler®	Eppendorf AG, Hamburg
pH-Meter Seven Easy PH S20-K	Mettler Toledo, Schwerzenbach, Switzerland
Pipetboy	Integra Biosciences AG, Zizers, Switzerland
Pipette (0.1-2.5 µl; 0.5-10 µl; 10-100 µl; 20-200 µl; 100-1000 µl)	Eppendorf AG, Hamburg
Precision balance LC6200S	Sartorius AG, Göttingen
Pure water system Nanopure Diamond D11931	Thermo Fisher Scientific GmbH, Bremen
Rotating incubator PerfectBlot	PEQLAB Biotechnologie GmbH, Erlangen
Rotating incubator Polymax 1040	Heidolph Instruments GmbH & Co. KG, Schwabach
RT PCR CFX96 Touch™	Bio-Rad Laboratories GmbH, Munich
RT PCR LightCycler® 480	Roche Diagnostics, Basel, Switzerland
Spectrophotometer NanoDrop NP-100	PEQLAB Biotechnologie GmbH, Erlangen
Steam sterilizer E14 Hydromat	WEBECO Hygiene in Medizin und Labor GmbH & Co. KG, Selmsdorf
Suction system Vacusafe 158310	Integra Biosciences GmbH, Fernwald
Table centrifuge	Carl Roth GmbH & Co. KG, Karlsruhe
Trans-Blot SD semi-dry transfer cell	Bio-Rad Laboratories GmbH, Munich
Ultra-low temperature freezer, -80 °C	SANYO Electrics Co., Japan
VacuGene Pump	Pharmacia, Belgium
Vortex-Genie 2	Scientific Industries Inc., New York, USA

2.2.2 Software

Table 2.10 Used software for data collection and analysis.

Program	Manufacturer
BD FACSDiva 7.0	BD Biosciences, San Jose, USA
CFX Maestro™ Software	Bio-Rad Laboratories GmbH, Munich
EndNote X8.2	Clarivate Analytics, Philadelphia, USA
FlexiVent Software 5.3	SCIREQ Scientific Respiratory Equipment Inc., Montreal, Canada
FlowJo X	FlowJo, LLD, Ashland, USA
FluoView 2.1c	Olympus Corporation, Tokyo, Japan
GraphPad Prism 8.0	Graph Pad Software Inc., LaJolla, USA
ImageJ	Wayne Rasband, NIH
Imaris 9.2.1	Bitplane, Concord, USA
Inspector Pro	LaVision, Goettingen
Leica Application Suite 2.0.0	Leica Microsystems GmbH, Heerbrugg, Switzerland
LightCycler® 480 Software 1.5	Roche Life Science, Indianapolis, USA
Leica Application Suite 2.0.0	Leica Mikrosysteme Vertrieb GmbH, Wetzlar
Microsoft Excel 2016	Microsoft Corporation, Redmond, USA
Microsoft Powerpoint 2016	Microsoft Corporation, Redmond, USA
Microsoft Word 2016	Microsoft Corporation, Redmond, USA
MARS – Data Analysis Software 2.30 R2	BMG Labtech GmbH, Ortenberg
Zen 2011	Carl Zeiss, Oberkochen

2.3 Methods

2.3.1 Animals

Wild-type (WT) mice were either purchased from Charles River Laboratories (Balb/c), Jackson Laboratories (C57BL/6J), or came from internal breeding (Balb/cAnNRj, WT C57BL/6JRj breeder) in the specific-pathogen free (SPF) animal facility of the University of Lübeck. In addition, *C3ar1*$^{-/-}$, *C5ar1*$^{-/-}$, *tdTomato-C3ar1*$^{fl/fl}$, *tdTomato-C5ar2*$^{fl/+}$ mice were also bred and kept in our specific-pathogen free (SPF) animal facility from the University of Lübeck. All animals were used at 8-16 weeks of age and handled in accordance with the appropriate institutional and national guidelines. Animals were used for organ removal and experimental allergic asthma studies. All studies were reviewed and, according to protocols, approved by the local authorities of the Animal Care and Use Committee from Schleswig-Holstein state authorities (Ministerium für Landwirtschaft, Energiewende, Umwelt und ländliche Räume, Kiel, Germany) (V312-7224.122-39 (37-2/13), V242-30278/2016 (50-4/16), V242-389/2016 (75-6/16), V242-23572/2018 (44-5/18) respectively). Mice were anesthetized by i.p. injection of a 10x

anesthetic (75-100µl 76mg/ml Ketamine, 4.8mg/ml Xylazine), and euthanized subsequently by cervical dislocation if not stated otherwise.

2.3.2 Intratracheal application of substances

Mice were anesthetized with 6.9 mg/kg bodyweight Xylazine and 114.5 mg/kg bodyweight Ketamine by intraperitoneal (i.p.) injection. Deeply narcotized mice were fixed on an immunization board by their incisors and an elastic band. The tongue was carefully pulled out and a total volume of 50 µl of the respective substance was applied to the throat. Pulling out the tongue and closing the nose at the same time forced the inhalation of the fluid into the airways. After the treatment, mice were transferred back into their cages and placed on bedding material to avoid any backflow of the administered substance. During narcosis animals were kept (in a distance of 30-40 cm) under red light to prevent them from cooling.

2.3.3 Models of experimental allergic asthma

2.3.3.1 Induction of HDM-mediated sensitization

The sensitization phase model used here derived from the established effector phase model of allergic asthma (259, 278). Briefly, WT and *tdTomato-C3ar1*$^{fl/fl}$ BALB/c mice were sensitized by an intratracheal (i.t.) application (2.3.2) of 100 µg house dust mite (HDM) extract in 50 µl PBS once, on day 0 (Figure 2.1A), or twice on day 0 and 7 (Figure 2.1B). Control mice were treated the same way with 50 µl PBS. Mice were euthanized and organs were harvested 72 hours after the last immunization for further analysis.

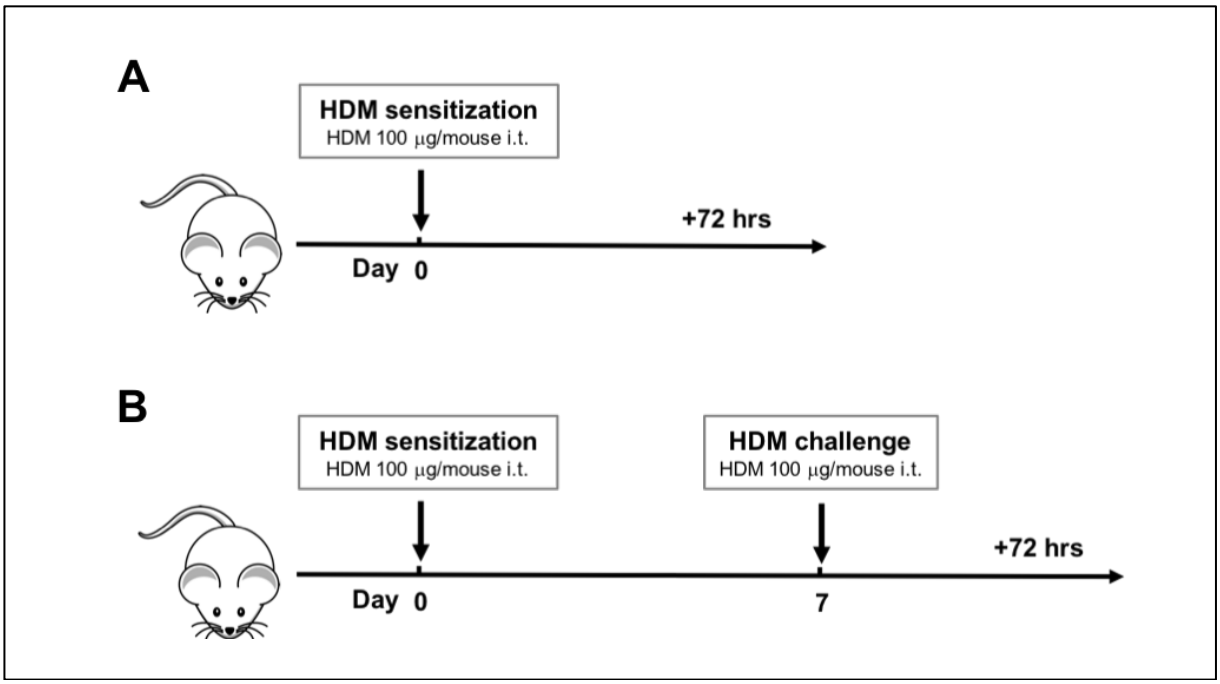

Figure 2.1 Experimental models of a house dust mite (HDM)-mediated sensitization in Balb/c mice. Mice were immunized i.t. with 100µg HDM in 50µl PBS i.t. (**A**) once on day 0 or (**B**) twice on day 0 and 7. Control mice were treated the same way with 50 µl PBS. 72hrs after final immunization mice were euthanized and organs were harvested.

2.3.3.2 Induction of HDM-mediated effector phase in BALB/c mice

For the effector phase of experimental allergic asthma (259, 278), WT, *C3ar1*$^{-/-}$, *C5ar1*$^{-/-}$, ST2$^{-/-}$, *IL-13Ra1*$^{-/-}$, and *tdTomato-C3ar1*$^{fl/fl}$ BALB/c mice were sensitized by an i.t. application (2.3.2) of 100 µg HDM extract in 50 µl PBS on day 0 and additionally challenged with 100 µg HDM on day 7, 14, and 21. Control mice were treated the same way with 50 µl PBS. Mice were sacrificed, and organs were harvested 72 hours after the last immunization for further analysis (Figure 2.2A).

2.3.3.3 Induction of HDM-mediated effector phase in C57BL/6 mice

For the effector phase of experimental allergic asthma, WT and *Ccr2*$^{-/-}$ C57BL/6 mice (494) were sensitized by an i.p. injection of HDM (10 µg in 100 µl PBS) on day 0 and 7. In addition they were challenged with 100 µg HDM in 50 µl PBS intratracheally (2.3.2) on day 14 and 21. Control mice were treated the same way with 100 µl PBS for the i.p. injection and 50 µl PBS for the i.t. treatment. Mice were euthanized, and organs were harvested 72 hours after the last immunization for further analysis (Figure 2.2B).

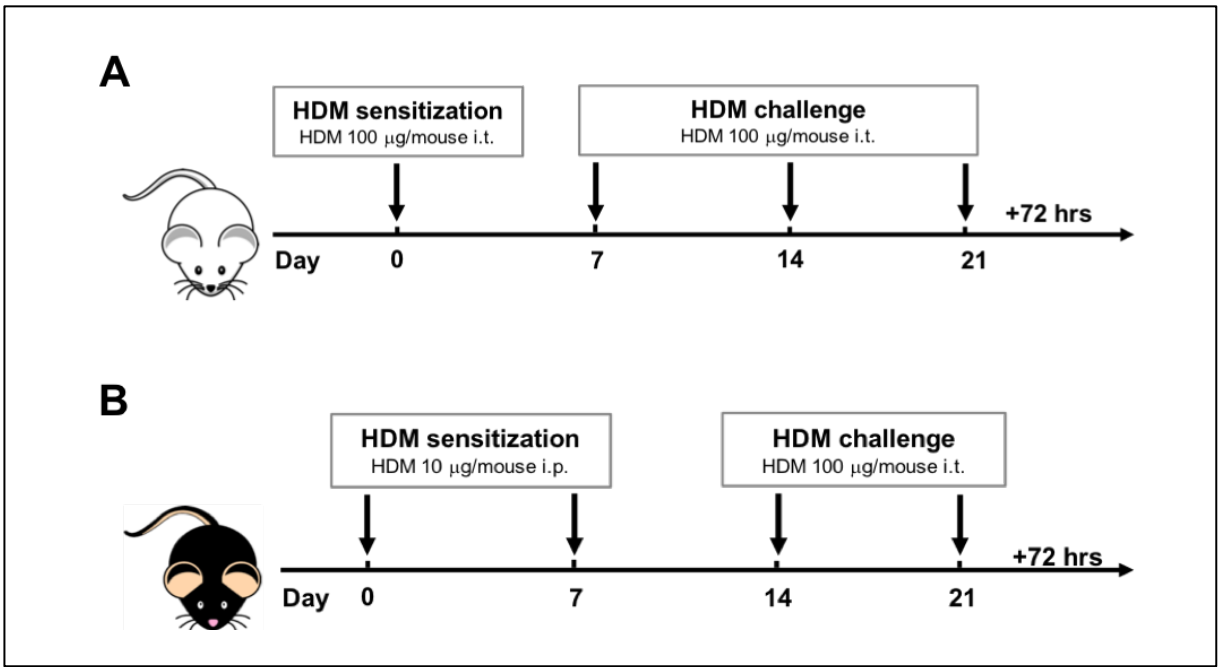

Figure 2.2 Experimental models of a house dust mite (HDM)-mediated effector phase. (**A**) HDM-mediated effector phase in Balb/c mice. Mice were immunized 4 times i.t. with 100 µg HDM in 50 µl PBS on day 0, 7, 14 and 21. Control mice were treated the same way with 50 µl PBS. 72hrs after final immunization mice were euthanized and organs were harvested. (**B**) HDM-mediated effector phase in C57BL/6 mice. Mice were immunized twice i.p. with 10 µg HDM in 100 µl PBS on day 0 and 7, and subsequently twice i.t. with 100 µg HDM in 50 µl PBS on days 14 and 21. Control mice were treated the same way with PBS. 72 hrs after final immunization mice were euthanized and organs were harvested.

2.3.4 Models of a cytokine induced pulmonary inflammation

2.3.4.1 IL-33-mediated pulmonary inflammation

For the induction of a strong pulmonary inflammation, WT, *C3ar1*$^{-/-}$, *C5ar1*$^{-/-}$, *tdTomato-C3ar1*$^{fl/fl}$, and *tdTomato-C5ar2*$^{fl/+}$ mice were immunized by i.t. application (see 2.3.2) of mouse recombinant IL-33 (500 ng in 50 µl PBS) on four consecutive days (495). Control mice were treated with 50 µl PBS. Mice were sacrificed, and organs were harvested 24 hours after the last immunization for further analysis (Figure 2.3A).

2.3.4.2 IL-13-mediated pulmonary inflammation

For the induction of a mild pulmonary inflammation, WT and *tdTomato-C3ar1*$^{fl/fl}$ mice were immunized by an i.t. application (see 2.3.2) of 5 µg recombinant IL-13 in 50 µl PBS on day 0, 3 and 6 (407). Control mice were treated with 50 µl PBS. Mice were euthanized and organs were harvested 24 hours after the last immunization for further analysis (Figure 2.3B).

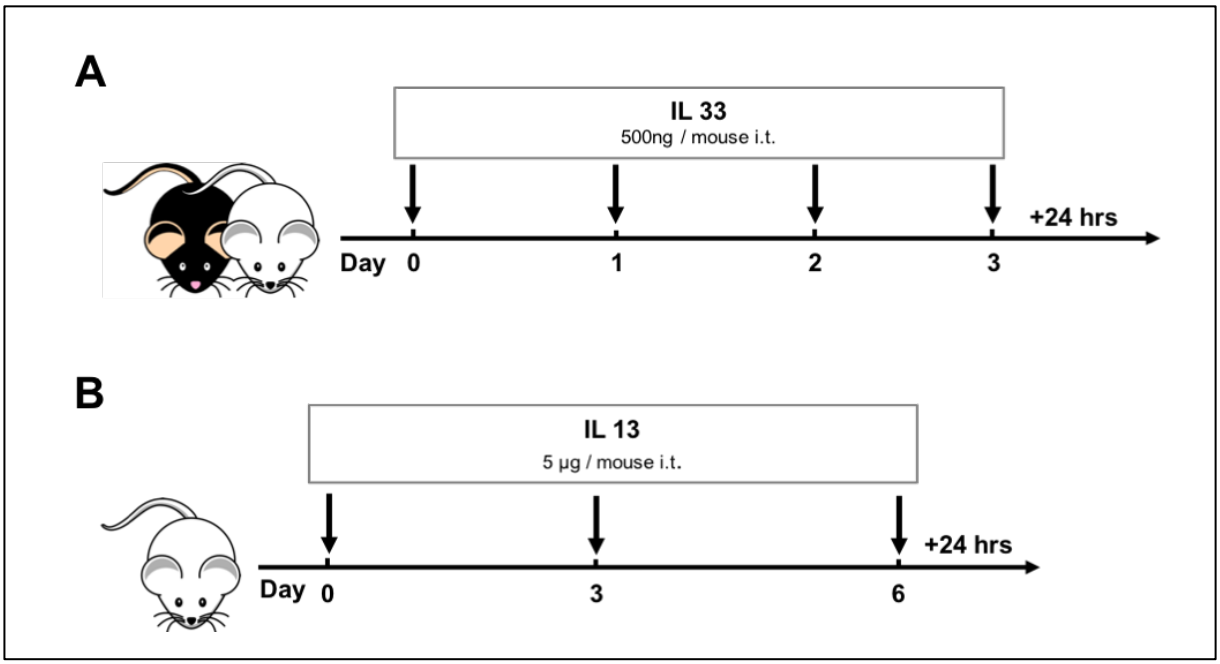

Figure 2.3 Induction of a pulmonary inflammation in mice. (**A**) Induction of a strong pulmonary inflammation with IL-33 in Balb/c and C57BL/6 mice. Mice were immunized 4 times i.t. with 500 ng IL-33 in 50µl PBS on day 0, 1, 2 and 3. Control mice were treated the same way with 50 µl PBS. 24 hrs after final immunization mice were euthanized and organs were harvested. (**B**) Induction of a mild pulmonary inflammation with IL-13 in Balb/c mice. Mice were immunized 3 times i.t. with 5 µg IL-13 in 50 µl PBS on day 0, 3 and 6. Control mice were treated the same way with 50 µl PBS. 24 hrs after final immunization mice were euthanized and organs were harvested.

2.3.5 Measurement of the airway hyperresponsivness

In allergic asthma, the chronic inflammation of the airways is associated with airway hyperresponsiveness (AHR) that leads to recurrent episodes of wheezing, chest tightness, and coughing. Bronchial provocation tests (BPTs) are objective tests for AHR that are useful to evaluate the phenotype of the disease. AHR is defined as the predisposition of the airways to narrow excessively in response to stimuli that would produce little or no effect in healthy subjects. However, our understanding of AHR in asthma remains complicated by the multitude of potential underlying mechanisms, which in reality are likely to have different contributions. In mouse models usually direct BPTs are used. In particular nebulization of methacholine, a pharmacological agonist of muscarinic (M_3) receptors, leads to direct airway smooth muscle cell contraction. AHR is quantified by the airway response, usually measured as airway resistance, to increased nebulized concentrations of methacholine. There have been two abnormalities observed on the dose response curve to a direct contractile agonist. Either a shift in the dose response curve or an increase in the maximum of the curve. A shift in the curve to the left suggests that epithelial damage, neural control, inflammatory cells and mediators may cause an increased sensitivity while airway smooth muscle contractility, increased wall thickness and decreased elastic loads may increase the maximal response (496, 497).

The measurement of lung function was performed using the forced oscillation technique in a mechanically ventilated animal (flexiVent™ system). The calibration of the flexiVent™ system was performed according to the manufacturer's suggestions. Immunized mice (see 2.3.3.2) were anaesthetized by i.p. injection of 50 µl 10x anesthetic solution and kept on a warming plate. Then, trachea was freed of surrounding muscles and opened at the upper third part by half-incision. A metal cannula, connected to the endo-tracheal tubing of the flexiVent™ system, was inserted into the trachea and fixed with sewing cotton. To ensure the paralysis of the respiratory muscles, 50 µl of the muscle relaxant agent Esmeron® (10 mg/ml) were injected additionally i.p.. The positive end-respiratory pressure was adjusted to 2.3 cm H_2O. Then, increasing concentrations of Acetyl-β-Methyl-Choline (methacholine) (0, 2.5, 5, 10, 25 and 50 mg/ml) were aerosolized by an ultrasonic nebulizer and delivered in-line through the inhalation port for 10 seconds. Methacholine binding to muscarinic acetylcholine receptors induces a dose-dependent bronchoconstriction, which is reflected by an increase of the airway resistance. Airway resistance was measured 2 min after nebulization by perturbating the lung 8 times in a row with 3 ventilations between each perturbation.

2.3.6 Induction and collection of thioglycolate-elicited peritoneal macrophages

BALB/c WT and *tdTomato-C3ar1*$^{fl/fl}$ mice were injected i.p. with 1 ml of 3% thioglycolate medium (Sigma-Aldrich) (227). Seventy-two hours later, peritoneal cell exudates were collected. For that, a syringe with 10 ml of ice-cold PBS was pre-filled. Mice were sacrificed by CO_2 and the peritoneal cavity was flushed with 10 ml PBS. Exudate was collected into a 15 ml tube. Subsequently, cells were identified as F4/80$^+$ cells by flow cytometry (2.3.8) and used for the assessment of C3a-mediated mobilization of intracellular Ca^{2+} (2.3.9.1).

2.3.7 Cell preparation from different organs

2.3.7.1 Bronchoalveolar lavage

To obtain the bronchoalveolar lavage (BAL) the murine thorax was opened, the trachea freed of surrounding muscles and opened at the upper third part by half-incision. The plastic part of a catheter (Vasofix® Safety, 18 G, 1.3x45 mm) was inserted and lung lobes were flushed once with 1 ml ice-cold PBS. Subsequently, the BAL fluid was collected in a 1.5 ml micro tube, centrifuged (10 min, 250 x g, 4°C) and erythrocytes were lysed with 100 µl red blood cell lysis (RBCL) buffer (2 min, room temperature (RT)). The lysis was stopped by addition of 900 µl PBS and cells were counted (see section 2.3.7.8). Cells were either used for subsequent flow cytometric analysis (see 2.3.8) or prepared for later microscopic morphological examination by spinning them on examination-slides using a cytospin centrifuge (see 2.3.14).

2.3.7.2 Mediastinal lymph nodes

For collection of the mediastinal lymph nodes (mLN) a 6 well plate, equipped with 40 µm cell strainers, was pre-filled with 5 ml RPMI 1640 and kept on ice. Opening widely the murine thorax, the three mLN were isolated under the upper right lung at the triangle between heart, trachea, and lung. Collected mLN were transferred into the prepared plate, the tissue disrupted mechanically with the plunger of a 5ml syringe, and the cells collected. The cell strainer was washed with 5 ml medium of the corresponding well. Then, the cell suspension was centrifuged (10 min, 350 x g, 4°C) and the supernatant discarded. The cell pellet was resuspended in 1 ml PBS and the cell number determined (2.3.7.8). The isolated mLN cells were further analyzed by flow cytometry (2.3.8.3).

2.3.7.3 Lung

Lung tissue was collected in a 6 well plate equipped with 40 µm cell strainers, pre-filled with 5 ml RPMI 1640 and kept on ice. After bronchoalveolar lavage collection (see 2.3.7.1) to remove cells from the airways and alveolar space, either all lung lobes or only right lobes (the left one being reserved for histology sampling (see 2.3.13.1)) were collected into the cell strainer and then gently chopped by using dissection scissors. The lung tissue was digested for 45 min at 37 °C in presence of 0.25 mg/ml Liberase TL (Roche) and 0.5 mg/ml DNase I (Sigma-Aldrich) under gentle agitation. After incubation, the content of each cell strainer was transferred to a 50 ml tube and lung cells were separated further by mechanical disaggregation using the plunger of a 5 ml syringe. The cell strainer was washed with 5 ml digestion medium and additionally with 10 ml wash medium (2.1.6). The single cell suspension was centrifuged (4 °C, 350 x g, 10 min), supernatant discarded, and erythrocytes lysed with 3 ml of RBCL buffer (3 min, RT). The reaction was terminated by addition of PBS to a final volume of 30 ml and the cell number was determined (see 2.3.7.8). Subsequently, the cells were used for flow cytometric analysis (2.3.8.3, 2.3.8.5), fluorescence activated cell sorting (FACS) (2.3.8.7), *ex vivo* re-stimulation (2.3.11.1) or intracellular T-cell staining (2.3.11.1).

2.3.7.4 Bone marrow isolation

For bone marrow (BM) preparation, femurs and tibias were removed, freed from muscles, placed in PBS on ice, and subsequently flushed with 2 ml PBS, and the marrow disrupted mechanically with the plunger of a 5ml syringe through a 40 µM cell strainer. The cells were collected into a 50 ml tube and the cell strainer was washed with additional 8 ml PBS. The cell suspension was centrifuged (5 min, 350 x g, 4°C) and the supernatant discarded. RBCs were lysed by incubating the cells with RBCL buffer for 3 min at RT. The reaction was stopped by addition of a large volume of PBS. The prepared BM cells were then used for flow cytometric analysis (2.3.8.3) or FACS (2.3.8.7).

2.3.7.5 Peritoneal lavage

To collect cells from the peritoneal cavity, the mice were sacrificed by CO_2 inhalation followed by cervical dislocation. Then, the peritoneal cavity (PerC) of the mice was gently flushed with 10 ml ice-cold PBS by using a 10 ml syringe and a needle (26G 0.45x13 mm). Collected cells were transferred to a 15 ml tube, washed once with PBS and centrifuged at 350 x g for 10 min at 4°C. If necessary, RBCs were lysed by incubating the cells in RBCL buffer for 3 min at RT. The reaction was terminated by addition of a large volume of PBS. The obtained cell suspension was further used for flow cytometric analysis (2.3.8.3, 2.3.8.5), FACS (2.3.8.7) or functional assays (2.3.9).

2.3.7.6 Visceral-adipose tissue

For visceral-adipose tissue (VAT) cell preparation, a 6 well plate equipped with 40 µm cell strainers, was pre-filled with 5 ml RPMI 1640 and kept on ice. The perigonadal fat tissue was harvested, taking care not to remove the gonads, transferred into the prepared plate and chopped into small pieces by using dissection scissors. The tissue was digested using 0.25 mg/ml Liberase TL (Roche) and 0.5 mg/ml DNase I (Sigma-Aldrich) for 45 min at 37°C. After incubation, the tissue-containing cell strainer was transferred to a 50 ml tube, the tissue disrupted mechanically with a plunger of a 5ml syringe. Further, the cells were collected and the strainer was washed with 5 ml medium of the corresponding well and additionally washed with 10 ml of wash medium (2.1.6). The cells were centrifuged at 350 x g for 10 min at 4°C, supernatant discarded, and RBCs were lysed using 1 ml RBCL buffer for 1 min at RT. Cells were transferred into a fresh 15 ml tube to limit the amount of contaminating lipid droplets and lysis was terminated by addition of a PBS to a final volume of 15 ml. The obtained single cell suspension was further analyzed by flow cytometry (2.3.8.3, 2.3.8.5).

2.3.7.7 Small Intestine Lamina Propria

Lamina propria (LP) cell suspension was obtained using a Lamina Propria Dissociation Kit (mouse, Miltenyi Biotec), following the manufacturer's instructions. Briefly, the small intestine was removed from the mice, quickly collected in predigestion medium (2.1.6) and cleared from feces, residual fat, and Peyer's patches. Then, the small intestine was cut longitudinally and washed once with HBSS (w/o) (see 2.1.1). The cleaned tissue was transferred to a 50 ml tube containing 10 ml predigestion medium. Samples were incubated under continuous rotation for 10 min at 37°C and afterwards vortexed well for 20 seconds. The intestine was removed, stretched and unknotted, the existing cell solution discarded. The same procedure was repeated once with 10 min incubation and twice with 5 min of incubation time. Afterwards, the intestine was removed, washed in HBSS (w/o), transferred into a tube with fresh 25 ml HBSS (w/o) and incubated for 20 min (37°C, continuous rotation). For digestion, the tissue was removed, chopped into small pieces and transferred into a gentleMACS™ Tube (Miltenyi

Biotec) containing the manufacturer's enzyme mixture (2.1.6), incubated for 30 min (37°C, continuous rotation) and afterwards homogenized with the gentleMACS Dissociator™ (Miltenyi Biotec) by using the program m_intestine_01. Then, the cell suspension was transferred to 50 ml tubes and centrifuged (600 x g, 5 min). The pellet was resuspended in 1 ml PBS, filtered through a 100 µm cell strainer and the strainer washed with 10 ml digestion medium. The cell suspension was again filtered through a 40 µm cell strainer and the strainer washed with 3 ml digestion medium. Lamina propria cells were centrifuged (10 min, 350 x g, 4°C), the supernatant discarded, and resuspended cells further analyzed by flow cytometry (2.3.8.3, 2.3.8.5).

2.3.7.8 Purification of naïve $CD4^+$ T cells from spleen

For co-culture of tissue-associated alveolar macrophages with T cells, splenic naïve $CD4^+$ T cells from WT mice were isolated by negative magnetic selection using the mouse $CD4^+$ T cell isolation kit (Miltenyi Biotec) according to the manufacturer's instructions. Briefly, for collection of the spleen a 6 well plate was equipped with 40 µm cell strainers, pre-filled with 5 ml PBS and kept on ice. Mice were sacrificed by CO_2 followed by cervical dislocation. Spleens were harvested, placed into the cell strainer, which was transferred to a 50 ml tube. Cells were obtained by mechanical disruption of the spleen with the plunger of a 5 ml syringe. The cell strainer was washed with 5 ml medium of the corresponding well, the cell suspension centrifuged (350 x g, 4°C, 8 min) and the supernatant discarded. Cells were resuspended with MACS buffer to $5x10^7$ cells/400 µl, 100 µl of antibody cocktail and incubated 10 minutes at 4°C in the dark. Further, 300 µl MACS buffer and 200 µl MicroBeads UltraPure per $5x10^7$ cells were added and additionally incubated 15 min at 4°C in the dark. Cells were washed by adding 10 ml MACS buffer, centrifuged (300 x g, 4°C, 8min) and the supernatant discarded. The cell pellet was then resuspended with 1 ml MACS buffer. During the incubation times, MACS LS columns were placed in a MACS separator and rinsed with 3ml MACS buffer. The labeled bead/cell suspension was added and unlabeled $CD4^+$ T cells passed through the column and were collected in a 15 ml tube. After washing the column using 6 ml of MACS buffer, the collection was passed once more through the column, which was finally washed additionally with 3 ml MACS buffer. An aliquot of the 10 ml spleen cell suspension (20 µl) was taken for cell counting. Cell suspension was centrifuged (300 x g, 4°C, 8min) and resuspended in appropriate medium to a concentration of 150,000 cells per 100 µl and used for fluorescence labeling with PKH26 (Sigma-Aldrich) or 5,6-Carboxyfluorescein N-hydroxysuccinimidyl ester (CFSE) (Invitrogen) (2.3.8.6).

2.3.7.9 Determination of cell numbers

For determination of the cell number, an aliquot of the cell suspension was taken and mixed with the same volume of trypan blue. By using a Neubauer counting chamber, living cells, which did not incorporate the Trypan blue, were counted under a transmitted-light microscope. The number of cells was calculated according to the following formula:

$$\text{Total cell number} = \frac{\text{counted cells}}{\text{number of counted big squares}} \times \text{dilution factor} \times 10^4 \times \text{Volume (ml)}$$

2.3.8 Analysis and purification of cell populations by flow cytometry and fluorescence activated cell sorting

2.3.8.1 Principals of flow cytometry

Flow cytometry is a laser-based measurement technology that allows a simultaneous multiparametric analysis of single cells in a heterogeneous cell population and has the ability to collect information from millions of cells in a matter of seconds.

A flow cytometer contains of four main components: the fluidics, optics, detectors and electronics. The fluidics system directs the sample suspension into the instrument, organizes the initial sample suspension into a single-cell stream, presents the sample to the interrogation point, and carries away the waste. The optical system which includes lasers, lenses, mirrors and filters leads to light scattering and fluorescence, and captures, filters and directs the light. The detection system, which consists of sensors, the so-called photomultiplier tubes (PMTs), detects the filtered fluorescence at a specified wavelength and generates a photocurrent. The electronics then digitize the photocurrent from the detector and save data for subsequent analysis.

A typical experiment begins with fluorescently labeled cells in a single-cell suspension. Once the sample is taken up into the flow cytometer, it is transported through the interrogation point, where the cells pass the laser light. To achieve precise data, cells in the single-file stream pass at best the laser beam one cell at a time. When a single cell passes the laser light beam, some of the light will hit physical structures within the cell and will cause scattering of light. This scattered light can be measured and correlated with relative cell size and structures inside the cell. The forward scatter (FSC) is the amount of light that scatters in the forward direction and is proportional to the size of the cell. A laser light that strikes a cell will scatter light also to the side. The so-called side scatter (SSC) is caused by granularity and structural complexity of the cell. In the end, the detectors will translate the intensity of the forward and side scattered light into voltage pulses.

In addition to separating cells based on FSC and SSC, cells can also be characterized by whether they express a particular protein. In this case, fluorescent molecules, such as fluorophore labeled antibodies are often used to stain the protein of interest. When passing through the laser beam those fluorochromes get excited by a laser with the corresponding excitation wavelength to a higher energy level and return back to their original position by emission of light. That emitted light is then directed to the optics, where it is split into defined wavelengths and channeled by a number of filters and mirrors within the flow cytometer. Subsequently, the filtered fluorescent light is delivered to the detection system so that each PMT can detect fluorescence only at a specified wavelength. The sensors translate the amount of fluorescence light proportionally into voltage pulses. Finally, the voltage pulses are recorded by the electronics and are ready for further analysis.

2.3.8.2 Compensation in flow cytometry

The range of light wavelengths that is able to bring a fluorochrome to a higher energy level is called excitation spectrum. The subsequent emission of light in another range of wavelengths, is the emission spectrum. All fluorochromes have excitation and emission spectra. Within a flow cytometer, the appropriate ranges of excitation and emission wavelengths are selected by bandpass filters. However, in case that many fluorophores are used simultaneously, emission spectra can overlap, and the fluorescence from more than one fluorochrome may be detected. To correct this spectral overlap, a process of fluorescence compensation is used, and a compensation matrix needs to be created. This ensures that the fluorescence light detected in a particular detector derives from the fluorochrome that is being measured.

Two different strategies were used to create a compensation matrix. On the one hand, I used a bead-based compensation method. For this purpose, single stained compensation beads were used to design and calculate the matrix automatically by the Diva software of the flow cytometer. For the preparation of the beads, 150 µl flow buffer containing one drop of negative bead and one drop of anti-rat/anti-hamster positive bead were placed into a tube. In addition, 0.5 µl of a single fluorophore-labeled antibody was added to every tube. Ideally, same antibodies that were used for the preparation of the antibody master mix, were also used for the staining of the beads. To compensate a tdTomato signal, (which emits at 581 nm), a PE-labeled antibody (emitting at 578 nm) was used. A tube without fluorophore staining was used as a negative/unstained control. Each fluorophore emission was measured in all the wavelengths used for the measurements, and the percentage of fluorescence attributed to overlapping emission was calculated and used to build the matrix.

On the other hand, since a staining for a single-cell suspension of the lung often requires a staining with multiple fluorophores and the cell suspension consists of variant cell populations, the bead-based

compensation do not always work satisfactory, the spectral overlap was also corrected by the manual creation of a compensation matrix using the analysis software FlowJo.

2.3.8.3 Fluorescence staining of surface markers

For fluorescence staining of surface markers, the single cell suspension was adjusted to a density of 0.5-1 x 10^6 cells/100 µl in PBS, and then incubated with a 1:100 dilution of an anti-CD16/32 containing Fc-block in flow buffer (4 °C, 15 min) to saturate non-specific bindings to Fc receptor II and III. The excess of unbound antibodies was removed by washing cells with flow buffer supplemented with BSA. Then, cells were pelleted by centrifugation (RT, 30 s, maximum speed) and the supernatant aspirated. For the specific staining of surface markers, antibodies catalogued in Table 2.2 were used at the specified dilution in an antibody master mix prepared in flow buffer as diluent. Staining was performed by resuspending 0.5-1 x 10^6 cells with 100 µl of the prepared antibody master mix and incubated at 4 °C for 20 min. Subsequently, unbound antibodies were removed by washing the cell suspension with 1 ml PBS, centrifugated (RT, 30 s, maximum speed) and the supernatant carefully aspirated. Finally, cells were resuspended for flow cytometric analysis in 150-300 µl flow buffer and analyzed with a cell analyzer BD FACS Aria™ III or BD™ LSR II. For the analysis of cell populations 3x 10^5 cells were recorded when possible, setting a threshold for the FSC at 25,000, in order to exclude small particles and cell debris.

2.3.8.4 Fluorescence-labeling of antibody

Unlabeled rat C3aR-specific murine antibody (clone 14D4), without protein carrier (bovine serum albumin (BSA)-free) was purchased from Hycult Biotech. Labeling of the antibody was performed using an AF647™ Antibody Labeling Kit (Invitrogen) according to manufacturer's instructions. Briefly, a 1 M solution of sodium bicarbonate was prepared by adding 1 ml of deionized water (dH_20) to the provided vial of sodium bicarbonate (Component B). The solution was vortexed until fully dissolved. A part of the antibody was diluted in PBS to obtain 90 µl antibody solution at a concentration of 1 mg/ml. Then 10 µl of 1 M sodium bicarbonate buffer was added, and the whole was transferred to the vial of containing the reactive dye. The vial was capped and gently inverted to fully dissolve the dye. The reaction was incubated (1 hour, RT) and every 10-15 minutes the vial was gently inverted in order to mix the two reactants and to increase the labeling efficiency. During labeling time, the spin column was prepared by adding 1 ml of purification resin (Component C) into the column and allowing it to settle by gravity. More resin was added until the resin bed volume was 1.5 ml. The spin column was placed in one of the provided collection tubes, and centrifuged (1100 x g, 3min). After incubation, 100 µl reaction volume were loaded dropwise onto the center of the spin column to allow the solution to absorb into the resin bed. The spin column was placed into the empty collection tube and centrifuged

(1100 x g, 5 min). After centrifugation, the collection tube contained the labeled protein that was used for direct fluorescence staining of C3aR (2.3.8.3., 2.3.8.5).

Fluorescence staining of surface C3aR expression

Cells that showed a positive tdTomato-C3aR signal, were also assessed for C3aR expression on the cell surface using an unlabeled rat C3aR-specific murine antibody (clone 14D4, Hycult Biotech) and a secondary $F(ab')_2$ anti-rat allophycocyanin antibody (Cell Signaling Technology) or a AF647™ fluorescence-labeled C3aR (14D4, Hycult Biotech) (2.3.8.4) at the catalogued dilutions (2.1.2). When the AF647™ fluorescence-labeled C3aR (14D4, Hycult Biotech) was used for staining, C3aR staining was performed according to the protocol described in 2.3.8.3. However, when the unlabeled rat C3aR-specific murine antibody and a secondary $F(ab')_2$ anti-rat allophycocyanin antibody was used, the staining was performed according to the following protocol. First, 0.5-1 x 10^6 cells per sample were blocked using 100 µl PBS supplemented with 20% FCS (PBS20) for 30 min at 4 °C. Usually, Fc block is used to block unspecific antibody binding. However, Fc block cannot be used since the secondary antibody recognizes rat antibodies, such as most of the labeled-antibodies. Then, cells were centrifuged (RT, 30 s, maximum speed), supernatant aspirated and stained with 100 µl C3aR antibody in PBS20 (30 min, 4 °C). After washing with 1 ml PBS20 and centrifugation (RT, 30 s, maximum speed), cells were stained with 100 µl of the secondary antibody in PBS20 as diluent. Excessive unbound antibody was removed by washing the cell suspension three times with 1 ml PBS20, centrifugation (RT, 30 s, maximum speed) and aspiration of the supernatant. Hereafter, cell specific marker staining was performed as described above (2.3.8.3). Finally, cells were resuspended for flow cytometric analysis in 150-300 µl flow buffer and analyzed with a cell analyzer BD FACS Aria™ III or BD™ LSR II, as mentioned before.

Evaluation of anti-mouse C3aR antibody specificity by flow cytometry

To evaluate the specifity of flow cytometry-approved anti-mouse C3aR antibodies, PM from WT and *tdTomato-C3ar1*$^{fl/fl}$ mice were stained for surface C3aR expression with two different antibody clones (D-20, Santa Cruz; 14D4, Hycult). Cells from *C3ar1*$^{-/-}$ mice served as controls. As shown in Figure 2.4, the clone 14D4 showed a C3aR signal in WT and *tdTomato-C3ar1*$^{fl/fl}$ cells, but no signal in *C3ar1*$^{-/-}$ control cells. However, using the clone D-20, both WT and *tdTomato-C3ar1*$^{fl/fl}$ cells, but in addition also cells from *C3ar1*$^{-/-}$ mice showed a signal for surface C3aR expression.

These data revelaed that the clone 14D4 shows C3aR-specific binding at steady-state, but the clone D-20 binds unspecifically. Therefore, to investigate C3aR expression at steady-state, I always used the clone 14D4.

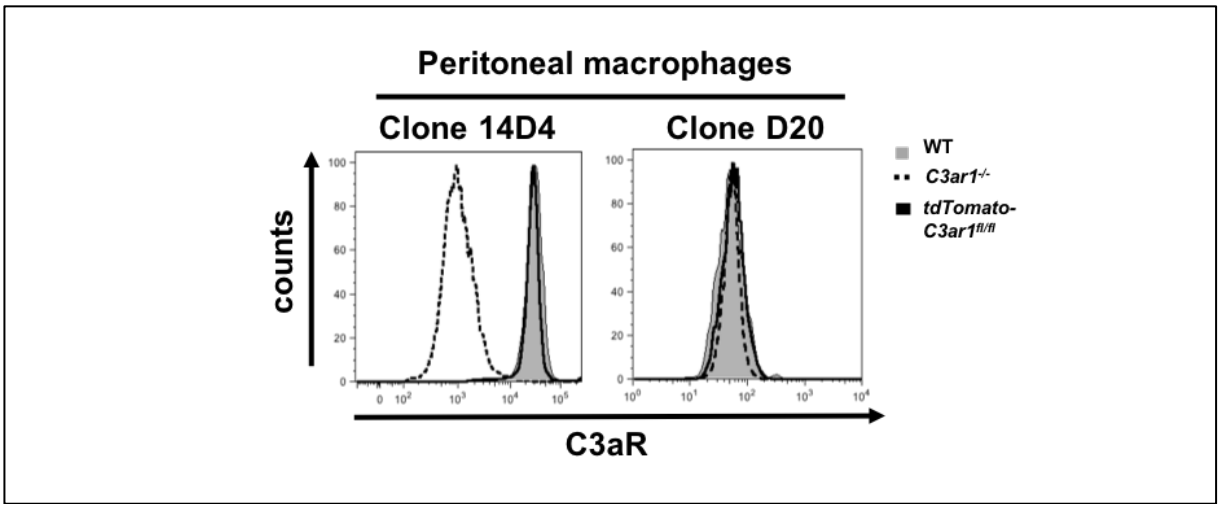

Figure 2.4 Anti-mouse C3aR (clone D-20) shows unspecific binding. Flow cytometric assessment of C3aR surface expression of F4/80$^+$ peritoneal macrophages from WT, *tdTomato-C3ar1$^{fl/fl}$* and *C3ar1$^{-/-}$* mice using antibody clone 14D4 and D-20. The grey histogram depicts C3aR signal from WT mice; the black line shows the signal of *tdTomato-C3ar1$^{fl/fl}$*, the dashed line the signal of *C3ar1$^{-/-}$* mice.

2.3.8.5 Intracellular fluorescence staining

Intracellular fluorescence staining is a method to detect intracellular or intraorganellar proteins like cytokines, receptors or transcription factors by flow cytometry. At first, it is important to fix cells before intracellular staining to ensure stability of the cell membrane, soluble antigens and antigens with a short half-life. In addition, it retains the target protein in the original cellular location. Typically, cells are fixed using a cross-linking agent like formaldehyde. Furthermore, the detection of intracellular antigens requires the permeabilization of cell membranes with detergent or alcohol to allow antibodies to access and bind intracellular targets.

Although several methods are available to fix and permeabilize cells, I used a saponin-based permeabilization method to stain intracellularly C3aR. Saponin interacts with membrane cholesterol and enables antibodies to go through pores without totally dissolving the plasma membrane. It is suitable for antigens in the cytoplasm or the cytoplasmic face of the plasma membrane and soluble nuclear antigens. Furthermore, for the detection of nuclear antigens such as transcription factors but also for the detection of secreted cytokines following activation *in vitro* a special Foxp3/Transcription Factor Staining Buffer Set was used according to manufacturer's suggestions.

In addition, I used a methanol-based permeabilization for intracellular staining to detect phosphorylated proteins and transcription factors, because it can increase the reactivity of antibodies to certain nuclear antigens.

Saponin-based permeabilization and intracellular staining of C3aR

Cells that showed a positive tdTomato-C3aR signal, but no surface C3aR expression, were also assessed for intracellular C3aR. To do so, single cell suspension was adjusted to a density of 0.5-1 x 10^6 cells/100 µl in PBS. Cells were centrifuged (RT, 30 s, maximum speed), supernatant aspirated and the pellet fixed with in 100 µl 1.5% paraformaldehyde (4°C, 30 min). Cells were centrifuged (RT, 30 s, maximum speed) and supernatant discarded before cell permeabilization, performed by resuspending cells in 100 µl of a saponin-based permeabilization buffer containing 20% FCS (2.1.6). After 30 min incubation at 4°C, cells were centrifuged and stained with 100 µl of C3aR-specific antibody (clone 14D4, Hycult) at the listed dilution (Table 2.2) in permeabilization buffer. After washing with 1 ml permeabilization buffer and centrifugation (RT, 30 s, maximum speed), cells were stained with 100 µl $F(ab')_2$ anti-rat antibody (Cell Signaling Technology) at the listed dilution (2.1.2) in permeabilization buffer (30 min, 4°C). Unbound antibody was removed by washing the cell suspension three times with 1 ml permeabilization buffer, centrifugation (RT, 30 s, maximum speed) and aspiration of supernatant. Then, the staining, using cell specific markers, was performed as described above (2.3.8.3). Finally, cells were resuspended in 150-300 µl flow buffer for flow cytometric analysis with a cell analyzer BD FACS Aria™ III or BD™ LSR II. For the analysis of cell populations 3x 10^5 cells were recorded when possible, setting a threshold for the FSC at 5,000, to avoid loss of shrunken cells harboring low FSC.

Methanol-based permeabilization and intracellular staining of pERK1/2

For intracellular pERK1/2 staining, 1-2 x 10^6 stimulated cells (2.3.9.3) were fixed with 1.5% formaldehyde (4 µl of a 37% formaldehyde stock solution for 100 µl cell suspension) and incubated for 10 min at RT in the dark. Then, cells were centrifuged (500 x g, 5 min) and the supernatant aspirated. Cells were permeabilized with 500 µl/10^6 cells pre-cooled (-20°C) methanol and incubated for 10 min at -20°C (NOTE: Once in methanol, cells can be stored at < -20°C for up to 4 weeks). Subsequently, cells were centrifuged at 500 x g for 5-10 min (NOTE: 500 x g should never be exceeded after permeabilization because cells are prone to rupture; wash not recommended because of difficulty pelleting) and supernatant aspirated. Then, cells 100 µl anti-CD16/32 containing Fc-block buffer (1:100 dilution) was added and cells were incubated additionally at 4 °C for 15 min. Finally, after centrifugation (500 x g, minimum 5 min), the supernatant was discarded, and staining performed. For that, cells were stained with 100 µl of a prepared antibody master mix containing anti-pERK1/2 antibody and specific surface markers (antibodies catalogued in 2.1.2) in PBS as diluent and incubated at 4 °C for 30-60 min. Subsequently, cell suspension was centrifugated (500 x g, 10 min; wash not recommended!), and supernatant was discarded. Finally, cells were resuspended in 150-300 µl flow buffer for flow cytometric analysis and analyzed with a cell analyzer BD FACS Aria™ III or BD™ LSR II, as mentioned above.

Foxp3/Transcription Factor Staining Buffer Set

For intranuclear T-cell staining of transcription factors and secreted cytokines a special Foxp3/Transcription Factor Staining Buffer Set (eBioscience) was used according to manufacturer's suggestions. Briefly, 1-2 x 10^6 stimulated cells (2.3.11.1) were centrifuged (600 x g, 5 min) and washed with 200 µl PBS, before being fixed with 100 µl fixation/permeabilization buffer using the Fixation/Permeabilization Concentrate at a 1:4 dilution with Fixation/Permeabilization Diluent and incubated for 1 hour at 4°C. Then, 100 µl anti-CD16/32 containing Fc-block buffer in permeabilization buffer (1:100 dilution) was added and cells were incubated additionally at 4 °C for 20 min. Finally, after centrifugation (96-well plate: 600 x g, 5 min; 1.5 ml micro tube: max. speed, 1 min), the supernatant was discarded and permeabilization together with staining was performed. For that, cells were stained with 100 µl of a prepared antibody master mix containing anti-FoxP3 or anti-cytokine antibodies and specific surface markers (antibodies catalogued in 2.1.2) using a 1:10 dilution of Permeabilization Buffer 10x in deionized water as diluent and incubated at 4 °C for 20 min. Subsequently, unbound antibodies were removed by washing the cell suspension twice with fixation/permeabilization buffer, centrifugated (96-well plate: 600 x g, 5 min; 1.5 ml micro tube: max. speed, 1 min), and supernatant was discarded. Finally, cells were resuspended in 150-300 µl flow buffer for flow cytometric analysis and analyzed with a cell analyzer BD FACS Aria™ III or BD™ LSR II, as mentioned before.

2.3.8.6 Fluorescence-labeling of live cells for *in vitro* culture

Labeling of purified cells with PKH26

PKH26 is a red fluorescent cell linker for general cell membrane labeling. It can be useful for *in vitro* cell labeling, *in vitro* proliferation studies and long term, *in vivo* cell tracking. In described assays (2.3.12.4, 2.3.12.5), it was used for *in vitro* cell labeling in order to track cells in a co-culture system with confocal microscopy in the PE channel.

For cell labeling, a PKH26 Fluorescent Cell Linker Kit (Sigma-Aldrich) was used according to manufacturer's protocol. Briefly, 1 µl of PKH26 stock dye was diluted in 100 µl of Diluent C. Then, purified cell pellet was resuspended with 100 µl of Diluent C and the diluted dye was added to the cell suspension. Cells were incubated at 37 °C for 10 min and the reaction stopped by addition of 1 ml of 100% FCS. After centrifugation (4 °C, 350 x g, 5 min), cells were resuspended into 1 ml of FCS, transferred in a fresh 1.5 ml micro tube and centrifuged again at the same conditions. Finally, cells were resuspended in complete medium and used for cell culture or manipulation as planned.

Labeling of purified cells with carboxyfluoresceine succinimidyl ester (CFSE)

CFSE (5,6-Carboxyfluorescein N-hydroxysuccinimidyl ester) is a cell permeable, non-fluorescent pro-dye. Intracellular esterases in live cells cleave the acetate groups, which results in the green fluorescent

molecule carboxyfluorescein that is now membrane impermeable. The succinimidyl ester group reacts indiscriminately with intracellular free amines to generate covalent dye-protein conjugates. The result is live cells with an intracellular fluorescent label that can be used for *in vitro* cell labeling, *in vitro* proliferation studies and long term, *in vivo* cell tracking. In the described assay (2.3.12.4), it was used for *in vitro* cell labeling in order to track cells in a co-culture system with confocal microscopy in the FITC channel.

For cell labeling a CellTrace™ CFSE Cell Proliferation Kit (Invitrogen) was used according to manufacturer's instructions. Briefly, purified cells were adjusted to a concentration of 10^7 cells/ml in PBS. CFSE was added to a final concentration of 1 µM and incubated at 37°C for 10 min. Then, 1 ml ice cold PBS was added to the cell suspension and incubated for 1 min on ice. Cells were centrifuged (4°C, 350 x g, 5 min), the supernatant discarded, and the pellet was re-suspended in 5 ml PBS to wash away toxic remnants of CFSE. When used for co-culture, an aliquot of the T cell suspension (10 µl) was taken for cell counting and staining efficiency.

2.3.8.7 Purification of cell populations by fluorescence activated cell sorting (FACS)

Fluorescence activated cell sorting is a flow cytometry-based sorting technique to separate live cells into purified cell populations based on fluorescent labeling. It involves more complex mechanisms in the flow cytometer than a non-sorting analysis. Cells stained using fluorophore-conjugated antibodies can be separated from one another depending on the fluorophore. Every individual cell enters a single droplet as it leaves the nozzle tip. This drop is given an electronic charge, depending on the fluorescence of the cell inside the drop. Deflection plates attract or fend the cells accordingly into collection tubes. Finally, sorted cell populations are then analyzed for purity to ensure successful cell sorting. Sorted cells can then be used for different approaches.

For the purification of alveolar macrophages and their subpopulations by FACS the whole lung single-cell suspension (obtained as described in 2.3.7.3) was centrifuged (4°C, 600 x g, 5 min) and then incubated with 1000 µl of an anti-CD16/32 containing Fc-block buffer (4°C, 15 min) to saturate non-specific binding sites. Unbound antibodies were removed by centrifugation (4°C, 600 x g, 5 min) and supernatant was aspirated. For the specific staining of surface markers, antibodies listed in 2.1.2 were used at the specified dilution for the preparation of an antibody master mix in flow buffer as diluent. Staining was performed by resuspending cells with 1000 µl of the prepared antibody master mix and incubated at 4°C for 20 min. After that, unbound antibodies were removed by washing the cell suspension with 5 ml PBS. Cells were centrifuged (4°C, 600 x g, 5 min) and supernatant was aspirated. Finally, for the Fluorescence-Activated Cell Sorting cells were resuspended in 1000 µl flow buffer and clumps were removed by filtering the cell suspension through a 40 µm cell strainer into a FACS tube. The cell population was purified with a cell sorter BD FACS Aria™ III or BD FACS Aria™ II, respectively,

equipped with a 100 µm nozzle. If not stated otherwise, purified cells were collected into tubes prefilled with 1 ml 100% FCS. FACS purified cells were used directly for RNA extraction or further *in vitro* culture, respectively (2.3.12.1, 2.3.12.2, 2.3.12.3, 2.3.12.4, 2.3.12.5, 2.3.15).

2.3.9 Functional assays

2.3.9.1 C3a-mediated increase in intracellular calcium

The C3a-induced increase in intracellular Ca^{2+} concentration ($[Ca^{2+}]_i$) was determined, as described (249, 498), using thioglycolate-elicited $F4/80^+$ peritoneal macrophages (PM). Cells were collected from the peritoneal cavity by peritoneal lavage and processed as described (2.3.7.5). Then, the cells were loaded with 5 mM of the Ca^{2+}-sensitive fluorophore Fluo-4AM (Invitrogen) according to the manufacturer's recommendations. Briefly, 1 ml peritoneal cell-suspension was prepared and incubated with 10 µl Fluo-4 AM (final concentration of 10 µM) in the dark for 30 min, RT. Then, the cells were washed twice with 500 µl PBS, centrifuged (350 x g, 5 min, RT) and the supernatant was discarded. Finally, the pellet was resuspended in 500 µl PBS and incubated for another 30 min in the dark, RT.

Subsequently, cells were stained with F4/80 for 20 min in flow buffer (2.3.8.3). $F4/80^{hi}$ cells were then analyzed on the LSR II flow cytometer. The background signal was recorded for 30 s. Then, 37 nM recombinant human C3a (hC3a, Hycult Biotech) was added, and recorded continuously for another 90 s. The increase in $[Ca^{2+}]_i$ was calculated by assessment of the maximal Ca^{2+} peak using the kinetic plug-in tool of the FlowJo software (version 9; Tree Star, Ashland, OR). The mean background signal recorded during the 30 s was subtracted from the Ca^{2+} peak signal to determine the final change in relative mean fluorescence intensity (ΔMFI).

2.3.9.2 C3aR internalization assay

Cells from the peritoneal cavity were collected and handled as described (2.3.7.5). After centrifugation, cells from WT or *tdTomato-C3ar1*$^{fl/fl}$ mice were resuspended at 1-3 x 10^6 cells per ml in PBS and allowed to rest for 5 min at 37°C. Cells were left untreated or stimulated either with 1, 10, and 100 nM hC3a (Hycult Biotech) for 3 min at 37°C, or with 10 nM for 1, 3, and 9 min at 37°C. The reaction was stopped by addition of paraformaldehyde (1.5% final concentration) and cells were immediately placed on ice. After 30 min fixation, cells were additionally blocked for 30 min with PBS supplemented with 20% FCS (PBS20), and then stained first with anti-C3aR mAb (clone 14D4; Hycult Biotech) in PBS20 for 30 min at 4°C. After washing with PBS20, cells were stained with an F(ab)2 anti-rat secondary Ab (Cell Signaling Technology). After three washes with PBS20, the cells were resuspended in flow buffer containing Fc

Block (eBioscience) and stained with an F4/80-specific Ab. Expression of C3aR in F4/80^{+} cells was determined by flow cytometry (2.3.8.3).

2.3.9.3 C3a-mediated phosphorylation of ERK1/2

Cells from the peritoneal cavity (PerC) (2.3.7.5) or bone marrow (2.3.7.4) were collected and handled as described. After centrifugation, cells from WT and *C3ar1*$^{-/-}$ mice were resuspended at 1.0 x 10^{6} cells per ml in PBS and allowed to rest for 5 min at 37°C. Cells from PerC were left untreated or stimulated either with 10, 50 or 100 nM hC3a (Hycult Biotech) for 5 min at RT. Bone marrow cells were stimulated with 10 nM hC5a (Hycult Biotech) for 5 min at RT. The reaction was stopped by addition of formaldehyde (1.5% final concentration) and cells were immediately placed on ice. Subsequently, intracellular pERK1/2 staining was performed as described in 2.3.8.5.

2.3.10 *In vitro* differentiation of BMDCs and BMMs

BM was prepared as described in 2.3.7.4. BM-derived dendritic cells (BMDCs) were generated as described (479). Briefly, BM cells were differentiated for 9 days (d) with GM-CSF (20 ng/ml). BMDCs were defined as CD11c^{+}CD11b^{+}MHCII^{hi}CD115^{-} cells. To generate BM-derived macrophages (BMMs), BM cells were cultured for 6 d in the presence of L929 cell-conditioned medium (499) or alternatively, BM cells were cultured in GM-CSF (20 ng/ml) for 9 d and identified as CD11c^{+}CD11b^{+}MHCII^{lo}CD115^{+} BMMs as described (482). After differentiated cells were used for flow cytometric analysis (2.3.8.3) or purification by FACS (2.3.8.7) and western immunoblot (2.3.18).

2.3.11 *In vitro* and *ex vivo* culture models of whole lung single-cell suspension

2.3.11.1 Intracellular cytokine secretion and T cell staining

Intracellular flow cytometry of an activated lung single cell suspension makes it possible to easily measure multiple cytokine secretion simultaneously and thus helps to identify T-cell differentiation and plasticity. Since cytokines typically are secreted proteins, they must first be trapped inside the cell by using a protein transport inhibitor. The two most commonly used protein transport inhibitors are monensin and brefeldin A. Monensin prevents protein secretion by interacting with the Golgi transmembrane Na^{++}/H^{+} transport, while brefeldin A redistributes intracellularly produced proteins from the cis/medial Golgi complex to the endoplasmatic reticulum.

Cytokine secretion and intracellular T-cell staining was performed with 2 x 10^{6} cells/200 µl in re-stimulation medium. Single cell suspension was seeded on a 96-well U-bottom plate and stored overnight at 4°C. The next day, cells were activated for 4 hours at 37°C, 5% CO_2 with 50 ng/ml phorbol 12-myristate 13-acetate (PMA) and 500 ng/ml ionomycin (both unspecific stimulators) and

simultaneously Golgi apparatus was blocked with 1x brefeldin and 1x monensin by adding 50 µl of a freshly prepared 5x stimulation mix (2.1.6). Afterwards cells were fixed, permeabilized and stained intracellularly for multiple cytokines and transcription factors as well as for specific surface markers following the protocol for the Foxp3/Transcription factor staining buffer set (2.3.8.5).

2.3.11.2 *Ex vivo* re-stimulation of lung single-cell suspension

Whole lung single-cell suspension was seeded at a density of 250,000 cells/150 µl in re-stimulation medium in a 96-well U-bottom plate and rested at 37°C, 5%CO_2. After 24 hours cells were re-stimulated with 30µg/ml HDM extract for additional 72 hours at 37°C, 5% CO_2. Then, the plate was centrifuged (600 x g, 5 min) and the supernatants were transferred into new micro tubes, frozen and stored at -20°C for subsequent ELISA.

2.3.12 *In vitro* culture models of naive tissue-associated alveolar macrophages

2.3.12.1 *In vitro* stimulation of naïve alveolar macrophages for mRNA extraction

SiglecF$^+$CD11c$^+$ tissue-associated alveolar macrophages (tAMs) of naïve WT mice were sorted from whole lung single-cell suspension by FACS as described in 2.3.8.7. Cells were washed with PBS, centrifuged (600 x g, 5 min) and resuspended in complete medium at a density of 30,000 cells/50 µl. Then, cells were seeded on a 96-well U-bottom plate and stimulated with 100 ng/ml granulocyte-macrophage colony-stimulating factor (GM-CSF), 100 ng/ml Interleukin (IL)-13, 100 ng/ml IL-5, 100 ng/ml IL-13 + 100 ng/ml IL-5, 100 ng/ml IL-4 or 10 nM human C3a, respectively, by adding 50 µl of a freshly prepared 2x concentrated stimulation solution. As negative control, 50 µl of complete medium was used. Cells were stimulated for 72 hours at 37°C and 5% CO_2, then cells were resuspended in Trizol for RNA extraction and cDNA synthesis (2.3.15, 2.3.16). Finally, the mRNA level of C3aR was evaluated by semi-quantitative Polymerase Chain Reaction (sqPCR) (2.3.17).

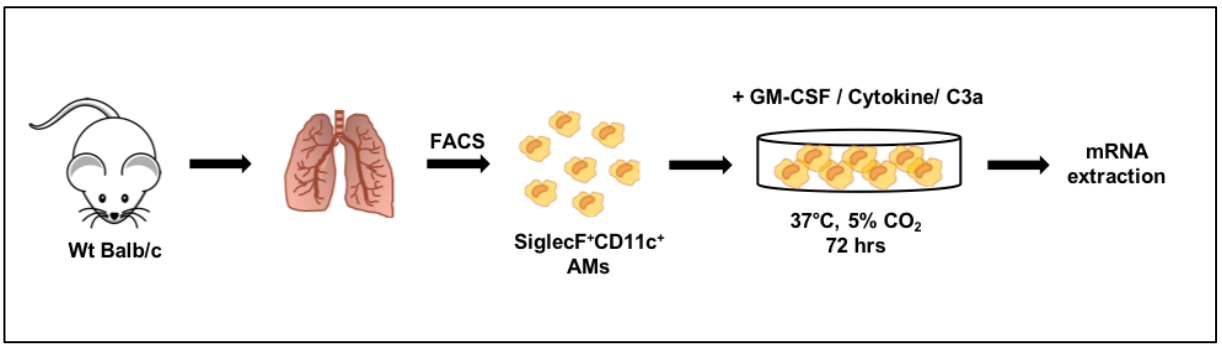

Figure 2.5 *In vitro* stimulation of naïve tissue-associated alveolar macrophages for mRNA extraction. Naïve WT mice were euthanized, lungs harvested and digested and whole single-cell suspension stained with SiglecF and CD11c for tissue-associated (t)AMs. tAMs were purified by FACS and 30,000 cells/ 100 µl complete medium stimulated with GM-CSF, cytokines and/or hC3a. After 72 hrs cells were lysed in Trizol and mRNA as well as cDNA prepared.

2.3.12.2 *In vitro* stimulation of naïve alveolar macrophages to determine C3aR expression by confocal microscopy

SiglecF$^+$CD11c$^+$ tAMs from naïve WT and *tdTomato-C3ar1$^{fl/fl}$* mice were sorted from whole lung single-cell suspension by FACS as described in 2.3.8.7. Cells were washed with PBS, centrifuged (600 x g, 5 min), resuspended in complete medium at a density of 100,000-150,000 cells/200 µl and seeded on a Permanox® slide for later microscopy. Furthermore, cells were stimulated with 100 ng/ml GM-CSF or 1% IL-4, respectively, by adding 200 µl of a freshly prepared 2x concentrated stimulation solution. As negative control, 200 µl complete medium was used. Cells were stimulated for 5 days at 37°C and 5% CO_2. Stimulation medium was changed on day 1 and 2 by aspirating the supernatant and replacing it with 400 µl of a freshly prepared 1x concentrated stimulation solution (Figure 2.6). After 5 days cells were used for confocal microscopy as described in 2.3.14.1. To determine C3aR expression, images were acquired by defining the tdTomato-C3aR signal in the PE channel. Image processing was conducted using Imaris software (Bitplane).

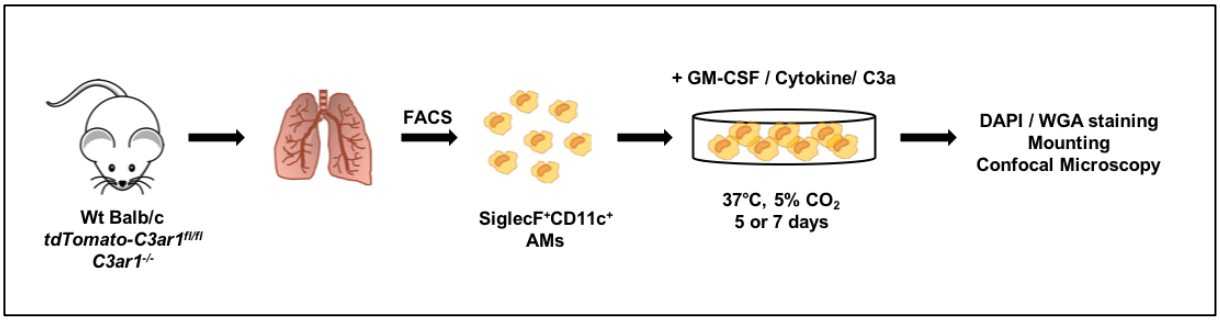

Figure 2.6 *In vitro* model of naïve tAMs to induce C3aR expression and generate multinucleated macrophages. Naïve WT Balb/c, *tdTomato-C3ar1$^{fl/fl}$* and *C3ar1$^{-/-}$* mice were euthanized and lungs harvested. SiglecF$^+$CD11c$^+$ tAMs were purified by FACS from whole lung single-cell suspension and 100,000-150,000 cells per 400 µl complete medium cultured on Permanox® slides with GM-CSF or IL-4 for 5 or 7 days. Then, cells were stained for their nuclei (DAPI) and membrane (Wheat Germ Agglutinin (WGA)) and analyzed by confocal microscopy.

2.3.12.3 *In vitro* stimulation of naïve alveolar macrophages for the induction of multinucleated tAMs

SiglecF$^+$CD11c$^+$ tAMs of naïve WT and *C3ar1$^{-/-}$* mice were sorted from whole lung single-cell suspension by FACS as described in 2.3.8.7. After washing with PBS and centrifugation (600 x g, 5 min), cells were resuspended in complete medium at a density of 100,000-150,000 cells/200 µl and seeded on a Permanox® slide for later microscopy (Figure 10). Then, cells were stimulated with 10, 20 or 100 ng/ml GM-CSF, 100 ng/ml IL-5, 1% IL-4, or 10 nM hC3a, respectively, by adding 200 µl of a freshly prepared 2x concentrated stimulation solution. As negative control 200 µl complete medium was used. Stimulation medium was changed on day 1, 2 and 5 and kept for 5-7 days. Changes were done by discarding the supernatants replacing it by 400 µl of freshly prepared 1x concentrated stimulation

solution. Cells were stimulated for at 37°C and 5% CO_2 (Figure 2.6), before staining for confocal microscopy as described in 2.3.14.1. Images were acquired and the frequency of polyploid tAMs was evaluated by using Imaris software (Bitplane). For that, I counted and calculated the frequency of binucleated (BiN) (nuclei =2) and MuN (>2 nuclei) cells on 6-9 pictures that were taken evenly distributed over one well.

2.3.12.4 CFSE- and PKH26-labeled naïve alveolar macrophages culture for the assessment of cell fusion

SiglecF$^+$CD11c$^+$ tAMs of naïve WT mice were sorted from whole lung single-cell suspension by FACS as described in 2.3.8.7. Cells were washed with PBS, centrifuged (600 x g, 5 min) and resuspended in complete medium at a density of 100,000-150,000 cells/200 µl. Cells were divided into half and labeled either with PKH26 (Sigma-Aldrich) or CFSE (Invitrogen) as described in 2.3.8.6. After respective washing procedures, differently labeled cells were combined and 100,000-150,000 cells/200 µl in complete medium and seeded on a Permanox® slide. Then, cells were stimulated with 10 ng/ml GM-CSF by adding 200 µl of a freshly prepared 2x concentrated stimulation solution. Stimulation medium was changed on day 1 and 2 by aspirating the supernatant and adding 400 µl of a freshly prepared 1x concentrated stimulation solution. Cells were stimulated for 5 days at 37°C and 5% CO_2 (Figure 2.7). Further, cells were used for confocal microscopy as described in 2.3.14.1. Images were acquired and multinucleated tAMs were investigated for fusion by identifying red, green, and double positive red-green multinucleated cells (MuNCs) using Imaris software (Bitplane).

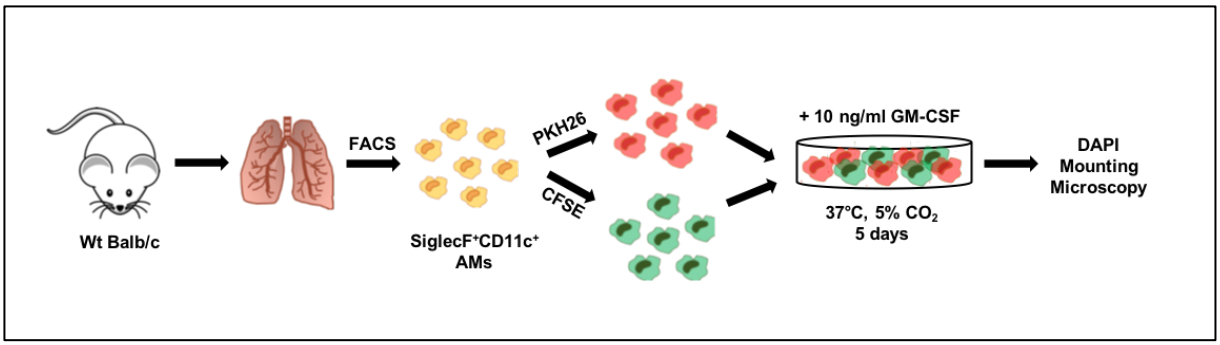

Figure 2.7 *In vitro* co-culture of CFSE- and PKH26-labeled naïve alveolar macrophages for the assessment of cell fusion. Naïve WT Balb/c mice were euthanized, and lungs harvested. SiglecF$^+$CD11c$^+$ tAMs were purified by FACS from whole lung single-cell suspension and equal number of cells were labeled with PKH26 or CFSE and co-cultured on Permanox® slides in 400 µl complete medium with GM-CSF for 5 days. Then, cells were stained for their nuclei (DAPI) and analyzed by confocal microscopy for cell fusion.

2.3.12.5 Evaluation of activated PKH26-labeled CD4⁺ T cells uptake by in vitro generated multinucleated tAMs culture

SiglecF⁺CD11c⁺ tAMs of naïve WT mice were sorted from whole lung single-cell suspension by FACS as described in 2.3.8.7. Purified cells were washed with PBS, centrifuged (600 x g, 5 min) and resuspended in complete medium at a density of 100,000-150,000 cells/200 µl seeded on a Permanox® slide. Firstly, MuN tAMs were generated by stimulation with 10 ng/ml GM-CSF as described (see 2.3.12.3) and changed on day 1, 2 and 5 by freshly prepared 1x concentrated stimulation solution. On day 5, in vitro pre-activated PKH26-labeled CD4⁺ T cell were added for co-culture. These cells were generated by activation on an anti-CD3 (2 µg/ml) covered 96-well plate (the plate was kept at 37°C, 5% CO2 for at least 2 h before discarding the coating solution and adding the cell suspension) for 3 days at 37°C and 5% CO2 in presence of anti-CD28 (10 µg/ml) of naïve CD4⁺ T cells isolated from spleen as described (2.3.7.8). Then, activated CD4⁺ T cells were labeled with PKH26 as described (2.3.8.6), and 450,000 labeled CD4⁺ T cells were added to the MuN tAMs culture. The co-culture was kept for 1 day at 37°C and 5% CO_2. After that, cells were used for confocal microscopy as described in 2.3.14.1. Images were acquired and the potential of tAMs to engulf PKH26⁺ T cells was evaluated using Imaris software (Bitplane).

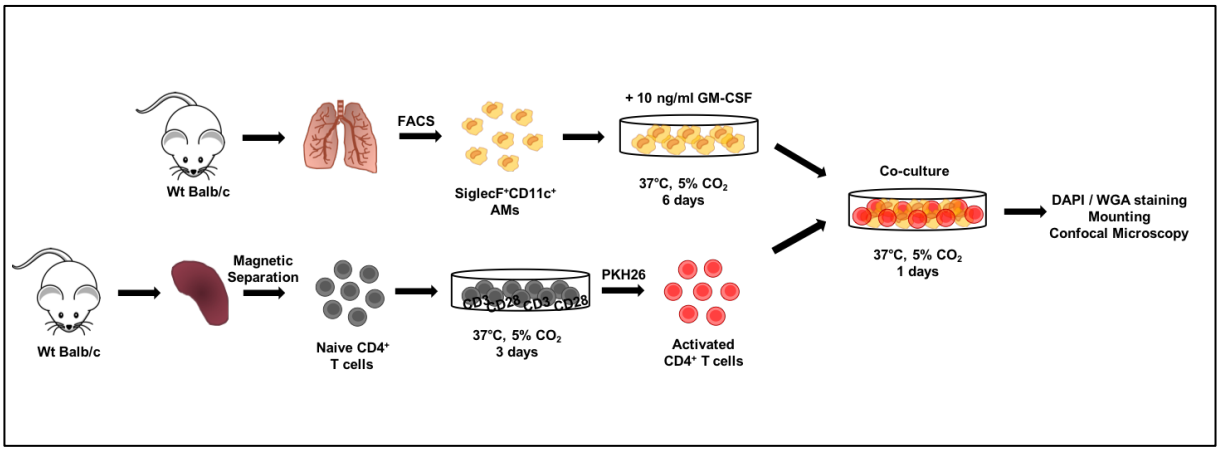

Figure 2.8 *In vitro* co-culture of PKH26-labeled activated T cells with naïve tAMs for the assessment of phagocytosis. Naïve WT Balb/c mice were euthanized, and lungs harvested. SiglecF⁺CD11c⁺ tAMs were purified by FACS from whole lung single-cell suspension and the formation of multinucleated cells induced by stimulation with GM-CSF slides in 400 µl complete medium on Permanox® for 5 days. On day 5, from WT spleen MACS-isolated, CD3/CD28 activated and PKH26-labeled CD4⁺ T cells were added, and MuN and T cells were co-cultured for one day. Then, cells were stained for their nuclei (DAPI) and membrane (WGA), and analyzed by confocal microscopy for engulfment of apoptotic T cells by macrophages.

2.3.13 Histology

2.3.13.1 Paraffin embedding of left lung lobe

After measuring the AHR (see 2.3.5) and obtaining the BAL (2.3.7.1), the left lung lobe was collected into an embedding cassette and fixed for 2-3 h in a 3.7% phosphate-buffered formalin solution (2.1.6).

Then, the cassette was rinsed with tap water under continuous shaking conditions over night to avoid formaldehyde artefacts in the lung lobe for further staining. Afterwards, tissue waste was transferred into 70% isopropanol and subsequently, tissue dehydration was performed by using an increasing ethanol-series with final replacement of ethanol by paraffin. The duration of the different incubation steps is listed in Table 2.11. Afterwards, the tissue sample was embedded in paraffin and cut into 5 µm histologic slices by using a microtome and used for H&E staining as described in 2.3.13.2.

Table 2.11 Ethanol and Paraffin series. For the dehydration of lung tissue an increasing Ethanol series was used. Thereafter, the Ethanol was replaced by Paraffin.

Concentration	Incubation time
70% ethanol	24-72 h
80% ethanol	24-72 h
90% ethanol	24-72 h
96% ethanol	24 h
100% ethanol I	24 h
100% ethanol II	24 h
100% ethanol III	24 h
Mixture paraffin:ethanol 1:2	24 h
Paraffin I	24 h
Paraffin II	24 h
Paraffin III	24 h

2.3.13.2 Hematoxylin and eosin (H&E) staining

The H&E staining was used to identify multinucleated macrophages in the lung of HDM-induced allergic asthma mice. At a low pH hematoxylin is a positively charged dye that binds to negatively charged structures such as the DNA of the chromatin, which appear blue after staining. In contrast, eosin is a negatively charged dye that can be used for counterstaining other structures that will appear in different shades of red after staining.

Prior to the staining, the histological slices were deparaffinized by a decreasing ethanol-series and rehydrated. The procedure and duration of the different incubation steps is listed in Table 2.12. Then, lung slices were stained with hemalaun and eosin-phloxine solution. This staining was developed during the following ethanol steps until the cytoplasm of the eosinophil granulocytes became red enough. After the replacement of ethanol by xylol the slices were mounted with Entellan® (Merck Millipore).

Table 2.12 Protocol of the HE staining. Lung slices were re-hydrated, stained with Hemalaun and Eosin and mounted with mounting medium.

Solution	Incubation time
100% ethanol	5 min
96% ethanol	5 min
90% ethanol	5 min
80% ethanol	5 min
70% ethanol	5 min
A. dest	5 min
Hemalaun	10 min
Eosin-phloxine solution	35 s
96% ethanol	20 s
100% ethanol I	1 min
100% ethanol II	1 min
100% ethanol III	2 min
Xylol I	5 min
Xylol II	5 min
Xylol III	5 min
Xylol IV	5 min
Mounting with Entellan®	

2.3.13.3 May-Grünwald Giemsa staining

To characterize the morphology of tAM subpopulations, lung single-cell suspension was obtained from HDM-treated mice as described in 2.3.7.3 and MHCII$^-$, MHCII$^+$C3aR^{low} and MHCII$^+$C3aR^{hi} tAMs were purified by FACS (2.3.8.7). Then, purified tAM subpopulations were spotted on a microscope slide with a cyto-centrifuge for 5min (600 x g, RT). Subsequently, dried cells were stained with May-Grünwald stain (4 min, RT, pH 7) in a microscope slide staining jar, gently washed and rinsed with water and then stained with a Giemsa-solution (1:15 dilution with dH_2O, 40min, RT, pH 7). After additional washing and drying, cells were mounted with VectaMount™ (Vector Laboratories) permanent mounting medium, and pictures were taken with a transmitted-light microscope (Leica DM IL LED).

2.3.14 Microscopy

2.3.14.1 Confocal microscopy of *in vitro* stimulated alveolar macrophages

To perform confocal microscopy of *in vitro* stimulated alveolar macrophages, first the supernatant in the wells of the Permanox® slide was aspirated and wells were washed once with 400 µl PBS. Then, cells were fixed with 400 µl of a 1.5% paraformaldehyde solution for 15 min at RT. Afterwards, the

supernatant was aspirated, the wells of the Permanox® slide were removed and the glass slide was washed again in PBS. Subsequently, cells were stained for DNA with 4',6-diamidino-2-phenylindole (DAPI) and/or with an Alexa Fluor™ 488 conjugated Wheat Germ Agglutinin (WGA) to stain their membrane. WGA is a lectin and a versatile cationic probe for detecting glycoconjugates, i.e., N-acetylglucosamine and N-acetylneuraminic acid (sialic acid) residues, on cell membranes. It can be used in fixed and live cells that have not been permeabilized. For the staining, fluorescent compounds catalogued in 2.1.2 were used at the specified dilution for the preparation of a master mix in PBS as diluent. Staining was performed by covering the glass slide with 2000 µl of the prepared master mix and cells were incubated at RT for 10 min in the dark. After that, the Permanox® slide was washed in PBS, dried carefully, and coverslipped with Fluoroshield™ as mounting medium. Images were acquired with an FV1000 confocal laser-scanning microscope (Olympus) with a 20x oil immersion and 40x 0.95 numerical aperture objective. FluoView 2.1c software (Olympus) was used as acquisition software. Image processing was conducted using Imaris software (Bitplane).

2.3.14.2 Immunofluorescence microscopy of whole lung slices

WT and *tdTomato-C3ar1*$^{fl/fl}$ mice were sacrificed by isoflurane inhalation (Baxter), and blood was removed from pulmonary vasculature by perfusion with 5 ml of 37°C HEPES-Ringer buffer (10 mM HEPES, 136.4 mM NaCl, 5.6 mM KCl, 1 mM $MgCl_2$, 2.2 mM, $CaCl_2$, 11 mM glucose (pH 7.4)) containing 300 ml of heparin-natrium (25000; Ratiopharm) via the right ventricle. Then, the airways were filled via the cannulated trachea with 3% low melting point agarose (Bio-Rad) dissolved in HEPES-Ringer buffer. The lungs were removed in bloc and transferred into ice-cold HEPES-Ringer buffer to solidify the agarose. The lungs were cut as precision-cut lung slices into 300-mm-thick slices using a Vibratome (VT1200S; Leica). For fixation and freezing, slices were placed in 1% paraformaldehyde (Sigma-Aldrich), then washed three times in PBS and incubated overnight with 20% D(+)-saccharose (Carl Roth) and frozen at -20°C until further use.

Immunohistochemical stainings were performed in 24-well plates (tissue culture OrPlate; Orange Scientific) in the dark to protect the fluorophores from light. Precision-cut lung slices were defrosted at room temperature on a shaker and washed three times in 1 ml of TBS for 10 min. Primary antibodies were diluted in 500 ml of TBS and incubated on a shaker overnight at RT. The next day, the slices were washed three times in TBS for 10 min. The slices were transferred to an object slide (Superfrost; Menzel Gläser), dried carefully, and coverslipped with Mowiol as mounting medium (Mowiol 4-88 (Hoechst), 200 mM Tris buffer (pH 8.5; Roth), glycerin (Merck)). Images were acquired with an LSM 710 confocal laser-scanning microscope (Carl Zeiss) with a 320/0.5 M27 objective and an immersion oil objective 340/1.30 oil differential interference contrast M27 (Carl Zeiss). Emitted light was detected by three wavelength-separated photomultiplier tubes at 505–534, 555–593, and 657–723 nm. Zen 2011 (Carl

Zeiss) was used as acquisition software. Image processing was conducted using Imaris software (Bitplane).

2.3.14.3 2-Photon microscopy

Imaging of fixed lung slices was performed using the TriM Scope II multiphoton microscope (LaVision BioTec) equipped with a XLUMPLFL 320 W/0.95 water immersion objective (Olympus). Images were acquired at 740 and 1100 nm performed by a Mai Tai HP (Spectra-Physics) and an InSight DeepSee (Spectra-Physics). Emitted light was detected by three wavelength-separated photomultiplier tubes (Hamamatsu) at 435–495, 495–560, and 560 nm. Inspector Pro (LaVision BioTec) was used as acquisition software. Image processing was conducted using Imaris software (Bitplane) and ImageJ (National Institutes of Health).

2.3.15 RNA extraction

For cell lysis 3 x 10^3 - 1 x 10^6 cells were centrifuged at 600 x g for 5 minutes, washed twice with PBS and centrifuged (300 x g, 5 min) again. Once the supernatant was removed, cell pellet was lysed by mixing in 100 µl of Trizol reagent. Cell lysate was directly transferred into a 1.5 ml micro tube pre-filled with 400 µl Trizol reagent and RNA isolated by addition of 200 µl of 100% chloroform and mixed by vortexing. Then, samples were incubated at room temperature for 3 minutes and centrifuged at 12,000 x g at 4°C for 15 minutes. After centrifugation, the RNA is located in the clear aqueous phase, the DNA is in the buffy coat interface, and protein is in the underlying organic phase. The clear aqueous phase was then transferred into fresh 1.5 ml micro tubes containing 500 µl of isopropyl alcohol and ~50 µg (1 µl) of glycogen and incubated either at RT for 10 min or at -20°C up to overnight. Afterwards, samples were centrifuged (12,000 x g, 4°C, 10 min), the supernatant discarded, and the RNA pellet was washed with 750µl of 75% ethanol (if necessary, samples could be stored at -20°C for one month). Samples were centrifuged again (7,500 x g, 4°C, 5 min) and the supernatant carefully discarded. Subsequently, the pellet was dried for 30-60 minutes at RT. Finally, the pellet was resuspended in 15-20 µl of nuclease-free water and either stored at -80°C or directly used to determine RNA purity and concentration. The NanoDrop (PEQLAB) was used to define RNA purity and concentration according to manufacturer's protocol. For this, samples were heated at 65°C for ~2 minutes to denaturate RNA, mixed well and snap-cooled on ice. The samples were then pulsed in the centrifuge to condense the volume and the samples were stored at -80°C until time of cDNA preparation.
Purity and concentration were determined by the NanoDrop according to the following formulae:

$$Purity\ ratio = \mathrm{A260/A280}$$

$$Total\ RNA\ \mu g = A_{260} \times 40\,\mu g/ml \times Dilution\ Factor \times Sample\ in\ ml$$

$$RNA\ \mu g/ml = RNA\ \mu g/\ Total\ Volume\ Sample\ in\ \mu l$$

2.3.16 cDNA synthesis

First-strand cDNAs were synthesized in a final reaction volume of 20 µl per sample according to manufacturer's suggestions. For that 1 µl of random primers (50 µM) (Life technologies Corporation), 300 ng of RNA (whole amount of RNA if total RNA <300 ng) and 1 µl of deoxynucleotide triphosphate (dNTP) mix (10 mM) (Life technologies Corporation) was added to a nuclease-free micro tube and filled with nuclease-free water to a volume of 13 µl. The mixture was heated to 65°C for 5 minutes and then incubated on ice for at least 1 minute. The content of the tube was collected by brief centrifugation and 7 µl of a polymerase chain reaction (PCR) pre-mix containing 4 µl 5X First-Strand Buffer (Life technologies Corporation), 2 µl 0.1 M (dithiothreitol) DTT (Life technologies Corporation), 0.5 µl murine RNase Inhibitor (40 units/µl) (New England Biolabs)), 0.5 µl nuclease-free water and 0.25 µl SuperScript™ II RT (200 units/µl) (Life technologies Corporation) was added. The samples were then mixed by pipetting gently up and down.

Subsequently, the PCR was set up with the following PCR program on a Mastercycler® (Eppendorf). Samples were first incubated at 25°C for 10 minutes followed by an increased reaction temperature to 42°C for 50 minutes. The Reverse Transcriptase reaction was then inactivated by heating at 70°C for 15 minutes. Finally, the cDNA was diluted 5-6-fold by adding nuclease-free water to each tube and used for real-time (RT)-PCR analysis (2.3.17).

2.3.17 Real-Time PCR

Semi-quantitative Real Time (RT)-PCR was performed using SYBR Green I (Bio-Rad). The gene-specific forward and reverse primer pair concentrations were normalized and mixed. Each primer (forward or reverse) in the mixture was used with a 20 µM/ml concentration. RT-PCR was performed in a final reaction volume of 10 µl per sample using 5 µl of SYBR Green Mix, 2 µl cDNA, 1 µl of primer pair mix and 2 µl nuclease-free water. The experiment was set up on a LightCycler®480 (Roche) or a CFX96 Touch™ Real-Time PCR Detection System (Bio-Rad). Primer sequences and specific annealing temperature are listed above (2.1.3). RT-PCR results were analyzed with the LightCycler®480 Software or CFX Maestro™ Software. Raw data were checked for any bimodal dissociation curve or abnormal amplification plot. The PCR program was run according to the procedure listed in Table 2.13.

Table 2.13 Program for semi-quantitative RT-PCR. Sequence, temperature, time and cycles for denaturation, amplification, melting curve and cooling.

Program	Temperature	Time	Cycles
Denaturation	95°C	10 min	1
Amplification	95 °C annealing temperature °C 72 °C	5 s 10 s 11 s	45
Melting Curve	95°C 65 °C 97 °C	5 s 60 s continous	1
Cooling	40°C	10 s	1

Finally, mRNA abundance was determined. For that, Cp values of the housekeeping gen (*S14*) and of the analyzed gen (e.g. *C3ar1*) of the same sample were used according to the following formulae:

$$mRNA\ abundance = (1.8^{(Cp\ S14 - Cp\ gene)}) \times 100000$$

2.3.18 Western immunoblot

0.5-1.0 x 10^6 cells per 90 µl PBS were lysed with 30 µl volume of 4x Laemmli sample buffer (Bio-Rad), which was freshly complemented with ß-mercaptoethanol (1:10 dilution at a final concentration of 355 mM) and preheated at 95°C. Lysates were homogenized through a needle (18G 1.2x40 mm) until they were very smooth and no longer viscous. Then the samples were denaturized at 95°C for 5 minutes, centrifuged (max. speed, 30 s) and either directly used for running a gel or stored at -20°C. Cell lysates were separated by a discontinuous sodium dodecyl sulfate polyacrylamide gel electrophoresis (SDS-PAGE) according to standard procedures using a 4-15% Mini-PROTEAN®TGX™ Precast Protein Gel (Bio-Rad). Briefly, gels were removed from the storage pouch and assembled in gel cassettes placed into the electrode holder. Then, the electrophoresis module was placed into the tank and the buffer chambers were filled with 1x SDS running buffer. Before loading the gel, the wells were rinsed with 1x SDS running buffer by using a syringe or disposable transfer pipet to clean the wells and to eliminate air bubbles.

Up to 50 µl of the denatured protein samples were loaded, together with a protein marker Kaleidoscope™ Prestained Standards (Bio-Rad) and the gel was run first with 100 Volt (V) for 15 min in order to concentrate the proteins in the collection part of the gel (neutral pH), then at 180 V to separate the proteins in the separating part of the gel (basic pH). The run was stopped when the migration front was reaching the bottom of the gel. Then, the gel was disassembled for subsequent

blotting using the Trans-Blot SD semi-dry transfer system (Bio-Rad). Gel, filter papers, and a 0.45μm pore size nitrocellulose membrane (Schleicher & Schnell GmbH) were soaked independently in 100 ml of 1x transfer buffer containing 20% methanol. Then, the blot was assembled for transfer placing on the cathode the filter paper, the membrane, the gel and the 2nd filter paper, from bottom to the top and closing with the anode. Between each layer air bubbles were removed by gently rolling with a half of a plastic pipette. The Trans-Blot SD system was connected, and the proteins were transferred upon application of an electric field at 15V/5.5mA for 15 min. After the semi-dry transfer, the membrane was directly incubated with a Tris-buffered saline (TBS) supplemented with 0.1% Tween 20 blocking buffer (TTBS) complemented by 5% BLOTTO low-fat dry milk (Rockland Immunochemicals) (TTBS-milk) under agitation for 60 min at RT. After blocking, the membrane was incubated with the primary antibody in TTBS-milk (dilution specified by the manufacturer) with agitation for 60 min (at RT) or overnight (at 4°C). The blot was washed with TTBS three times, 5 min each at room temperature with agitation. Then the secondary antibody was diluted with TTBS-milk and the membrane incubated (RT, agitation, 60 min) again. After final washing steps with three times TTBS, 5 min each (RT, agitation), the blot was incubated with 750 μl luminol/enhancer and 750 μl peroxide solution (for a 7 x 8.5 cm membrane) from an Amersham ECL Prime Western Blotting Detection Reagent (GE Healthcare Life Science), for 1 min RT. Then, the excess substrate was aspirated, and the membrane was placed in a protective plastic wrap sleeve to prevent drying prior light detection. Light emission was documented using and the chemiluminescence imaging system Fusion SL (Vilbert Lourmat) with an optimized appropriate time, starting with a low exposure of 2 min. If necessary, the exposure was repeated with a shorter or longer duration.

To evaluate the specificity of anti-mouse C3aR antibodies, I performed western blot analysis of peritoneal macrophages (PMs), BM neutrophils and BM-derived DCs (BMDCs) as well as macrophages (BMMs) of WT and *tdTomato-C3ar1*$^{fl/fl}$ mice. Cells from *C3ar1*$^{-/-}$ mice were used as controls. Used were three different WB-approved monoclonal or polyclonal C3aR antibodies (monoclonal D-12; polyclonal D-20; polyclonal H-300, Santa Cruz). As shown in Figure 2.9A,B, polyclonal C3aR antibody (D-20) showed a band in the range of the molecular weight of C3aR (54 kDa), but revealed also a band in PM and BM neutrophils of *C3ar1*$^{-/-}$ mice. In addition, similar results were also obtained with BMDCs and BMMs (Figure 2.9C). Moreover, investigation of monoclonal D-12 and polyclonal H-300 Ab (Figure 2.9C) revealed similar results to the D-20 Ab. Whenever a band in WT and *tdTomato-C3ar1*$^{fl/fl}$ cells appeared (for D-12 only in BMMs), a band appeared also in cells of *C3ar1*$^{-/-}$ mice.
These data revealed that all three antibodies showed unspecific binding and were not adequate for investigation of C3aR expression in my project.

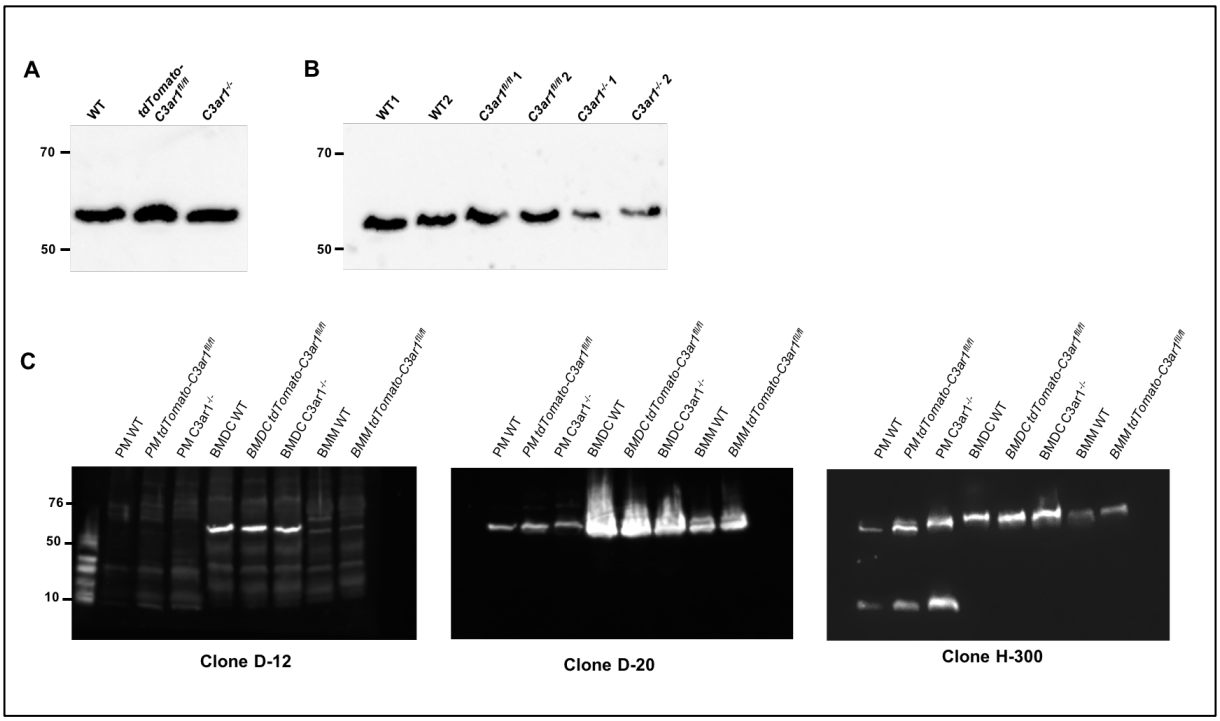

Figure 2.9 Western blot analysis of C3aR expression. Cell lysates were prepared from sorted (A) F4/80^{+} peritoneal macrophages and (B) Ly6G^{+} BM neutrophils of WT, *tdTomato-C3ar1$^{fl/fl}$*, and *C3ar1$^{-/-}$* mice. The membrane was probed with anti-C3aR antibody D-20. (C) Lysates from peritoneal macrophages (PMs), BMDCs or BMMs from WT, *tdTomato-C3ar1$^{fl/fl}$*, and *C3ar1$^{-/-}$* mice were separated and tested with 3 different anti-C3aR antibody clones (D12, D20, and H300).

2.3.19 Statistical Analysis

Statistical analysis was performed using GraphPad Prism (version 8.0.1; GraphPad Software, Inc.). The graphs are presented as scatter plots with bars showing the individual samples and the mean ± standard error of the mean (SEM). Normal distribution of data was tested using the Kolmogorov-Smirnov and D'Agostino-Pearson tests, some after log transformation. When groups were normally distributed, statistical differences between two groups were assessed by unpaired t test. Comparisons involving multiple groups were first evaluated by an analysis of variance (ANOVA) followed by Tukey's multiple comparison test. When groups were not normally distributed, they were analyzed using a Mann-Whitney U (two groups), or ANOVA on ranks (multiple groups) followed by a Dunn's multiple comparison test. A p value < 0.05 was considered statistically significant (* or § $p < 0.05$, ** or §§ $p < 0.01$, *** or §§§ $p < 0.001$).

3 Results

3.1 Variable expression of anaphylatoxin receptors in alveolar macrophages at steady state

The anaphylatoxins C3a and C5a, generated by the proteolytic cleavage of C3 and C5 either after complement activation or by allergen-associated proteases, have been shown to play an important role regulating the development and severity of allergic asthma through the activation of their cognate G-protein-coupled receptors C3aR, C5aR1 and C5aR2 (259, 278, 407, 460, 484, 485). However, the expression and functions of the anaphylatoxins in pulmonary innate and adaptive immune cells, in particular on alveolar macrophages, during allergic asthma development and in allergic asthma severity, remain unclear.

Until recently, the expression level of anaphylatoxin receptors (ATRs) on murine cells was ill defined due to the lack of appropriate antibodies and tools, in particular for C5aR2. Therefore, our lab generated a floxed tandem-dye Tomato (tdTomato)-C3ar1 and a tdTomato-C5ar2 reporter knock-in mouse. These mice gave us the opportunity to monitor C3aR and C5aR2 expression, using tdTomato as a surrogate, by flow cytometry and immunofluorescence microscopy.

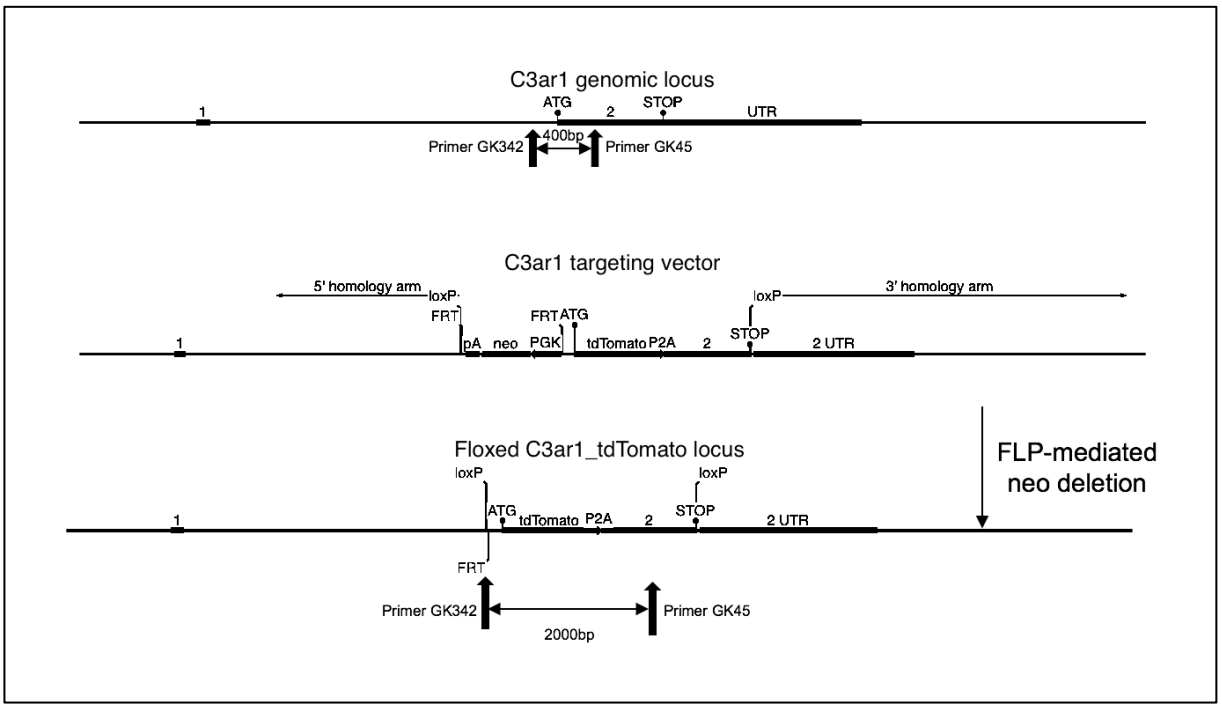

Figure 3.1 Generation of the floxed tdTomato-C3aR knock-in mouse. Scheme of the gene-targeting strategy used. The exon 2 of the WT gene of C3ar1 was replaced with a cassette encoding a fusion protein comprising tdTomato and C3aR, flanked with loxP sites by homologous recombination. The fusion contains a P2A cleavage site allowing the splitting of both the tdTomato and C3aR, leading in fine to the expression of 2 independent proteins.

The construct of the tdTomato-C3ar1 reporter knock-in mouse is shown in Figure 3.1. A tdTomato cassette was inserted directly upstream of the 5' end of exon 2 of the C3ar1 gene, because structural data have shown that the N-terminal part of the C3aR does not bind C3a (217, 500). In contrast, the C-terminal part of the C3aR harbors important phosphorylation sites, conserved in human and mice that drive receptor internalization and signal transduction (223). To allow a conditional deletion of the C3ar1 gene, two loxP sites were placed upstream of the tdTomato coding sequence and downstream of exon 2 of the C3ar1 gene. Instead of a bis-cystronic vector containing an internal ribosomal entry site (IRES), the porcine teschovirus-1 2A (P2A) mRNA sequence was inserted in frame, between the tdTomato and the C3aR moiety of the mRNA. This short length sequence, when translated ensures a higher level of transgene expression and a, high self-cleavage efficiency during gene transcription, providing a stoichiometric expression of the proteins flanking the 2A peptidic sequence (501-504). Finally, this vector leads to the synthesis of two autonomous and separated proteins – the tdTomato protein and the C3aR protein – without affecting the functions of C3aR.

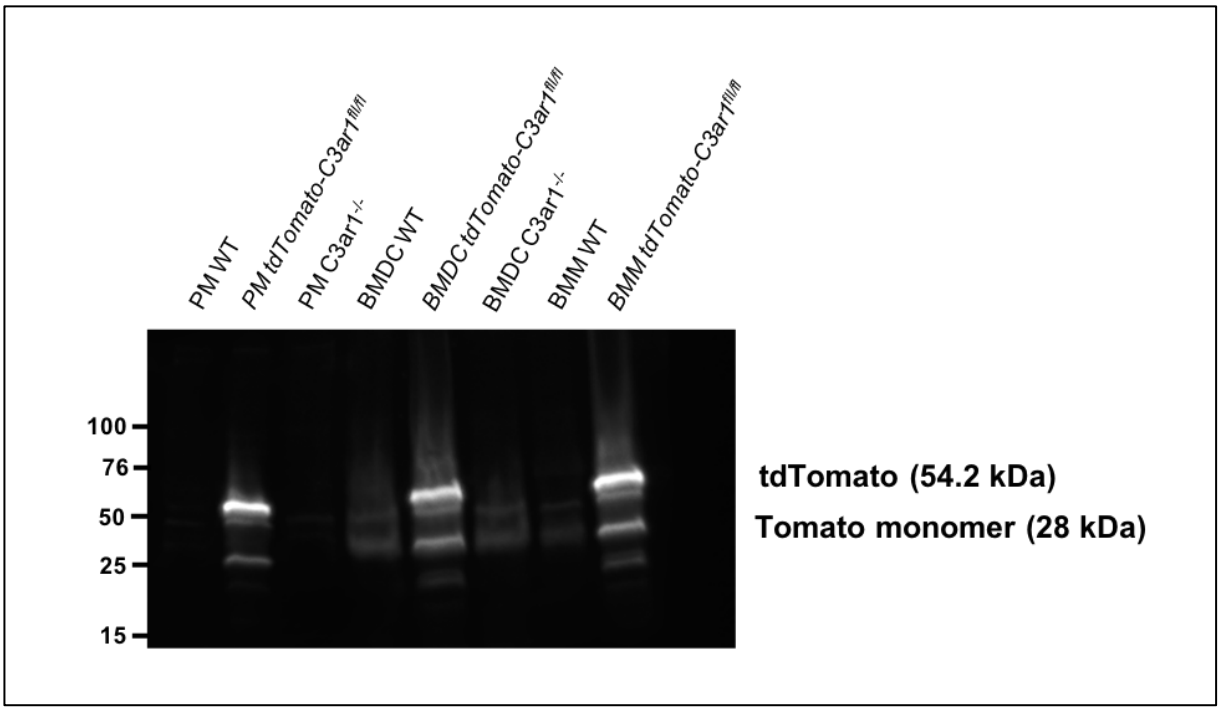

Figure 3.2 Western immunoblot of the cleaved tdTomato protein. Analysis of tdTomato has been performed by a Tomato/tdTomato-specific antibody (DsRed) of cell sorted peritoneal macrophages (PM), BM-derived DCs (BMDCs) and BM-derived macrophages (BMM) of WT, *tdTomato-C3ar1*$^{fl/fl}$ and *C3ar1*$^{-/-}$ mice by light emission with a chemiluminescence imaging system Fusion SL (Vilbert Lourmat).

To confirm the cleavage of the tdTomato from the C3aR protein, I performed a western immunoblot (WB) for the tdTomato (with DsRed) by using cell lysates from sorted peritoneal macrophages (PMs), bone marrow-derived dendritic cells (BMDCs) and bone marrow-derived macrophages (BMM) of WT, *tdTomato-C3ar1*$^{fl/fl}$ and *C3ar1*$^{-/-}$ mice (2.3.8.7). Cells were obtained as mentioned above (2.3.7.5,

2.3.7.4, 2.3.8.7) and WB performed as described in 2.3.18. Indeed, WB stained with a Tomato/tdTomato-specific antibody (Living Color® DsRed, Takara Biotech) showed a single band for Tomato and a band for a tandem-Tomato protein, but no band for a tdTomato-C3aR protein (molecular weight ~ 108 kDa) (Figure 3.2), revealing a reliable cleavage of the tdTomato during the translation of the tdTomato-C3aR sequence.

3.1.1 Alveolar macrophages show high expression levels of C5aR1 and C5aR2, but do not express C3aR at steady-state

The airways is the most continuously challenged anatomic site of the body. A variety of foreign invaders including microbial pathogens, allergens, particulates, and chemicals are stimulating the airways day and night. Therefore, an excellent balance between maintenance of physiologic homeostasis and necessary inflammatory responses is required. One cell type that can orchestrate such a fine balance is the alveolar macrophage (AM). AMs reside at the mucosal surface, have a high functional plasticity, and have the ability to communicate with neighboring cells in a paracrine manner. AMs are a good candidate to serve as a guide to either promote or suppress inflammatory responses in the airways. Hence, alveolar macrophages (AMs) are a cell type with major importance in allergic asthma. However, macrophages have been relatively overlooked in that regard and are not well characterized in the context of allergic inflammation and therefore require further investigation both at steady-state and upon allergic inflammation.

In order to get a better understanding of the function of the ATRs, my first aim was the investigation of C3aR, C5aR1 and C5aR2 receptor expression in pulmonary leukocytes, with a specific focus on alveolar macrophages at steady-state.

Airway alveolar macrophages (aAMs) are defined as cells that are washed out by bronchoalveolar lavage, whereas tissue-associated alveolar macrophages (tAMs) remain attached to the tissue. Further, they are both characterized by the expression of the C-type lectin receptor Siglec F (129, 505) and CD11c. Interestingly, although aAMs (Figure 3.3A) and tAMs (Figure 3.3B) showed high signals for tdTomato-C5aR2 and C5aR1 stained with an anti C5aR1 murine antibody (clone 20/70, Biolegend) under steady-state conditions, neither macrophage subtype expressed tdTomato-C3aR (Figure 3.3A,B).

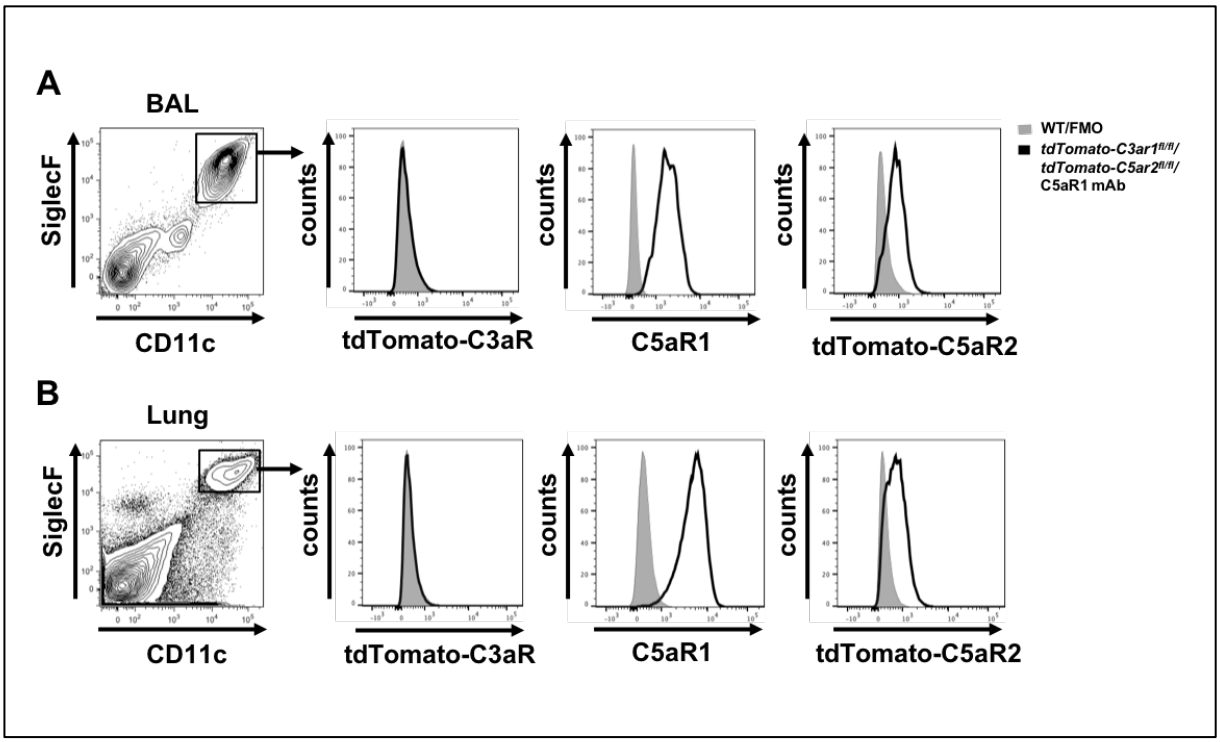

Figure 3.3 Flow cytometric assessment of tdTomato-C3aR, tdTomato-C5aR2 and C5aR1 expression in airways and tissue-associated alveolar macrophages at steady state. The grey histograms show the WT/FMO signal; the black lines correspond to the signal in the *tdTomato-C3ar1*$^{fl/fl}$, *tdTomato-C5ar2*$^{fl/fl}$ mice or the signal of the C5aR1 mAb (clone 20/70) staining. (**A-B**) Flow cytometric analysis of the tdTomato or C5aR1 signal in SiglecF$^+$CD11c$^+$ alveolar macrophages from (A) BAL fluid and (B) lung tissue.

Supporting these findings, characterizing the tdTomato-C3aR signal in lung slices by two-photon microscopy, I identified a tdTomato-C3aR signal around the airways, but only scarcely in the alveolar space (Figure 3.4A). Furthermore, a detailed look by immunofluorescence microscopy showed that CD11c$^+$SiglecF$^+$ tAMs did not express tdTomato-C3aR (Figure 3.4B). Instead of that, tdTomato-C3aR$^+$ cells around the airways were identified as CD11c$^+$ but SiglecF$^-$ cells, likely CD11c$^+$ dendritic cells (DCs). Finally, PCR analysis of *C3ar1* mRNA of purified tAMs by fluorescence activated cell sorting (2.3.8.7) provided last evidence that, in contrast to C5aR1 and C5aR2, C3aR was not expressed by alveolar macrophages upon steady-state (Figure 3.4C).

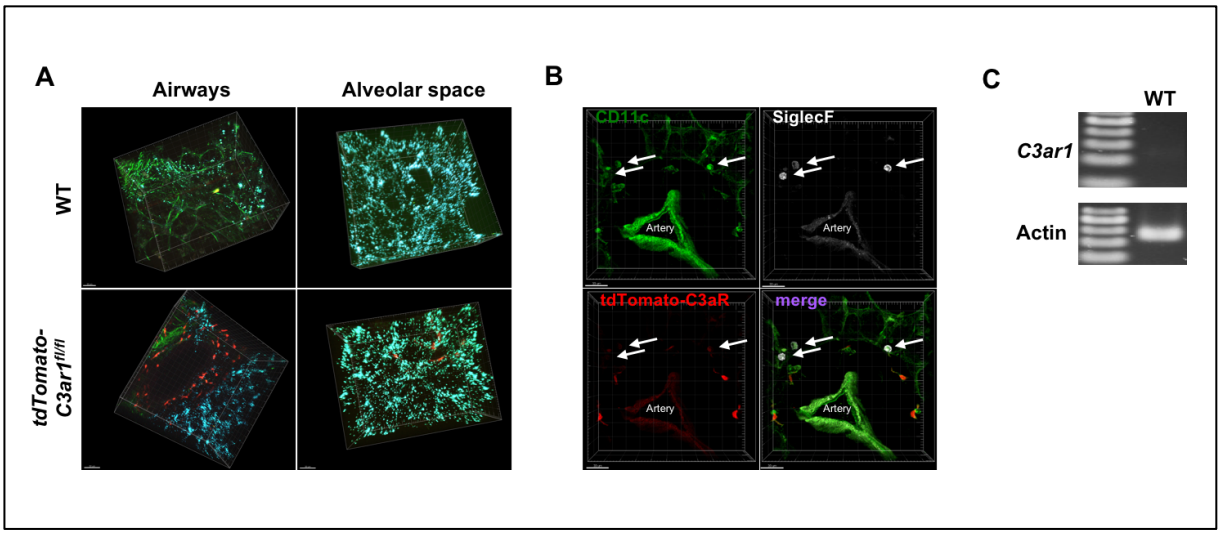

Figure 3.4 Alveolar macrophages lack C3aR expression at steady-state. (**A**) Assessment of tdTomato-C3aR expression in the lung and the airways of WT and *tdTomato-C3ar1*$^{fl/fl}$ mice by two-photon microscopy (original magnification x20). Shown is the fluorescence signal from the tdTomato-C3aR (red), from the autofluorescent connective tissue cells of the airways (green) and from the alveolar epithelial cells (turquoise). (**B**) Lung sections showing the fluorescence signal of tdTomato-C3aR (red) were stained for SiglecF (white) and CD11c (green) expression and assessed by confocal microscopy. Bars represent 30 µm. (**C**) *C3ar1* mRNA expression in tissue-associated sorted CD11c^{+}SiglecF^{+} AMs from the lungs of WT mouse.

3.1.2 C3aR expression is restricted to the myeloid lineage

Investigating the tdTomato-C3aR expression in lung tissue by flow cytometry, I found roughly two percent of all lung cells expressing tdTomato-C3aR (Figure 3.5A). Among those cells, SiglecF^{+}CD11c^{-} lung resident eosinophils, were strongly positive for the tdTomato-C3aR signal (Figure 3.5B). To determine whether tdTomato-C3aR expression correlated with C3aR protein expression, I additionally stained WT and tdTomato^{+} eosinophils with a C3aR-specific murine antibody (clone 14D4, Hycult) as described in 2.3.8.3. The C3aR specificity was verified by flow cytometry using C3aR-deficient cells as control (Figure 3.5B). Interestingly, I found no surface expression of C3aR on eosinophils. However, after saponin-based permeabilization (2.3.8.5), tdTomato^{+} eosinophils and their WT counterparts stained positive for C3aR, whereas eosinophils from *C3ar1*$^{-/-}$ mice stained negative, suggesting that lung eosinophils only express intracellular C3aR.

In previous studies, human neutrophils have been reported to strongly express C3aR (221). However, evidence for C3aR expression in mouse neutrophils is controversial (237, 277, 506). Therefore, I assessed the expression of tdTomato-C3aR in Ly6G^{+} neutrophils from lung tissue and observed that, in contrast to human neutrophils, murine pulmonary neutrophils did not express C3aR (Figure 3.5C).

Finally, several dendritic cell (DCs) subsets in the lung have been described in the past (129). Four distinct DCs populations can be discriminated as CD11b^{+} and CD103^{+}conventional DCs (cDCs), CD64^{+} monocyte-derived DCs (moDCs) and plasmacytoid DCs (pDCs). In contrast to cDCs, lungs harbor only a minor population of moDCs and pDCs at steady-state, which increases under inflammatory conditions (86, 507). In the lung, only CD11b^{+} cDCs and moDCs showed a tdTomato signal (Figure 3.5E), whereas

pDCs (Figure 3.5D) and CD103$^+$ cDCs (Figure 3.5E) did not. To correlate the tdTomato-C3aR signal with C3aR surface expression, counterstaining of pulmonary tdTomato$^+$ DCs with murine antibody (mAb) 14D4 showed surface expression of C3aR only on moDCs (Figure 3.5E), whereas CD11b$^+$ cDCs expressed C3aR in low amounts, and entirely intracellularly as shown in permeabilized cells (Figure 3.5E).

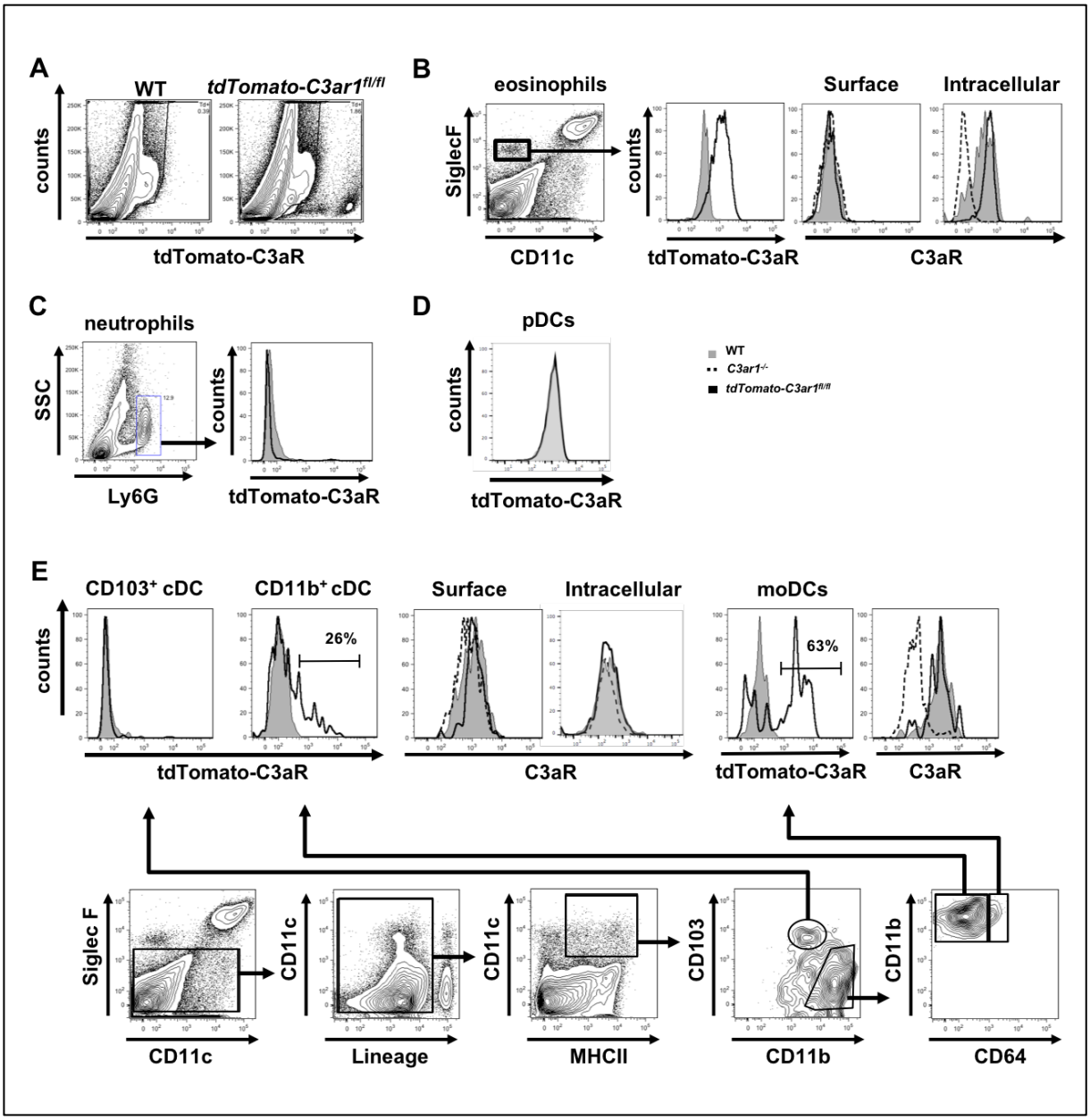

Figure 3.5 tdTomato-C3aR expression in myeloid cells from lung tissue. Flow cytometric determination of tdTomato-C3aR expression in lung cells is shown. The grey histograms show the WT signal; the black lines correspond to the signal in the *tdTomato-C3ar1$^{fl/fl}$* mice. In case of C3aR surface or intracellular expression, the dashed lines depict the staining of cells from *C3ar1$^{-/-}$* mice. (**A**) tdTomato-C3aR signal of whole lung single cell suspension of WT and *tdTomato-C3ar1$^{fl/fl}$* mice (**B-E**) tdTomato-C3aR and/or C3aR expression in (B) Siglec-F$^+$CD11c$^-$ eosinophils; (C) Ly6G$^+$ neutrophils; (D) pDCs (pre-gated on mPDCA-1 and B220); and (E) in different pulmonary DC subsets. After excluding Siglec-F$^+$ eosinophils and AMs as well as lineage$^+$ cells (CD19, CD49b, CD3e, Ly6G), DCs were identified as CD11c$^+$MHCII$^+$ cells. In the DC population, CD103$^+$ cDCs and CD11b$^+$ DCs could be distinguished. The latter population was further subdivided into CD11b$^+$ cDCs and CD64$^+$ moDCs.

In contrast to the myeloid lineage, the expression of the anaphylatoxin receptors by murine innate or adaptive lymphoid cells is controversial (188, 249, 258, 508, 509). Therefore, I used the tdTomato-C3aR reporter mouse to monitor C3aR expression by flow cytometry in pulmonary Innate Lymphoid Cells Type 1 (ILC1/NK cells), and ILC2s as well as B- and T cells. Innate lymphoid cells encompass three populations (510): group 1 with ILC1s and NK cells, ILC2s and ILC3s. Within these subpopulations ILC2s (511) and NK cells (512) reside in the lung at steady-state. Neither ILC2s (Figure 3.6A) nor NK cells (Figure 3.6C) expressed tdTomato-C3aR. In addition, also $CD4^+$ T cells (Figure 3.6B) and B cells (Figure 3.6D) lacked a tdTomato-C3aR signal. The negativity of these cells was confirmed by PCR (data not shown).

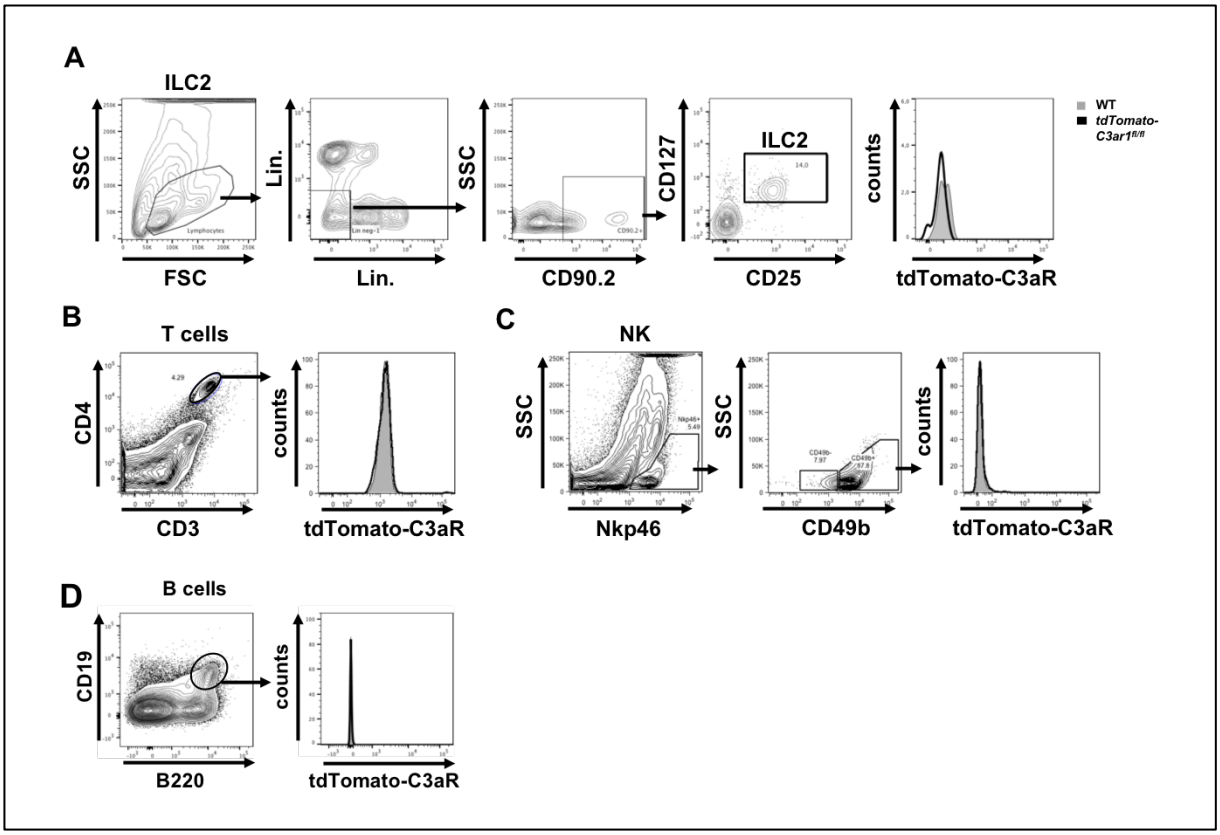

Figure 3.6 Lymphoid cells from lung tissue lack tdTomato-C3aR expression. Flow cytometric assessment of tdTomato-C3aR expression in different lymphoid populations from the lung is shown. The grey histograms show the WT signal; the black lines correspond to the signal in the *tdTomato-C3ar1*$^{fl/fl}$ mice. (**A**) tdTomato-C3aR expression in pulmonary ILC2. After excluding lineage$^+$ cells (CD19, CD49b, CD3e, Ly6G, CD11c, CD11b), ILC2s were identified as CD90.2$^+$CD127$^+$CD25$^+$ cells. (**B-D**) tdTomato-C3aR expression in pulmonary (B) CD3$^+$CD4$^+$ T cells; (C) NKp46$^+$CD49b$^+$ NK cells; (D) CD19$^+$B220$^+$ B cells.

Altogether, my results show that the expression of C3aR in pulmonary leukocytes is restricted to the myeloid lineage, albeit with exception of aAMs/tAMs, $CD103^+$ cDCs, pDCs, and neutrophils, which do not express C3aR at steady-state. Furthermore, C3aR localized either on the surface or intracellularly.

3.1.3 SiglecF$^-$ macrophages express high levels of functional C3a receptor at steady-state

F4/80 is considered as a key lineage marker for macrophages (49), except for alveolar and tissue-associated AMs, which are characterized by a high expression level of Siglec-F. In contrast to AMs, F4/80$^+$SiglecF$^-$ macrophages from visceral adipose tissue (VAT) (Figure 3.7A), from lamina propria (LP) of the small intestine (Figure 3.7B), from brain (Figure 3.7C), as well as from peritoneal cavity (PerC) (Figure 3.7D) showed a strong tdTomato-C3aR signal. Further, brain macrophages and LP macrophages were homogeneously positive for tdTomato-C3aR, whereas VAT macrophages, and microglia could be divided into C3aR$^+$ and C3aR$^-$ subpopulations (Figure 3.7). In addition, counterstaining of tdTomato$^+$ cells using the mAb 14D4, showed a C3aR surface expression in some but not all macrophage subpopulations. In particular, peritoneal macrophages (PMs) showed strong surface expression of C3aR (Figure 3.7D) whereas microglia showed only a slight surface expression (Figure 3.7C). In contrast, brain, LP, and VAT macrophages stained negative for C3aR suggesting an intracellular localization of C3aR (Figure 3.7). Indeed, for macrophages from the VAT, I could show an intracellular staining of C3aR in permeabilized cells (Figure 3.7A). Unfortunately, high background in permeabilized LP and brain macrophages precluded the intracellular assessment of C3aR in such cells. In summary, my data demonstrate that only F4/80$^+$SiglecF$^-$ macrophages express C3aR and that their C3aR surface expression is heterogeneous in the investigated organs.

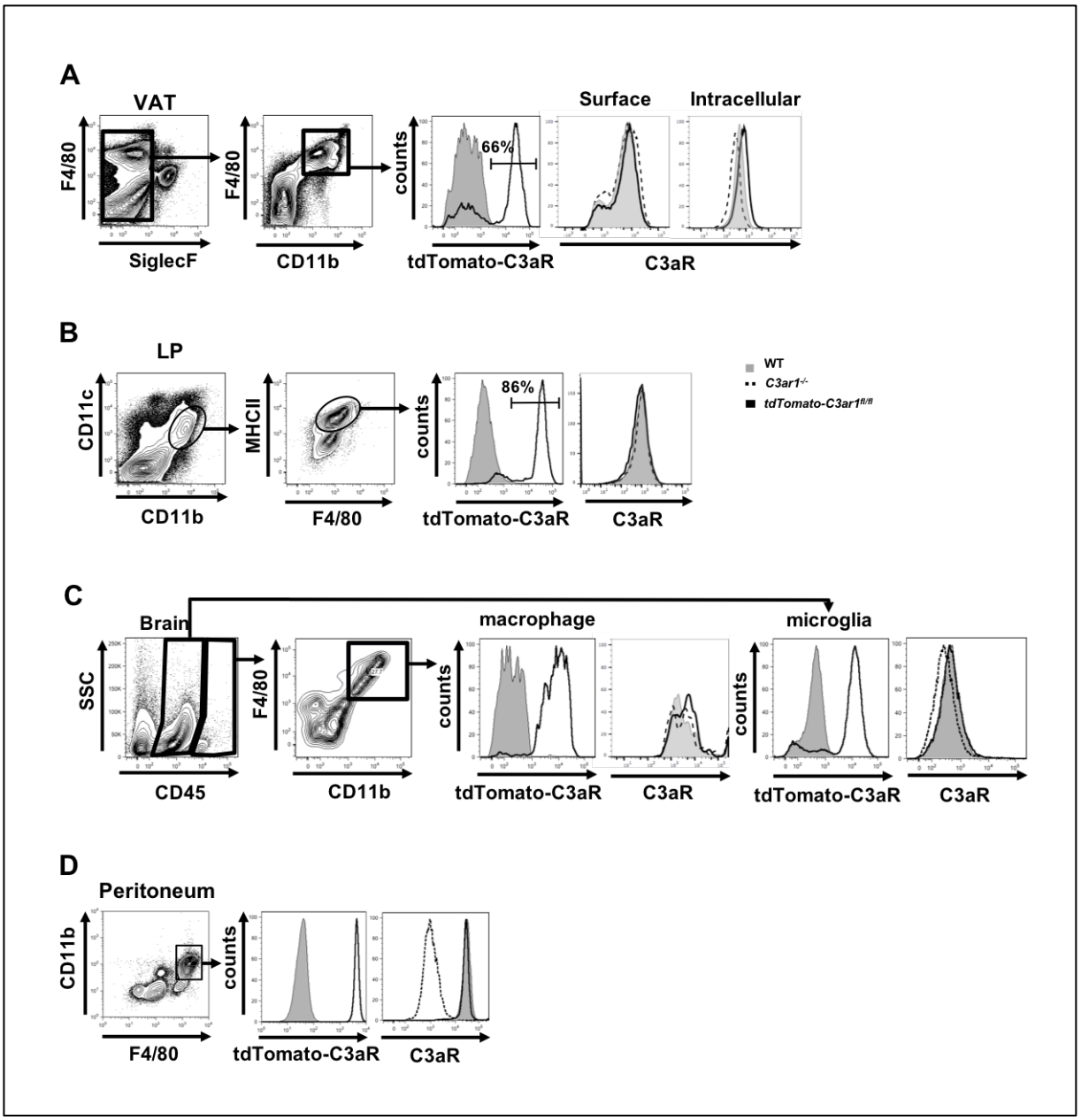

Figure 3.7 SiglecF$^-$F4/80$^+$ macrophages express tdTomato-C3aR and C3aR. Flow cytometric assessment of tdTomato-C3aR expression in different macrophage populations. The grey histograms show the WT signal; the black lines correspond to the signal in the *tdTomato-C3ar1$^{fl/fl}$* mice. In case of C3aR surface expression, the dashed lines depict the staining of cells from *C3ar1$^{-/-}$* mice. (**A-F**) tdTomato-C3aR and C3aR expression in (A) SiglecF$^-$F4/80$^+$CD11b$^+$ macrophages from VAT; (B) Lineage$^-$ CD11c$^+$CD11b$^+$MHCII$^+$F4/80$^+$ macrophages from the LP of the small intestine; (C) CD45^{hi}F4/80$^+$CD11b$^+$ macrophages and CD45^{int} microglia from brain; and (D) F4/80$^+$CD11b$^+$ peritoneal macrophages.

To assess whether the genomic construct of tdTomato with C3aR alters the functionality of the receptor, I compared functional responses of the receptor from WT and *tdTomato-C3ar1$^{fl/fl}$* mice side by side. The complement component C3a activates cells via its cell surface G protein coupled receptor (GPCR) C3aR. For most GPCRs, agonist-induced receptor phosphorylation leads to receptor desensitization due to internalization (513), and previous studies showed that stimulation of C3aR with C3a resulted in rapid internalization (7, 69). As I found strong C3aR surface expression in PMs, I used

this cell population to evaluate the C3a-driven C3aR internalization. PMs were obtained from peritoneal lavage as described in 2.3.7.5 and identified as F4/80^{+}C3aR^{+} cells. As shown, WT and *tdTomato-C3ar1*$^{fl/fl}$ macrophages expressed similar levels of C3aR at their surface (Figure 3.8A) and when incubated with increasing concentrations of C3a, they showed a rapid and similar dose-dependent decrease of C3aR surface expression. The maximum of C3aR internalization was reached 3 min after C3a stimulation using a concentration of 10 nM C3a (Figure 3.8B, Figure 3.8C), although most of the fluorescence signal disappeared within 1 min, suggesting a rapid internalization of the C3aR upon C3a stimulation (Figure 3.8C). Between 1 and 3 min after C3a administration, the fluorescence signal further declined although at a much slower pace. Eventually, the normalized C3aR MFI decreased to 30% of unstimulated controls (Figure 3.8C).

Previous studies have shown that stimulation with C3a leads to an intracellular calcium mobilization in thioglycolate-elicited PMs (223, 224, 514). In order to have an additional proof of functionality of the tdTomato-C3aR construct, I determined C3a-induced mobilization of $[Ca^{2+}]_i$ in cells from WT and *tdTomato-C3ar1*$^{fl/fl}$ mice. To do so, thioglycolate-elicited PMs were induced and collected as described in 2.3.6. The stimulation of PMs with C3a resulted in a transient increase in $[Ca^{2+}]_i$ in cells from WT and *tdTomato-C3ar1*$^{fl/fl}$ mice (Figure 3.8D). The amplitude of the response, measured as the ΔMFI, was similar in PMs of both strains. In line with the flow cytometric analysis, microscopic assessment of the C3a-mediated change in $[Ca^{2+}]_i$ confirmed the rapid and transient influx of calcium into macrophages from WT and *tdTomato-C3ar1*$^{fl/fl}$ macrophages. I observed a peak of $[Ca^{2+}]_i$ 6 s after C3a stimulation (Figure 3.8E). In contrast, we observed no change in $[Ca^{2+}]_i$ in thioglycolate-elicited PMs from *C3ar1*-deficient mice upon C3a challenge by flow cytometry.

A frequent feature of GPCR activation is the agonist-induced activation of downstream signaling pathways such as ERK1/2 phosphorylation. In particular, C3a causes a transient ERK1/2 phosphorylation of cells of a human mast cell line-1 (HMC-1) (224, 225) and human bone marrow derived-mesenchymal stem cells (226). Therefore, I investigated C3a-induced ERK1/2 phosphorylation in PMs from WT mice. In addition, *C3ar1*-deficient macrophages were used as negative control. Surprisingly, when I incubated F4/80^{+} WT PMs with different concentrations of C3a for 5 min, stimulation did not result in any intracellular ERK1/2 phosphorylation (Figure 3.8F). In order to evaluate the validity of my protocol, I used bone marrow (BM) neutrophils as a positive control, since it is well established that stimulation with C5a of BM neutrophils leads to ERK1/2 phosphorylation (251, 280, 515). I could show that stimulating these cells with 10 nM C5a for 5 min and performing the same methanol-based permeabilization and staining protocol for pERK1/2, was leading to a positive pERK1/2 staining compared to my *C5ar1*$^{-/-}$ neutrophils used as negative control. Therefore, I concluded that C3a stimulation of PMs does not trigger a downstream ERK1/2 phosphorylation.

In conclusion, my findings demonstrate that the C3aR expression in *tdTomato-C3ar1*$^{fl/fl}$ and WT macrophages is similar. Furthermore, C3a-mediated internalization of C3aR and mobilization of intracellular calcium follows the same pattern in WT and *tdTomato-C3ar1*$^{fl/fl}$ macrophages, indicating that the C3aR in *tdTomato-C3ar1*$^{fl/fl}$ mice is functional.

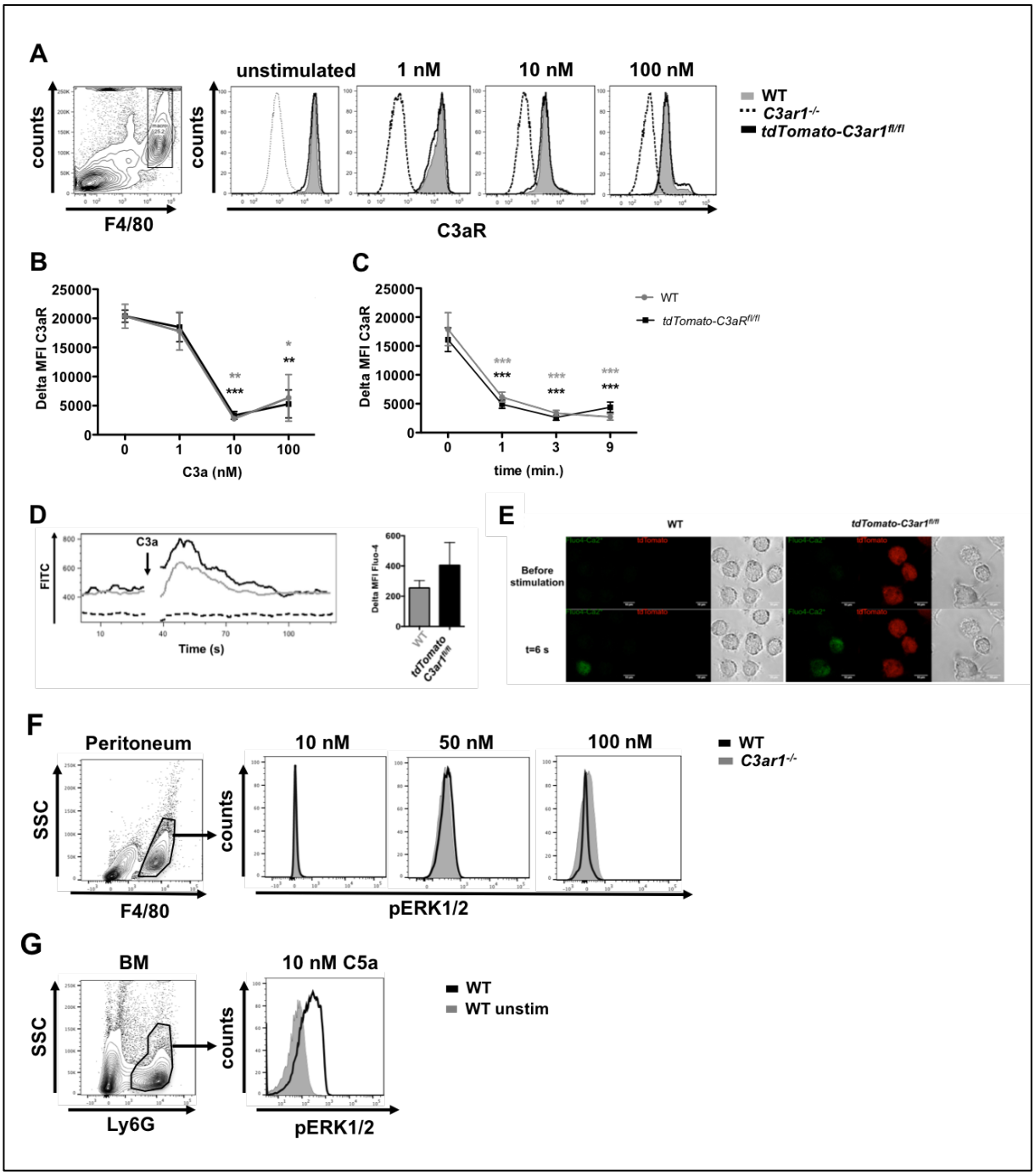

Figure 3.8 C3a drives rapid C3aR internalization and mobilization of intracellular calcium in peritoneal macrophages (PMs) from WT and *tdTomato-C3ar1*$^{fl/fl}$. (**A**) Determination of C3aR surface expression in F4/80^{+} PMs from WT (grey histogram) and *tdTomato-C3ar1*$^{fl/fl}$ mice (black line) by flow cytometry. PMs from *C3ar1*$^{-/-}$ mice (dashed line) served as controls. Data show representative histograms of the C3aR signal in unstimulated PMs as compared with 1, 10, and 100 nM C3a stimulation for 3 min at 37°C. (**B**) Comparison of C3aR surface expression in PMs from WT and *tdTomato-C3ar1*$^{fl/fl}$ mice in response to stimulation with increasing concentrations of C3a (1, 10, 100 nM) for 3 min at 37°C. Shown is the ΔMFI of C3aR staining, which is defined as the MFI obtained by C3aR staining of cells from WT or *tdTomato-C3ar1*$^{fl/fl}$ mice corrected by the C3aR

staining obtained with PMs from C3aR-deficient mice. Values shown are the mean ± SEM; n = 6 per group. (**C**) Comparison of C3aR surface expression before as well as 1, 3, and 9 min after stimulation with 10 nM C3a at 37°C. Shown is the △MFI of C3aR staining. Values shown are the mean ± SEM; n = 5–6 per group. (**D**) C3a-mediated increase of $[Ca^{2+}]_i$ in F4/80$^+$ thioglycolate-elicited PMs from WT mice (grey line), *tdTomato-C3ar1$^{fl/fl}$* mice (black line), or *C3ar1$^{-/-}$* (dashed line) mice. Shown is the △MFI of the fluorescence peak. Values shown are the mean ± SEM; n = 7 per group. Statistical differences between groups were assessed by a Student t test. (**E**) Microscopic evaluation of the C3a-mediated change of $[Ca^{2+}]_i$ in thioglycolate-elicited PMs from WT and *tdTomato-C3ar1$^{fl/fl}$* mice. Adherent thioglycolate-elicited PMs from both groups were loaded with Fluo4-AM and challenged with C3a (37 nM). The images show the fluorescence emission in the FITC (Fluo4 emission) and PE channels (tdTomato), as wells as from polarized light before and 6 s after C3a stimulation (x40 objective). Scale bar, 10 mm. Data are representative of three independent experiments. (**F-G**) Flow cytometric assessment of pERK1/2 in (F) F4/80$^+$ PMs and (G) Ly6G$^+$ BM neutrophils from WT mice (black line). *C3ar1$^{-/-}$* mice or unstimulated WT cells (grey histogram) served as controls. Data show representative histograms of phosphorylated ERK1/2 in PMs stimulated with 10, 50 and 100 nM hC3a or BM neutrophils stimulated with 10 nM hC5a both for 5 min at 37°C. * $p < 0.05$, ** $p < 0.01$, *** $p < 0.001$.

3.2 C3aR is involved in the severity of a house dust mite-mediated allergic asthma model

Two decades ago, the C3a receptor was shown to play an important role in the development of allergic asthma (460, 484). Therefore, C3a has been described as a strong pro-inflammatory factor that is a critical driver of bronchoconstriction during the effector phase of allergic asthma (407, 460, 484). However, the airway resistance was determined using different measurement techniques and new data coming from different studies led to controversial discussions about the functions of C3aR (516). Therefore, the role and function of the C3a/C3aR axis required renewed investigation and evaluation.

3.2.1 Absence of C3aR decreased the airway hyperresponsivness during the effector phase of allergic asthma

In order to delineate the role and functions of C3aR in the effector phase of allergic asthma, I investigated the asthmatic phenotype of *C3ar1$^{-/-}$* mice compared to WT mice after four times HDM i.t. administration, evaluated by changes in airway resistance compared to a PBS control in response to increased concentration of nebulized methacholine (Figure 3.9). Mice were immunized as described in 2.3.3.3. Control mice were immunized with PBS according to the same protocol.

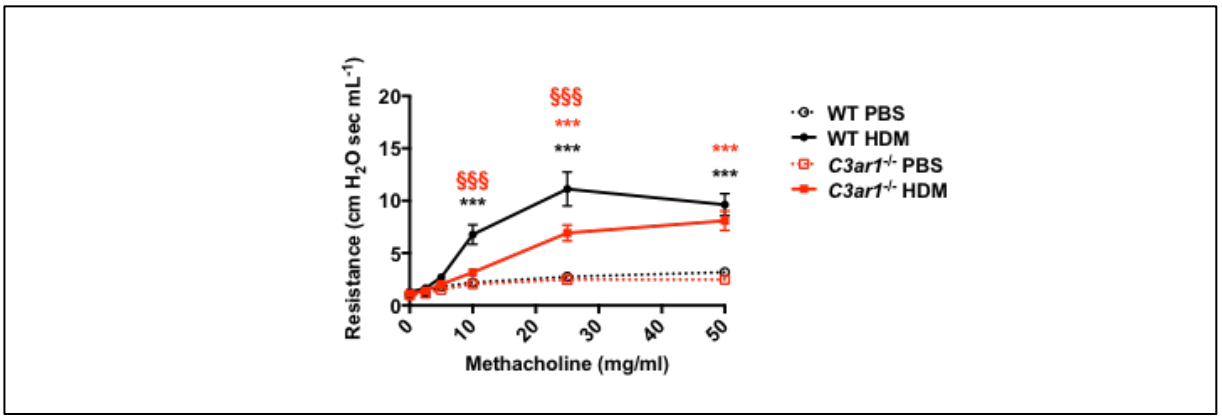

Figure 3.9 *C3ar1*-deficient mice develop a milder AHR compared to WT. AHR in response to i.t. administration of methacholine measured as airway resistance. Shown are dose-response curves after four times HDM i.t. administration from WT (black line) or *C3ar*1-deficient mice (red line) using 10, 25, or 50 mg/ml methacholine. WT (dashed black line) or *C3ar1*-deficient mice (dashed red line) treated with PBS were used as controls. Values shown are the mean ± SEM; n = 6–10 per group; * or § $p < 0.05$, ** or §§ $p < 0.01$, *** or §§§ $p < 0.001$. § is used to indicate significant differences between WT and *C3ar1*$^{-/-}$ groups.

C3ar1$^{-/-}$ mice showed a significant reduced asthmatic phenotype at 10 and 25 mg/ml nebulized methacholine compared to WT mice. However, at 50 mg/ml C3aR-deficient mice reached a similar plateau than WT mice.

3.2.2 C3aR is dispensable for the pulmonary recruitment and the composition of immune cells during the effector phase of allergic asthma

Inhaled allergens drive airway epithelial cell activation and damages, which cause the secretion of various alarmins. These epithelial-derived mediators promote type 2 inflammation through their indirect actions on DCs and their direct actions on ILC2s and $CD4^+$ T cells. Both Th2 cells as well as ILC2s elaborate characteristic type 2 cytokines including interleukin (IL)-4, IL-5, and IL-13, instrumental for the activation and recruitment of other immune cells to the lung e.g. eosinophils.

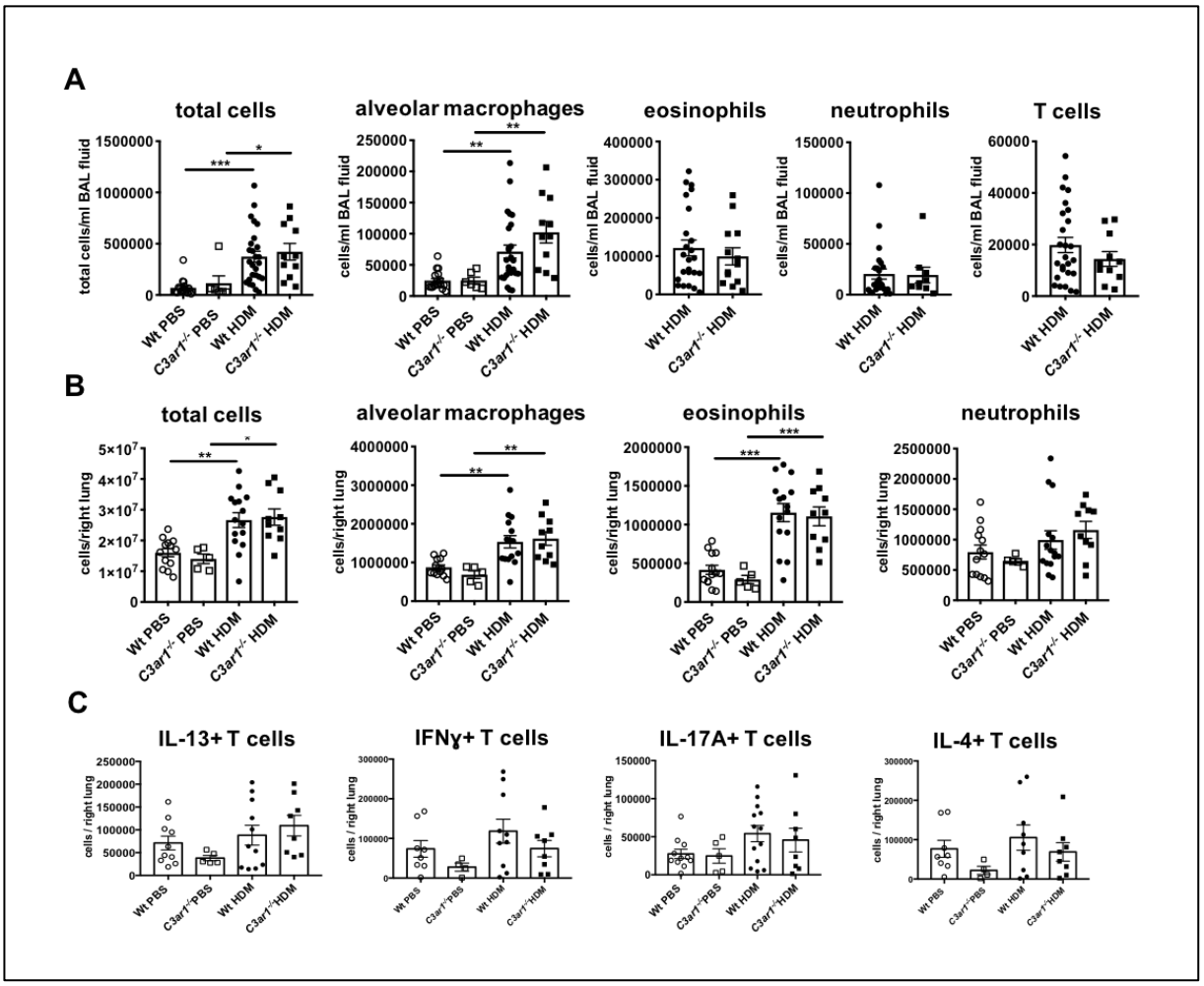

Figure 3.10 WT and mice *C3ar1*$^{-/-}$ mice show a strong and similar pulmonary recruitment of inflammatory cells during the allergic effector phase. (**A-B**) Differential cell counts of PBS-treated or HDM-immunized WT or *C3ar1*$^{-/-}$ animals in (A) BAL fluid and (B) lung tissue. Values shown are the mean ± SEM; n = 6-25 per group. (**C**) Differential cell counts of T cells from PBS-treated or HDM-immunized WT or *C3ar1*$^{-/-}$ animals. For that, whole lung single cell suspension was stimulated with PMA, ionomycin, brefeldin and monensin and intracellular cytokine secretion of $CD3^{+}CD4^{+}$ T cells determined by flow cytometry. Values shown are the mean ± SEM; n = 4-12 per group. * $p < 0.05$, ** $p < 0.01$, *** $p < 0.001$.

In agreement, HDM-induced allergic asthma in WT mice led to an increase in the total number of immune cells in BAL fluid (Figure 3.10A) and lung tissue (Figure 3.10B) compared to PBS-treated controls. They also showed increased levels of aAMs (Figure 3.10A) and tAMs (Figure 3.10B) as well as a strong eosinophilia (Figure 3.10A and Figure 3.10B). Since the absence of C3aR was responsible for a decrease in the dose response curve of the measured airway hyperresponsiveness (see 3.2.1), I expected a reduced cell recruitment and differences in the cell composition in absence of C3aR. However, *C3ar1*$^{-/-}$ mice treated with HDM showed no differences in cell recruitment and composition compared to WT mice in BAL fluid and lung tissue, with similar numbers of alveolar macrophages, eosinophils, neutrophils and T cells (Figure 3.10A and Figure 3.10B). In addition, T cell activation and intracellular cytokine staining for IL-13, IL-4, IFN-ɣ, and IL-17A (see 2.3.8.5) were the same in WT and in absence of C3aR (Figure 3.10C).

Therefore, my data show that C3aR has an impact on an allergen-induced AHR without influencing the development of Th2 immunity and airway inflammation.

3.2.3 HDM-mediated allergic asthma leads to a *de novo* upregulation of C3aR in airway and tissue-associated alveolar macrophages

Although there were no differences in the cell composition and cell recruitment between WT and *C3ar1*$^{-/-}$ mice, there was the reduction in the airway hyperresponsivness in absence of C3aR. Since pulmonary epithelial cells do not express C3aR at steady-state (227, 517), also shown by the lack of tdTomato-signal of alveolar epithelial cells in 2-photon microscopy (Figure 3.4A), it was still unclear which cells actually express C3aR upon induction of allergic asthma and could therefore participate in airway contraction and sensitivity through C3aR in allergic asthma.

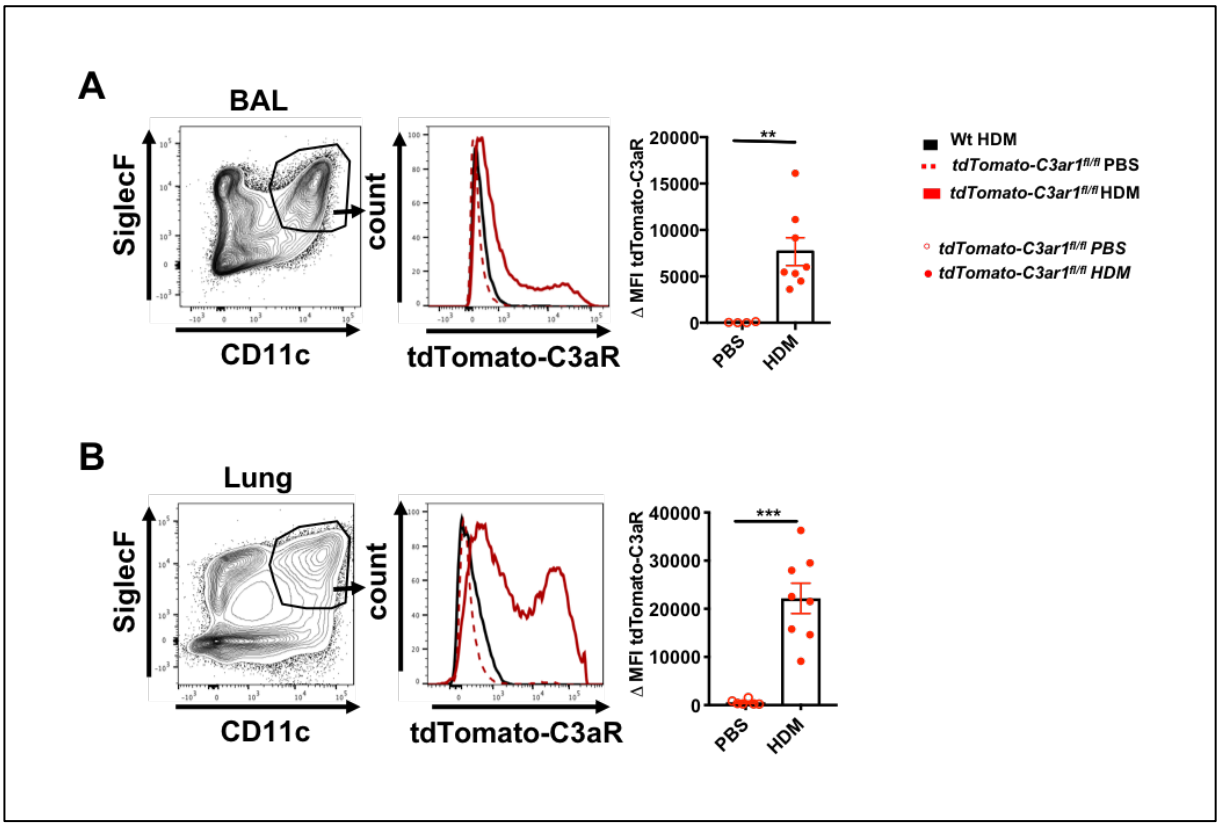

Figure 3.11 *De novo* C3aR expression of AMs upon HDM-mediated allergic asthma. Flow cytometric assessment of tdTomato-C3aR expression in alveolar macrophages after 4 times PBS- or HDM-treated WT and *tdTomato-C3ar1*$^{fl/fl}$ mice. The black histograms show the WT signal; the red lines correspond to the signal in the HDM-treated *tdTomato-C3ar1*$^{fl/fl}$ mice; the dashed red lines depict the signal in PBS-treated *tdTomato-C3ar1*$^{fl/fl}$ control mice. (**A-B**) tdTomato-C3aR in SiglecF^{+}CD11c^{+} alveolar macrophages from (A) BAL fluid or (B) lung tissue. In addition, it is shown the ΔMFI of the tdTomato-C3aR signal, which is defined as the MFI obtained by the tdTomato-C3aR signal of cells from *tdTomato-C3ar1*$^{fl/fl}$ mice treated with PBS (red open circles) or HDM (red circles) corrected by the tdTomato-C3aR signal obtained with cells from WT mice**.** Values shown are the mean ± SEM; n = 4-8 per group. ** $p < 0.01$, *** $p < 0.001$.

Interestingly, when I drove an HDM-mediated effector phase in WT and *tdTomato-C3ar1*$^{fl/fl}$ mice, SiglecF^{+}CD11c^{+} aAMs and tAMs, which did not express C3aR at steady-state (3.1.1), showed by flow cytometry a massive *de novo* upregulation of tdTomato-C3aR (Figure 3.11A and Figure 3.11B). Furthermore, looking more in detail, tAMs showed a stronger increase in tdTomato-C3aR in comparison to airway alveolar macrophages. Moreover, SiglecF^{+}CD11c^{+} AMs showed a C3aR^{hi} and a C3aR^{low} subpopulation. In line with the flow cytometry data, I could identify a strong increase of the tdTomato-C3aR signal around the airways in lung slices by two-photon microscopy (Figure 3.12A). Further, immunohistochemistry staining revealed that CD11c^{+}SiglecF^{+} aAMs and tAMs were positive for the tdTomato-C3aR signal, although not all tAMs seemed to be tdTomato^{+}, recapitulating the result of a C3aR^{hi} and C3aR^{low} population (Figure 3.12B).

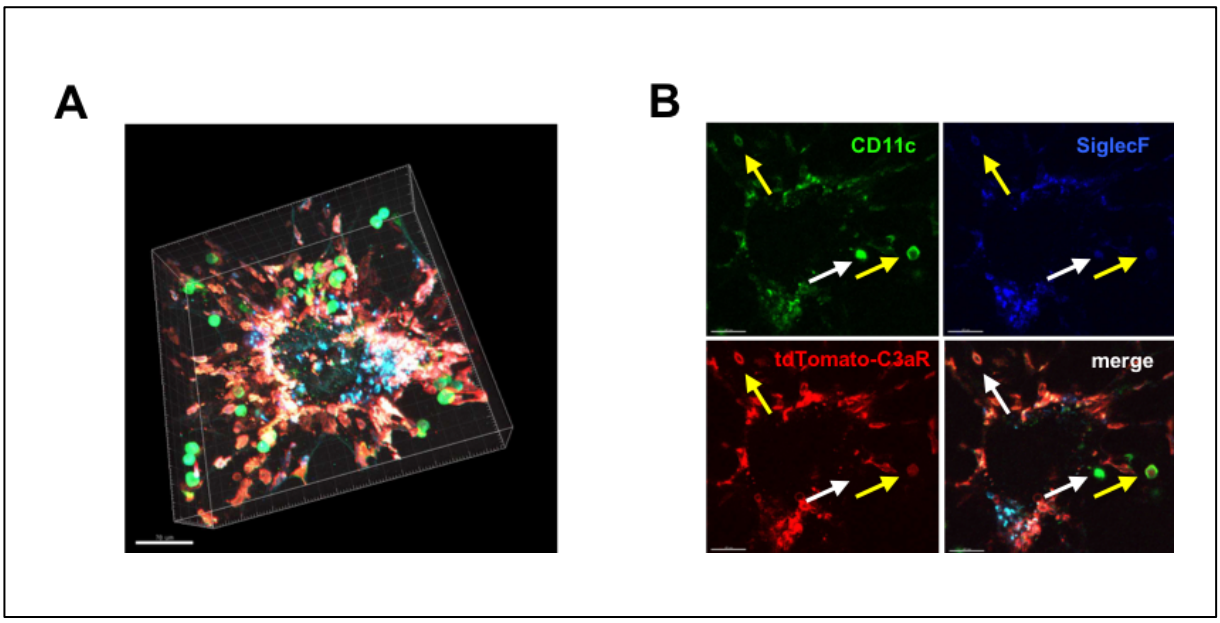

Figure 3.12 tdTomato-C3aR expression of AMs upon allergic asthma. (**A**) Assessment of tdTomato-C3aR expression in the lung of WT and *tdTomato-C3ar1*$^{fl/fl}$ mice by two-photon microscopy (original magnification x20). Shown is the fluorescence signal of tdTomato-C3aR (red) from autofluorescent connective tissue cells of the airways (turquoise) and from CD11c^{+} (green), SiglecF^{+} (blue) cells. Bars represent 70 µm. (**B**) Lung sections showing the fluorescence signal of tdTomato-C3aR (red) were stained for SiglecF (blue) and CD11c (green) expression and assessed by confocal microscopy. Yellow arrows mark tdTomato^{+} AMs; white arrows mark tdTomato^{-} AMs. Bars represent 30 µm.

3.2.4 C3aR upregulation in alveolar macrophages increases upon repeated allergen exposure

Although I identified a strong *de novo* upregulation of C3aR during the effector phase of allergic asthma, I was interested in assessing the C3aR expression during the sensitization phase of allergic asthma. Therefore, I induced an HDM-mediated allergen sensitization (2.3.3.1) in WT and *tdTomato-C3ar1*$^{fl/fl}$ mice. As shown in Figure 3.13A, tAMs started to upregulate C3aR already after one allergen contact, but this increase in C3aR expression strengthen upon repeated allergen exposure. In detail,

mice showed a 5-fold increase in the ΔMFI of tdTomato-C3aR between one and four times HDM-administration (Figure 3.13C). Further, mice that were treated four times with HDM showed 8-times higher levels of tdTomato^{hi} tAMs compared to mice which were treated only once with HDM (Figure 3.13D).

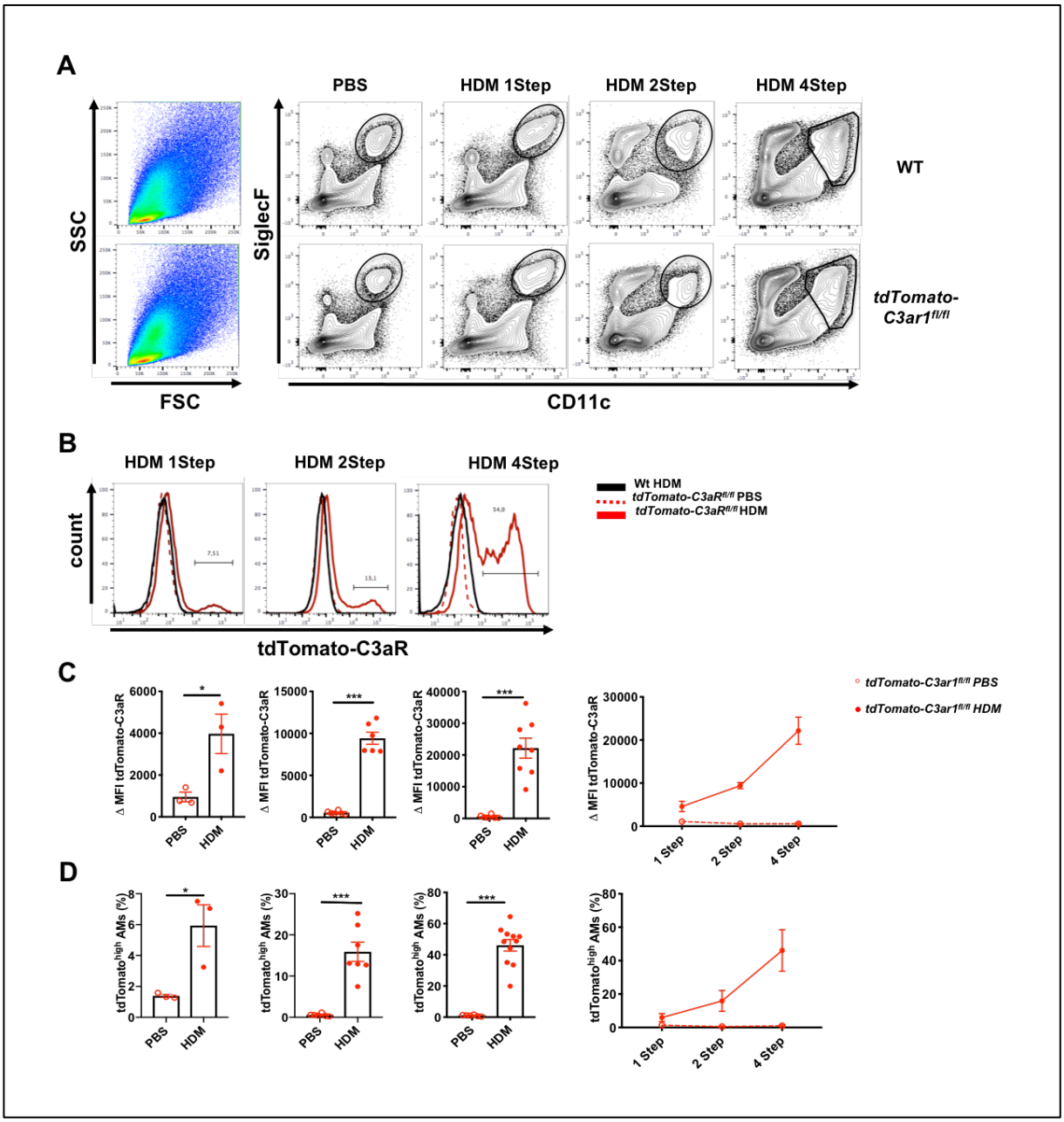

Figure 3.13 AMs upregulate C3aR upon repeated HDM-exposure. (**A**) Flow cytometric gating strategy of SiglecF+CD11c+ AMs of WT and *tdTomato-C3ar1$^{fl/fl}$* mice after 1, 2 or 4 times i.t. administration of PBS or HDM extract. (**B**) Flow cytometric assessment of tdTomato-C3aR expression in alveolar macrophages after 1, 2 or 4 times i.t treatment with PBS or HDM in WT and *tdTomato-C3ar1$^{fl/fl}$* mice. The black histograms show the WT signal; the red lines correspond to the signal in the HDM-treated *tdTomato-C3ar1$^{fl/fl}$* mice; the dashed red lines depict the signal in PBS-treated *tdTomato-C3ar1$^{fl/fl}$* control mice. (**C-D**) Increase in the (C) ΔMFI of the tdTomato-C3aR signal and (D) the frequency of tdTomato^{high} AMs after 1,2 or 4 i.t. administration of PBS or HDM in *tdTomato-C3ar1$^{fl/fl}$* mice**.** The red circles correspond to the signal in the HDM-treated *tdTomato-C3ar1$^{fl/fl}$* mice; the open red circles depict the signal in PBS-treated *tdTomato-C3ar1$^{fl/fl}$* control mice. Values shown are the mean ± SEM; n = 3-11 per group. * $p < 0.05$, ** $p < 0.01$, *** $p < 0.001$.

3.2.5 Both, airway and tissue-associated alveolar macrophages show elevated levels of C3aR in comparison to other pulmonary leukocytes in a house dust mite-mediated allergic asthma model

Besides the AMs, the expression of C3aR in other immune cells participating to the severity of allergic asthma was evaluated in the *tdTomato-C3ar1*$^{fl/fl}$ mice. In addition to alveolar macrophages, eosinophils from BAL fluid showed increased levels of tdTomato-C3aR (Figure 3.14A). Comparing the amplitude of the tdTomato MFI of both cell types showed that the level of C3aR expression was 6-fold higher in alveolar macrophages (Figure 3.11A) compared to eosinophils (Figure 3.14A). Furthermore, in lung tissue, CD11b^{+} cDCs, which were already C3aR^{+} at steady-state (3.1.2), showed an increase in tdTomato-C3aR whereas moDCs did not, compared to naïve conditions (Figure 3.14B). Analyzing the ΔMFI of tdTomato-C3aR, showed a 3-fold higher level of C3aR in tAMs (Figure 3.11A) compared to CD11b^{+} cDCs (Figure 3.14B). Furthermore, cells from the lymphoid lineage showed only minor increases (CD4^{+} T cells) or no changes in the tdTomato-C3aR expression compared to cells from PBS-treated control mice (Figure 3.14B).

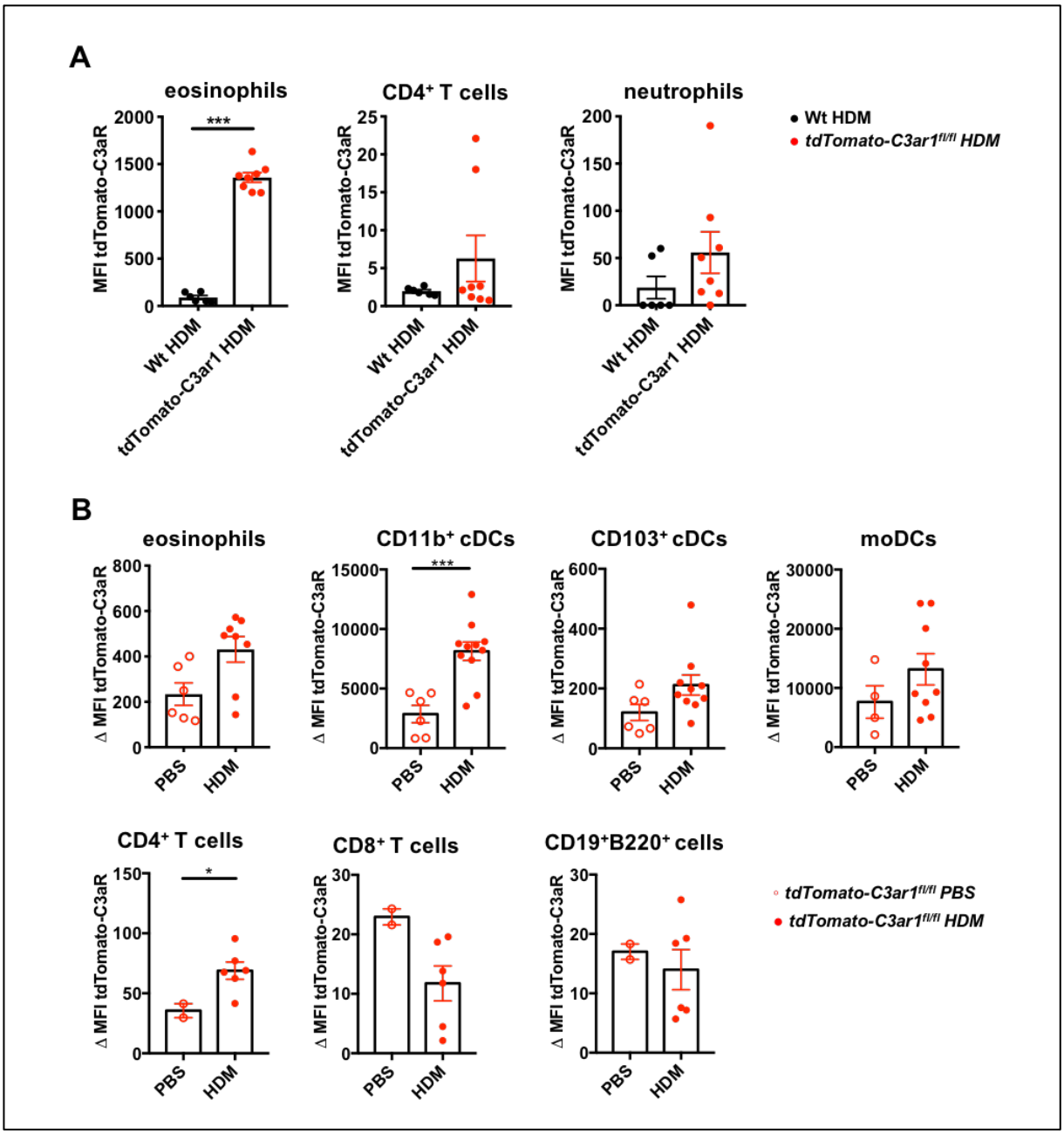

Figure 3.14 tdTomato-C3aR expression in pulmonary leukocytes from BAL and lung tissue during the effector phase of allergic asthma. (**A**) Assessment of the MFI of the tdTomato-C3aR signal in various pulmonary leukocytes from BAL fluid after 4 times i.t. treatment with HDM in WT and *tdTomato-C3ar1*$^{fl/fl}$ mice. The data show only measures in BAL from HDM-triggered airway inflammation in Wt and *tdTomato-C3ar1*$^{fl/fl}$ mice, since these leukocytes are not present in the airways at steady state/PBS. Black circles show the WT signal; the red circles correspond to the signal in the HDM-treated *tdTomato-C3ar1*$^{fl/fl}$ mice. (**B**) Assessment of the ΔMFI of the tdTomato-C3aR signal in various pulmonary leukocytes from lung tissue after 4 times i.t. treatment with PBS or HDM in *tdTomato-C3ar1*$^{fl/fl}$ mice. The filled red circles correspond to the signal in the HDM-treated *tdTomato-C3ar1*$^{fl/fl}$ mice; the open red circles depict the signal in PBS-treated *tdTomato-C3ar1*$^{fl/fl}$ control mice. Values shown are the mean ± SEM; n = 2-10 per group. * $p < 0.05$, ** $p < 0.01$, *** $p < 0.001$.

In conclusion, airway and tissue-associated AMs show the highest upregulation of C3aR in comparison to other pulmonary leukocytes. Except of CD4⁺ T cells, AMs are the only cell type which upregulated C3aR *de novo* upon an HDM-mediated allergic asthma development. Taking all results into consideration leads me to the finding that alveolar macrophages are a very important pulmonary cell

type that is involved in the effector phase of allergic asthma through the upregulation of C3aR and has been so far underestimated.

3.2.6 Alveolar macrophages show a reciprocal regulation of C3aR and C5aR1 upon allergic asthma conditions

In a mouse model it has been shown that reciprocal modulation of C3aR and C5aR expression, in pulmonary DCs, resulted in reciprocal suppression of C3aR- and C5aR-mediated biological functions (478). Although alveolar macrophages did not express C3aR upon steady-state, they show a relatively high expression level of C5aR1 (249, 518). In contrast, the expression of C5aR1 has been shown to be down regulated in an OVA-induced allergic asthma model (518). Therefore, I hypothesized that a reciprocal regulation of C3aR and C5aR1 would be observed in AM populations following allergen treatment.

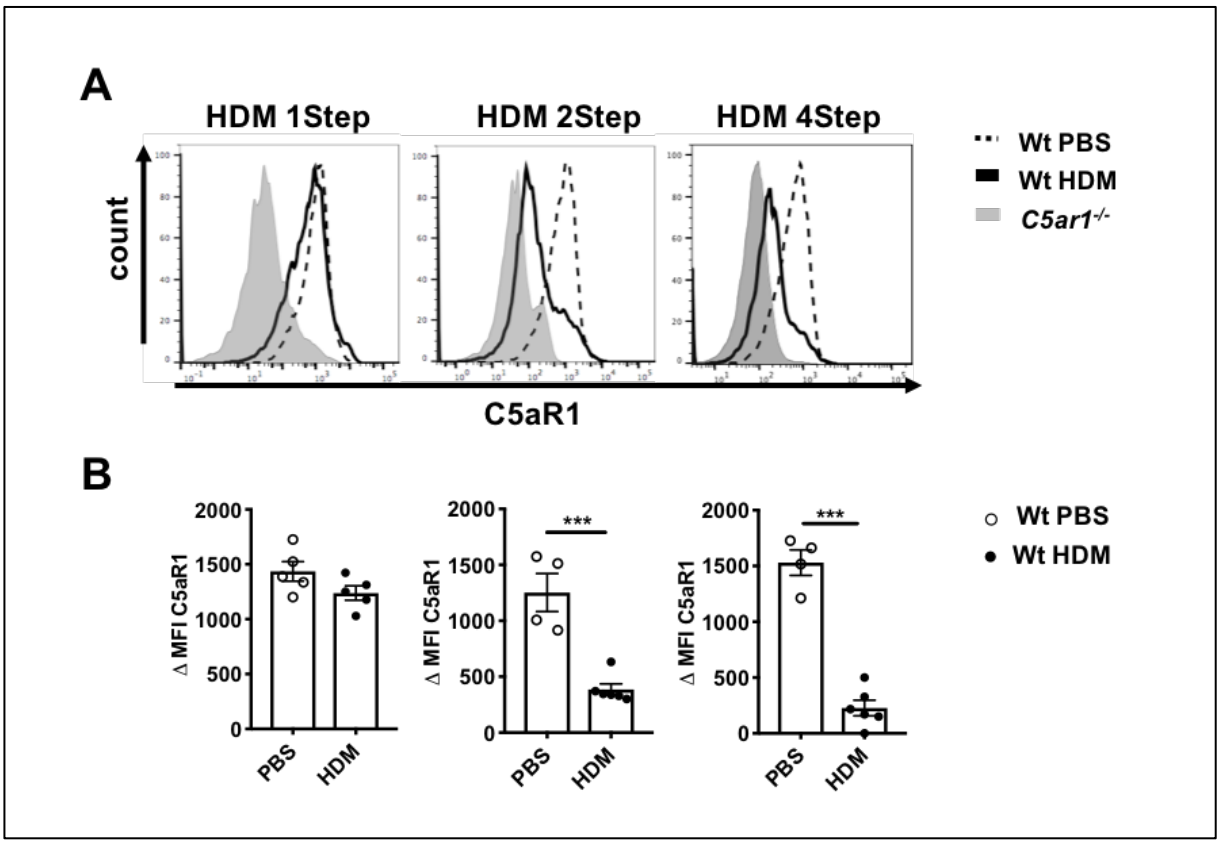

Figure 3.15 AMs downregulate C5aR1 expression upon repeated allergen exposure. (A) Flow cytometric assessment of C5aR1 mAb (20/70) staining in SiglecF^{+}CD11c^{+} AMs from WT mice upon 1, 2 or 4 times i.t. treatment with PBS or HDM. The black lines correspond to the signal in the WT HDM-treated mice; the dashed lines depict the staining of WT mice treated with PBS; the grey histogram depict the staining of cells from *C5ar1*$^{-/-}$ mice. (**B**) ΔMFI of C5aR1 signal in WT mice i.t treated 1, 2 or 4 times with PBS or HDM. ΔMFI was defined as the MFI obtained by C5aR1 signal of cells from WT mice treated with PBS or HDM corrected by the C5aR1 signal obtained with cells from *C5ar1*$^{-/-}$ mice**.** The black circles show the WT HDM signal; the open black circles depict the signal in PBS-treated WT mice. Values shown are the mean ± SEM; n = 4-6 per group. *** p < 0.001.

To test this hypothesis, I investigated the dynamic changes of C5aR1 expression during an HDM-induced allergic asthma development. I immunized WT and *C5ar1*$^{-/-}$ mice once, twice or four times with 100 μg HDM as described in 2.3.3.1, 2.3.3.2. and recapitulated our observations made in the OVA model. Indeed, tissue-associated AMs downregulated C5aR1 upon repeated allergen exposure, although one i.t. administration of HDM the expression level of C5aR1 did not show a significant reduction in comparison to PBS treated control mice (Figure 3.15). However, after a second HDM exposure the ΔMFI of C5aR1 on alveolar macrophages decreased 3-fold in HDM-treated mice compared to PBS control mice. Finally, in the 4-times exposed effector allergic asthma phase, the MFI was nearly on the same level as of mice deficient in C5aR1 (Figure 3.15).

Since AMs upregulate C3aR expression already after one allergen challenge, but C5aR1 is downregulated only after a second allergen contact, these data suggest that C3aR may preclude the downregulation of C5aR1.

3.3 Anaphylatoxin receptor expression in alveolar macrophages is regulated by IL-33 and IL-13

3.3.1 C3aR^{hi} and C3aR^{low} tAMs express different levels of major histocompatibility complex II, but show both a characteristic macrophage phenotype

Major histocompatibility complex (MHC) molecules are highly polymorphic cell-surface proteins encoded by MHC class I and MHC class II genes and are involved in presentation of peptide antigens to T cells. MHC class II molecule is expressed primarily on specialized antigen-presenting cells, where it presents antigenic peptides derived from internalized extracellular proteins, to CD4^{+} T cells and also binds to the co-receptor CD4. While investigating C3aR in SiglecF^{+}CD11c^{+} tAMs during the effector phase of allergic asthma, I observed an upregulation of MHCII molecules in HDM treated WT mice in comparison to PBS control mice (Figure 3.16A and Figure 3.16B). Interestingly, not only the upregulation was homogeneously distributed, and cells could be rather divided in a MHCII^{-} and MHCII^{+} subpopulation, but also that MHCII^{+} tAMs were C3aR^{hi}, whereas MHCII^{-} tAMs were C3aR^{low} in tdTomato-C3ar1$^{fl/fl}$ mice (Figure 3.16C). Interestingly, fluorescence activated cell sorted (2.3.8.7) WT HDM-induced MHCII^{+} and MHCII^{-} cells showed a similar expression level of the *C3ar1* mRNA in both groups (Figure 3.16B) by RT-PCR analysis (2.3.17).

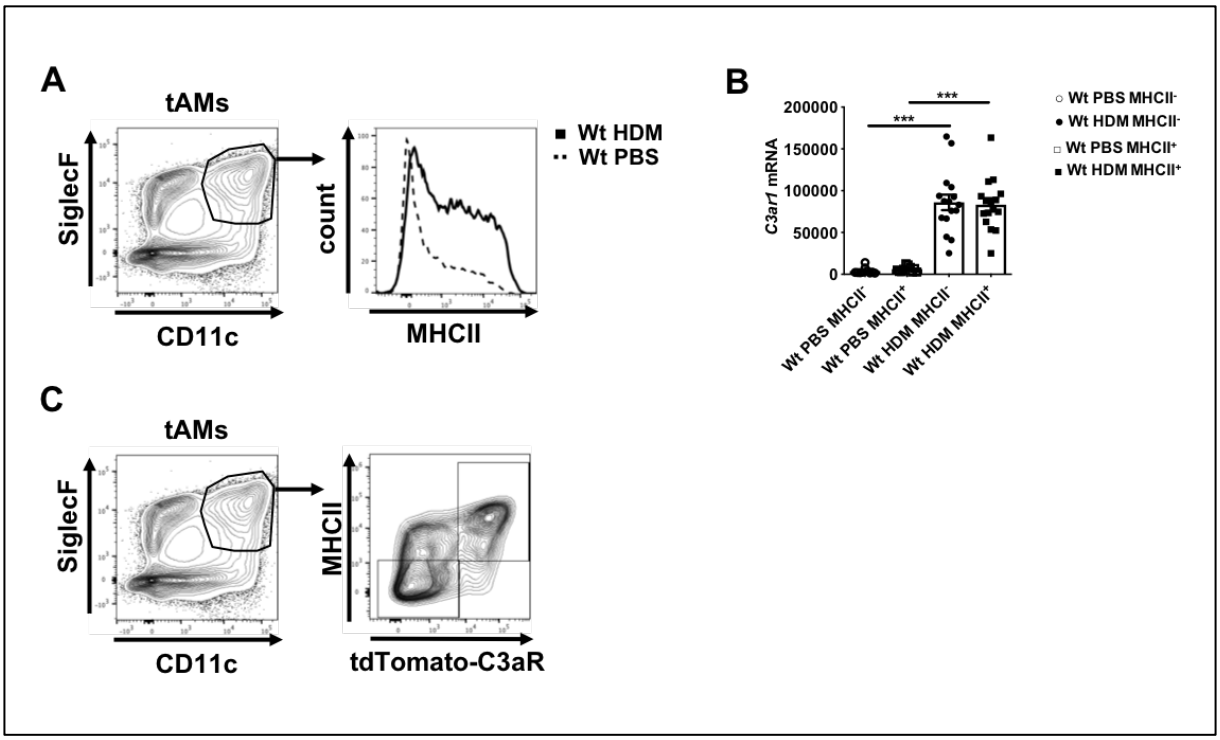

Figure 3.16 tAMs encompass a C3aR^{hi}MHCII^{+} and C3aR^{low}MHCII^{-} subpopulation during an established allergic asthma. (A) Flow cytometric assessment of MHCII mAb (I-A/I-E) staining in SiglecF^{+}CD11c^{+} AMs from WT mice treated 4 times with PBS or HDM. The black lines correspond to the signal in the WT HDM-treated mice; the dashed lines depict the staining of WT mice treated with PBS. (**B**) Analysis of C3ar1 mRNA levels of MHCII^{+} (squares) and MHCII^{-} (circles) AMs from WT mice either treated 4 times with HDM (filled symbol) extract or with PBS (open symbol) as control. (**C**) Flow cytometric assessment of tdTomato-C3aR and MHCII signal in SiglecF^{+}CD11c^{+} AMs from *tdTomato-C3ar1$^{fl/fl}$*. Values shown are the mean ± SEM; n = 6-14 per group. *** $p < 0.001$.

To further evaluate the origin and characteristics of the MHCII^{+}C3aR^{hi} and MHCII^{-}C3aR^{low} population, I investigated the two populations for specific macrophage markers. Although a large number of markers are used to commonly identify and characterize macrophages, the exact set of markers to use depends on the subset of macrophage and the conditions of their local environment. In addition to the expression of Siglec-F and CD11c (505), resident a/tAMs are characterized by high levels of CD64 (505) and Mer tyrosine kinase (MerTK) (519, 520), but low expression levels of CD11b (130, 520) and F4/80 (128).In addition, as stated in the introduction, when macrophages become activated upon recognition and initiate a response to certain stimuli, they polarize according these conditions into M1 and/or M2 macrophages. M1 macrophages express high levels of nitric oxide synthase 2 (NOS2) and low levels of Arginase 1 (Arg1), and have pro-inflammatory properties (107). In contrast, M2 macrophages are Arg1^{hi} and NOS2^{low}, while developing, in context of a Th2 immune response, tissue remodeling and repair functions (107). Interestingly, both MHCII^{+}C3aR^{hi} and MHCII^{-}C3aR^{low} cells expressed similar levels of MerTK and CD64, while they remained CD11b low and F4/80 negative (Figure 3.17B) confirming their macrophage phenotype. Moreover, fluorescence activated cell sorting (2.3.8.7) of WT HDM MHCII^{+} and MHCII^{-} cells, followed by RT-PCR analysis (2.3.17) revealed a similar macrophage phenotype characterized by high levels of *Arg1* and low levels of *Nos2* (Figure 3.17A) reflecting an M2

macrophage polarization. In addition, both MHCII^{+} and MHCII^{-} AMs showed a low expression level of *Ccr2* mRNA (Figure 3.17A), suggesting that they did not derive from blood recruited monocytes.

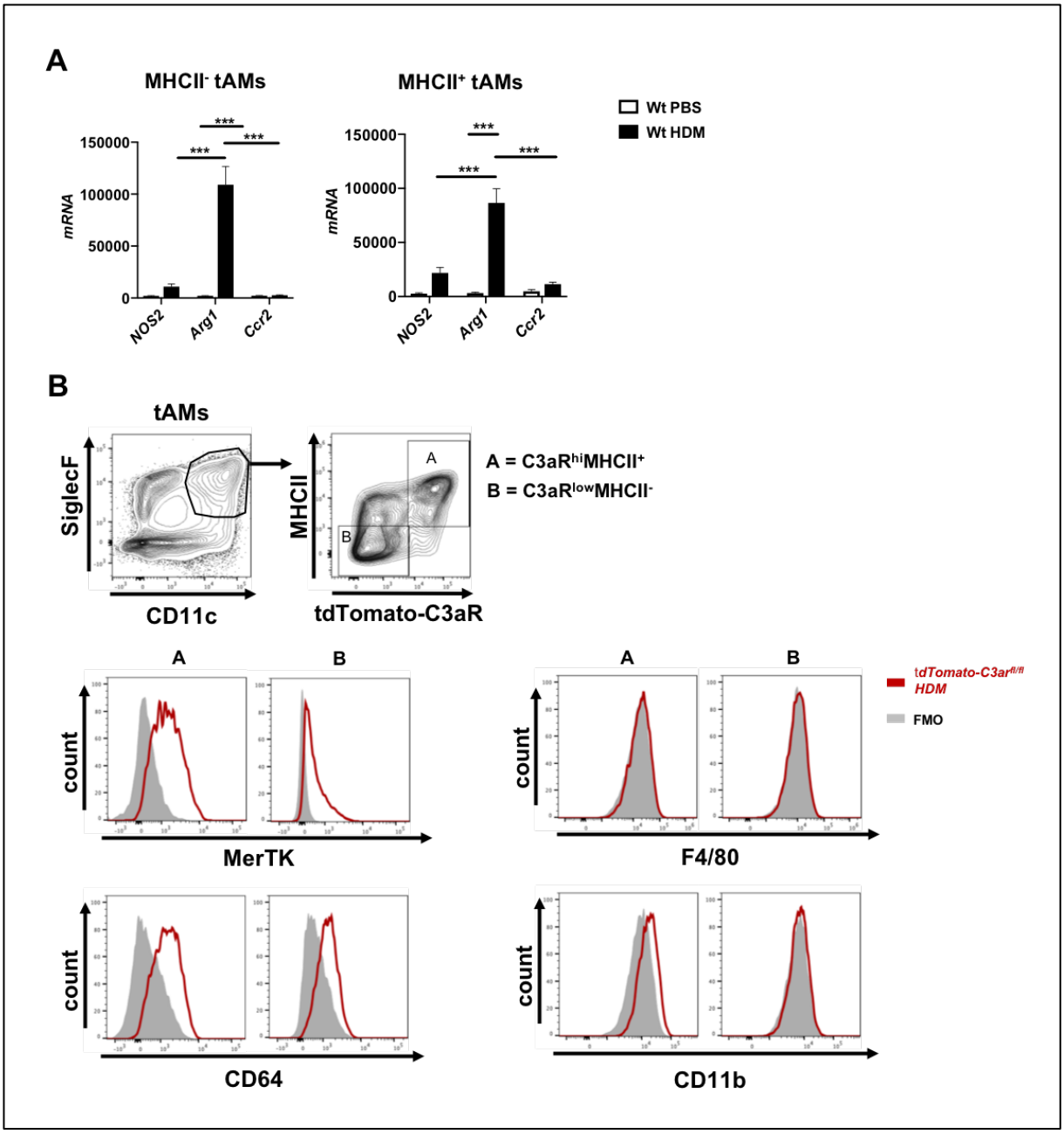

Figure 3.17 Both C3aR^{hi}MHCII^{+} and C3aR^{low}MHCII^{-} tAMs show similar expression levels of characteristic macrophage markers. (**A**) RT-PCR analysis of MHCII^{+} and MCHII^{-} tAMs for mRNA levels of *NOS2, Arg1* and *Ccr2* from WT mice treated 4 times i.t with HDM (black bars) or PBS (open bars) as controls. (**B**) Flow cytometric assessment of MerTK, F4/80, CD64 and CD11b expression in C3aR^{hi}MHCII^{+} and C3aR^{low}MHCII^{-} cells pre-gated on SiglecF^{+}CD11c^{+} tAMs of HDM-treated *tdTomato-C3ar1$^{fl/fl}$*. The red lines correspond to the signal in *tdTomato-C3ar1$^{fl/fl}$* mice; the grey histograms depict the FMO from these mice. Values shown are the mean ± SEM; n = 6-14 per group. *** $p < 0.001$.

3.3.2 Molecular mechanisms involved in C3aR upregulation in tAMs upon inflammatory conditions

3.3.2.1 Naïve tAMs as targets for alarmins and Type 2 cytokines

Various cytokines are involved in the allergic asthma development among interleukin (IL)-33, thymic stromal lymphopoietin (TSLP), IL-25, IL-13, IL-4 and IL-5 (332). Recently it has been well recognized that epithelial cells, as a layer lining the airways, not only consists in a physical barrier to protect against environmental particulates and pathogens, but can also be activated by TLRs, in particular TLR4 and TLR9, as well as PARs by environmental stimuli which leads to subsequent activation of the NF-κB pathway and the release of growth factors such as GM-CSF, and a triad of cytokines, including interleukin (IL)-25, thymic stromal lymphopoietin (TSLP), and IL-33 (521), which together with IL-13, IL-4 and IL-5, are involved in the allergic asthma development (332). IL-33 (522-524), considered an alarmin, mediates its biological effects via ST2 (also known as IL1RL1), a member of the IL-1 superfamily (525, 526), which activates ILC2s and $CD4^+$ T cells and thus drives production of IL-4, IL-5, and IL-13 (527). Furthermore, ST2 exists in two forms as splice variants (528): a soluble form (sST2), which acts as a decoy receptor, neutralizing free IL-33, and does not signal, and a trans-membrane receptor (ST2L), which activates the MyD88/NF-κB signaling pathway to enhance Th2 (527, 529), and ILC2 functions (529). To delineate which cytokines could directly act on naïve macrophages upon developing the disease, I investigated the expression level of ST2, the receptor for the alarmin IL-33 and IL-13Rα1, the receptor for the Th2 cytokine IL-13 at steady state, and could show that naïve tAMs expressed ST2 as well as IL-13Rα1, as shown in Figure 3.18.

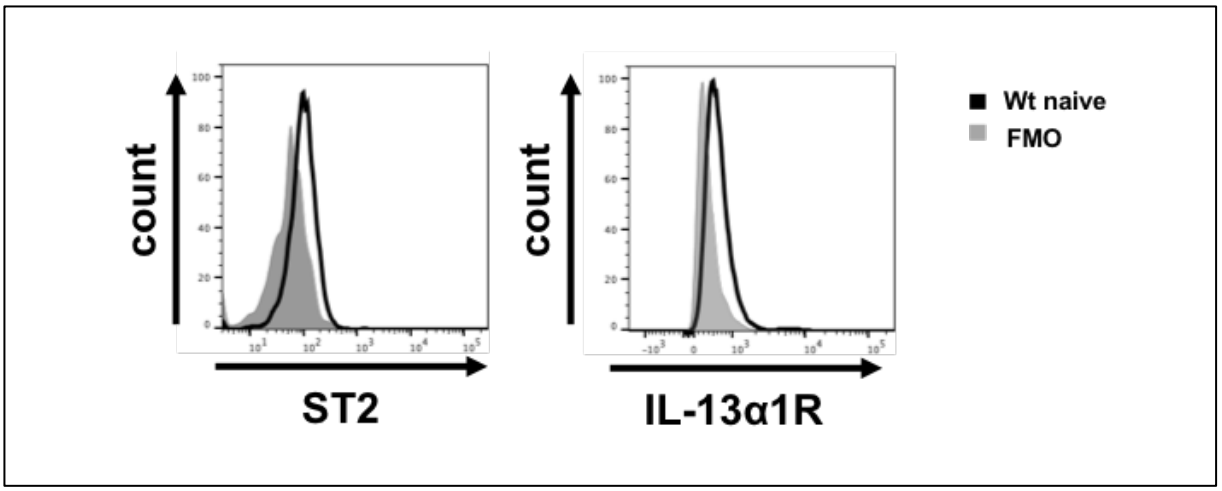

Figure 3.18 Naïve tAMs express markers for alarmins and Th2 cytokines. Flow cytometric assessment of ST2 and IL-13Rα1 expressions in tAMs at steady-state. The black histograms show the WT signal; the grey histograms correspond to the signal of the FMO controls.

This expression of ST2 at their surface suggests that tAMs may be a direct target for IL-33-driven activation. Thus, as *ST2*$^{-/-}$ mice are lacking both the soluble and trans-membrane form of ST2, and cannot respond to IL-33, I used *ST2*$^{-/-}$ mice to delineate the effect of IL-33 on C3aR and MHCII upregulation in tAMs upon an HDM-mediated effector phase of allergic asthma. Firstly, WT and *ST2*$^{-/-}$ mice were immunized four times with HDM (2.3.3.2) and characterized for the frequency of MHCII^{+} tAMs, with WT and *ST2*$^{-/-}$ mice immunized with PBS as controls. Upon HDM, WT mice show a 2-fold increased frequency of MHCII^{+} tAMs whereas *ST2*$^{-/-}$ mice showed a frequency similar to the PBS controls (Figure 3.19A). In addition, analysis of *C3ar1* mRNA expression in WT FACS purified MHCII^{-} tAMs showed a significant upregulation of *C3ar1* expression upon HDM compared to their PBS-controls, whereas the *ST2*$^{-/-}$ mice cells did not show such an increase (Figure 3.19B). Similarly, HDM significantly increased the expression of *C3ar1* in WT MHCII^{+} tAMs compared to PBS, while the *C3ar1* expression in the few MHCII^{+} cells from HDM *ST2*$^{-/-}$ showed no significant reduction (Figure 3.19B).

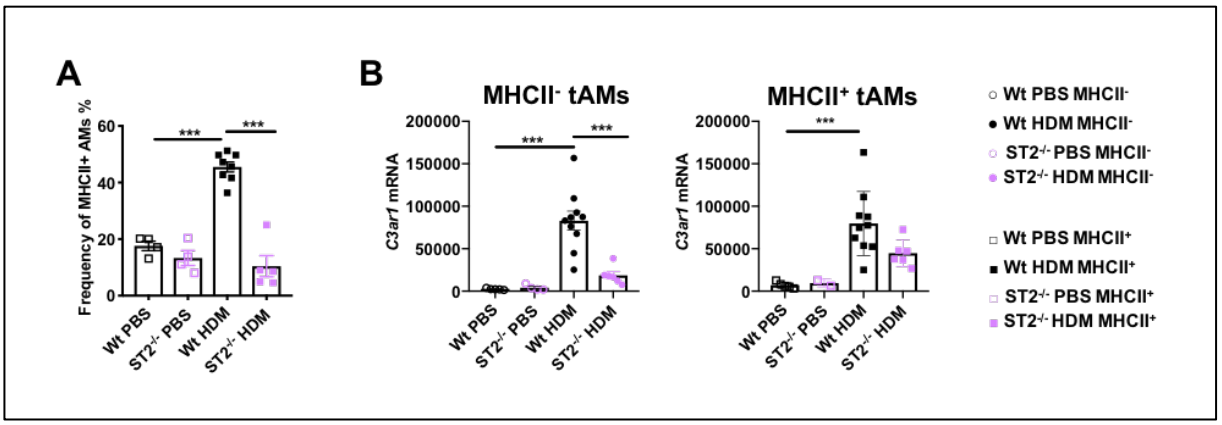

Figure 3.19 IL-33 is involved in C3aR and MHCII upregulation during the effector phase of allergic asthma. (**A**) Frequency of MHCII^{+} and MHCII^{-} tAMs pre-gated on SiglecF^{+}CD11c^{+} tAM from WT and ST2-deficient mice treated 4 times i.t with HDM or PBS as controls. (**B**) RT-PCR analysis of MHCII^{+} and MCHII^{-} tAMs for mRNA levels of *C3ar1* from WT and ST2-deficient mice treated 4 times i.t with HDM or PBS as controls. MHCII^{+} cells are depicted as squares; MCHII^{-} are depicted as circles; WT mice are shown in black; ST2-deficient mice are shown in purple; PBS-treatment is pictured as open symbols; HDM-treatment is pictured as filled symbols. Values shown are the mean ± SEM; n = 3-10 per group. *** $p < 0.001$.

Altogether, these findings suggest that IL-33, which is released upon an HDM-mediated allergic asthma, is involved in both C3aR and MHCII upregulation in tAMs. Further, IL-33 may act either directly on tAMs by binding to ST2 or indirectly via the recruitment and activation of ILC2s and Th2 cells and their subsequent release of Th2 cytokines, or even both.

3.3.2.1 IL-33-induced pulmonary inflammation leads to an upregulation of C3aR on alveolar macrophages

Since tissue-associated AMs express ST2, and that ST2-deficient mice showed a reduced expression in *C3ar1* and a lower frequency of MHCII upon HDM, I hypothesized that i.t. administration of IL-33, would promote C3aR and MHCII upregulation.

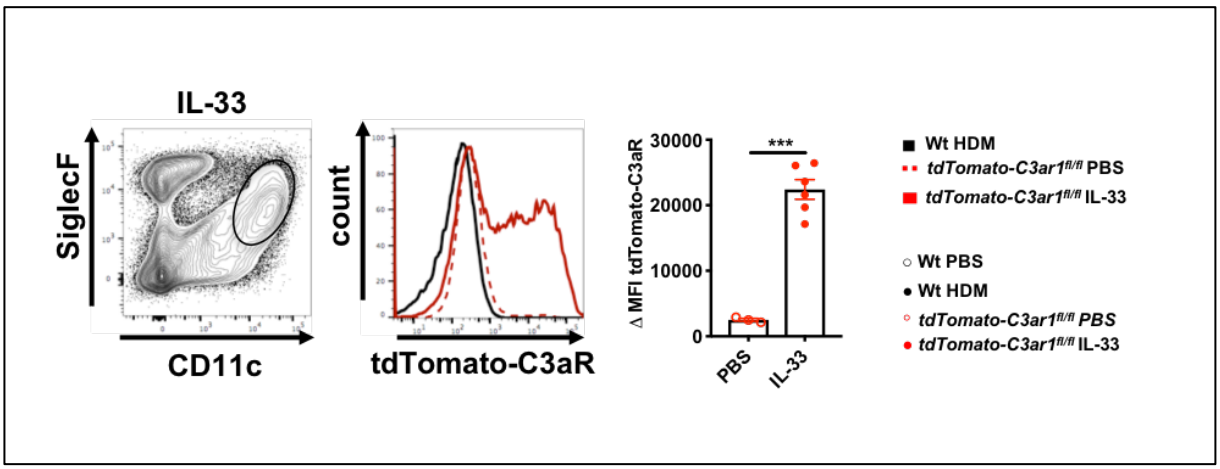

Figure 3.20 IL-33-induced airway inflammation leads to *de novo* upregulation of C3aR in *tdTomato-C3ar1*$^{fl/fl}$ mice. **(A)** Flow cytometric assessment of tdTomato-C3aR expression in tAMs after 4 times PBS- or IL-33 treatment of WT and *tdTomato-C3ar1*$^{fl/fl}$ mice. The black histograms show the WT signal; the red lines correspond to the signal in the IL-33-treated *tdTomato-C3ar1*$^{fl/fl}$ mice; the dashed red lines depict the signal in PBS-treated *tdTomato-C3ar1*$^{fl/fl}$ control mice. In addition, it is shown the ΔMFI of the tdTomato-C3aR signal, which is defined as the MFI obtained by the tdTomato-C3aR signal of cells from *tdTomato-C3ar1*$^{fl/fl}$ mice treated with PBS (red open circles) or IL-13 (red circles) corrected by the tdTomato-C3aR signal obtained with cells from WT mice**.** Values shown are the mean ± SEM; n = 3-6 per group. *** $p < 0.001$.

To assess whether IL-33 is leading to C3aR upregulation in tAMs, I treated WT and *tdTomato-C3ar1*$^{fl/fl}$ mice intra-tracheally with IL-33 (2.3.4.1) to induce a cytokine-mediated pulmonary inflammation. Control mice were treated with PBS according to the same protocol. The tdTomato signal was used as a surrogate to analyze C3aR expression in tAMs by flow cytometry. As shown in Figure 3.20, mice that were treated with IL-33 showed a pronounced tdTomato-C3aR signal compared to WT and PBS-treated *tdTomato-C3ar1*$^{fl/fl}$ mice, indicating that strong *de novo* upregulation of C3aR in SiglecF^{+}CD11c^{+} tAMs was at play. Of note, the normalized MFI increased 10-fold between PBS and IL-33 treated mice (Figure 3.20).

3.3.2.2 IL-13 is involved in the upregulation of C3aR on alveolar macrophages

As mentioned above, ILC2s and Th2 cells secrete pro-inflammatory cytokines among which IL-13 is a potent inducer which can target and activate AMs, based on their IL-13Rα1 expression. To evaluate, whether IL-13 was leading to C3aR upregulation, I treated WT and *tdTomato-C3ar1*$^{fl/fl}$ mice intra-tracheally with IL-13 (2.3.4.2) to induce an IL-13-mediated pulmonary inflammation. As a control

group, mice were treated with PBS the same way. Indeed, mice that were treated with IL-13 showed an increased tdTomato-C3aR signal in SiglecF^{+}CD11c^{+} tAMs compared to WT and PBS-treated *tdTomato-C3ar1*$^{fl/fl}$ mice (Figure 3.21A). However, comparing the ΔMFI of the tdTomato-C3aR signal between *tdTomato-C3ar1*$^{fl/fl}$ mice that have been treated with IL-33 (Figure 3.20A) compared with mice treated with IL-13 (Figure 3.21A), showed that C3aR increased considerably more (5-fold) upon an IL-33-mediated pulmonary inflammation.

IL-13 is a signature cytokine of the type II inflammatory response. IL-13 binds to two receptors, namely, IL-13Rα1 and IL-13Rα2. The role of IL-13 binding to IL-13Rα2 has been somewhat elusive. IL-13Rα2 has been considered as a decoy receptor that binds strongly free IL-13, without eliciting signaling and thus would serve as a neutralizer of IL-13. But when IL-13 binds to IL-13Rα1 it initiates the typical IL-13 signaling cascades. Mice lacking IL-13Rα1 cannot generate the functional IL-13/IL-13Rα1 complex and thereby the typical Januskinase (JAK)/STAT signaling cascade cannot take place (530, 531).

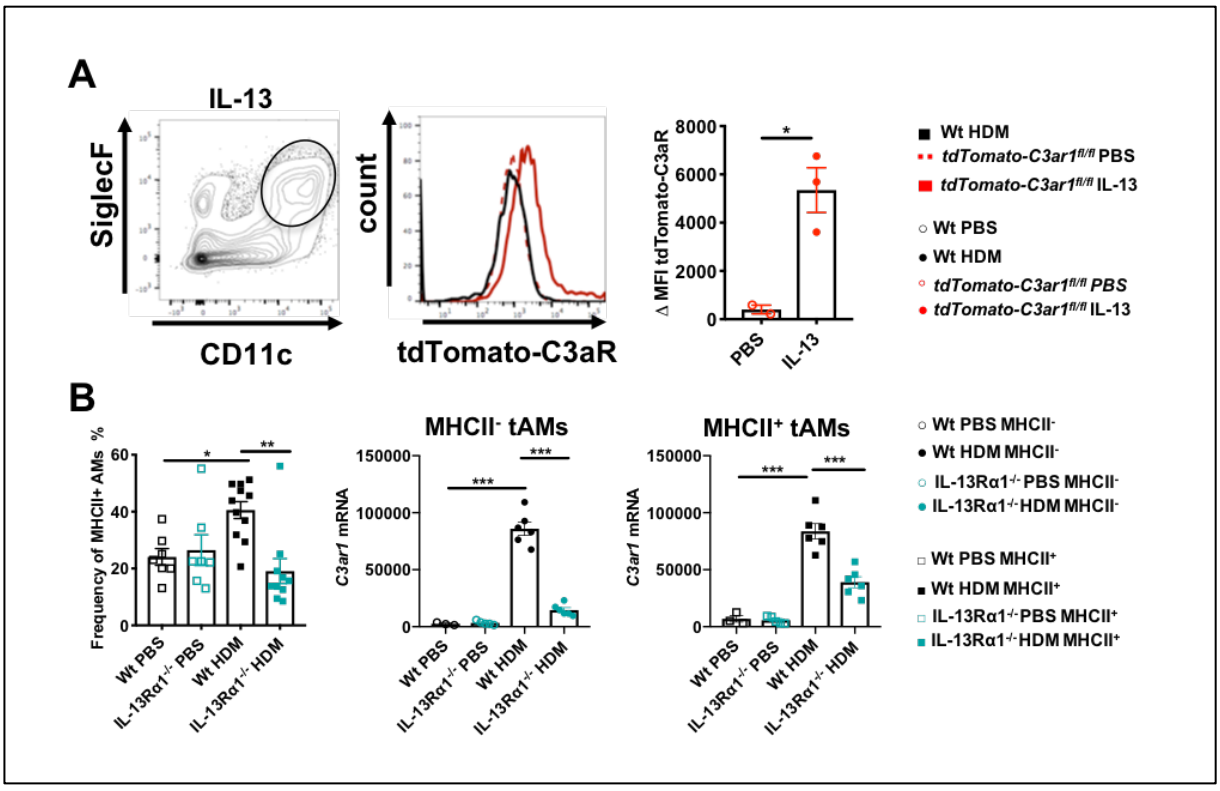

Figure 3.21 IL-13 is involved in the *de novo* upregulation of C3aR and MHCII in tAMs. (**A**) Flow cytometric assessment of tdTomato-C3aR expression in tAMs after PBS- or IL-13 treatment of WT and *tdTomato-C3ar1*$^{fl/fl}$ mice. The black histograms show the WT signal; the red lines correspond to the signal in the IL-13-treated *tdTomato-C3ar1*$^{fl/fl}$ mice; the dashed red lines depict the signal in PBS-treated *tdTomato-C3ar1*$^{fl/fl}$ control mice. In addition, it is shown the ΔMFI of the tdTomato-C3aR signal, from *tdTomato-C3ar1*$^{fl/fl}$ mice treated with PBS (red open circles) or IL-13 (red circles)**.** Values shown are the mean ± SEM; n = 2-3 per group. * $p < 0.5$. (**B**) Frequency of MHCII^{+} and MHCII^{-} tAMs pre-gated on SiglecF^{+}CD11c^{+} tAM from WT and *IL-13Rα1*-deficient mice treated i.t with HDM or PBS as controls. RT-PCR analysis of MHCII^{+} and MCHII^{-} tAMs for mRNA levels of *C3ar1* from WT and *IL-13Rα1*-deficient mice treated 4 times i.t with HDM or PBS as controls. MHCII^{+} cells are depicted as squares; MCHII^{-} are depicted as circles; WT mice are shown in black; *IL-13Rα1*-deficient mice are shown in turquoise; PBS-treatment is pictured as open symbols; HDM-treatment is pictured as filled symbols. Values shown are the mean ± SEM; n = 3-11 per group. *** $p < 0.001$.

To evaluate the direct impact of IL-13 on the upregulation of C3aR and MHCII in tAMs, I used *IL-13Rα1*-deficient mice during the induction of an HDM-mediated effector phase of allergic asthma. For that, WT and *IL-13Rα1*$^{-/-}$ mice were immunized four times with HDM (2.3.3.2) and characterized for the frequency of MHCII^{+} tAMs. Mice immunized with PBS were used as control groups. As observed previously, the frequency of MHCII^{+} tAMs of WT mice treated with HDM was 2-fold higher that the frequency observed in the PBS control (Figure 3.21B). In contrast, MHCII^{+} tAMs from HDM-treated *IL-13Rα1*$^{-/-}$ mice showed a similar frequency to PBS-treated control groups. Furthermore, to evaluate the expression of C3aR, MHCII^{-} and MHCII^{+} tAMs from WT and *IL-13Rα1*$^{-/-}$ mice were purified by FACS (2.3.8.7) and analyzed for their *C3ar1* mRNA expression (2.3.15, 2.3.16, 2.3.17). As shown in Figure 3.21B, WT MHCII^{-} tAMs showed a significant upregulation of *C3ar1* expression compared to their PBS-controls as well as a significant increase compared to their HDM-treated *IL-13Rα1*$^{-/-}$ counterparts. Similarly, *C3ar1* mRNA expression in MHCII^{+} tAMs from HDM WT mice was also significantly elevated compared to PBS, and also compared to MHCII^{+} cells from HDM *IL-13Rα1*$^{-/-}$ mice. However, I observed that both the HDM MHCII^{-} and the HDM MHCII^{+} cells of the *IL-13Rα1*$^{-/-}$ mice showed a slight increase in *C3ar1* mRNA compared to their corresponding PBS controls. However, the abundance of *C3ar1* mRNA HDM MHCII^{+} tAMs of IL-13Rα1$^{-/-}$ mice was significantly lower compared to their WT counter parts. (Figure 3.21B).

In summary, the underlying mechanism leading to the upregulation of C3aR and MHCII in tAMs is mediated by IL-33 and also IL-13.

3.3.3 C3aR^{hi} tAMs originate from resident alveolar macrophages and develop independently from peripheral blood-recruited monocytes

During the effector phase of allergic asthma, I observed that alveolar macrophages generated two subpopulations, an MHCII^{-}C3aR^{low} and an MHCII^{+}C3aR^{hi} population. However, their origin remained elusive, as either they may derive from mature long-lived-macrophages or from blood-circulating monocytes that were recruited upon airway inflammation. Usually, AMs enter the tissue during embryonic development, and then self-renew at steady-state during life (26-29). However, during infection or inflammation, monocytes that develop in the bone marrow and circulate in the blood, can be rapidly recruited from the bloodstream to sites of infection and inflammation to exert their pro-inflammatory and antimicrobial roles (532). They are marked by high expression levels of Ly6C, CD11b, and CD115 and can be in addition identified as a monocyte subset that expresses high levels of C-C chemokine receptor type 2 (CCR2) but low levels of CX_3C chemokine receptor 1 (CX_3CR1) (533-535). A second major subset of circulating monocytes in mice expresses also high levels of CD11b and CD115, but low levels of CCR2 and Ly6C (533-535) and high levels of CX_3CR1 (535). These Ly6C^{low} monocytes have a role in patrolling, recruitment to noninflamed tissues, and tissue repair (533, 536, 537). As

mentioned above, my mRNA data of HDM-treated WT mice showed that the MHCII$^+$ AMs were *Ccr2*$^-$ (Figure 3.17A), suggesting a monocytic-independent origin.

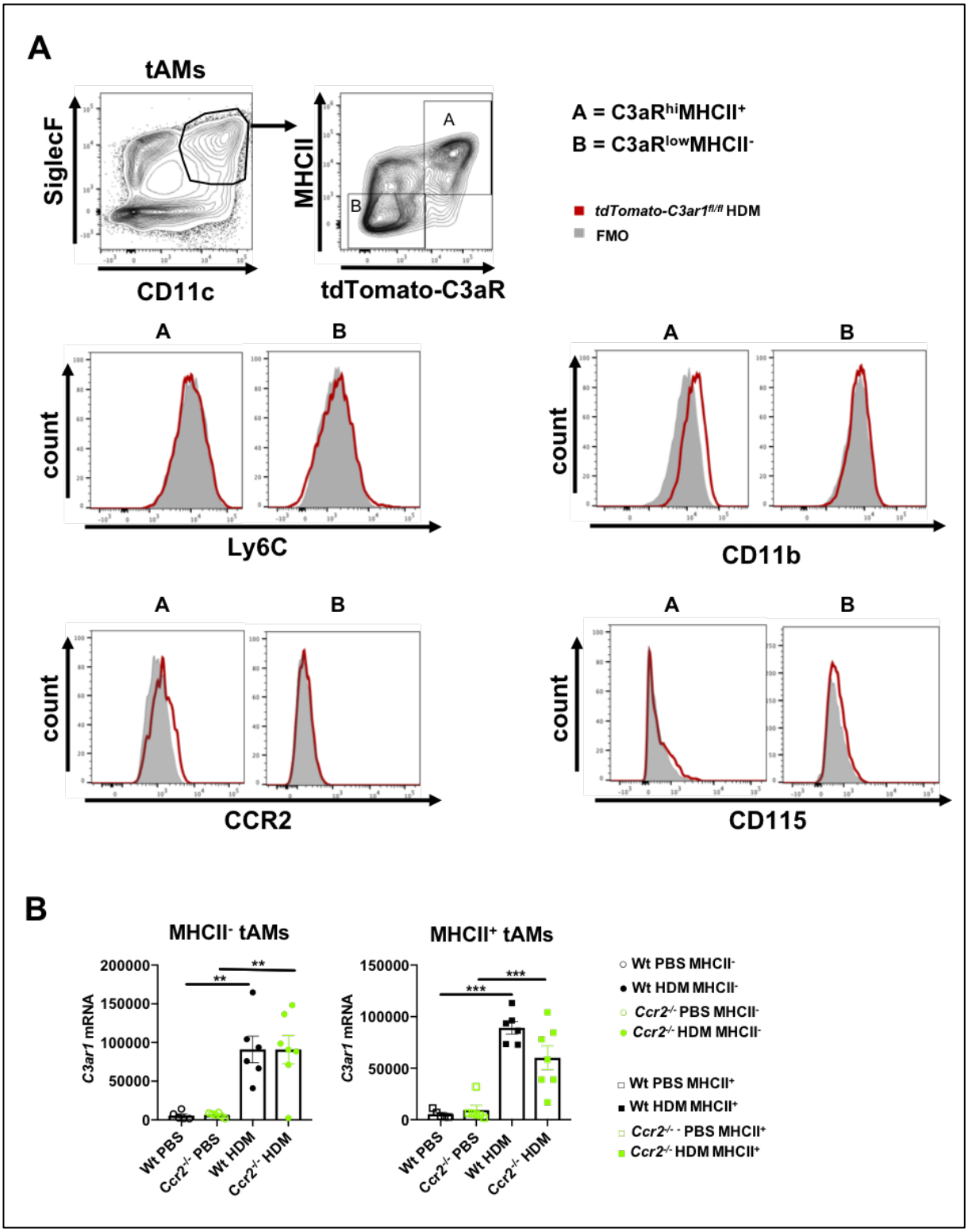

Figure 3.22 C3aR^{hi}MHCII$^+$ tAMs do not express monocytic markers. (**A**) Flow cytometric assessment of different monocytic markers of C3aR^{hi}MHCII$^+$ and C3aR^{low}MHCII$^-$ tAMs of HDM-treated *tdTomato-C3ar1$^{fl/fl}$* mice. The red histograms show the signal of *tdTomato-C3ar1$^{fl/fl}$* mice; the grey histograms show the signal of the corresponding FMO control. A= C3aR^{hi}MHCII$^+$ tAM subpopulation; B= C3aR^{low}MHCII$^-$ tAM subpopulation. (**B**) RT-PCR analysis of MHCII$^+$ and MCHII$^-$ tAMs for mRNA levels of *C3ar1* from WT and *Ccr2*-deficient mice treated 4 times i.t with HDM or PBS as controls. MHCII$^+$ cells are depicted as squares;

MCHII$^-$ cells are depicted as circles; WT mice are shown in black; *Ccr2*-deficient mice are shown in green; PBS-treatment is pictured as open symbols; HDM-treatment is pictured as filled symbols. Values shown are the mean ± SEM; n = 4-7 per group. * $p < 0.01$; *** $p < 0.001$.

To more precisely delineate the origin of these two subpopulations, I investigated the expression of additional specific monocytic markers. Both C3aR^{low}MHCII$^-$ and a C3aR^{hi}MHCII$^+$ populations showed no expression of the general monocyte marker CD115 and only a very low level of CD11b (Figure 3.22A). Further, CCR2 that has been described as a crucial receptor to efficiently recruit LY6C^{hi} monocytes from the bone marrow to the blood and into inflamed tissue via the binding of either C-C chemokine ligand 2 (CCL2; also known as monocyte chemoattractant protein-1 (MCP-1)) and CCL7 (also known as MCP-3) (538). As shown in Figure 3.22A, neither C3aR^{low}MHCII$^-$ nor C3aR^{hi}MHCII$^+$ cells showed expression of CCR2 and Ly6C that can be used to identify the inflammatory monocyte subset that is usually recruited to inflamed tissue.

In addition, mice lacking CCR2 have markedly decreased blood monocytes and are not able to recruit monocytes from the bloodstream into tissue (537, 538). To confirm that CCR2$^+$Ly6C^{hi} inflammatory monocytes were not involved in the appearance of C3aR$^+$ tAMs, I immunized WT C57BL/6 and *Ccr2*$^{-/-}$ mice with HDM (2.3.3.3). Then, the abundance of *C3ar1* mRNA in FACS purified MHCII$^-$ and MHCII$^+$ tAMs from WT and *Ccr2*$^{-/-}$ was evaluated. Indeed, *C3ar1* mRNA expression data showed that in MHCII$^+$ and MHCII$^-$ tAMs from WT and *Ccr2*$^{-/-}$ mice treated with HDM *C3ar1* abundance was similar and was significantly higher in comparison to their PBS-controls (Figure 3.22B).

Summarizing my results, I could demonstrate that C3aR^{hi}MHCII$^+$ tAMs originate from resident tissue-associated alveolar macrophages and that they develop independently from blood recruited monocytes.

3.3.4 IL-33-IL-13 signaling axis is involved in the cross-regulation of C3aR and C5aR1 on alveolar macrophages

Since I identified a cross-regulation of C3aR and C5aR1 during the effector phase of allergic asthma (3.2.6) and, in addition, I could demonstrate that the underlying mechanism leading to C3aR upregulation in tAMs was dependent on IL-33 and IL-13, I therefore determined if C5aR1 downregulation upon HDM was also dependent on a similar mechanism. In order to evaluate this hypothesis, I induced a cytokine-mediated pulmonary inflammation either with IL-33 (2.3.4.1) or IL-13 (2.3.4.2) or PBS control mice in WT and *C5ar1*$^{-/-}$ mice. Indeed, staining and flow cytometric assessment of C5aR1 showed that tAMs of WT mice treated with IL-33 decreased intensively their level of C5aR1 expression compared to cells from WT mice treated with PBS (Figure 3.23A). Analyzing the normalized MFI showed a 3-fold decrease of C5aR1 in WT IL-33 mice compared to their PBS control. Furthermore,

treatment with IL-13 showed an even stronger effect, since tAMs from WT mice treated with IL-13 showed almost the same level of C5aR1 as cells from mice that were deficient in C5aR1. Treatment with IL-13 led to a 10-fold reduction in the ΔMFI of C5aR1 in tAMs from WT IL-13 mice compared to WT mice treated with PBS (Figure 3.23A).

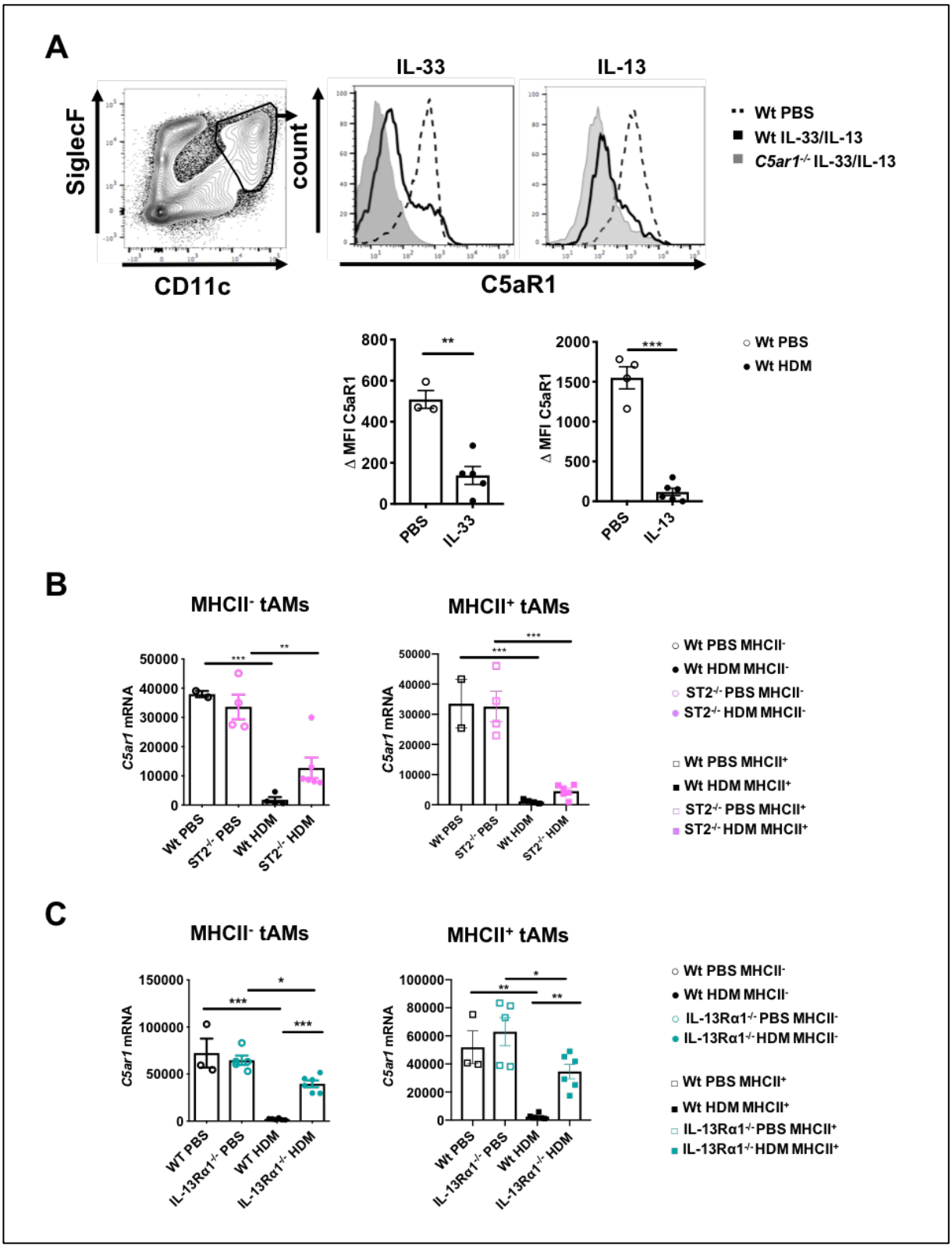

Figure 3.23 IL-33 and IL-13 are involved in the downregulation of C5aR1 in tAMs upon pulmonary inflammation. (**A**) Flow cytometric assessment of C5aR1 expression in tAMs after PBS-, IL-33 or IL-13 treatment of WT mice. The black histograms show the WT signal treated with IL-33 or IL-13; the dashed lines depict the signal in PBS-treated WT control mice; the grey histogram correspond to the signal of IL-33/IL-13-treated *C5ar1*-deficient mice. In addition, it is shown the ΔMFI of the C5aR1 signal, from WT mice treated with PBS (open circles) or IL-33/IL-13 (filled circles)**.** Values shown are the mean ± SEM; n = 3-6 per group. *** $p < 0.001$. (**B**) RT-PCR analysis of mRNA levels for *C5ar1* of sorted MHCII$^+$ and MCHII$^-$ tAMs pre-gated on SiglecF$^+$CD11c$^+$ tAMs from WT and *IL-13Rα1*-deficient mice treated 4 times i.t with HDM or PBS as controls. MHCII$^+$ cells are depicted as squares; MCHII$^-$ are depicted as circles; WT mice are shown in black; *IL-13Rα1*-deficient mice are shown in turquoise; PBS-treatment is pictured as open symbols; HDM-treatment is pictured as filled symbols. Values shown are the

mean ± SEM; n = 3-11 per group. *** p < 0.001. (**C**) RT-PCR analysis of mRNA levels for *C5ar1* of sorted MHCII$^+$ and MCHII$^-$ tAMs pre-gated on SiglecF$^+$CD11c$^+$ tAMs from WT and *ST2*-deficient mice treated 4 times i.t with HDM or PBS as controls. MHCII$^+$ cells are depicted as squares; MCHII$^-$ are depicted as circles; WT mice are shown in black; *ST2*-deficient mice are shown in purple; PBS-treatment is pictured as open symbols; HDM-treatment is pictured as filled symbols. Values shown are the mean ± SEM; n = 3-11 per group. *** p < 0.001.

To confirm the involvement of IL-33 in the downregulation of C5aR1 in tAMs, I quantified *C5ar1* mRNA in MHCII$^+$ and MHCII$^-$ tAMs of *ST2*$^{-/-}$ mice during an HDM-mediated effector phase of allergic asthma. For that, WT and *ST2*$^{-/-}$ mice were immunized four times with HDM (2.3.3.2). Mice immunized with PBS were used as control groups. MHCII$^+$ and MHCII$^-$ tAMs were purified by FACS (2.3.8.7) and analyzed for their *C5ar1* mRNA expression (2.3.15, 2.3.16, 2.3.17). As shown in Figure 3.23B, as expected WT MHCII$^-$ tAMs showed a significant downregulation of *C5ar1* expression following 4 allergen treatments compared to their PBS-controls. However, comparing WT MHCII$^-$ tAMs to their HDM-treated *ST2*$^{-/-}$ counterparts (Figure 3.23B) revealed a higher, but insignificant difference of *C5aR1* mRNA level of WT mice compared to *ST2*$^{-/-}$ mice. Similarly, *C5ar1* mRNA expression in MHCII$^+$ tAMs from HDM WT mice was also significantly diminished compared to PBS, but no difference were identified compared to MHCII$^+$ cells from HDM *ST2*$^{-/-}$ mice (Figure 3.23B).

Additionally, to confirm the downregulation of C5aR1 in tAMs by IL-13, I delineated the abundance of *C5ar1* mRNA of MHCII$^+$ and MHCII$^-$ tAMs in *IL-13Rα1*$^{-/-}$ mice same way as described above. As shown in Figure 3.23C, WT MHCII$^-$ tAMs showed a significant downregulation of *C5ar1* expression compared to their PBS-controls and indeed showed also a significant decrease compared to their HDM-treated *IL-13Rα1*$^{-/-}$ counterparts (Figure 3.23C). Similarly, *C5ar1* mRNA expression in MHCII$^+$ tAMs from HDM WT mice was also significantly reduced compared to PBS, and also compared to MHCII$^+$ cells from HDM *IL-13Rα1*$^{-/-}$ mice (Figure 3.23C).

Therefore, my data suggest that the downregulation of C5aR1 in tAMs is mediated by the IL-33-IL-13 signaling axis. However, in contrast to the direct effect of IL-13, shown by both i.t. application of IL-13 and HDM-treatment of *IL-13Rα1*$^{-/-}$, IL-33 seems to have no direct effect on the downregulation of C5aR1, but might be rather involved by an indirect effect via its downstream signaling.

3.3.5 C5aR2 expression in alveolar macrophages remains unaffected by IL-33-induced pulmonary inflammation

The current understanding is that most of the C5a effects result from binding to the canonical C5aR1. However, C5aR2 as a second receptor for C5a is thought to regulate the C5a-C5aR1 effects. Although discovered in 2000 (215, 268), it remains unclear whether C5aR2 is a decoy receptor with anti-inflammatory properties and/or a signaling receptor with mixed pro- or anti-inflammatory properties. Upon steady-state tAMs expressed high levels of C5aR1 and C5aR2 (3.1.1), while C5aR1 was

downregulated during repeated HDM exposure (3.2.6) as well as upon an cytokine-induced inflammation (3.3.4). Therefore, I next evaluated the expression of C5aR2 during IL-33 pulmonary inflammation in a *tdTomato-C5ar2*$^{fl/+}$ mouse model. Hence, WT and *tdTomato-C5ar2*$^{fl/+}$ mice received four doses of IL-33 to induce a pulmonary inflammation (2.3.4.1) and the tdTomato-C5aR2 signal was evaluated in airways and tissue-associated alveolar macrophages. Interestingly, in contrast to the observed downregulation of C5aR1 upon these conditions, C5aR2 expression in a/tAMs remained unaffected. The normalized MFI between PBS and IL-33 treated groups showed similar levels of C5aR2 (Figure 3.24A,B). The same was validated by the percentage of tdTomato-C5aR2^{+} cells. IL-33 treated *tdTomato-C5ar2*$^{fl/+}$ mice showed similar frequencies of tdTomato-C5aR2^{+} cells compared to PBS-treated controls (Figure 3.24A,B). These data suggest, that C5aR2 in a/tAMs remains unaffected by an IL-33 pulmonary inflammation.

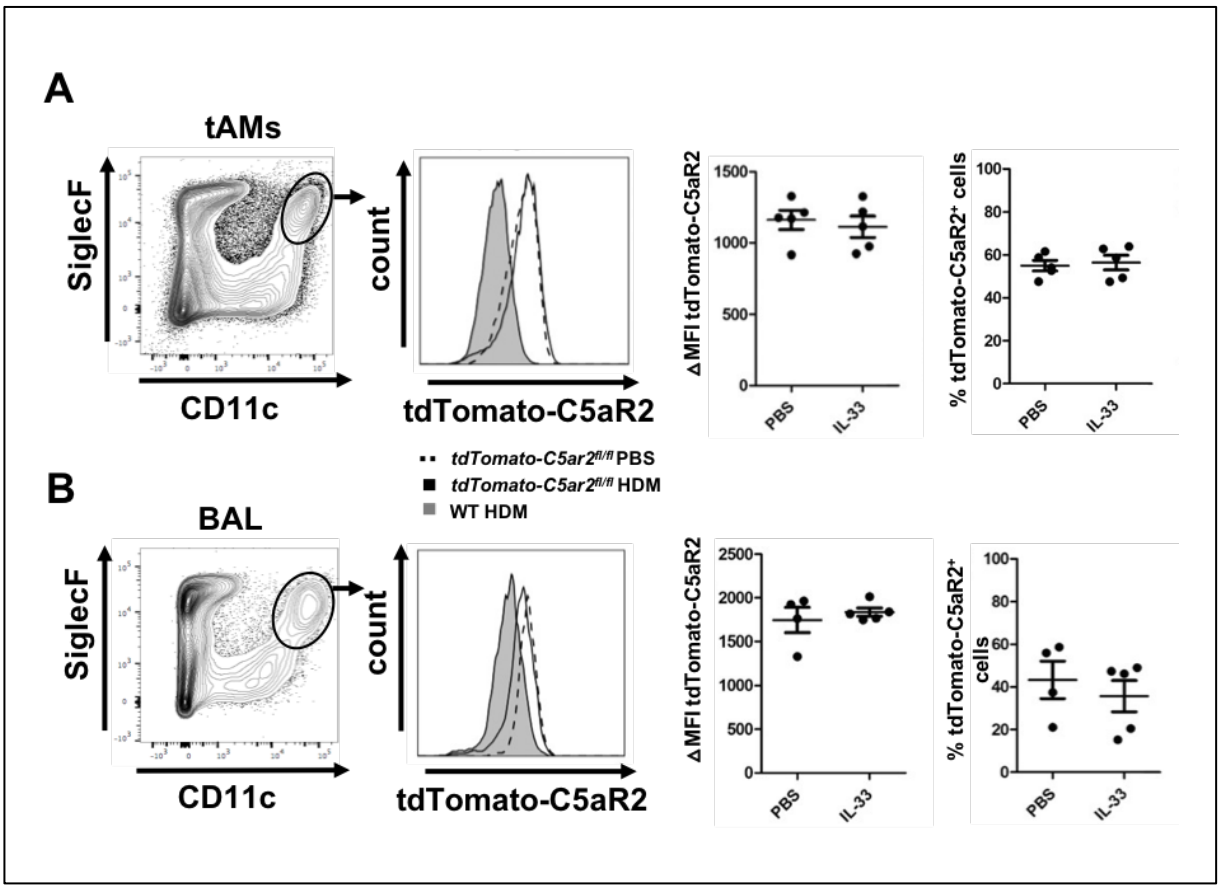

Figure 3.24 aAMs and tAMs do not downregulate C5aR2 expression upon pulmonary inflammation. Flow cytometric assessment of tdTomato-C5aR2 expression in airway and tissue-associated AMs. The gray histograms show the WT signal; the black lines show the signal obtained with heterozygous *tdTomato-C5ar2*$^{fl/+}$ mice upon IL-33 treatment, and the dashed lines correspond to the signal obtained upon PBS control treatment. (A-B) tdTomato-C5aR2 in SiglecF^{+}CD11c^{+} alveolar macrophages from (A) BAL fluid or (B) lung tissue. In addition, quantitative evaluation of tdTomato-C5aR2 expression in SiglecF^{+}CD11c^{+} alveolar macrophages from (A) BAL fluid or (B) lung tissue Shown is the MFI of the tdTomato signal normalized to WT control fluorescence (ΔMFI) in cells from mice treated with PBS or IL-33. Values shown are the mean ± SEM; n = 3-5 per group. *p < 0.5, **p < 0.01, ***p < 0.001, Student t test. Quantitative evaluation of tdTomato-C5aR2^{+} alveolar macrophages from (A) BAL fluid or (B) lung tissue. Shown is the frequency of tdTomato- tdTomato-C5aR2^{+} cells in response to PBS or IL-33 treatment. Values shown are the mean ± SEM; n = 3-5 per group. *p < 0.5, **p < 0.01, ***p < 0.001, Student t test.

3.3.6 *In vitro* stimulation of naïve tAMs recapitulates the upregulation of C3aR

Alveolar macrophages upregulated *de novo* C3aR expression in different allergic asthma and pro-inflammatory *in vivo* experiments (3.2.3, 3.2.4, 3.3.2.1). Two subpopulations, a MHCII^{-}C3aR^{low} and a MHCII^{+}C3aR^{hi} population developed. Additionally, I could demonstrate that both subpopulations originate from tissue-resident alveolar macrophages and developed independent from periphery blood-recruited monocytes (3.3.3). Therefore, I wanted to evaluate if *in vitro* stimulation of naïve tissue-associated macrophages with cytokines could lead to an upregulation of C3aR. As described above, allergen contact leads to epithelial cell damage and activation leading to the release of growth factors and cytokines. Additionally, during the development of the type 2 immune response that underlies allergic asthma, pro-inflammatory cytokines like IL-4 are released by ILC2s (539) and T cells.

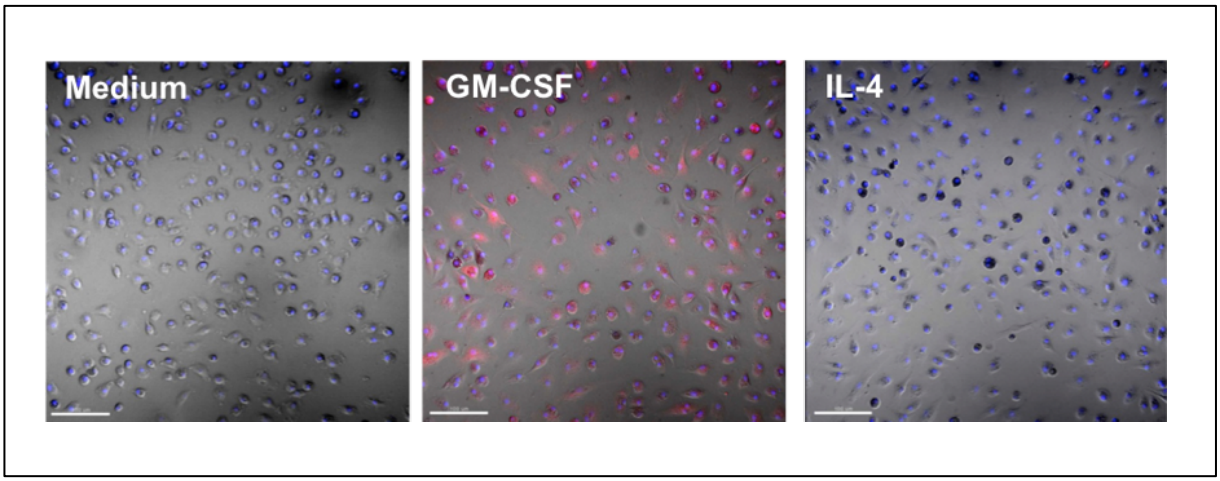

Figure 3.25 In vitro stimulation with GM-CSF leads to C3aR upregulation of tAMs. Assessment of the tdTomato-C3aR signal of sorted tAMs from naïve *tdTomato-C3ar1$^{fl/fl}$* and stimulated with 100ng/ml GM-CSF, 1% IL-4 supernatant or medium alone by confocal microscopy (original magnification x20). Shown is the fluorescence signal of tdTomato-C3aR (red) from SiglecF^{+}CD11c^{+} tAMs and their nuclei staining (blue). Bars represent 20 µm.

To delineate the effects of these cytokines, I used GM-CSF and IL-4 to stimulate sorted naïve tAMs from WT and *tdTomato-C3ar1$^{fl/fl}$* mice in vitro (2.3.12.2) and evaluated their C3aR expression by confocal microscopy (2.3.14.1), using the tdTomato signal as a surrogate for C3aR. tAMs from *tdTomato-C3ar1$^{fl/fl}$* mice stimulated with medium alone were used as control. As shown, tAMs stimulated with 100 ng/ml GM-CSF showed a tdTomato^{+} signal compared to cells that were stimulated with medium alone (Figure 3.25). Interestingly, tAMs that were stimulated with 1% IL-4 did not show C3aR expression after 5 days (Figure 3.25). Conclusively, my data reveal that induction of the C3aR protein expression *in vitro* by stimulating naïve tAMs is possible, but dependent on the stimulus and its concentration as well as the stimulation period that is used. In addition, these data confirmed that C3aR^{+} AMs can arise independently from monocytes.

3.4 C3aR^{hi}MHCII^{+} tissue-associated alveolar macrophages form a multinucleated macrophage subpopulation upon experimental allergic asthma

As shown in paragraph 3.3.1, induction of an HDM-mediated effector phase was leading to the formation of two subpopulations: a MHCII^{-}C3aR^{low} and a MHCII^{+}C3aR^{hi} population. Since my investigations regarding these populations were, until now, limited to flow cytometry and semi-quantitative Real-Time PCR, I was interested in their morphological appearance. Therefore, I purified MHCII^{-}, MHCII^{+}C3aR^{low}, and MHCII^{+}C3aR^{hi} cells by fluorescence activated cells sorting (2.3.8.7), put these cells with a cyto-centrifuge on microscopy slides, and examined their morphology after a May-Giemsa staining (2.3.13.3) with a transmitted-light microscope. As expected, MHCII^{+}C3aR^{low} cells (Figure 3.26A) and MHCII^{-} (Figure 3.26C) showed a characteristic macrophage morphology. Interestingly, the morphology of MHCII^{+}C3aR^{hi} cells, revealed that in addition to the morphologically classical macrophages, macrophage harboring between one and four nuclei (Figure 3.26B) were readily observed. These data suggest that upon allergic inflammation, tAMs formed multinucleated (MuN) cells.

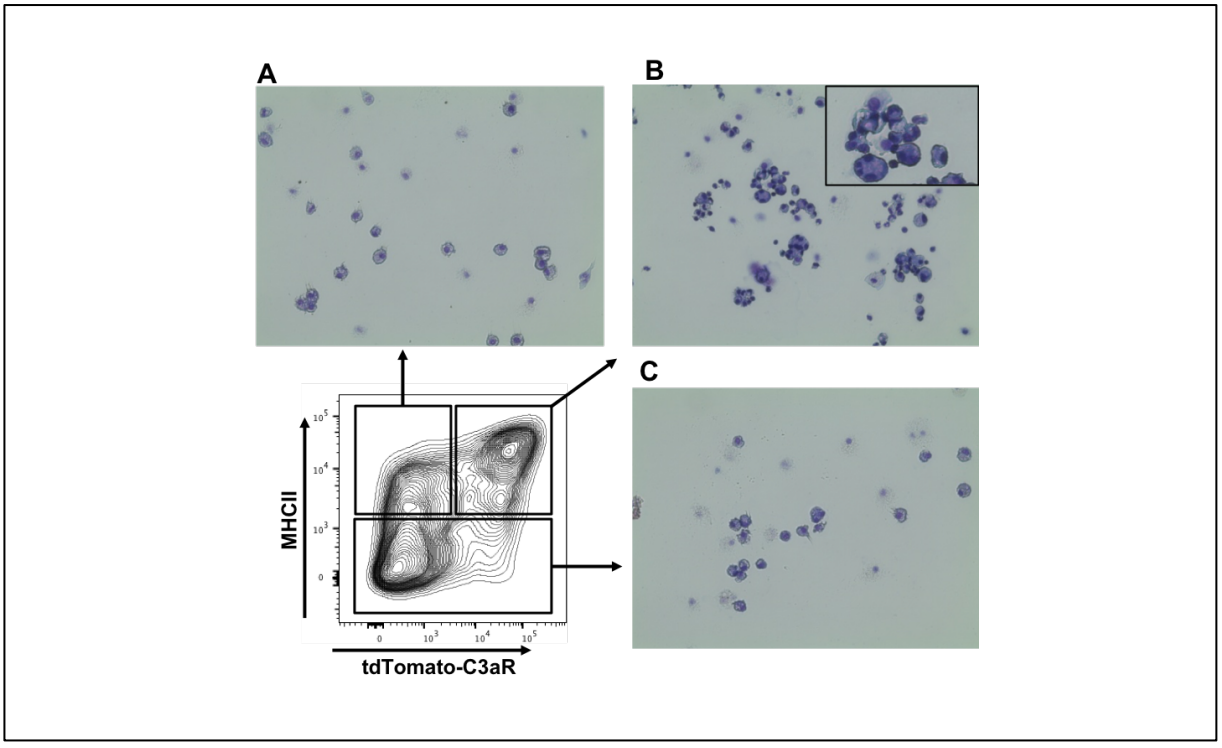

Figure 3.26 C3aR^{hi}MHCII^{+} tAM population contains a multinucleated macrophage subset upon an HDM-mediated allergic asthma. Transmitted-light microscopy of sorted, cyto-centrifuged and May-Giemsa-stained (A) MHCII^{+}C3aR^{low}, (B) MHCII^{+}C3aR^{hi} and (C) MHCII^{-} tAMs. Original magnification x20.

3.4.1 MuN macrophages can be found during the effector phase of allergic asthma *in vivo*

Multinucleated (MuN) cells or giant cells are frequently associated with the formation of osteoclasts and may participates to the formation of granuloma observed in *Mycobacteria* infections. Under strong pro-inflammatory conditions macrophages have been reported to engage fusion processes leading to the formation of multinucleated giant cells (540). Although the molecular mechanisms involved in their formation *in vivo* and their detailed function are still poorly understood, Th2 cytokines have been described as potent fusion triggers (112-114, 541). However, although Th2 immune response is also a hallmark of allergic asthma inflammation, evidences for the presence of multinucleated cells (MuNCs) in allergic asthma are scarce.

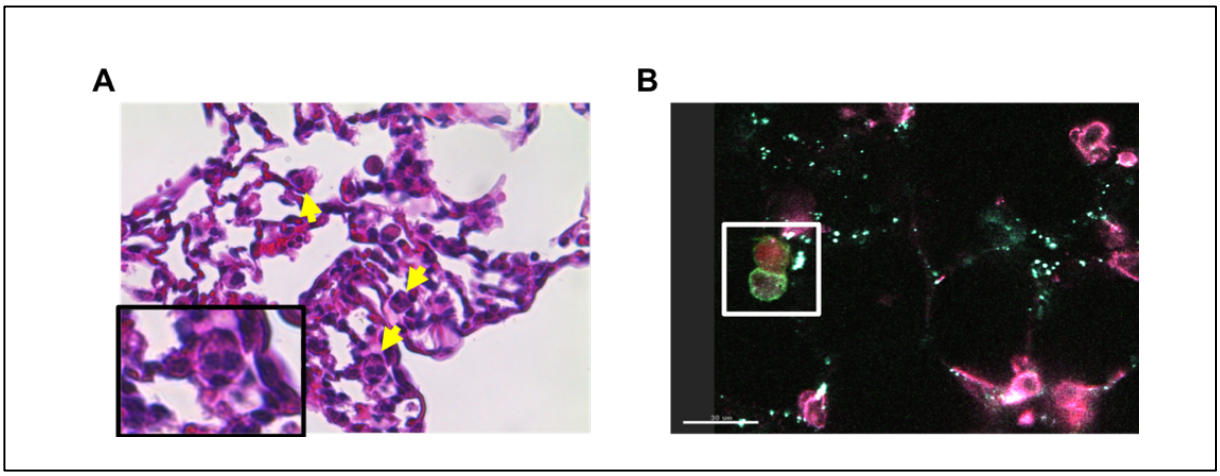

Figure 3.27 Multinucleated macrophages develop *in vivo* during the effector phase of allergic asthma. (**A**) Transmitted-light microscopy of a H&E-stained lung slice of an HDM-treated WT mouse (original magnification x20). (**B**) Immunofluorescence microscopy of lung tissue. 200 µm lung slices were stained for SiglecF (blue), CD11c (green) and MHCII (purple). tdTomato-C3aR expression is shown in red. Original magnification x20. Bar represents 30 µm.

Since I identified MuNCs after purification of tAM subpopulations from lung isolates, I wanted to evaluate if these cells can be detected also *ex vivo*/*in vivo* or if these cells only arise because of lung digestion and processing. Therefore, I used 50 µm histology slices from whole lung tissue of HDM-treated (2.3.3.2) WT for Hematoxylin/Eosin (H&E staining) (2.3.13.2) to identify such MuNCs. Indeed, MuNCs could be identified in H&E stained lung slices (Figure 3.27A). Furthermore, most of the MuNCs were located around the alveoli. In addition, immunofluorescence microscopy of VPLC sections (2.3.14.3, 2.3.14.2) of HDM-immunized lungs, revealed *in vivo* cell-cell interactions between tdTomato-C3aR$^+$SiglecF$^+$CD11c$^+$ tAMs and tdTomato-C3aR$^-$SiglecF$^+$CD11c$^+$ tAMs (Figure 3.27B). Altogether, my findings demonstrate that MuNCs develop *in vivo* from SiglecF$^+$CD11c$^+$ tAMs during the effector phase of allergic asthma.

3.4.2 *In vitro* stimulation of naïve tAMs with GM-CSF leads to a multinucleated cell formation

To delineate if *in vitro* stimulation could also induce MuN macrophage formation, I purified naïve tAMs from WT and *tdTomato-C3ar1*$^{fl/fl}$ mice by fluorescence activated cell sorting (2.3.8.7), and stimulated cells *in vitro* for 5 days (2.3.12.3) with either GM-CSF or IL-4. Indeed, GM-CSF was able to induce C3aR expression *in vitro* (Figure 3.25) and both GM-CSF and IL-4 have been reported to serve as inducers of multinucleated giant cell (MNGC) formation (113, 541). As a control, I stimulated cells with medium alone. While cells in medium did not show MuN macrophages, cells stimulated with GM-CSF, showed a significant increase in MuN macrophage formation (Figure 3.28A). Intriguingly, IL-4 that was described as an inducer for multinucleated giant cells (MNGCs) did not induce multinucleated macrophage formation, since the frequency of MuN macrophages was similar to medium alone (Figure 3.28A).

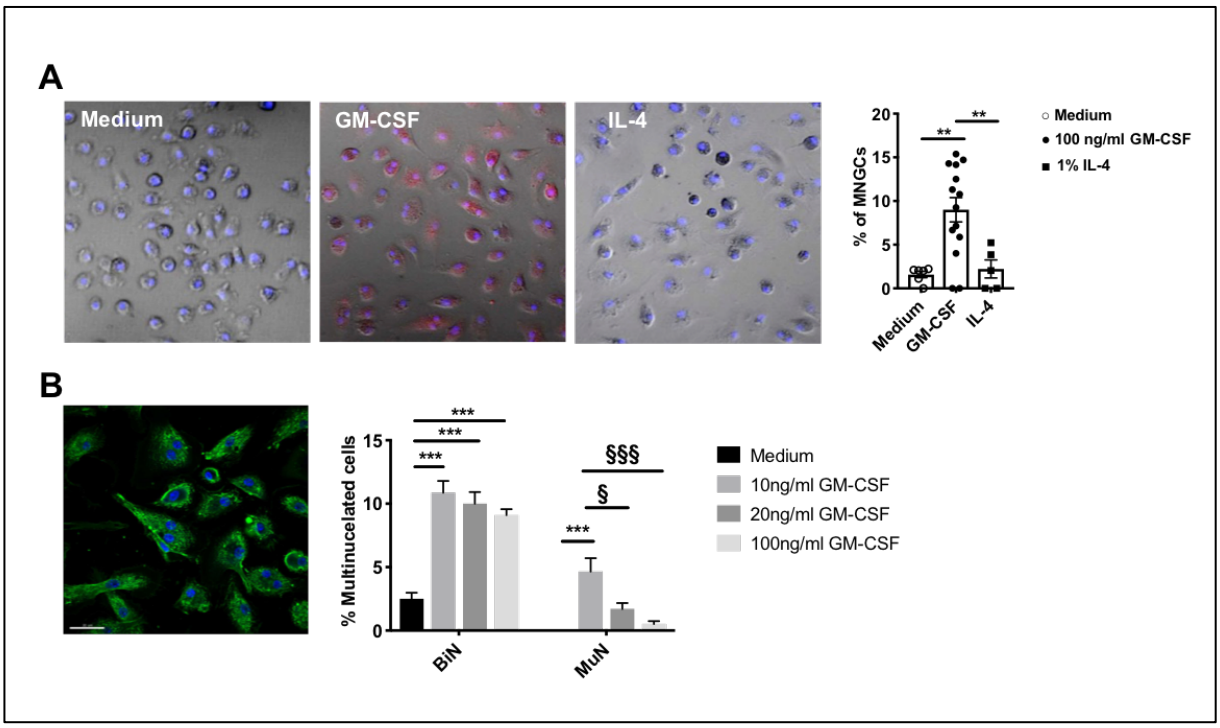

Figure 3.28 Naïve tAMs stimulated *in vitro* with GM-CSF form bi- and multinucleated cells. (**A**) Assessment of multinucleated macrophages by confocal microscopy (original magnification x20). Sorted tAMs from naïve *tdTomato-C3ar1*$^{fl/fl}$ mice were stimulated with 100ng/ml GM-CSF, 1% IL-4 supernatant or medium alone. Shown is the fluorescence signal of tdTomato-C3aR (red) from SiglecF^{+}CD11c^{+} tAMs and their nuclei staining (blue). Bars represent 100 µm. In addition, shown is the frequency of multinucleated cells in response to stimulation with GM-CSF, IL-4 or medium alone. Values shown are the mean ± SEM; n = 5-14 per group. *p < 0.5, **p < 0.01, ***p < 0.001. (B) Assessment of bi- and multinucleated macrophages by confocal microscopy (original magnification x40). For that, sorted tAMs from naïve *tdTomato-C3ar1*$^{fl/fl}$ mice were stimulated with 10ng/ml GM-CSF or medium alone. Shown is the fluorescence signal of DAPI for the DNA content (blue) from SiglecF^{+}CD11c^{+} tAMs and their membrane staining (green). Bars represent 30 µm. In addition, shown is the frequency of bi- and multinucleated cells in response to stimulation with GM-CSF or medium alone. Values shown are the mean ± SEM; n = 5-14 per group. * or § p < 0.5, ** or §§ p < 0.01, *** or §§§ p < 0.001.

Furthermore, stimulating naïve tAMs with different concentrations of GM-CSF showed a dose-response relationship. The maximum of binucleated (BiN) cells was reached at a concentration of 10 ng/ml GM-CSF, whereas stimulation with 20 ng/ml and 100 ng/ml showed already a decrease in BiN macrophage formation (Figure 3.28B) but still a significant increase compared to cells stimulated with medium alone. However, whereas stimulation with 10ng/ml GM-CSF showed significant elevated levels of MuN cells compared to cells stimulated with medium alone, 20 ng/ml and 100ng/ml GM-CSF did not promote the formation of MuN macrophages since such conditions led to similar levels of MuN compared to the medium alone (Figure 3.28B).

3.4.3 C3aR participates in the formation of MuNCs upon GM-CSF

Since stimulating of tAMs with GM-CSF lead to *de novo* upregulation of C3aR and in addition to multinucleated macrophage formation *in vitro*, I hypothesized that C3aR may play a role in the development of MuN macrophage formation. In order to evaluate that hypothesis, I isolated naïve tAMs from WT and *C3ar1*$^{-/-}$ mice by fluorescence activated cell sorting (2.3.8.7), and stimulated them *in vitro* for 5 days (2.3.12.3). Cells stimulated with medium alone were used as control. After fixation and staining of the nuclei, I analyzed the frequency of MuN macrophages. Indeed, I could observe a statistically significant reduction in the frequency of MuN macrophage formation in *C3ar1*$^{-/-}$ mice compared to cells from WT mice (Figure 3.29). Therefore, my data suggested that upregulation of C3aR on alveolar macrophages upon an HDM-mediated allergic asthma participates to the induction of multinucleated macrophage formation *in vivo*.

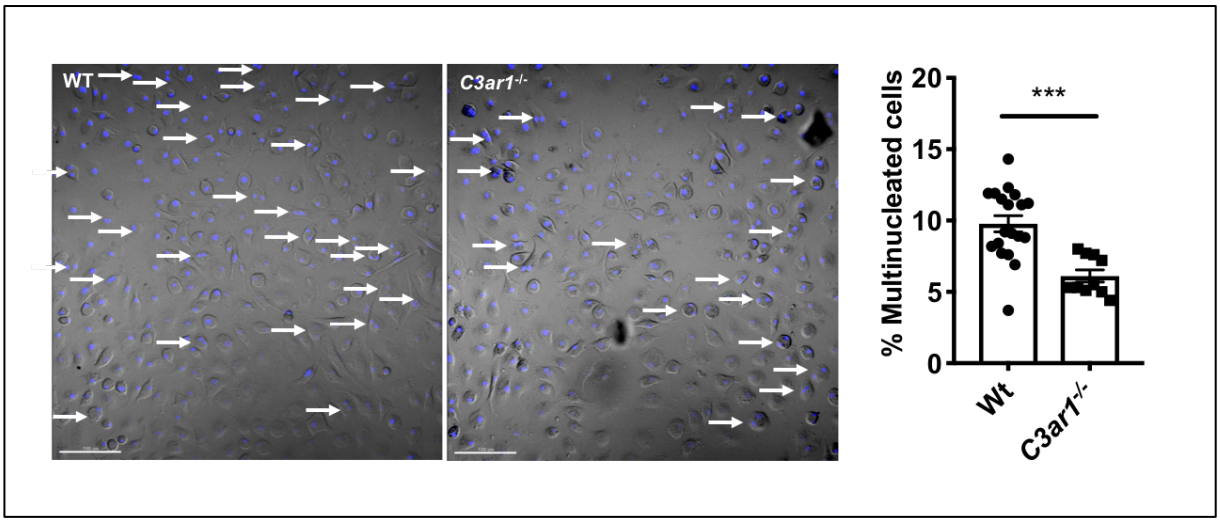

Figure 3.29 *C3ar1*$^{-/-}$ mice form less MuN cells in comparison to WT mice. Assessment of multinucleated macrophages by confocal microscopy (original magnification x20). Sorted tAMs from naïve *C3ar1*$^{-/-}$ and WT mice were stimulated with 100ng/ml GM-CSF. Shown is the fluorescence signal of DAPI for their DNA content (blue). Bars represent 100 µm. In addition, shown is the difference in the frequency of multinucleated cells of *C3ar1*$^{-/-}$ and WT mice in response to stimulation with GM-CSF. Values shown are the mean ± SEM; n = 10-20 per group. *p < 0.5, **p < 0.01, ***p < 0.001.

3.4.4 Both fusion and division defects are sources for tAMs polyploidy

Multinucleated giant cells are mainly described as cells that form through fusion under pro-inflammatory conditions (114, 123, 541). However, novel data have been shown that polyploid granuloma-resident macrophages formed via modified cell divisions and mitotic defects such as endoreplication and cytokinesis failure or recurrent cytokinesis failure (121). Therefore, I wondered if the observed MuNCs in lung tissue and lung cell isolations, but also *in vitro* generated multinucleated macrophages were arising from fusion or cell division defects.

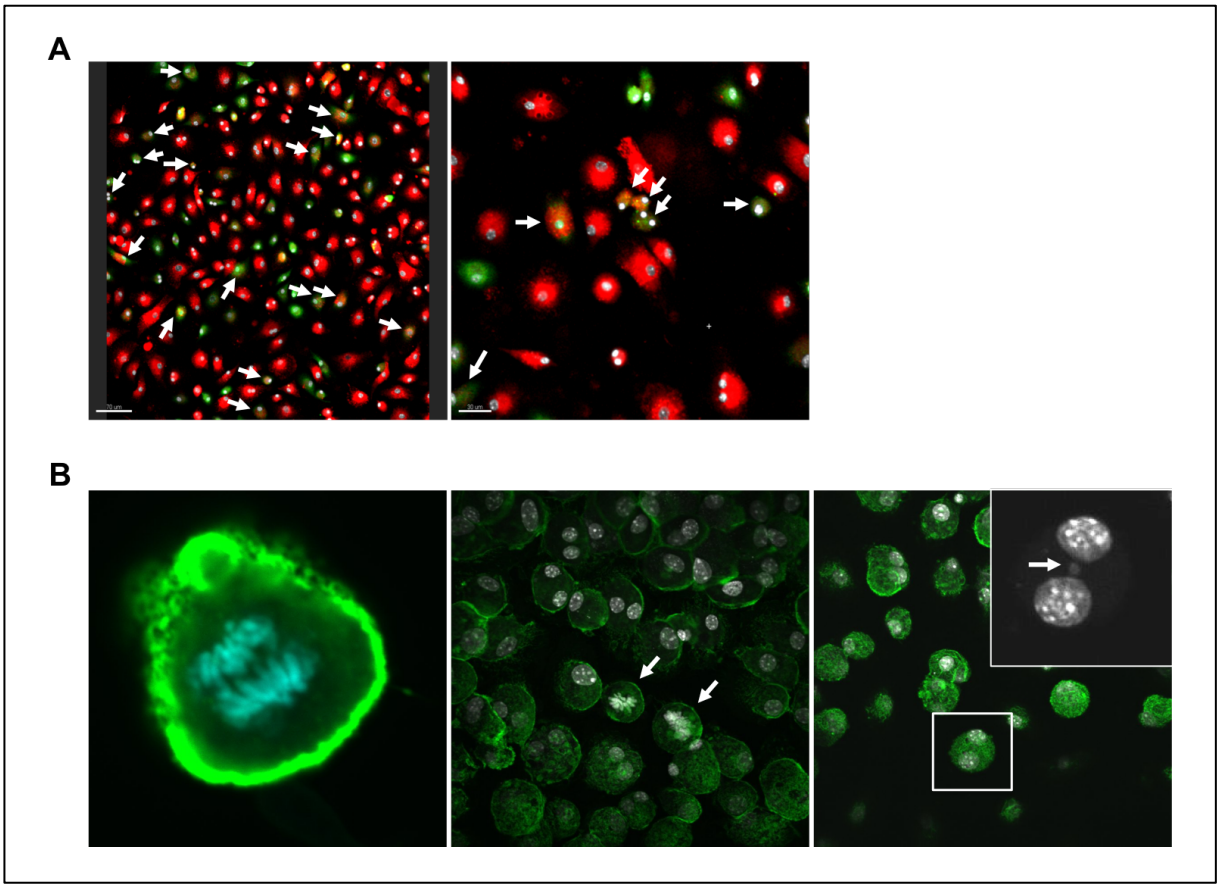

Figure 3.30 tAMs form both through fusion and division defects. (**A**) Assessment of fused macrophages by confocal microscopy (original magnification x20/x40). Membrane of MuN macrophages were stained with PKH26 or CFSE and cells where co-cultured for 5 days. Shown is the fluorescence signal of DAPI for the DNA content (white) from tAMs and membrane staining with PKH26 (red) or CFSE (green). Bars represent 70/30 µm. Arrows show cells holding both red and green staining. (**B**) Assessment of proliferation and division defects of alveolar macrophages by confocal microscopy (original magnification x40/x60). Shown is the fluorescence signal of DAPI for the DNA content (white) from tAMs and their membrane staining with WGA (green). White arrows show mini-nucleus.

To delineate the mechanism leading to MuNC formation of tAMs, I used an *in vitro* model, where I firstly purified naïve tAMs by FACS (2.3.8.7), labeled tAMs either with PKH26 or CFSE (2.3.8.6) and co-cultured differently labeled tAMs together in presence of GM-CSF (2.3.12.4) to induce MuNC formation. I could identify binucleated cells that were either red or green, but in addition I could report binucleated cells that had a red and green (merged yellow) staining (Figure 3.30A). Although this

suggested that MuN macrophages formed by fusion, I could also observe mononucleated cells showing a double staining, which may either indicate phagocytosis of dying tAMs or that in addition to the membrane also the nuclei of the macrophages fused. In contrast, careful examination of pictures taken from *in vitro* MuN cell induction with 10 ng/ml GM-CSF for 7 days (2.3.12.3), showed that cells actively proliferated since I could observe cells that were under mitosis (Figure 3.30B). Additionally, in such conditions, micronuclei, as a sign of defective cytokinesis, could also be observed (Figure 3.30B). Altogether, my data suggest that fusion and cell division defects are both sources for the formation of MuN cells from tAMs.

3.4.5 Binucleated cells are more potent to engulf T cells than mononuclear cells

I could demonstrate that tAMs were able to form MuNCs upon an HDM-mediated effector phase *in vivo* and also by stimulation with GM-CSF *in vitro*. In general, MNGCs have been described as cells that are better in phagocytosis of pathogens and big particles (541). However, the role and function of MuNCs derived from tAMs remained elusive. Therefore, I hypothesized that MuNCs could show a higher capacity to clear apoptotic T cells. In order to answer this question, I performed a co-culture experiment of *in vitro* generated MuNCs with PKH26-labeled activated $CD4^+$ splenic T cells (2.3.12.5).

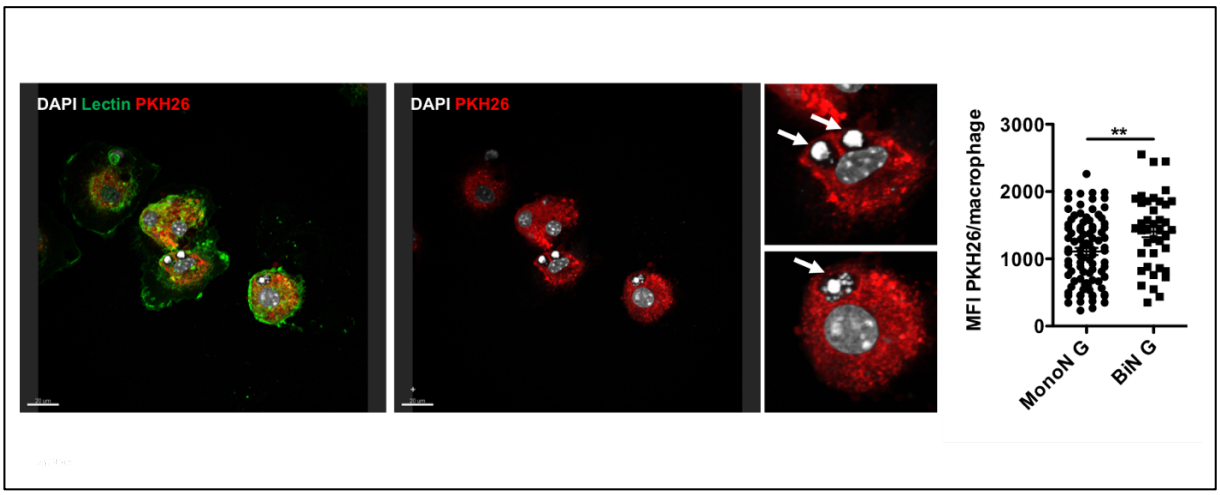

Figure 3.31 Binucleated cells show a better phagocytic capacity than mononucleated cells. (**A**) Assessment of mono- and binucleated macrophages capabilities to engulf activated T cells by confocal microscopy (original magnification x40/x60). Pictures show the fluorescence signal of DAPI for the DNA content (white), PKH26-labeled T cells (red) and membrane staining of macrophages (green) after 1 day co-culture of anti-CD3 activated T cells and in GM-CSF-induced multinucleated macrophages. Bars represent 20 µm. In addition, shown is the difference in the MFI signal of PKH26 of mono- and binucleated cells in response to co-culture with T cells reflecting their engulfment. Values shown are the mean ± SEM; n = 4 per group. *p < 0.5, **p < 0.01, ***p < 0.001.

After one day of co-culture, nearly all tAMs showed a red staining and in addition small nuclei (Figure 3.31), suggesting that PKH26-labeled T cells were phagocyted by tAMs and their membrane has already been digested, whereas the nuclei remained inside the endosomes. A preliminary semi-quantitative

analysis of the PKH26 fluorescence intensity in MuNCs and mononuclear (MonoN) macrophages revealed that MuNCs were significantly better in engulfing T cells than MonoN cells (Figure 3.31).
Therefore, my data suggest, that MuNCs are better phagocytes than mononuclear macrophages and may ensure accelerated inflammatory clearing upon allergic asthma conditions. However, their high level of MHCII expression also suggest that they are better in presenting antigens to $CD4^+$ T cells, although that function has not been tested and requires further investigation.

3.5 Conclusion

The conclusion of ATR expression during the effector phase of allergic asthma on alveolar macrophages is pictured in Figure 3.32. Briefly, $SiglecF^+CD11c^+$ tissue-associated alveolar macrophages show different anaphylatoxin receptor (C3aR, C5aR1 and C5aR2) expression levels. At steady-state they express high levels of C5aR1 and C5aR2, whereas C3aR is neither expressed on protein nor mRNA level. Intriguingly, all other $F4/80^+SiglecF^-$ macrophages express C3aR either on their surface or intracellularly. In contrast, upon an HDM-induced pulmonary inflammation associated with allergic asthma, tAMs upregulate *de novo* C3aR and in addition MHC class II and downregulate C5aR1. The underlying mechanism leading to the reciprocal regulation of C3aR and C5aR1, is IL-33 and IL-13 dependent and independent of peripheral blood recruited monocytes. Furthermore, during the effector phase of allergic asthma $C3aR^{hi}MHCII^+$ tAMs start to form multinucleated cells, a process which could be mimicked by *in vitro* cultivation of naive tAMs with GM-CSF. In addition, the formation of MuN cells is dependent on C3aR and they form both through cell-to-cell fusion as well as through cell division defects. Mechanistically, one role of these cells is to provide a better phagocytosis of apoptotic cells that occur during pulmonary inflammation.
Altogether, my data suggest that C3aR activation in tAMs plays an underestimated role in allergic asthma severity via the control of tAMs involved in MuNCs formation.

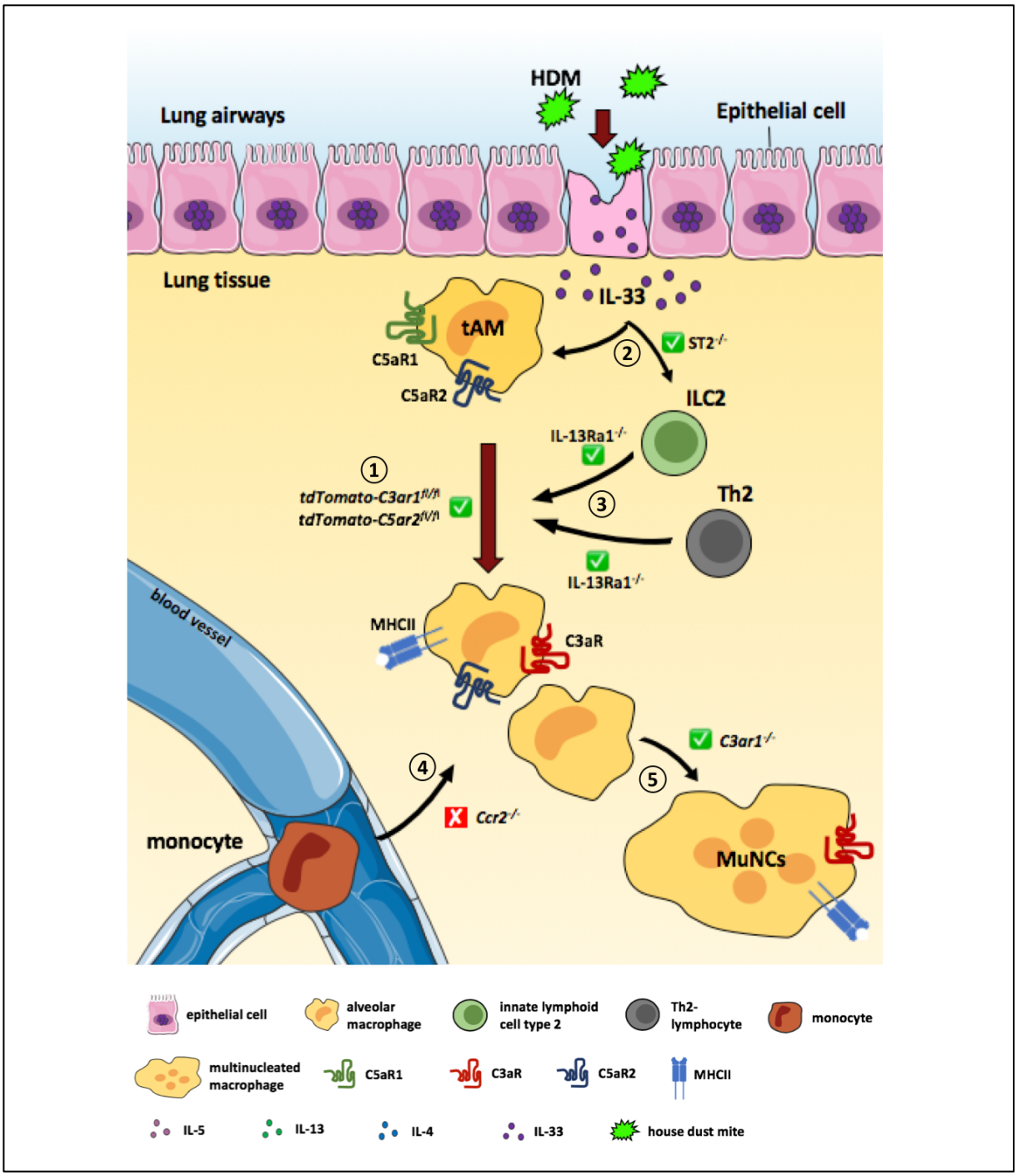

Figure 3.32 Visual conclusion of ATR expression during the effector phase of allergic asthma. (**1**) AMs express C5aR1 and C5aR2 at steady-state, but lack C3aR expression Upon an HDM immunization they start de novo expression C3aR, downregulate C5aR1 but keep C5aR2 expression. (**2-4**) HDM-treatment of different knockout mice strains were used to validate the hypothesis that IL-33-IL13-signals drive C3aR expression in resident AMs, leading to changes in ATR expression upon allergic asthma. (2) HDM treatment of *ST2*-deficient mice can block the activation of AMs, but also ILC2s and Th2 cells. Subsequent release of pro-inflammatory cytokines, like IL-13 and IL-5, is prevented. As a consequence, AMs do not upregulate C3aR and MHCII expression. (3) Immunization of *IL-13Rα1*-deficient mice is preventing the binding of IL-13 on AMs. As a consequence, C3aR and MHCII are not upregulated. (4) Investigation of C3aR expression and MHCII upregulation in HDM-treated *Ccr2*$^{-/-}$ mice is showing that resident pulmonary macrophages, but not allergen-recruited monocyte-derived AMs, upregulate C3aR expression. (**5**) Resident alveolar macrophages form multinucleated cells during the effector phase of allergic asthma. *In vitro* culture of *C3ar1*$^{-/-}$ mice showed that C3aR participates in the formation of MuNCs.

4 Discussion

Asthma is a chronic inflammatory disorder of the airways caused by innocuous environmental allergens leading, through airway remodeling, mucus hyperplasia, and smooth muscle cell contractions, to persistent bronchial hyperreactivity, chest tightness and difficulties in breathing (334). The chronic inflammation caused by adaptive, innate and stromal cells plays a key role in the development of the disease (336). Further, several studies have revealed a central role of the complement system, in particular the anaphylatoxins (AT) and their cognate receptors (ATRs), on the development of the disease (263, 282, 464). However, most of these studies have concentrated on the role of the ATs on the development of allergic asthma at the level of the DC/T cell interface without taking into consideration other immune cells, such as alveolar macrophages or eosinophils, present at steady state and upon inflammation. In addition, the detailed understanding of the ATR expression in tissue-residing immune and stromal cells, in particular in alveolar macrophages, at steady-state and under allergic asthma conditions remained elusive due to the lack of adequate antibodies and/or tools to investigate the receptor expression level.

In this study, I used newly generated C3aR and C5aR2 reporter knock-in mouse strains in order to investigate ATR expression in a wide range of pulmonary immune cells and could show that at steady-state C3aR is mainly expressed by cells of the myeloid lineage, with a major exception since the SiglecF^{+}CD11c^{+}F4/80^{-} alveolar macrophages, which expressed high levels of C5aR1 and C5aR2, did not express C3aR at steady-state. However, upon HDM-mediated allergic asthma, AMs started *de novo* expression of C3aR and MHCII and downregulated C5aR1. Furthermore, using relevant knockout strains and pro-inflammatory cytokine models, I could demonstrate that the underlying mechanisms of a reciprocal C3aR-C5aR1 regulation depends on IL-33 and/or IL-13 signaling and do not require monocyte-derived macrophages. Moreover, I could demonstrate that C3aR is involved in multinucleated cell formation during the effector phase of allergic asthma, although the functions of these cells in the disease phenotype remained elusive. Altogether, I could show that the anaphylatoxins and their receptors on alveolar macrophages play an underestimated role on allergic asthma development and severity.

4.1 New insights into the expression pattern of C3aR in mice at steady-state

Although the mouse gene encoding C3aR was cloned in 1997, a detailed understanding of its expression in tissue-residing immune and stromal cells remained elusive (542, 543). While up to now, most of the expression and functional data existing, in terms of C3a/C3aR signaling axis have been

mostly obtained with humans (221, 224, 225), direct evidence for the expression of C3aR in murine immune and non-immune cells, at steady-state or under inflammatory conditions, are scarce and partly contradictory. The main reason might be due to the lack of C3aR-specific mAbs. Indeed, various studies worked with polyclonal Abs against C3aR in western immunoblots and immunohistochemistry (262, 506, 517). However, Tschernig et al. reported that most of these antibodies bind unspecifically, while only the monoclonal antibody clone 14D4 worked in immunofluorescence microscopy (517). Moreover, my own western blot analysis revealed that all of the commercially antibodies used in the past, such as the clone H-300 (281), D-12, and D-20 (277), give non-specific signals in western immunoblot (Figure 2.9). In addition, my data also showed non-specific signals in peritoneal macrophages by flow cytometry using the clone D-20 (Figure 2.4). In contrast, the clone 14D4, was appropriate in flow cytometry, although it proved useless for western blotting (data not shown). All together, these antibody limitations were calling for other methods to evaluate the expression of C3aR in mice. Therefore, in my studies, I used a newly developed floxed tdTomato-C3aR reporter knock-in mouse. The reporter strain contains the coding sequence for a tandem dye (td)dTomato-C3aR self-processing polyprotein, flanked by two loxP sites (227). Using this mouse, I was able to determine murine C3aR expression in pulmonary leukocytes and macrophages from various tissues, including the LP of the small intestine, the VAT, and the brain. Furthermore, cells, which showed a positive tdTomato-C3aR signal, were evaluated for C3aR surface expression using the anti-C3aR mAb (clone 14D4), which was tested for its specificity using cells from C3aR-deficient mice. This approach provided novel and detailed insights into the C3aR expression pattern in immune and stromal cells of mice at steady-state.

4.1.1 Mice as a model organism for the allergic asthma

The house mouse (*Mus musculus*) is one of the most important model organisms used in biology and medicine. Various disease models have proven the usage of the laboratory mouse and the benefit in research. Likewise, the laboratory mouse has developed into the preferred model system for biomedical lung research, not only because of the relative unsophisticated standardized housing condition and short timeframe of generation but also for the high degree of resemblance between men and mice in terms of genetics and immunology (544). Furthermore, the usage of inbred strains enables a high reproducibility of experiments and the breeding of knockout and reporter knock-in strains facilitates the research of specific genes.

Nevertheless, it is important to keep in mind that, although mice are genetically closely related to humans, the anatomy, function and physiology of their respiratory tract differ significantly (545). The macroscopic structure of the lung shows already marked differences. Whereas the human lung consists of 3 left and 2 right lung lobes, the murine lung is made of one left and 4 right lobes. In

addition, the mouse lacks respiratory bronchioles. Here, the terminal bronchiole is the smallest airway structure and leads directly to the alveolar ducts. Furthermore, while in humans the complete trachea consists of rings, in mice the cartilage system is less organized and only the upper part of the trachea has complete rings. In addition, there are differences in the cell amount and composition in the airway wall between mice and humans, for instance the mouse Clara cells can be found also in the trachea while they are normally only found in terminal bronchioles (545).

However, selecting the right mouse strain and allergen, a laboratory mouse provides a good model organism for the investigation of the allergic asthma development with a recapitulation of the main characteristic of a pulmonary inflammation. It opens the window for research of the Th2/Th17 cell immune response, the infiltration of various immune cells, mucus overproduction and production of allergen-specific IgE. In addition, various measurement techniques for physiological parameters like airway hyperresponsiveness (AHR), have been developed and open the opportunity to easily determine the asthmatic phenotype of a mouse. Finally, repeated allergen challenge leads to pathological changes in lung tissue that can be similar observed in chronic asthma patients.

4.1.2 Differential expression pattern of C3aR in humans and mice

My data highlighted some strong differences between humans and mice in terms of C3aR expression. Firstly, functional studies as well as binding studies have reported the expression of C3aR in human neutrophils (221, 546, 547). Although some reports suggested also an expression of C3aR in murine neutrophils (277, 548), I could not, using the tdTomato-C3aR reporter mouse, confirm the neutrophilic expression of C3aR, either in the lung (see Figure 3.5) or in other tissues (227). Interestingly, the previous study reported C3aR expression in Gr-1$^+$ cells based on Western immunoblot analysis and by flow cytometry (277). However, Gr-1 recognizes both Ly6C and Ly6G, hence targets not only neutrophils but also other immune cells, including eosinophils, monocytes and DCs. In contrast, I used a specific anti-Ly6G clone (1A8) that has been described as a far more reliable antibody to identify neutrophils (549). In addition, studies re-examining anaphylatoxin receptor expression, revealed lack of antibody specificity (262, 277) and caused disparate findings (227, 517), suggesting that the previous identification of C3aR in steady state neutrophils could be a false positive result. Of note, upon LPS activation, neutrophils have been reported to express C3aR, which in turn are important for neutrophil NETosis (237), although HDM-induced asthma did not (227).

Similarly, studies regarding the expression of C3aR on human T cells are contradictory. While older studies failed to detect C3aR surface expression in naive T cells, more recent publications have shown low levels of C3aR expression in naïve human T cells (188, 221, 231, 508, 550). Further, such low surface expression increased upon CD3 and CD28 stimulation (550). Moreover, C3aR expression was found intracellularly in resting human T cells and was translocated to the cell surface upon CD3 or CD3$^+$CD46

stimulation (188). In mice, one study reported surface expression of C3aR in naive T cells (509). Furthermore, *C3ar1* mRNA expression was reported in naive $CD4^+Foxp3^+$ natural (n)Treg cells, which was enhanced in response to CD3 and CD28 stimulation (508). In contrast to these reports, I could detect a tdTomato-C3aR signal neither in pulmonary naïve $CD4^+$ T cells nor in murine naïve $CD4^+$ T cells from the circulation, spleen and mediastinal lymph nodes as well as upon CD3/CD28 activation of splenic $CD4^+$ T cells (227). The absence of C3aR in T cells was also confirmed by mRNA analysis. So far, the original description of C3aR in T cells used antibodies with inadequate specificity (281).

Likewise the opposing data about C3aR in human neutrophils and T cells, receptor expression in human B cells seems to be controversial. Indeed, tonsil-derived human B cells have been shown in one study to express C3aR and in another the receptor has not been detected on peripheral blood-derived B lymphocytes and on tonsillar B cells before and after stimulation with IL-2/*Staphylococcus aureus* (200, 221, 547). In contrast, data about C3aR in murine B cells are lacking. Using the tdTomato-C3aR reporter mouse, I could demonstrate that murine $CD19^+B220^+$ B cells from lung tissue do not express C3aR. Moreover, B cells from mediastinal lymph nodes (mLN), peritoneum, blood and spleen do not show C3aR expression (227). Although my data support the observation made in humans, that C3aR is not expressed in peripheral B cells, data related to C3aR expression in tonsils remain to be generated.

Summarizing my data, I could demonstrate that the expression pattern of C3aR in human and mice vary significantly, in particular in neutrophils, T cells. Hence, it is necessary to consider this fact for future research of diseases where the complement system plays a role.

4.1.3 C3aR expression in the lung is restricted to the myeloid lineage

Investigating lymphoid cells from the pulmonary compartment, I could demonstrate that both B and T lymphocytes lack tdTomato-C3aR expression at steady-state. In addition, C3aR was neither expressed in innate lymphoid cells, in particular ILC2s, nor in NK cells in the lung. These data suggest a restriction of C3aR expression to the myeloid compartment of the lung. The expression of C3aR mirrored the restriction in expression observed for C5aR1 (249, 259, 518) and C5aR2 (280).

The expression of C3aR in lung parenchymal cells is controversial. RNA hybridization of lung sections or immunohistochemical C3aR staining with polyclonal Abs, suggested an expression of C3aR on bronchial, alveolar epithelial cells and on smooth muscle cells but not in leukocytes (262, 551-553). In contrast, another study demonstrated C3aR expression solely on leukocytes using C3aR-specific mAb 14D4 for surface staining and mentioned unspecific binding for other Abs (517). In line with this observation, my 2-photon microscopy data provided evidences for a main tdTomato-C3aR signal around the airways but sparsely in the alveolar space. In addition, assessment of C3aR expression by confocal microscopy and flow cytometry did not reveal C3aR expression on naive alveolar or airway epithelial cells (227).

However, I could show two different cell populations expressing the tdTomato-C3aR signal in the lung. Firstly, I found that eosinophils from lung tissue express tdTomato-C3aR and C3aR. Interestingly, a large set of studies delineated the expression and function of C3aR in human eosinophils. Indeed, human blood eosinophils have been shown to express C3aR. Further, in these cells, C3a was reported to trigger reactive oxygen species, calcium flux, and to be chemotactic (196, 221, 514, 554, 555). In contrast, studies about C3aR expression in murine eosinophils were missing. I could show that C3aR is expressed by SiglecF$^+$CD11c$^-$ resident eosinophils from lung tissue. In addition, I could also show that C3aR is expressed in eosinophils from the blood, LP and peritoneum (227).

The second population largely expressing tdTomato-C3aR was the dendritic cell (DC). The expression of C3aR has been previously reported in *in vitro*-generated DC populations of human (556-558) and murine origin (229, 478, 486, 556, 558). Moreover, one study has revealed that, in BMDCs, the C3a/C3aR signaling axis is important for antigen uptake and T cell activation (486). However, the *in vitro*-derived BMDC are known to be poor surrogates to pulmonary DCs (482). Despite evidence showing that C3aR is expressed in human primary CD11c$^+$ conventional (c)DCs (557), little is known about the expression of C3aR in human pulmonary DC subsets. Similarly, evidences for the expression of C3aR in pulmonary DCs of mice are lacking. I observed that, in the lung, among the 4 DC subsets, only the monocyte-derived (mo)DCs and the CD11b$^+$ cDCs express tdTomato-C3aR and C3aR, whereas CD103$^+$ cDCs and the pDCs did not. In the lung, CD11b$^+$ cDCs have been shown to be critical drivers of Th2/Th17 maladaptive immune response in allergic asthma (86, 129).

In conclusion, my data indicate that the expression of C3aR in the lung is restricted to cells from the myeloid lineage.

4.1.4 Intracellular expression of complement

Interestingly, my results show a heterogeneous cellular distribution of C3aR expression in macrophages from different tissues. Peritoneal macrophages (PMs) and microglia showed surface expression, in contrast to brain, LP, and VAT macrophages that displayed solely intracellular localization of C3aR (see Figure 3.7). The exclusive intracellular localization was also confirmed in eosinophils and DCs from lung tissue (Figure 3.5) and other compartments (227). Recent studies already reported intracellular complement expression and activation in human cells, a concept recently designed as “complosome” (160). Resting human CD4$^+$ T cells were shown to contain intracellular stores of C3 which is cleaved in vesicles by CTSL into active fragments C3a and C3b. This C3a generation was demonstrated to be essential for homeostatic T cell survival. In addition, shuttling of the intracellular C3-activation-system to the cell surface upon T cell stimulation induced autocrine proinflammatory cytokine production (188). In fact, intracellular C3 activation is not limited to T cells but is observed in a wide range of immune and stromal cells including B cells, monocytes, neutrophils,

epithelial cells and fibroblasts, suggesting that intracellular complement activation could be of broad physiological significance (188). Moreover, human $CD4^+$ T cells also contain intracellular C5, which can be cleaved intracellularly by a yet unknown protease/convertase into C5a and C5b upon TCR engagement. The binding of the intracellular C5a to C5aR1 is required for normal ROS production and triggers NLRP3 inflammasome assembly which leads to intrinsic IL-1β secretion that sustains Th1 induction during T cell migration into tissues in an autocrine manner (190). In addition, it has been shown that autocrine and intracellular complement drives *per se* key T cell metabolic pathways during the Th1 induction (559). Interestingly, IL-1ß plays a major role in the regulation of the experimental allergic asthma phenotype through its impact on Th2/Th17 immune responses (560), and human eosinophils have been shown to secrete IL-1ß and to drive the production of IL-17A by $CD4^+$ T cells (561). Although a functional role of intracellular complement in eosinophils of human or mice has not yet been investigated, my data reveal new insight into intracellular complement expression in murine cells and suggest that likewise in human cells these processes play major role in survival, metabolism but also in inflammatory processes of pulmonary eosinophils.

4.1.5 C3aR in *tdTomato-C3ar1$^{fl/fl}$* knock-in mice is functional

In this study, I used a newly generated reporter knock-in mouse, designed to express a fluorescent tdTomato complex and C3aR (227). A tdTomato cassette was directly inserted in frame upstream of the 59 end of exon 2 of the *C3ar1* gene, because structural data have shown that the N-terminal part of the C3aR does not bind C3a (217, 500), while in contrast, the C-terminal part of the C3aR harbors important phosphorylation sites, conserved in humans and mice that drive receptor internalization and signal transduction (223). To allow a conditional deletion of the tdTomato-*C3ar1* locus, two loxP sites were placed upstream of the tdTomato coding sequence and downstream of exon 2 of the C3ar1 gene. Furthermore, instead of an internal ribosomal entry site (IRES), the porcine teschovirus-1 2A (P2A) was used to provide effective co-expression of tdTomato and C3aR from a single mRNA. P2A insertion is short length, provides a high self-cleavage efficiency, a higher level of transgene expression and ensures a stoichiometric expression of proteins flanking the 2A peptide (501-504). Finally, this vector leads to the efficient generation of two autonomous and separated proteins – the tdTomato protein and the C3aR protein. However, I wanted to ensure of the functionality of the C3aR protein, since ATR produced by bi-cistronic system showed reduced activity (249).

It is well established that GPCR phosphorylation by GRKs leads to the recruitment of β-arrestin, which results in receptor desensitization and internalization (562, 563). I could show that the C3a concentration necessary in mouse cells from WT and *tdTomato-C3ar1$^{fl/fl}$* to drive the maximal C3aR internalization, was 10 nM C3a as compared with 100 nM using human granulocytes (228). Similar, the observed internalization of C3aR was quicker in mouse cells compared to human cells, where most of

the C3aR signal was lost only 10 min after C3a stimulation (228). Additionally, I could show a similar rapid and transient increase in intracellular calcium concentration in thioglycolate-elicited PMs from WT and *tdTomato-C3ar1*$^{fl/fl}$ mice.

Similarly, C3a-induced ERK1/2 phosphorylation has been reported in human mast cell line-1 (HMC-1) and human bone marrow derived-mesenchymal stem cells (224-226). However, stimulation of PMs with C3a did not lead to ERK1/2 phosphorylation, although they express the receptor on their surface. This could be due to a different cell type or because of a different method to analyze pERK1/2. Indeed, while most studies analyzed ERK1/2 phosphorylation by western blot, I used a flow cytometric approach because of its versatility and ability to study cytoplasmic and nuclear phosphoproteins (564-568). However, I could show a C5a-driven ERK1/2 phosphorylation in neutrophils using the same protocol, suggesting that the absence of phosphorylation was not the result of a technical problem. Although it could be that phosphorylated ERK1/2 was below detection limit in flow cytometry, an alternative explanation will be that the C3a-induced signaling may alternatively, due to a rapid internalization and desensitization of the receptor, could not been detected anymore. Intriguingly, one study showed that GRK5/GRK6 inhibited C3a-induced ERK1/2 phosphorylation via distinct pathways (225), suggesting that an active inhibition of the C3a-ERK1/2 may also be at play here.

Summarizing my data, I could demonstrate that, although ERK1/2 phosphorylation in PMs was not confirmed, the C3aR protein from *tdTomato-C3ar1*$^{fl/fl}$ mice is functional as shown by an equivalent C3aR internalization and calcium mobilization in peritoneal macrophages from *tdTomato-C3ar1*$^{fl/fl}$ and WT mice in response to C3a stimulation.

4.2 C3aR on alveolar macrophages plays a dual role in allergic asthma

The role and function of both alveolar macrophages and C3aR in the allergic asthma development and severity are diverse and complex. Indeed, alveolar macrophages have been described as either tolerogenic, pro-inflammatory or pro-resolving depending on the conditions (110, 489). Moreover, C3aR has been mainly described to play a pro-inflammatory role in established allergic asthma (460, 484, 485). However, studies usually focused on the role of C3aR on the allergic asthma development at the level of the DC/T cell interface (478, 480). The initial report attributing a pro-inflammatory role to C3aR in allergic asthma was published nearly 2 decades ago. Since then, although the absence of C3aR gives a clear phenotype, characterized by a decreased allergen-induced airway hyperresponsivness, the role of immune cells besides DCs and T cells are unclear. Moreover, data related to the C3aR expression profile or the putative changes of C3aR expression upon asthmatic inflammatory conditions are scarce.

Firstly, I could recapitulate the reduction in AHR in comparison to WT mice reported in the past (407, 460, 478, 484, 485). However, C3aR was dispensable for the recruitment and composition of immune

cells in the lung. These results are supported by various other studies using C3 and C3aR-deficient animals revealing a strong pro-inflammatory immune response during the allergic asthma development together with reduction of AHR and bronchoconstriction in these animals (407, 460, 478, 483-485). Interestingly, only some, but not all studies showed differences in the Th2 immune response with induction of airway inflammation, mucus production, and IgE secretion likely depending on the allergen (HDM;OVA/aluminum hydroxide; OVA/*Asperigullus fumigatus*), the species (mouse (Balb/c, C57BL/6); guinea pig) and the sensitization route (i.t., i.p., aerosol) that have been used.

In addition, my data give new insides of C3aR pattern of expression upon allergic inflammation. They show that the CD11b$^+$ cDCs are the cells mostly affected in terms of expression. No other major changes could be observed in C3aR-expressing cells (moDCs, eosinophils) or C3aR negative cells (neutrophils, T, B cells). So far, no data exists on the role of C3aR in pulmonary DC/T cells cross talk, although locally produced anaphylatoxins in DC/T cell cross talk have been shown to be important for co-stimulatory and survival signals of naïve CD4$^+$ T cells (509) and the engagement of C3aR or C5aR of human monocyte-derived DCs enhances the cell activation and their capacity for allostimulation and may regulate T cell mediated immunity (556). Moreover, my data suggest that C3aR play a key but complex role in the establishment of airway hypersensitivity. Although the nature of the cells involved has to be clarified since I could not observe an expression of C3aR in stromal pulmonary cells (227). These data suggest also that in the lung of allergic mice C3aR on CD11b$^+$ DCs may be involved in the regulation of T cell survival and immune response.

4.2.1 C3aR upregulation in alveolar macrophages as a critical driver of bronchoconstriction during the effector phase

While CD11b$^+$ cDCs show a strong upregulation of C3aR in my tdTomato-C3aR reporter upon HDM-driven allergic asthma, they do not represent the main cell type upregulating C3aR. Indeed, using the tdTomato-C3aR reporter mouse and mRNA analysis, I could demonstrate that alveolar macrophages, which do not express C3aR at steady-state, start *de novo* C3aR expression upon allergen exposure.

Alveolar macrophages have been shown to develop a pro-inflammatory, M2a-phenotype, upon repeated allergen exposure (110, 489, 490). These activated AMs secrete pro-inflammatory cytokines like IL-4, IL-13 and chemokines like CCL17 and CCL22 causing persistent Th2 immune response, tissue remodeling, mucus hypersecretion and smooth muscle cell hyperplasia (489, 490). Although C3aR expression itself had no influence on the total cell number of alveolar macrophages during the effector phase of allergic asthma and did not lead to differences in the Th2 immune response, my results suggest that C3aR upregulation on alveolar macrophages might be a critical driver of bronchoconstriction either via increased secretion of IL-13 (421, 569, 570) or via a direct interaction of AMs with stromal cells (569, 571, 572). Indeed, AMs have been shown to produce IL-13 in sheep

following allergen challenge, in fibrotic lung of humans, and other airway diseases (489, 573-577). Although, AMs in rat have been shown to reduce AHR (578), another study has demonstrated that AMs are promoting AHR in a cockroach-induced airway inflammation (579) and are instrumental in viral exacerbation of asthma via the M2 muscarinic receptor (580). Of note, although eosinophils have also been reported to act on smooth muscle cell contraction via the M2 muscarinic receptor, the fact that no change of expression could be observed upon asthma suggest that C3aR in eosinophils do not play a role in such effect. Interestingly, these processes are independent of DCs, since adoptive transfer of *C3ar1*$^{-/-}$ BMDCs in contrast promoted a strong asthmatic phenotype associated with a marked AHR, strong Th2 cytokine and mucus production, as well as mixed eosinophilic and neutrophilic airway inflammation which do not differ from the WT controls (480).

4.2.2 Reciprocal modulation of C3aR and C5aR expression in alveolar macrophages as a potential mechanism to regulate the development of Th2 immune responses

Intriguingly, my data showed that while C3aR is *de novo* upregulated upon repeated allergen exposure, the high expression level of C5aR1 in AMs at steady-state is completely downregulated. These observations were in line with a previous study showing that, in an OVA-driven allergic asthma model, the expression of C5aR1 was down regulated upon allergic asthma (518). Furthermore, several studies have described a cross-regulation between C3aR and C5aR signaling in immune and stromal cells. One study showed that ligand-induced C3aR internalization on granulocytes, monocytes and mast cells has been dramatically decreased by co-stimulation with C5a, which could be blocked by neutralizing C5aR1 (228). In addition, in a model of respiratory syncytial virus disease C5-deficient mice showed elevated C3aR expression in bronchial epithelial and smooth muscle cells as compared with WT mice (551). Furthermore, C5aR1 expression in C3aR-deficient pulmonary DCs was increased when compared with WT DCs (478). Finally, in pulmonary DCs, the expression of C3aR and C5aR1 have been shown to be reciprocally modulated after HDM exposure (478). Interestingly, the protective effect of the C5a/C5aR1 signaling axis during allergen sensitization has been shown in detail. Thereby, ablation of C5aR1 led to excessive airway inflammation and a Th2/Th17 immune response associated with an increased allergic phenotype regarding AHR, airway inflammation and mucus production (259). However, the absence of C5aR1 in AMs or DCs do not impact the establishment and/or severity of allergic asthma in an OVA model (581). In contrast, C3aR has been mainly reported to have a strong pro-inflammatory effect during the allergic asthma development leading to increased bronchoconstriction (460, 484, 485). Since I could demonstrate that C5aR1 is highly expressed on alveolar macrophages at steady-state and C3aR is not, but strongly upregulated upon allergen

exposure, it gives rise to the hypothesis that the slight reduced allergic phenotype in C3aR-deficient mice after 4 times HDM exposure results from a protective C5aR1 signaling on alveolar macrophages during the allergen sensitization. Once C5aR1 is completely downregulated upon repeated allergen exposure in alveolar macrophages, C3aR is taking over with its pro-inflammatory functions, therefore, leading to increase in AHR. One may speculate that repeated allergen contact would additionally lead to an increased airway inflammation. Indeed, a reciprocal modulation of C5aR1 and C3aR expression and its regulatory role in a Th2 immune response has been already shown in pulmonary DCs. This study suggests that the reduced asthma phenotype in C3aR-deficient mice is mainly driven by the protective C5aR1 signaling of pulmonary DCs (478). However, examining closely the expression of C5aR1 and C3aR on alveolar macrophages, indicates that the obtained allergic phenotype resulted from a reciprocal receptor regulation on AMs during the allergic asthma development. This assumption can be supported by the fact, that adoptive transfer of either *C3ar1*$^{-/-}$ or *C5ar1*$^{-/-}$ BMDCs led to the opposite asthma phenotype than *in vivo* models with these knockout strains (479, 480). Of note, the expression levels of C5aR2 in AMs upon allergic asthma has not been studied yet. However, an important point could be the balance of expression between C5aR1/C5aR2 at steady state shifting to a balance C3aR/C5aR2 upon inflammation. Such shift would probably result in significant functional changes in AMs functions.

Altogether, my data reveal that the HDM-induced sensitization and effector phase leads to a reciprocal regulation of C3aR and C5aR1 in alveolar macrophages and may play a role in the regulation of a Th2 immune response.

4.2.3 C3aR^{hi}MHCII^{+} AMs may play a role in local innate immune memory cells

Immunological memory has long been described as a main feature of the T and B adaptive immunity in vertebrates. However, accumulating evidences show that in plants and invertebrates (that do not develop adaptive immunity), phagocytes respond much better to a challenge if they had already a first contact with the microbe (582). Indeed, new insights into cell biology have weakened the old concept of a memory response only by adaptive immune cells, revealing that monocytes, macrophages, and NK cells may also acquire an immune memory after primary immunologic exposure to enhance host defense, a process now known as trained immunity (583-587). Thus, innate immunity has the ability to form a memory, although different from adaptive immune memory. Nevertheless, in the case of a related or unrelated microbial exposure, it can initiate an enhanced inflammatory response. The molecular mechanisms responsible for initiating and instructing innate immune memory formation remain elusive. Recent studies have described the mechanisms setting up this innate memory. Trained immunity is mediated by epigenetic, metabolic, and functional reprogramming of innate immune cells, such as myeloid cells and NK cells (584), and is systemically induced at the level of bone marrow

progenitors (585, 588). However, recent data about innate immune memory at mucosal sites revealed that, in contrast to previous studies, long-lived resident mucosal macrophages arose upon respiratory adenoviral infection. These viral-induced long-term memory AMs were characterized by high expression of MHCII, a specific defense-ready gene signature, increased glycolytic metabolism, and heightened chemokine production (589). In addition, examination of the RNA-based gene microarray of the AMs of the viral-infected lung from Yao *et al.* revealed that memory AMs also showed an increased level of *C3ar1* similar to the AMs of the HDM-mediated allergic asthma model (589). Moreover, their data demonstrate that while the priming of memory AMs requires the help of effector $CD8^+$ T cells in an IFN-γ- and contact-dependent manner, the generation and maintenance of these memory AMs are autonomous processes and involve a low rate of *in situ* proliferation, independently from circulating monocytes or bone marrow progenitors (589). In agreement with these data, my $C3aR^{hi}MHCII^+$ AM subpopulation develop independently from blood-recruited monocytes as shown by experiments of *Ccr2*$^{-/-}$ mice exposed to HDM. Re-analyzing some previous data with HDM-exposed *Rag2*$^{-/-}$ mice generated by a former PhD student reveal that mice deficient in B and T cells do not develop $MHCII^+$ AMs (data not shown) which is in analogy to the long-term memory AMs of the viral infected lung that requires T cell priming. However, viral infection in general involves the help of $CD8^+$ T cells and IFN-γ, whereas allergic asthma mainly involves $CD4^+$ T cells and the Th2 cytokines IL-4 and IL-13 (1). Therefore, the priming of memory AMs in an allergic asthma model may require presumably the help of effector $CD4^+$ T cells and/or ILC2 in an IL-13 and/or IL-4-dependent manner. This assumption can be supported by the results I obtained with an IL-13-induced pulmonary inflammation and HDM-treated *IL-13Rα1*$^{-/-}$ mice showing also upregulation of C3aR and MHCII in tissue-associated AMs.

Taking these similarities into account, my data showed that upon HDM exposure, the AMs showed some phenotypic overlap with memory AMs, suggesting that $C3aR^{hi}MHCII^+$ AMs may serve as long-term memory AMs, and that allergen activated alveolar macrophages may provide a trained immunity in the context of allergic asthma.

4.3 Multinucleated cells in allergic asthma

For the first time, I report multinucleated cell (MuNC) formation by AMs *ex vivo* and *in vivo* during the effector phase of an experimental allergic asthma model. Only one publication from the 80s has described multinucleated giant cells in BAL and lung of patients suffering from respiratory disorders after metal particles exposure. These patients showed interstitial pneumonia and fibrosis with multinucleated giant cells, comprising both type II alveolar epithelial cells and AMs (590).

Knowledge of MuNCs (also referred in the literature as multinucleated giant cells -MNGCs) role and function in disease progression and/or resolution remains limited. While historically their role has been

mainly described in pathogen-induced granuloma, osteoporosis, bone cancer and foreign body material rejection, revealing a role in disease progression and tissue remodeling, MuNCs have been mainly considered as “bad guys”. However, they have also shown a better phagocytic capacity and may contribute to resolution of inflammation. Therefore, they may also be considered as "good guys". These opposing phenotypes and functions call for the necessity to no longer refer to MuNCs as "good" or "bad" cells, but instead characterize and describe them more specifically according to their distinct phenotype, as it was done for the macrophage subtypes (119). My data indicate that *in vitro* generated MuNCs show a better phagocytic capacity to engulf activated T cells under pro-inflammatory conditions than mononucleated AMs. These data are supported by a study showing that IL-4-induced large MNGCs (with more than 10 nuclei/cell) phagocytosed large and complement-opsonized materials more effectively than their unfused M2 macrophage precursors (541). Intriguingly, large MNGCs with more than 15 nuclei per cell that develop in an *in vitro* model of human tuberculous granulomas formed in presence of high-virulence mycobacterium (*Mycobacterium tuberculosis*) resulted in MNGC with defective phagocytic activity. In contrast, MNGCs with lower numbers of nuclei per cell (less than seven) in granuloma formed in presence of low-virulence mycobacterium species (*Mycobacterium avium* and *Mycobacterium smegmatis*) produced phagocytically-potent MNGCs (591). Interestingly, the MuNCs observed *in vivo*, as well as the MuNCs generated by *in vitro* stimulation of sorted naïve AMs never reached more than 4-5 nuclei per cell and show potent phagocytic activity.

Since MuNCs show a better phagocytic capacity, I hypothesized that the development of MuNCs by alveolar macrophages upon allergic asthma conditions may be crucial for a better resolution of airway inflammation. Indeed, clearance of apoptotic cells by macrophages in the airways play a vital role in airway resolution, since delayed clearance could induce secondary necrosis and subsequent release of toxic cellular contents resulting in tissue damage and persisting inflammation in allergic asthma and chronic inflammatory lung disease (435, 436).

Molecular basis of MuNCs formation

Cytokines

Classical MuNCs formation depends on type 2 cytokines, with a major role played by IL-4 and GM-CSF. IL-4 has been demonstrated to induce expression of E-cadherin and dendritic cell-specific transmembrane protein (DC-STAMP) as well as ß1, ß2 and ß5 integrins, in monocytes and macrophages which mediate adhesion during macrophage fusion and multinucleated foreign body giant cell formation (112, 114, 592, 593). Further, *in vitro* culture of rat alveolar macrophages in presence of GM-CSF promoted multinucleated macrophage formation via macrophage fusion receptor (MFR), P2X7 receptor (P2X7R) and Pannexin-1 (Panx-1) (123, 124, 594). Interestingly, I could demonstrate that

in vitro stimulation of sorted naïve AMs with GM-CSF but not IL-4, recapitulated bi- and multinucleated cell formation observed *in vivo*. Of note, IL-4 was potently driving the formation of MuNCs starting with BM-derived macrophages, suggesting that different mechanisms may initiate macrophage multinucleation. Moreover, although GM-CSF functions as a growth factor for the maturation and proliferation of macrophages and monocytes, it is also released as a pro-inflammatory mediator by activated and disrupted epithelial cells upon allergen exposure (332, 595). Therefore, stimulation of AMs with GM-CSF mimics the pro-allergic environment and confirms the finding of MuNCs formation in an i*n vivo* allergic asthma experiment.

Fusion and division defects

The formation of MNGCs is generally attributed to cell-to cell fusion (596). Such mechanisms can be triggered through receptor activator of NF-κB ligand (RANKL)-induced osteoclasts formation, which requires the fusion of osteoclast precursors (122). Similarly, stimulation of monocytes with mycobacteria lipoproteins *in vitro* promotes their fusion and the formation of MNGCs (597, 598). Mechanistically, Th2 cytokines, in particular IL-4, have been described to play a key role, mediating the adhesion of monocytes and macrophage during fusion (592). However, the inability of IL-4 to drive formation of alveolar macrophage-derived MuNCs *in vitro,* together with the absence of clear $CFSE^{+}PKH26^{+}$ labeled MuNC in my co-culture experiments, suggested that the role of fusion in the formation of MuN macrophages may be limited. Rather, my *in vitro* data suggest that MuN macrophage formation may occur by upon cytokinesis failure, in particular because of the high frequency of mitosis and micronuclei (MN) in GM-CSF treated cells. MN have been associated with genotoxic events and chromosomal instability leading to cytokinesis failure (121, 599), mechanisms involved in long-lived granuloma-resident multinucleated macrophages formation. Such events arise upon persistent inflammatory stimuli, a pathway previously linked to oncogene-initiated carcinogenesis (121, 600). However, my data do not formally exclude that fusion is taking place, since both fusion and cytokinesis failure in AMs can occur at the same time as observed in lung fibrosis, where it has been shown that AM proliferation appears to be prerequisite for cell fusion and MNGC formation as a feature of granulomatous disease (601).

In conclusion, for the first time my data show MuNCs formation by murine AMs in an experimental allergic asthma model. In addition, the generation of MuNCs under pro-inflammatory conditions *in vitro* occurs by both cell-to-cell fusion and through cytokinesis failure. With that, my data open a new window in the research field of multinucleated (giant) cells and their role in allergic asthma and other pulmonary diseases.

4.3.1 C3aR participates in the formation of MuNCs

So far, the molecular and cellular mechanisms of MNGC formation remain poorly defined. However, a number of common factors and mediators for adhesion and fusion have been demonstrated to contribute to MNGC formation. Thus, giant cells formation in mycobacterium-induced granulomas occurs through an ADAM9 and ß1 integrin-mediated pathway, while the formation of osteoclasts depends on the integrin $\alpha_v ß_3$ and RANKL, and the dendritic cell-specific transmembrane protein (DC-STAMP) has been identified as being required for the fusion of both osteoclasts and foreign body giant cells (598, 602). In addition, macrophage fusion receptor (MFR), P2X7R, Panx-1 and Cnx43 have been shown to play a functional role in MNGCs formation (123, 124, 603). However, the wide diversity of species, models, and cell types that have been used in these studies suggest that the formation of MuNCs is more complex and depends on way more factors than previously thought.

In addition to these mediators, I could demonstrate that *in vitro* generation of MuNCs by alveolar macrophages depends on C3aR, since *C3ar1*$^{-/-}$ AMs showed reduced bi- and multinucleated cell formation upon GM-CSF stimulation compared to WT AMs. Interestingly, other *in vitro* studies using BM progenitors for the generation of MNGCs showed that complement is involved in the formation or in the function of MNGCs. Also, analysis of scRNA-seq data from Herrtwich et al. (121) reveals that complement is upregulated in multinucleated cells. A significant increase of *C3* and partly in *C3ar1* mRNA occurred in FSL-1-stimulated cells (FSL-1 is a synthetic bacterial lipoprotein (BLP) acting as a ligand for the TLR2/6 complex) with a DNA content of 2c and >4c as compared to control cells (121). Moreover, it has been shown that the activated complement receptor (CR)3 (CD11b/CD18) specifically equips MNGCs to engulf large complement-coated targets (541). Although the influence of C3aR *in vivo* has not been investigated by my studies yet, these data suggest that C3aR may play a role in MuNC formation *in vivo* upon allergic asthma conditions. Supporting this idea, LPS and C3a have been shown to induce IL-1ß production in human macrophages and dendritic cells via adenosine triphosphate (ATP)-mediated P2X7R and TLR signaling, which together activate the inflammasome (229). Since P2X7R has been shown to induce MNGC formation in rat AMs (123), it is tempting to propose that both P2X7 and C3a/C3aR participates to initiation of MuNC formation by AMs.

4.3.2 MNGCs in pulmonary diseases

MNGCs have been shown in all pulmonary diseases, which are associated with granulomas. Also called granulomatous lung diseases, they are a heterogeneous group of disorders that have a wide spectrum of pathologies with variable clinical manifestations and outcomes. They include both infectious and noninfectious lung diseases, among which Mtb and *Histoplasma capsulatum* infection, but also in noninfectious lung fibrosis, lung injury and sarcoidosis (590, 601, 604-606). Although their incidence is widely distributed, the function of MNGCs in granulomas is incompletely understood. *In vitro* studies

of granulomas from human tuberculosis patients have demonstrated that MNGCs produce both pro-inflammatory and anti-inflammatory mediators such as the cytokines IL-1α, IL-10, IFN-γ, TNF-α, TGF-ß, chemokines such as CXCL10, CCL2 and enzymes like MMPs. However, compared to epithelioid macrophages, which share a common origin with MNGCs, giant cells express more anti-inflammatory cytokines i.e. TGF-ß and have higher antigen load and reduced mycobactericidal abilities (607-610). These studies reveal that MNGCs have, on the one hand, a pro-inflammatory role and on the other hand anti-inflammatory, wound healing and tissue remodeling functions. While the development of a pro-inflammatory milieu helps to dampen pathogen infection and/ or protects against infections in an injured lung, once the inflammation occurs, it is also necessary to start tissue repair. Therefore, MNGCs release also anti-inflammatory mediators. However, prolonged anti-inflammatory MNGC response can cause tissue remodeling and lung fibrosis.

The presumably dual role of MNGCs/MuNCs in pulmonary granulomatous diseases, give suggestions for their role in allergic asthma, where they may have both pro-inflammatory and anti-inflammatory / pro-resolving functions, likely depending on the time of occurrence. This would be supported by my findings that MuNCs formation depends on C3aR and occurs in the effector phase of allergic asthma and may participate to the airway remodeling and smooth muscle cell contraction. In line with this hypothesis, a study where polyploid cells induced by bacterial lipoproteins (BLPs) showed increased expression of genes encoding ECM remodeling proteases, such as *Mmp8*, *Mmp9*, *Chi3l3*, cathepsin K *(Ctsk)*, and lysosyl oxidase (*Lox)* (121). However, they may also have anti-inflammatory / pro-resolving functions indicated by their better phagocytic capacity compared to mononuclear macrophages. Therefore, it is indispensable to characterize and describe MuNCs in allergic asthma more specifically according to their time of occurrence and their possible phenotype in order to delineate their role at the different stage of the disease.

4.4 Alveolar macrophages are a peculiar population of macrophages

Besides expression profiles differing from human to mouse, my data allow me to exemplify heterogeneity of C3aR expression into cells from the same type. Indeed, while macrophages from LP, VAT, peritoneum and the brain showed a strong tdTomato-C3aR signal and C3aR expression, airway and tissue-associated alveolar macrophages do express C3aR neither on mRNA nor protein level. Intriguingly, this dichotomy in C3aR mirrored the specific expression of Siglec-F, limited to the airway and tissue-associated alveolar macrophage subset. In this context, the expression of C3aR parallels the expression profile of F4/80 or CD11b in macrophages.

4.4.1 AMs: what makes them so extraordinary

Alveolar macrophages are a peculiar population of macrophages differing from other tissue-resident macrophages in various aspects.

Firstly, AMs differ from all other macrophages throughout the body in terms of surface receptor expression. In agreement with other studies, I could demonstrate that AMs are characterized by a high expression of Siglec-F and CD11c and a low expression of F4/80 (128, 129, 505, 611). This is in marked contrast to other macrophages such as the macrophages from the PerC, the LP of the small intestine, the VAT and the brain, which can all be identified by their high expression level of F4/80 in combination with other markers (612). In addition, I could show that airway and tissue-associated SiglecF^{+}CD11c^{+} AMs are the only macrophage population that do not express C3aR at steady-state. Of note, AMs start *de novo* C3aR expression upon an experimental allergic asthma model or pulmonary pro-inflammatory cytokine-induced models, whereas other macrophage population did not change their expression level.

Moreover, AMs differ from other tissue-resident macrophages in their unique localization at the interface between pulmonary mucosa and external environment, meaning that they are the only macrophage population that is in direct contact with the environment evolved to ward off pathogens and restrain inflammation-mediated damage to maintain gas exchange. Because of their exceptional localization, their role in keeping homeostasis, and their capability to induce inflammatory immune response, they prove to have a strong plasticity allowing them to modify their phenotype into anti-inflammatory or pro-inflammatory macrophages according to their surroundings. They are prime candidates to serve as promotor or suppressor of airway inflammatory responses (127). However, this makes very difficult and complex to classify them. As I exemplified, AMs may play a key role in mediating inflammation and airway remodeling in part via the upregulation of C3aR and downregulation of C5aR1, causing disease progression and typical asthmatic symptoms as bronchoconstriction. In contrast, they are the most important cell type in resolution of inflammation by their competence in efferocytosis and the release of pro-resolving mediators (434, 443, 444) and C3aR in the context of MuNCs formation may play an important role. Further, a recent study revealed that AMs not only have their function in maintenance physiological homeostasis, inducing inflammatory immune response and participating in resolution of inflammation, but even have an autonomous memory function (589). Therewith, AMs are the first macrophage population that has been identified to form a long-lasting trained immunity that developed independently of monocytes or bone marrow progenitors and the first innate immune memory identified at mucosal sites.

So far, multinucleated cells have been only described in granulomas, osteoclast formation or foreign body reaction (116, 120, 613). My *in vivo* data reveal that AMs are the only macrophage population that form multinucleated cells beyond granulomas, osteoclasts or foreign bodies but are able to form

multinucleated cells upon allergic induced pulmonary inflammation. To that point, most of the publications have described multinucleated macrophage formation only by cells from the BM hematopoietic lineage (114, 121, 541, 614). However, my data reveal that AMs, as mature tissue-resident macrophages derived from Yolk sac macrophages and fetal liver monocytes, seems to be the only macrophage population that has the ability to generate MuNCs independently of monocytes or bone marrow macrophage progenitors. Indeed, multinucleated macrophage formation by alveolar macrophages has already been described in an *in vitro* model of rat AMs (121, 123). In addition, in patients with respiratory disorders associated with metal particles exposure showed interstitial pneumonia and fibrosis with unusual multinucleate giant cells comprised both type II alveolar epithelial cells and alveolar macrophages (590).

In conclusion, alveolar macrophages are an extraordinary macrophage population compared to other macrophages, due to their unique localization, specific expression of surface markers and their remarkable roles and functions.

4.5 Summary and future prospects

4.5.1 New targets for allergic asthma therapies

Alveolar macrophages play a complex role in the development and progression of allergic asthma. At steady-state and during the sensitization phase of allergic asthma they exert a tolerogenic phenotype trying to maintain physiological homeostasis. However, upon prolonged allergen contact they switch their tolerogenic phenotype to a pro-inflammatory phenotype by releasing pro-inflammatory mediators such as IL-13, IL-4 and eotaxin, leading to airway remodeling and disease progression. Certainly, they also play a vital role in the resolution of airway inflammation through increased efferocytosis and the release of pro-resolving mediators. With that, targeting alveolar macrophages in the different stages of the disease may a new therapeutic strategy. Reducing their pro-inflammatory mediators but increasing their capacity to engulf apoptotic cells and their release of pro-resolving mediators may be new approaches for pharmaceutical research.

Moreover, my data demonstrate that C3aR plays a pro-inflammatory role during the effector phase of allergic asthma but may also be involved in the development of long-term memory AMs. Targeting C3aR in the early phase of an allergic asthma by a C3aR antagonist or by a C3aR-neutralizing antibody could be a new therapeutic strategy to limit airway remodeling, which normally leads to increase in AHR, coughing and breathlessness. However, augmenting C3aR in the disease progression may help to induce priming of long-term memory AMs that are able to recognize rapidly the allergen identifying it as a harmless antigen and therefore dampening the pro-inflammatory reaction.

Finally, I demonstrated that AMs generate MuNCs during the effector phase of allergic asthma. This can occur through cell-to-cell fusion or by a DNA damage response leading to cytokinesis failure. Independently from their formation, my data and the literature suggest that MuNCs have pro-inflammatory but also anti-inflammatory functions. Augmenting their better capacity of phagocytosis and their anti-inflammatory role in the effector phase of allergic asthma may help to reinforce the resolution of airway inflammation.

4.5.2 Summary and future prospects

Alveolar macrophages reside at the mucosal surface with direct contact to the environment. With that they are the perfect cell type to keep an excellent balance between the maintenance of physiologic homeostasis and a necessary inflammatory response to defend the host against environmental invaders. However, their role and functions, in particular their role in allergic asthma development and severity, have massively been underestimated to that point. Summarizing my data, I could show that alveolar macrophages are a peculiar population of macrophages, which in contrast to all other macrophages, do not express C3aR at steady-state but start a strong *de novo* expression upon allergic asthma conditions. This triggers the generation of C3aR^{hi}MHCII^{+} and C3aR^{low}MHCII^{-} subpopulations. In addition, I could demonstrate that C5aR1 in AMs is reciprocal regulated and acts as a potential mechanism to regulate the development of a Th2 immune response. Moreover, mechanistically, the upregulation of C3aR and the downregulation of C5aR1 is dependent on the IL-33-IL-13 signaling axis. Further, I could demonstrate that upon the effector phase of allergic asthma AMs exert a pro-inflammatory role leading to increased AHR which is triggered by C3aR. However, besides of their pro-inflammatory role during the effector phase, there is growing evidence that C3aR^{hi}MHCII^{+} AMs may be primed by CD4^{+} T cells or ILC2s to develop into long-lived memory cells. To validate such hypothesis, exposing young WT or *C3ar1*$^{-/-}$ mice to allergen and rechallenging them at a later time point would help to delineate i) the fact that allergen triggers trained immunity, and ii) that C3aR is a critical player in the establishment of local immune memory cells.

Moreover, I could reveal that tissue-associated AMs generate MuNCs *in vivo* in the effector phase of allergic asthma and *in vitro* upon stimulation with GM-CSF, independently from blood-recruited monocytes and occurs through cell-to-cell fusion and/or cytokinesis failure. So far, the functions of such MuNCs during the establishment and resolution of inflammation is unclear. In addition, the exact role of C3aR in the formation and/or function of MuNCs has to be clarified, in order to envision targeting alveolar macrophages, C3aR, and/or the MuNCs in the different stages of allergic asthma.

Finally, my data show that not only allergic asthma inflammatory conditions, but also cytokine-induced airway inflammation drives the *de novo* expression of C3aR and the downregulation of C5aR1. Since AMs are participating to multiple lung disease, it is tempting to speculate that the reciprocal regulation

of C3aR and C5aR1 also occurs in other pulmonary diseases, suggesting that targeting C3aR could be a new therapeutic strategy to treat patients suffering from pulmonary inflammation, airway remodeling and/or tissue fibrosis.

References

1. Murphy K, Weaver C, Mowat A, Berg L, Chaplin D, eds. 2017. *Janeway's Immunobiology*. New York: Garland Science, Tayler Francis Group, LLC
2. Rottem M, Gershwin ME, Shoenfeld Y. 2002. Allergic disease and autoimmune effectors pathways. *Dev Immunol* 9: 161-7
3. Turvey SE, Broide DH. 2010. Innate immunity. *J Allergy Clin Immunol* 125: S24-32
4. Shishido SN, Varahan S, Yuan K, Li X, Fleming SD. 2012. Humoral innate immune response and disease. *Clin Immunol* 144: 142-58
5. Rettig TA, Harbin JN, Harrington A, Dohmen L, Fleming SD. 2015. Evasion and interactions of the humoral innate immune response in pathogen invasion, autoimmune disease, and cancer. *Clin Immunol* 160: 244-54
6. Pancer Z, Cooper MD. 2006. The evolution of adaptive immunity. *Annu Rev Immunol* 24: 497-518
7. Modlin RL. 2012. Innate immunity: ignored for decades, but not forgotten. *J Invest Dermatol* 132: 882-6
8. Pasquali JL, Martin T. 2012. Control of B cells expressing naturally occurring autoantibodies. *Adv Exp Med Biol* 750: 145-56
9. Avrameas S. 1991. Natural autoantibodies: from 'horror autotoxicus' to 'gnothi seauton'. *Immunol Today* 12: 154-9
10. Du Clos TW, Mold C. 2004. C-reactive protein: an activator of innate immunity and a modulator of adaptive immunity. *Immunol Res* 30: 261-77
11. Moalli F, Jaillon S, Inforzato A, Sironi M, Bottazzi B, Mantovani A, Garlanda C. 2011. Pathogen recognition by the long pentraxin PTX3. *J Biomed Biotechnol* 2011: 830421
12. Du Clos TW, Mold C. 2011. Pentraxins (CRP, SAP) in the process of complement activation and clearance of apoptotic bodies through Fcgamma receptors. *Curr Opin Organ Transplant* 16: 15-20
13. Du Clos TW. 2013. Pentraxins: structure, function, and role in inflammation. *ISRN Inflamm* 2013: 379040
14. Roh JS, Sohn DH. 2018. Damage-Associated Molecular Patterns in Inflammatory Diseases. *Immune Netw* 18: e27
15. Zhu J, Yamane H, Paul WE. 2010. Differentiation of effector CD4 T cell populations (*). *Annu Rev Immunol* 28: 445-89
16. Merien F. 2016. A Journey with Elie Metchnikoff: From Innate Cell Mechanisms in Infectious Diseases to Quantum Biology. *Front Public Health* 4: 125
17. Teti G, Biondo C, Beninati C. 2016. The Phagocyte, Metchnikoff, and the Foundation of Immunology. *Microbiol Spectr* 4
18. Abnave P, Muracciole X, Ghigo E. 2017. Macrophages in Invertebrates: From Insects and Crustaceans to Marine Bivalves. *Results Probl Cell Differ* 62: 147-58
19. Buchmann K. 2014. Evolution of Innate Immunity: Clues from Invertebrates via Fish to Mammals. *Front Immunol* 5: 459
20. Fricker M, Gibson PG. 2017. Macrophage dysfunction in the pathogenesis and treatment of asthma. *Eur Respir J* 50
21. Moore KJ, Sheedy FJ, Fisher EA. 2013. Macrophages in atherosclerosis: a dynamic balance. *Nat Rev Immunol* 13: 709-21
22. Prinz M, Priller J. 2014. Microglia and brain macrophages in the molecular age: from origin to neuropsychiatric disease. *Nat Rev Neurosci* 15: 300-12

23. McNelis JC, Olefsky JM. 2014. Macrophages, immunity, and metabolic disease. *Immunity* 41: 36-48
24. Noy R, Pollard JW. 2014. Tumor-associated macrophages: from mechanisms to therapy. *Immunity* 41: 49-61
25. van Furth R, Cohn ZA. 1968. The origin and kinetics of mononuclear phagocytes. *J Exp Med* 128: 415-35
26. Schulz C, Gomez Perdiguero E, Chorro L, Szabo-Rogers H, Cagnard N, Kierdorf K, Prinz M, Wu B, Jacobsen SE, Pollard JW, Frampton J, Liu KJ, Geissmann F. 2012. A lineage of myeloid cells independent of Myb and hematopoietic stem cells. *Science* 336: 86-90
27. Yona S, Kim KW, Wolf Y, Mildner A, Varol D, Breker M, Strauss-Ayali D, Viukov S, Guilliams M, Misharin A, Hume DA, Perlman H, Malissen B, Zelzer E, Jung S. 2013. Fate mapping reveals origins and dynamics of monocytes and tissue macrophages under homeostasis. *Immunity* 38: 79-91
28. Hashimoto D, Chow A, Noizat C, Teo P, Beasley MB, Leboeuf M, Becker CD, See P, Price J, Lucas D, Greter M, Mortha A, Boyer SW, Forsberg EC, Tanaka M, van Rooijen N, Garcia-Sastre A, Stanley ER, Ginhoux F, Frenette PS, Merad M. 2013. Tissue-resident macrophages self-maintain locally throughout adult life with minimal contribution from circulating monocytes. *Immunity* 38: 792-804
29. Ginhoux F, Greter M, Leboeuf M, Nandi S, See P, Gokhan S, Mehler MF, Conway SJ, Ng LG, Stanley ER, Samokhvalov IM, Merad M. 2010. Fate mapping analysis reveals that adult microglia derive from primitive macrophages. *Science* 330: 841-5
30. Hume DA. 2006. The mononuclear phagocyte system. *Curr Opin Immunol* 18: 49-53
31. Italiani P, Boraschi D. 2017. Development and Functional Differentiation of Tissue-Resident Versus Monocyte-Derived Macrophages in Inflammatory Reactions. *Results Probl Cell Differ* 62: 23-43
32. Hoffmann F, Ender F, Schmudde I, Lewkowich IP, Kohl J, Konig P, Laumonnier Y. 2016. Origin, Localization, and Immunoregulatory Properties of Pulmonary Phagocytes in Allergic Asthma. *Front Immunol* 7: 107
33. Tamoutounour S, Guilliams M, Montanana Sanchis F, Liu H, Terhorst D, Malosse C, Pollet E, Ardouin L, Luche H, Sanchez C, Dalod M, Malissen B, Henri S. 2013. Origins and functional specialization of macrophages and of conventional and monocyte-derived dendritic cells in mouse skin. *Immunity* 39: 925-38
34. Guilliams M, Ginhoux F, Jakubzick C, Naik SH, Onai N, Schraml BU, Segura E, Tussiwand R, Yona S. 2014. Dendritic cells, monocytes and macrophages: a unified nomenclature based on ontogeny. *Nat Rev Immunol* 14: 571-8
35. Onai N, Obata-Onai A, Schmid MA, Ohteki T, Jarrossay D, Manz MG. 2007. Identification of clonogenic common Flt3+M-CSFR+ plasmacytoid and conventional dendritic cell progenitors in mouse bone marrow. *Nat Immunol* 8: 1207-16
36. Naik SH, Sathe P, Park HY, Metcalf D, Proietto AI, Dakic A, Carotta S, O'Keeffe M, Bahlo M, Papenfuss A, Kwak JY, Wu L, Shortman K. 2007. Development of plasmacytoid and conventional dendritic cell subtypes from single precursor cells derived in vitro and in vivo. *Nat Immunol* 8: 1217-26
37. Hettinger J, Richards DM, Hansson J, Barra MM, Joschko AC, Krijgsveld J, Feuerer M. 2013. Origin of monocytes and macrophages in a committed progenitor. *Nat Immunol* 14: 821-30
38. Hoeffel G, Ginhoux F. 2015. Ontogeny of Tissue-Resident Macrophages. *Front Immunol* 6: 486

39. Palis J, Chan RJ, Koniski A, Patel R, Starr M, Yoder MC. 2001. Spatial and temporal emergence of high proliferative potential hematopoietic precursors during murine embryogenesis. *Proc Natl Acad Sci U S A* 98: 4528-33
40. Bertrand JY, Jalil A, Klaine M, Jung S, Cumano A, Godin I. 2005. Three pathways to mature macrophages in the early mouse yolk sac. *Blood* 106: 3004-11
41. Palis J, Robertson S, Kennedy M, Wall C, Keller G. 1999. Development of erythroid and myeloid progenitors in the yolk sac and embryo proper of the mouse. *Development* 126: 5073-84
42. Hoeffel G, Chen J, Lavin Y, Low D, Almeida FF, See P, Beaudin AE, Lum J, Low I, Forsberg EC, Poidinger M, Zolezzi F, Larbi A, Ng LG, Chan JK, Greter M, Becher B, Samokhvalov IM, Merad M, Ginhoux F. 2015. C-Myb(+) erythro-myeloid progenitor-derived fetal monocytes give rise to adult tissue-resident macrophages. *Immunity* 42: 665-78
43. Frame JM, McGrath KE, Palis J. 2013. Erythro-myeloid progenitors: "definitive" hematopoiesis in the conceptus prior to the emergence of hematopoietic stem cells. *Blood Cells Mol Dis* 51: 220-5
44. Bertrand JY, Kim AD, Violette EP, Stachura DL, Cisson JL, Traver D. 2007. Definitive hematopoiesis initiates through a committed erythromyeloid progenitor in the zebrafish embryo. *Development* 134: 4147-56
45. Muller AM, Medvinsky A, Strouboulis J, Grosveld F, Dzierzak E. 1994. Development of hematopoietic stem cell activity in the mouse embryo. *Immunity* 1: 291-301
46. Tavian M, Robin C, Coulombel L, Peault B. 2001. The human embryo, but not its yolk sac, generates lympho-myeloid stem cells: mapping multipotent hematopoietic cell fate in intraembryonic mesoderm. *Immunity* 15: 487-95
47. Gekas C, Dieterlen-Lievre F, Orkin SH, Mikkola HK. 2005. The placenta is a niche for hematopoietic stem cells. *Dev Cell* 8: 365-75
48. de Bruijn MF, Speck NA, Peeters MC, Dzierzak E. 2000. Definitive hematopoietic stem cells first develop within the major arterial regions of the mouse embryo. *EMBO J* 19: 2465-74
49. Kumaravelu P, Hook L, Morrison AM, Ure J, Zhao S, Zuyev S, Ansell J, Medvinsky A. 2002. Quantitative developmental anatomy of definitive haematopoietic stem cells/long-term repopulating units (HSC/RUs): role of the aorta-gonad-mesonephros (AGM) region and the yolk sac in colonisation of the mouse embryonic liver. *Development* 129: 4891-9
50. Gosselin D, Link VM, Romanoski CE, Fonseca GJ, Eichenfield DZ, Spann NJ, Stender JD, Chun HB, Garner H, Geissmann F, Glass CK. 2014. Environment drives selection and function of enhancers controlling tissue-specific macrophage identities. *Cell* 159: 1327-40
51. Lavin Y, Winter D, Blecher-Gonen R, David E, Keren-Shaul H, Merad M, Jung S, Amit I. 2014. Tissue-resident macrophage enhancer landscapes are shaped by the local microenvironment. *Cell* 159: 1312-26
52. Roberts AW, Lee BL, Deguine J, John S, Shlomchik MJ, Barton GM. 2017. Tissue-Resident Macrophages Are Locally Programmed for Silent Clearance of Apoptotic Cells. *Immunity* 47: 913-27 e6
53. Ajami B, Bennett JL, Krieger C, Tetzlaff W, Rossi FM. 2007. Local self-renewal can sustain CNS microglia maintenance and function throughout adult life. *Nat Neurosci* 10: 1538-43

54. Sevenich L. 2018. Brain-Resident Microglia and Blood-Borne Macrophages Orchestrate Central Nervous System Inflammation in Neurodegenerative Disorders and Brain Cancer. *Front Immunol* 9: 697
55. Ajami B, Bennett JL, Krieger C, McNagny KM, Rossi FM. 2011. Infiltrating monocytes trigger EAE progression, but do not contribute to the resident microglia pool. *Nat Neurosci* 14: 1142-9
56. Bain CC, Schridde A. 2018. Origin, Differentiation, and Function of Intestinal Macrophages. *Front Immunol* 9: 2733
57. Bain CC, Bravo-Blas A, Scott CL, Perdiguero EG, Geissmann F, Henri S, Malissen B, Osborne LC, Artis D, Mowat AM. 2014. Constant replenishment from circulating monocytes maintains the macrophage pool in the intestine of adult mice. *Nat Immunol* 15: 929-37
58. Denning TL, Norris BA, Medina-Contreras O, Manicassamy S, Geem D, Madan R, Karp CL, Pulendran B. 2011. Functional specializations of intestinal dendritic cell and macrophage subsets that control Th17 and regulatory T cell responses are dependent on the T cell/APC ratio, source of mouse strain, and regional localization. *J Immunol* 187: 733-47
59. Denning TL, Wang YC, Patel SR, Williams IR, Pulendran B. 2007. Lamina propria macrophages and dendritic cells differentially induce regulatory and interleukin 17-producing T cell responses. *Nat Immunol* 8: 1086-94
60. Bain CC, Scott CL, Uronen-Hansson H, Gudjonsson S, Jansson O, Grip O, Guilliams M, Malissen B, Agace WW, Mowat AM. 2013. Resident and pro-inflammatory macrophages in the colon represent alternative context-dependent fates of the same Ly6Chi monocyte precursors. *Mucosal Immunol* 6: 498-510
61. Gordon S, Pluddemann A. 2017. Tissue macrophages: heterogeneity and functions. *BMC Biol* 15: 53
62. Epelman S, Lavine KJ, Randolph GJ. 2014. Origin and functions of tissue macrophages. *Immunity* 41: 21-35
63. Arai M, Peng XX, Currin RT, Thurman RG, Lemasters JJ. 1999. Protection of sinusoidal endothelial cells against storage/reperfusion injury by prostaglandin E2 derived from Kupffer cells. *Transplantation* 68: 440-5
64. Crispe IN, Dao T, Klugewitz K, Mehal WZ, Metz DP. 2000. The liver as a site of T-cell apoptosis: graveyard, or killing field? *Immunol Rev* 174: 47-62
65. Liu ZX, Govindarajan S, Okamoto S, Dennert G. 2001. Fas-mediated apoptosis causes elimination of virus-specific cytotoxic T cells in the virus-infected liver. *J Immunol* 166: 3035-41
66. Helmy KY, Katschke KJ, Jr., Gorgani NN, Kljavin NM, Elliott JM, Diehl L, Scales SJ, Ghilardi N, van Lookeren Campagne M. 2006. CRIg: a macrophage complement receptor required for phagocytosis of circulating pathogens. *Cell* 124: 915-27
67. Klein A, Zhadkewich M, Margolick J, Winkelstein J, Bulkley G. 1994. Quantitative discrimination of hepatic reticuloendothelial clearance and phagocytic killing. *J Leukoc Biol* 55: 248-52
68. Gregory SH, Cousens LP, van Rooijen N, Dopp EA, Carlos TM, Wing EJ. 2002. Complementary adhesion molecules promote neutrophil-Kupffer cell interaction and the elimination of bacteria taken up by the liver. *J Immunol* 168: 308-15
69. Gregory SH, Wing EJ. 2002. Neutrophil-Kupffer cell interaction: a critical component of host defenses to systemic bacterial infections. *J Leukoc Biol* 72: 239-48

70. Shi J, Gilbert GE, Kokubo Y, Ohashi T. 2001. Role of the liver in regulating numbers of circulating neutrophils. *Blood* 98: 1226-30
71. Brown KE, Brunt EM, Heinecke JW. 2001. Immunohistochemical detection of myeloperoxidase and its oxidation products in Kupffer cells of human liver. *Am J Pathol* 159: 2081-8
72. Gregory SH, Wing EJ, Danowski KL, van Rooijen N, Dyer KF, Tweardy DJ. 1998. IL-6 produced by Kupffer cells induces STAT protein activation in hepatocytes early during the course of systemic listerial infections. *J Immunol* 160: 6056-61
73. Bleriot C, Dupuis T, Jouvion G, Eberl G, Disson O, Lecuit M. 2015. Liver-resident macrophage necroptosis orchestrates type 1 microbicidal inflammation and type-2-mediated tissue repair during bacterial infection. *Immunity* 42: 145-58
74. Scott CL, Zheng F, De Baetselier P, Martens L, Saeys Y, De Prijck S, Lippens S, Abels C, Schoonooghe S, Raes G, Devoogdt N, Lambrecht BN, Beschin A, Guilliams M. 2016. Bone marrow-derived monocytes give rise to self-renewing and fully differentiated Kupffer cells. *Nat Commun* 7: 10321
75. Anderson ER, Shah YM. 2013. Iron homeostasis in the liver. *Compr Physiol* 3: 315-30
76. Rishi G, Subramaniam VN. 2017. The liver in regulation of iron homeostasis. *Am J Physiol Gastrointest Liver Physiol* 313: G157-G65
77. Zhang X, Goncalves R, Mosser DM. 2008. The isolation and characterization of murine macrophages. *Current protocols in immunology / edited by John E. Coligan ... [et al.]* Chapter 14
78. Ghosn EE, Cassado AA, Govoni GR, Fukuhara T, Yang Y, Monack DM, Bortoluci KR, Almeida SR, Herzenberg LA, Herzenberg LA. 2010. Two physically, functionally, and developmentally distinct peritoneal macrophage subsets. *Proc Natl Acad Sci U S A* 107: 2568-73
79. Cassado Ados A, D'Imperio Lima MR, Bortoluci KR. 2015. Revisiting mouse peritoneal macrophages: heterogeneity, development, and function. *Front Immunol* 6: 225
80. Weisberg SP, McCann D, Desai M, Rosenbaum M, Leibel RL, Ferrante AW, Jr. 2003. Obesity is associated with macrophage accumulation in adipose tissue. *J Clin Invest* 112: 1796-808
81. Catrysse L, van Loo G. 2018. Adipose tissue macrophages and their polarization in health and obesity. *Cell Immunol* 330: 114-9
82. Boutens L, Stienstra R. 2016. Adipose tissue macrophages: going off track during obesity. *Diabetologia* 59: 879-94
83. Krinninger P, Ensenauer R, Ehlers K, Rauh K, Stoll J, Krauss-Etschmann S, Hauner H, Laumen H. 2014. Peripheral monocytes of obese women display increased chemokine receptor expression and migration capacity. *J Clin Endocrinol Metab* 99: 2500-9
84. Kamei N, Tobe K, Suzuki R, Ohsugi M, Watanabe T, Kubota N, Ohtsuka-Kowatari N, Kumagai K, Sakamoto K, Kobayashi M, Yamauchi T, Ueki K, Oishi Y, Nishimura S, Manabe I, Hashimoto H, Ohnishi Y, Ogata H, Tokuyama K, Tsunoda M, Ide T, Murakami K, Nagai R, Kadowaki T. 2006. Overexpression of monocyte chemoattractant protein-1 in adipose tissues causes macrophage recruitment and insulin resistance. *J Biol Chem* 281: 26602-14
85. Byrne AJ, Mathie SA, Gregory LG, Lloyd CM. 2015. Pulmonary macrophages: key players in the innate defence of the airways. *Thorax* 70: 1189-96
86. Hoffmann F, Ender F, Schmudde I, Lewkowich IP, Köhl J, König P, Laumonnier Y. 2016. Origin, Localization, and Immunoregulatory Properties of Pulmonary Phagocytes in Allergic Asthma. *Frontiers in immunology* 7: 107

87. Hussell T, Bell TJ. 2014. Alveolar macrophages: plasticity in a tissue-specific context. *Nat Rev Immunol* 14: 81-93
88. Morales-Nebreda L, Misharin AV, Perlman H, Budinger GR. 2015. The heterogeneity of lung macrophages in the susceptibility to disease. *Eur Respir Rev* 24: 505-9
89. Byrne AJ, Maher TM, Lloyd CM. 2016. Pulmonary Macrophages: A New Therapeutic Pathway in Fibrosing Lung Disease? *Trends Mol Med* 22: 303-16
90. Chandler DB, Brannen AL. 1990. Interstitial macrophage subpopulations: responsiveness to chemotactic stimuli. *Tissue Cell* 22: 427-34
91. N AG, Quintana JA, Garcia-Silva S, Mazariegos M, Gonzalez de la Aleja A, Nicolas-Avila JA, Walter W, Adrover JM, Crainiciuc G, Kuchroo VK, Rothlin CV, Peinado H, Castrillo A, Ricote M, Hidalgo A. 2017. Phagocytosis imprints heterogeneity in tissue-resident macrophages. *J Exp Med* 214: 1281-96
92. Gibbings SL, Thomas SM, Atif SM, McCubbrey AL, Desch AN, Danhorn T, Leach SM, Bratton DL, Henson PM, Janssen WJ, Jakubzick CV. 2017. Three Unique Interstitial Macrophages in the Murine Lung at Steady State. *Am J Respir Cell Mol Biol* 57: 66-76
93. Tan SY, Krasnow MA. 2016. Developmental origin of lung macrophage diversity. *Development* 143: 1318-27
94. Sabatel C, Radermecker C, Fievez L, Paulissen G, Chakarov S, Fernandes C, Olivier S, Toussaint M, Pirottin D, Xiao X, Quatresooz P, Sirard JC, Cataldo D, Gillet L, Bouabe H, Desmet CJ, Ginhoux F, Marichal T, Bureau F. 2017. Exposure to Bacterial CpG DNA Protects from Airway Allergic Inflammation by Expanding Regulatory Lung Interstitial Macrophages. *Immunity* 46: 457-73
95. Hoppstadter J, Diesel B, Zarbock R, Breinig T, Monz D, Koch M, Meyerhans A, Gortner L, Lehr CM, Huwer H, Kiemer AK. 2010. Differential cell reaction upon Toll-like receptor 4 and 9 activation in human alveolar and lung interstitial macrophages. *Respir Res* 11: 124
96. Kawano H, Kayama H, Nakama T, Hashimoto T, Umemoto E, Takeda K. 2016. IL-10-producing lung interstitial macrophages prevent neutrophilic asthma. *Int Immunol* 28: 489-501
97. Bedoret D, Wallemacq H, Marichal T, Desmet C, Quesada Calvo F, Henry E, Closset R, Dewals B, Thielen C, Gustin P, de Leval L, Van Rooijen N, Le Moine A, Vanderplasschen A, Cataldo D, Drion PV, Moser M, Lekeux P, Bureau F. 2009. Lung interstitial macrophages alter dendritic cell functions to prevent airway allergy in mice. *J Clin Invest* 119: 3723-38
98. Mills CD, Kincaid K, Alt JM, Heilman MJ, Hill AM. 2000. M-1/M-2 macrophages and the Th1/Th2 paradigm. *J Immunol* 164: 6166-73
99. Mosmann TR, Cherwinski H, Bond MW, Giedlin MA, Coffman RL. 1986. Two types of murine helper T cell clone. I. Definition according to profiles of lymphokine activities and secreted proteins. *J Immunol* 136: 2348-57
100. Martinez FO, Gordon S. 2014. The M1 and M2 paradigm of macrophage activation: time for reassessment. *F1000Prime Rep* 6: 13
101. Shapouri-Moghaddam A, Mohammadian S, Vazini H, Taghadosi M, Esmaeili SA, Mardani F, Seifi B, Mohammadi A, Afshari JT, Sahebkar A. 2018. Macrophage plasticity, polarization, and function in health and disease. *J Cell Physiol* 233: 6425-40
102. Akaike T, Maeda H. 2000. Nitric oxide and virus infection. *Immunology* 101: 300-8
103. Jamaati H, Mortaz E, Pajouhi Z, Folkerts G, Movassaghi M, Moloudizargari M, Adcock IM, Garssen J. 2017. Nitric Oxide in the Pathogenesis and Treatment of Tuberculosis. *Front Microbiol* 8: 2008

104. Malyshev I, Malyshev Y. 2015. Current Concept and Update of the Macrophage Plasticity Concept: Intracellular Mechanisms of Reprogramming and M3 Macrophage "Switch" Phenotype. *Biomed Res Int* 2015: 341308
105. Sica A, Mantovani A. 2012. Macrophage plasticity and polarization: in vivo veritas. *J Clin Invest* 122: 787-95
106. Murray PJ, Allen JE, Biswas SK, Fisher EA, Gilroy DW, Goerdt S, Gordon S, Hamilton JA, Ivashkiv LB, Lawrence T, Locati M, Mantovani A, Martinez FO, Mege JL, Mosser DM, Natoli G, Saeij JP, Schultze JL, Shirey KA, Sica A, Suttles J, Udalova I, van Ginderachter JA, Vogel SN, Wynn TA. 2014. Macrophage activation and polarization: nomenclature and experimental guidelines. *Immunity* 41: 14-20
107. Roszer T. 2015. Understanding the Mysterious M2 Macrophage through Activation Markers and Effector Mechanisms. *Mediators Inflamm* 2015: 816460
108. Porcheray F, Viaud S, Rimaniol AC, Leone C, Samah B, Dereuddre-Bosquet N, Dormont D, Gras G. 2005. Macrophage activation switching: an asset for the resolution of inflammation. *Clin Exp Immunol* 142: 481-9
109. Melgert BN, ten Hacken NH, Rutgers B, Timens W, Postma DS, Hylkema MN. 2011. More alternative activation of macrophages in lungs of asthmatic patients. *J Allergy Clin Immunol* 127: 831-3
110. Moreira AP, Hogaboam CM. 2011. Macrophages in allergic asthma: fine-tuning their pro- and anti-inflammatory actions for disease resolution. *J Interferon Cytokine Res* 31: 485-91
111. Nahrendorf M, Swirski FK. 2016. Abandoning M1/M2 for a Network Model of Macrophage Function. *Circ Res* 119: 414-7
112. Aghbali A, Rafieyan S, Mohamed-Khosroshahi L, Baradaran B, Shanehbandi D, Kouhsoltani M. 2017. IL-4 induces the formation of multinucleated giant cells and expression of beta5 integrin in central giant cell lesion. *Med Oral Patol Oral Cir Bucal* 22: e1-e6
113. Kao WJ, McNally AK, Hiltner A, Anderson JM. 1995. Role for interleukin-4 in foreign-body giant cell formation on a poly(etherurethane urea) in vivo. *J Biomed Mater Res* 29: 1267-75
114. Moreno JL, Mikhailenko I, Tondravi MM, Keegan AD. 2007. IL-4 promotes the formation of multinucleated giant cells from macrophage precursors by a STAT6-dependent, homotypic mechanism: contribution of E-cadherin. *J Leukoc Biol* 82: 1542-53
115. Gupta S, Kaur H., Gumber P., Fahmi N., Sharma K., Gumber A. 2016. Giant Cells in Health and Disease - a review. *Int J Com Health and Med Res* 2016;2(2):60-65
116. Brodbeck WG, Anderson JM. 2009. Giant cell formation and function. *Curr Opin Hematol* 16: 53-7
117. Gupta S, Kaur H, Gumber P, Fahmi N, Sharma K, Gumber A. 2016. Giant Cells in Health and Disease. *Int J Com Health and Med Res*
118. Quinn MT, Schepetkin IA. 2009. Role of NADPH oxidase in formation and function of multinucleated giant cells. *J Innate Immun* 1: 509-26
119. Miron RJ, Bosshardt DD. 2018. Multinucleated Giant Cells: Good Guys or Bad Guys? *Tissue Eng Part B Rev* 24: 53-65
120. Helming L, Gordon S. 2007. The molecular basis of macrophage fusion. *Immunobiology* 212: 785-93
121. Herrtwich L, Nanda I, Evangelou K, Nikolova T, Horn V, Sagar, Erny D, Stefanowski J, Rogell L, Klein C, Gharun K, Follo M, Seidl M, Kremer B, Munke N, Senges J, Fliegauf M,

Aschman T, Pfeifer D, Sarrazin S, Sieweke MH, Wagner D, Dierks C, Haaf T, Ness T, Zaiss MM, Voll RE, Deshmukh SD, Prinz M, Goldmann T, Holscher C, Hauser AE, Lopez-Contreras AJ, Grun D, Gorgoulis V, Diefenbach A, Henneke P, Triantafyllopoulou A. 2016. DNA Damage Signaling Instructs Polyploid Macrophage Fate in Granulomas. *Cell* 167: 1264-80 e18

122. Pereira M, Petretto E, Gordon S, Bassett JHD, Williams GR, Behmoaras J. 2018. Common signalling pathways in macrophage and osteoclast multinucleation. *J Cell Sci* 131
123. Lemaire I, Falzoni S, Zhang B, Pellegatti P, Di Virgilio F. 2011. The P2X7 receptor and Pannexin-1 are both required for the promotion of multinucleated macrophages by the inflammatory cytokine GM-CSF. *J Immunol* 187: 3878-87
124. Saginario C, Sterling H, Beckers C, Kobayashi R, Solimena M, Ullu E, Vignery A. 1998. MFR, a putative receptor mediating the fusion of macrophages. *Mol Cell Biol* 18: 6213-23
125. Yagi M, Miyamoto T, Sawatani Y, Iwamoto K, Hosogane N, Fujita N, Morita K, Ninomiya K, Suzuki T, Miyamoto K, Oike Y, Takeya M, Toyama Y, Suda T. 2005. DC-STAMP is essential for cell-cell fusion in osteoclasts and foreign body giant cells. *J Exp Med* 202: 345-51
126. Guilliams M, De Kleer I, Henri S, Post S, Vanhoutte L, De Prijck S, Deswarte K, Malissen B, Hammad H, Lambrecht BN. 2013. Alveolar macrophages develop from fetal monocytes that differentiate into long-lived cells in the first week of life via GM-CSF. *J Exp Med* 210: 1977-92
127. Kopf M, Schneider C, Nobs SP. 2015. The development and function of lung-resident macrophages and dendritic cells. *Nat Immunol* 16: 36-44
128. Gordon S, Pluddemann A, Martinez Estrada F. 2014. Macrophage heterogeneity in tissues: phenotypic diversity and functions. *Immunol Rev* 262: 36-55
129. Plantinga M, Guilliams M, Vanheerswynghels M, Deswarte K, Branco-Madeira F, Toussaint W, Vanhoutte L, Neyt K, Killeen N, Malissen B, Hammad H, Lambrecht BN. 2013. Conventional and monocyte-derived CD11b(+) dendritic cells initiate and maintain T helper 2 cell-mediated immunity to house dust mite allergen. *Immunity* 38: 322-35
130. Misharin AV, Morales-Nebreda L, Mutlu GM, Budinger SGR, Perlman H. 2013. Flow Cytometric Analysis of Macrophages and Dendritic Cell Subsets in the Mouse Lung. *American Journal of Respiratory Cell and Molecular Biology* 49
131. Lee YG, Jeong JJ, Nyenhuis S, Berdyshev E, Chung S, Ranjan R, Karpurapu M, Deng J, Qian F, Kelly EA, Jarjour NN, Ackerman SJ, Natarajan V, Christman JW, Park GY. 2015. Recruited alveolar macrophages, in response to airway epithelial-derived monocyte chemoattractant protein 1/CCl2, regulate airway inflammation and remodeling in allergic asthma. *Am J Respir Cell Mol Biol* 52: 772-84
132. Holt PG, Oliver J, Bilyk N, McMenamin C, McMenamin PG, Kraal G, Thepen T. 1993. Downregulation of the antigen presenting cell function(s) of pulmonary dendritic cells in vivo by resident alveolar macrophages. *J Exp Med* 177: 397-407
133. Soroosh P, Doherty TA, Duan W, Mehta AK, Choi H, Adams YF, Mikulski Z, Khorram N, Rosenthal P, Broide DH, Croft M. 2013. Lung-resident tissue macrophages generate Foxp3+ regulatory T cells and promote airway tolerance. *J Exp Med* 210: 775-88
134. Josefowicz SZ, Niec RE, Kim HY, Treuting P, Chinen T, Zheng Y, Umetsu DT, Rudensky AY. 2012. Extrathymically generated regulatory T cells control mucosal TH2 inflammation. *Nature* 482: 395-9

135. Lloyd CM, Hawrylowicz CM. 2009. Regulatory T cells in asthma. *Immunity* 31: 438-49
136. Westphalen K, Gusarova GA, Islam MN, Subramanian M, Cohen TS, Prince AS, Bhattacharya J. 2014. Sessile alveolar macrophages communicate with alveolar epithelium to modulate immunity. *Nature* 506: 503-6
137. Snelgrove RJ, Goulding J, Didierlaurent AM, Lyonga D, Vekaria S, Edwards L, Gwyer E, Sedgwick JD, Barclay AN, Hussell T. 2008. A critical function for CD200 in lung immune homeostasis and the severity of influenza infection. *Nat Immunol* 9: 1074-83
138. Kooguchi K, Hashimoto S, Kobayashi A, Kitamura Y, Kudoh I, Wiener-Kronish J, Sawa T. 1998. Role of alveolar macrophages in initiation and regulation of inflammation in Pseudomonas aeruginosa pneumonia. *Infect Immun* 66: 3164-9
139. Green GM, Kass EH. 1964. The Role of the Alveolar Macrophage in the Clearance of Bacteria from the Lung. *J Exp Med* 119: 167-76
140. Sun K, Gan Y, Metzger DW. 2011. Analysis of murine genetic predisposition to pneumococcal infection reveals a critical role of alveolar macrophages in maintaining the sterility of the lower respiratory tract. *Infect Immun* 79: 1842-7
141. Limper AH, Hoyte JS, Standing JE. 1997. The role of alveolar macrophages in Pneumocystis carinii degradation and clearance from the lung. *J Clin Invest* 99: 2110-7
142. Purnama C, Ng SL, Tetlak P, Setiagani YA, Kandasamy M, Baalasubramanian S, Karjalainen K, Ruedl C. 2014. Transient ablation of alveolar macrophages leads to massive pathology of influenza infection without affecting cellular adaptive immunity. *Eur J Immunol* 44: 2003-12
143. Schneider C, Nobs SP, Heer AK, Kurrer M, Klinke G, van Rooijen N, Vogel J, Kopf M. 2014. Alveolar macrophages are essential for protection from respiratory failure and associated morbidity following influenza virus infection. *PLoS Pathog* 10: e1004053
144. Laza-Stanca V, Stanciu LA, Message SD, Edwards MR, Gern JE, Johnston SL. 2006. Rhinovirus replication in human macrophages induces NF-kappaB-dependent tumor necrosis factor alpha production. *J Virol* 80: 8248-58
145. Chacon-Salinas R, Serafin-Lopez J, Ramos-Payan R, Mendez-Aragon P, Hernandez-Pando R, Van Soolingen D, Flores-Romo L, Estrada-Parra S, Estrada-Garcia I. 2005. Differential pattern of cytokine expression by macrophages infected in vitro with different Mycobacterium tuberculosis genotypes. *Clin Exp Immunol* 140: 443-9
146. Arango Duque G, Descoteaux A. 2014. Macrophage cytokines: involvement in immunity and infectious diseases. *Front Immunol* 5: 491
147. Ben-Sasson SZ, Hu-Li J, Quiel J, Cauchetaux S, Ratner M, Shapira I, Dinarello CA, Paul WE. 2009. IL-1 acts directly on CD4 T cells to enhance their antigen-driven expansion and differentiation. *Proc Natl Acad Sci U S A* 106: 7119-24
148. Vieira SM, Lemos HP, Grespan R, Napimoga MH, Dal-Secco D, Freitas A, Cunha TM, Verri WA, Jr., Souza-Junior DA, Jamur MC, Fernandes KS, Oliver C, Silva JS, Teixeira MM, Cunha FQ. 2009. A crucial role for TNF-alpha in mediating neutrophil influx induced by endogenously generated or exogenous chemokines, KC/CXCL1 and LIX/CXCL5. *Br J Pharmacol* 158: 779-89
149. Amrani Y, Panettieri RA, Jr. 1998. Cytokines induce airway smooth muscle cell hyperresponsiveness to contractile agonists. *Thorax* 53: 713-6
150. Hurst SM, Wilkinson TS, McLoughlin RM, Jones S, Horiuchi S, Yamamoto N, Rose-John S, Fuller GM, Topley N, Jones SA. 2001. Il-6 and its soluble receptor orchestrate a temporal switch in the pattern of leukocyte recruitment seen during acute inflammation. *Immunity* 14: 705-14

151. Scheller J, Chalaris A, Schmidt-Arras D, Rose-John S. 2011. The pro- and anti-inflammatory properties of the cytokine interleukin-6. *Biochim Biophys Acta* 1813: 878-88
152. Carre PC, Mortenson RL, King TE, Jr., Noble PW, Sable CL, Riches DW. 1991. Increased expression of the interleukin-8 gene by alveolar macrophages in idiopathic pulmonary fibrosis. A potential mechanism for the recruitment and activation of neutrophils in lung fibrosis. *J Clin Invest* 88: 1802-10
153. Grabiec AM, Hussell T. 2016. The role of airway macrophages in apoptotic cell clearance following acute and chronic lung inflammation. *Semin Immunopathol* 38: 409-23
154. Haslett C. 1999. Granulocyte apoptosis and its role in the resolution and control of lung inflammation. *Am J Respir Crit Care Med* 160: S5-11
155. Greenlee-Wacker MC. 2016. Clearance of apoptotic neutrophils and resolution of inflammation. *Immunol Rev* 273: 357-70
156. Shen ZJ, Malter JS. 2015. Determinants of eosinophil survival and apoptotic cell death. *Apoptosis* 20: 224-34
157. Fadok VA, Bratton DL, Konowal A, Freed PW, Westcott JY, Henson PM. 1998. Macrophages that have ingested apoptotic cells in vitro inhibit proinflammatory cytokine production through autocrine/paracrine mechanisms involving TGF-beta, PGE2, and PAF. *J Clin Invest* 101: 890-8
158. Kim KK, Dotson MR, Agarwal M, Yang J, Bradley PB, Subbotina N, Osterholzer JJ, Sisson TH. 2018. Efferocytosis of apoptotic alveolar epithelial cells is sufficient to initiate lung fibrosis. *Cell Death Dis* 9: 1056
159. Knapp S, Leemans JC, Florquin S, Branger J, Maris NA, Pater J, van Rooijen N, van der Poll T. 2003. Alveolar macrophages have a protective antiinflammatory role during murine pneumococcal pneumonia. *Am J Respir Crit Care Med* 167: 171-9
160. Arbore G, Kemper C, Kolev M. 2017. Intracellular complement - the complosome - in immune cell regulation. *Mol Immunol* 89: 2-9
161. Kolev M, Le Friec G, Kemper C. 2014. Complement--tapping into new sites and effector systems. *Nat Rev Immunol* 14: 811-20
162. Ricklin D, Hajishengallis G, Yang K, Lambris JD. 2010. Complement: a key system for immune surveillance and homeostasis. *Nat Immunol* 11: 785-97
163. Kohl J. 2006. The role of complement in danger sensing and transmission. *Immunol Res* 34: 157-76
164. Hajishengallis G, Reis ES, Mastellos DC, Ricklin D, Lambris JD. 2017. Novel mechanisms and functions of complement. *Nat Immunol* 18: 1288-98
165. Bloch EF, Knight EM, Carmon T, McDonald-Pinkett S, Carter J, Boomer A, Ogunfusika M, Petersen M, Famakin B, Aniagolu J, Walker J, Gant R, Walters CS, Gaither TA. 1997. C5b-7 and C5b-8 precursors of the membrane attack complex (C5b-9) are effective killers of E. coli J5 during serum incubation. *Immunol Invest* 26: 409-19
166. Tomlinson S, Taylor PW, Morgan BP, Luzio JP. 1989. Killing of gram-negative bacteria by complement. Fractionation of cell membranes after complement C5b-9 deposition on to the surface of Salmonella minnesota Re595. *Biochem J* 263: 505-11
167. Wurzner R. 2003. Deficiencies of the complement MAC II gene cluster (C6, C7, C9): is subtotal C6 deficiency of particular evolutionary benefit? *Clin Exp Immunol* 133: 156-9
168. Ricklin D, Reis ES, Mastellos DC, Gros P, Lambris JD. 2016. Complement component C3 - The "Swiss Army Knife" of innate immunity and host defense. *Immunol Rev* 274: 33-58

169. Schwaeble WJ, Reid KB. 1999. Does properdin crosslink the cellular and the humoral immune response? *Immunol Today* 20: 17-21
170. Fearon DT, Austen KF. 1975. Properdin: binding to C3b and stabilization of the C3b-dependent C3 convertase. *J Exp Med* 142: 856-63
171. Hourcade DE. 2006. The role of properdin in the assembly of the alternative pathway C3 convertases of complement. *J Biol Chem* 281: 2128-32
172. Bathum L, Hansen H, Teisner B, Koch C, Garred P, Rasmussen K, Wang P. 2006. Association between combined properdin and mannose-binding lectin deficiency and infection with Neisseria meningitidis. *Mol Immunol* 43: 473-9
173. Merle NS, Church SE, Fremeaux-Bacchi V, Roumenina LT. 2015. Complement System Part I - Molecular Mechanisms of Activation and Regulation. *Front Immunol* 6: 262
174. Noris M, Remuzzi G. 2013. Overview of complement activation and regulation. *Semin Nephrol* 33: 479-92
175. Tschopp J, Chonn A, Hertig S, French LE. 1993. Clusterin, the human apolipoprotein and complement inhibitor, binds to complement C7, C8 beta, and the b domain of C9. *J Immunol* 151: 2159-65
176. Alper CA, Johnson AM, Birtch AG, Moore FD. 1969. Human C'3: evidence for the liver as the primary site of synthesis. *Science* 163: 286-8
177. Morris KM, Aden DP, Knowles BB, Colten HR. 1982. Complement biosynthesis by the human hepatoma-derived cell line HepG2. *J Clin Invest* 70: 906-13
178. Alpert SE, Auerbach HS, Cole FS, Colten HR. 1983. Macrophage maturation: differences in complement secretion by marrow, monocyte, and tissue macrophages detected with an improved hemolytic plaque assay. *J Immunol* 130: 102-7
179. Passwell J, Schreiner GF, Nonaka M, Beuscher HU, Colten HR. 1988. Local extrahepatic expression of complement genes C3, factor B, C2, and C4 is increased in murine lupus nephritis. *J Clin Invest* 82: 1676-84
180. Naughton MA, Botto M, Carter MJ, Alexander GJ, Goldman JM, Walport MJ. 1996. Extrahepatic secreted complement C3 contributes to circulating C3 levels in humans. *J Immunol* 156: 3051-6
181. Naughton MA, Walport MJ, Wurzner R, Carter MJ, Alexander GJ, Goldman JM, Botto M. 1996. Organ-specific contribution to circulating C7 levels by the bone marrow and liver in humans. *Eur J Immunol* 26: 2108-12
182. Morgan BP, Gasque P. 1997. Extrahepatic complement biosynthesis: where, when and why? *Clin Exp Immunol* 107: 1-7
183. Circolo A, Pierce GF, Katz Y, Strunk RC. 1990. Antiinflammatory effects of polypeptide growth factors. Platelet-derived growth factor, epidermal growth factor, and fibroblast growth factor inhibit the cytokine-induced expression of the alternative complement pathway activator factor B in human fibroblasts. *J Biol Chem* 265: 5066-71
184. Gerritsma JS, van Kooten C, Gerritsen AF, van Es LA, Daha MR. 1998. Transforming growth factor-beta 1 regulates chemokine and complement production by human proximal tubular epithelial cells. *Kidney Int* 53: 609-16
185. West EE, Kolev M, Kemper C. 2018. Complement and the Regulation of T Cell Responses. *Annu Rev Immunol* 36: 309-38
186. Huber-Lang M, Sarma JV, Zetoune FS, Rittirsch D, Neff TA, McGuire SR, Lambris JD, Warner RL, Flierl MA, Hoesel LM, Gebhard F, Younger JG, Drouin SM, Wetsel RA, Ward PA. 2006. Generation of C5a in the absence of C3: a new complement activation pathway. *Nat Med* 12: 682-7

187. Broker K, Figge J, Magnusen AF, Manz RA, Kohl J, Karsten CM. 2018. A Novel Role for C5a in B-1 Cell Homeostasis. *Front Immunol* 9: 258
188. Liszewski MK, Kolev M, Le Friec G, Leung M, Bertram PG, Fara AF, Subias M, Pickering MC, Drouet C, Meri S, Arstila TP, Pekkarinen PT, Ma M, Cope A, Reinheckel T, Rodriguez de Cordoba S, Afzali B, Atkinson JP, Kemper C. 2013. Intracellular complement activation sustains T cell homeostasis and mediates effector differentiation. *Immunity* 39: 1143-57
189. Kolev M, Dimeloe S, Le Friec G, Navarini A, Arbore G, Povoleri GA, Fischer M, Belle R, Loeliger J, Develioglu L, Bantug GR, Watson J, Couzi L, Afzali B, Lavender P, Hess C, Kemper C. 2015. Complement Regulates Nutrient Influx and Metabolic Reprogramming during Th1 Cell Responses. *Immunity* 42: 1033-47
190. Arbore G, West EE, Spolski R, Robertson AAB, Klos A, Rheinheimer C, Dutow P, Woodruff TM, Yu ZX, O'Neill LA, Coll RC, Sher A, Leonard WJ, Kohl J, Monk P, Cooper MA, Arno M, Afzali B, Lachmann HJ, Cope AP, Mayer-Barber KD, Kemper C. 2016. T helper 1 immunity requires complement-driven NLRP3 inflammasome activity in CD4(+) T cells. *Science* 352: aad1210
191. Satyam A, Kannan L, Matsumoto N, Geha M, Lapchak PH, Bosse R, Shi GP, Dalle Lucca JJ, Tsokos MG, Tsokos GC. 2017. Intracellular Activation of Complement 3 Is Responsible for Intestinal Tissue Damage during Mesenteric Ischemia. *J Immunol* 198: 788-97
192. Zha H, Wang X, Zhu Y, Chen D, Han X, Yang F, Gao J, Hu C, Shu C, Feng Y, Tan Y, Zhang J, Li Y, Wan YY, Guo B, Zhu B. 2019. Intracellular Activation of Complement C3 Leads to PD-L1 Antibody Treatment Resistance by Modulating Tumor-Associated Macrophages. *Cancer Immunol Res* 7: 193-207
193. Klos A, Tenner AJ, Johswich KO, Ager RR, Reis ES, Kohl J. 2009. The role of the anaphylatoxins in health and disease. *Mol Immunol* 46: 2753-66
194. Elsner J, Oppermann M, Czech W, Kapp A. 1994. C3a activates the respiratory burst in human polymorphonuclear neutrophilic leukocytes via pertussis toxin-sensitive G-proteins. *Blood* 83: 3324-31
195. Murakami Y, Imamichi T, Nagasawa S. 1993. Characterization of C3a anaphylatoxin receptor on guinea-pig macrophages. *Immunology* 79: 633-8
196. Elsner J, Oppermann M, Czech W, Dobos G, Schopf E, Norgauer J, Kapp A. 1994. C3a activates reactive oxygen radical species production and intracellular calcium transients in human eosinophils. *Eur J Immunol* 24: 518-22
197. Kretzschmar T, Jeromin A, Gietz C, Bautsch W, Klos A, Kohl J, Rechkemmer G, Bitter-Suermann D. 1993. Chronic myelogenous leukemia-derived basophilic granulocytes express a functional active receptor for the anaphylatoxin C3a. *Eur J Immunol* 23: 558-61
198. el-Lati SG, Dahinden CA, Church MK. 1994. Complement peptides C3a- and C5a-induced mediator release from dissociated human skin mast cells. *J Invest Dermatol* 102: 803-6
199. Fukuoka Y, Hugli TE. 1988. Demonstration of a specific C3a receptor on guinea pig platelets. *J Immunol* 140: 3496-501
200. Fischer WH, Hugli TE. 1997. Regulation of B cell functions by C3a and C3a(desArg): suppression of TNF-alpha, IL-6, and the polyclonal immune response. *J Immunol* 159: 4279-86
201. Fischer WH, Jagels MA, Hugli TE. 1999. Regulation of IL-6 synthesis in human peripheral blood mononuclear cells by C3a and C3a(desArg). *J Immunol* 162: 453-9

202. Monsinjon T, Gasque P, Ischenko A, Fontaine M. 2001. C3A binds to the seven transmembrane anaphylatoxin receptor expressed by epithelial cells and triggers the production of IL-8. *FEBS Lett* 487: 339-46
203. Aksamit RR, Falk W, Leonard EJ. 1981. Chemotaxis by mouse macrophage cell lines. *J Immunol* 126: 2194-9
204. Ehrengruber MU, Geiser T, Deranleau DA. 1994. Activation of human neutrophils by C3a and C5A. Comparison of the effects on shape changes, chemotaxis, secretion, and respiratory burst. *FEBS Lett* 346: 181-4
205. Lett-Brown MA, Leonard EJ. 1977. Histamine-induced inhibition of normal human basophil chemotaxis to C5a. *J Immunol* 118: 815-8
206. Ottonello L, Corcione A, Tortolina G, Airoldi I, Albesiano E, Favre A, D'Agostino R, Malavasi F, Pistoia V, Dallegri F. 1999. rC5a directs the in vitro migration of human memory and naive tonsillar B lymphocytes: implications for B cell trafficking in secondary lymphoid tissues. *J Immunol* 162: 6510-7
207. Nataf S, Davoust N, Ames RS, Barnum SR. 1999. Human T cells express the C5a receptor and are chemoattracted to C5a. *J Immunol* 162: 4018-23
208. Mastellos D, Papadimitriou JC, Franchini S, Tsonis PA, Lambris JD. 2001. A novel role of complement: mice deficient in the fifth component of complement (C5) exhibit impaired liver regeneration. *J Immunol* 166: 2479-86
209. Hillebrandt S, Wasmuth HE, Weiskirchen R, Hellerbrand C, Keppeler H, Werth A, Schirin-Sokhan R, Wilkens G, Geier A, Lorenzen J, Kohl J, Gressner AM, Matern S, Lammert F. 2005. Complement factor 5 is a quantitative trait gene that modifies liver fibrogenesis in mice and humans. *Nat Genet* 37: 835-43
210. Benard M, Gonzalez BJ, Schouft MT, Falluel-Morel A, Vaudry D, Chan P, Vaudry H, Fontaine M. 2004. Characterization of C3a and C5a receptors in rat cerebellar granule neurons during maturation. Neuroprotective effect of C5a against apoptotic cell death. *J Biol Chem* 279: 43487-96
211. Strey CW, Markiewski M, Mastellos D, Tudoran R, Spruce LA, Greenbaum LE, Lambris JD. 2003. The proinflammatory mediators C3a and C5a are essential for liver regeneration. *J Exp Med* 198: 913-23
212. Bokisch VA, Muller-Eberhard HJ. 1970. Anaphylatoxin inactivator of human plasma: its isolation and characterization as a carboxypeptidase. *J Clin Invest* 49: 2427-36
213. Skidgel RA, Erdos EG. 2007. Structure and function of human plasma carboxypeptidase N, the anaphylatoxin inactivator. *Int Immunopharmacol* 7: 1888-99
214. Laumonnier Y, Karsten CM, Kohl J. 2017. Novel insights into the expression pattern of anaphylatoxin receptors in mice and men. *Mol Immunol* 89: 44-58
215. Lee DK, George SR, Cheng R, Nguyen T, Liu Y, Brown M, Lynch KR, O'Dowd BF. 2001. Identification of four novel human G protein-coupled receptors expressed in the brain. *Brain Res Mol Brain Res* 86: 13-22
216. Samson M, Edinger AL, Stordeur P, Rucker J, Verhasselt V, Sharron M, Govaerts C, Mollereau C, Vassart G, Doms RW, Parmentier M. 1998. ChemR23, a putative chemoattractant receptor, is expressed in monocyte-derived dendritic cells and macrophages and is a coreceptor for SIV and some primary HIV-1 strains. *Eur J Immunol* 28: 1689-700
217. Crass T, Raffetseder U, Martin U, Grove M, Klos A, Kohl J, Bautsch W. 1996. Expression cloning of the human C3a anaphylatoxin receptor (C3aR) from differentiated U-937 cells. *Eur J Immunol* 26: 1944-50

218. Ames RS, Li Y, Sarau HM, Nuthulaganti P, Foley JJ, Ellis C, Zeng Z, Su K, Jurewicz AJ, Hertzberg RP, Bergsma DJ, Kumar C. 1996. Molecular cloning and characterization of the human anaphylatoxin C3a receptor. *J Biol Chem* 271: 20231-4
219. Gao J, Choe H, Bota D, Wright PL, Gerard C, Gerard NP. 2003. Sulfation of tyrosine 174 in the human C3a receptor is essential for binding of C3a anaphylatoxin. *J Biol Chem* 278: 37902-8
220. Hollmann TJ, Haviland DL, Kildsgaard J, Watts K, Wetsel RA. 1998. Cloning, expression, sequence determination, and chromosome localization of the mouse complement C3a anaphylatoxin receptor gene. *Mol Immunol* 35: 137-48
221. Martin U, Bock D, Arseniev L, Tornetta MA, Ames RS, Bautsch W, Kohl J, Ganser A, Klos A. 1997. The human C3a receptor is expressed on neutrophils and monocytes, but not on B or T lymphocytes. *J Exp Med* 186: 199-207
222. Sayah S, Jauneau AC, Patte C, Tonon MC, Vaudry H, Fontaine M. 2003. Two different transduction pathways are activated by C3a and C5a anaphylatoxins on astrocytes. *Brain Res Mol Brain Res* 112: 53-60
223. Settmacher B, Rheinheimer C, Hamacher H, Ames RS, Wise A, Jenkinson L, Bock D, Schaefer M, Köhl J, Klos A. 2003. Structure-function studies of the C3a-receptor: C-terminal serine and threonine residues which influence receptor internalization and signaling. *European journal of immunology* 33: 920-7
224. Ali H, Ahamed J, Hernandez-Munain C, Baron JL, Krangel MS, Patel DD. 2000. Chemokine production by G protein-coupled receptor activation in a human mast cell line: roles of extracellular signal-regulated kinase and NFAT. *J Immunol* 165: 7215-23
225. Guo Q, Subramanian H, Gupta K, Ali H. 2011. Regulation of C3a receptor signaling in human mast cells by G protein coupled receptor kinases. *PloS one* 6
226. Schraufstatter IU, DiScipio RG, Zhao M, Khaldoyanidi SK. 2009. C3a and C5a Are Chemotactic Factors for Human Mesenchymal Stem Cells, Which Cause Prolonged ERK1/2 Phosphorylation. *The Journal of Immunology* 182: 3827-36
227. Quell KM, Karsten CM, Kordowski A, Almeida LN, Briukhovetska D, Wiese AV, Sun J, Ender F, Antoniou K, Schroder T, Schmudde I, Berger JL, Konig P, Vollbrandt T, Laumonnier Y, Kohl J. 2017. Monitoring C3aR Expression Using a Floxed tdTomato-C3aR Reporter Knock-in Mouse. *J Immunol* 199: 688-706
228. Settmacher B, Bock D, Saad H, Gartner S, Rheinheimer C, Kohl J, Bautsch W, Klos A. 1999. Modulation of C3a activity: internalization of the human C3a receptor and its inhibition by C5a. *J Immunol* 162: 7409-16
229. Asgari E, Le Friec G, Yamamoto H, Perucha E, Sacks SS, Kohl J, Cook HT, Kemper C. 2013. C3a modulates IL-1beta secretion in human monocytes by regulating ATP efflux and subsequent NLRP3 inflammasome activation. *Blood* 122: 3473-81
230. Legler DF, Loetscher M, Jones SA, Dahinden CA, Arock M, Moser B. 1996. Expression of high- and low-affinity receptors for C3a on the human mast cell line, HMC-1. *Eur J Immunol* 26: 753-8
231. Werfel T, Kirchhoff K, Wittmann M, Begemann G, Kapp A, Heidenreich F, Gotze O, Zwirner J. 2000. Activated human T lymphocytes express a functional C3a receptor. *J Immunol* 165: 6599-605
232. Kirchhoff K, Weinmann O, Zwirner J, Begemann G, Gotze O, Kapp A, Werfel T. 2001. Detection of anaphylatoxin receptors on CD83+ dendritic cells derived from human skin. *Immunology* 103: 210-7

233. Schraufstatter IU, Trieu K, Sikora L, Sriramarao P, DiScipio R. 2002. Complement c3a and c5a induce different signal transduction cascades in endothelial cells. *J Immunol* 169: 2102-10
234. Monsinjon T, Gasque P, Chan P, Ischenko A, Brady JJ, Fontaine MC. 2003. Regulation by complement C3a and C5a anaphylatoxins of cytokine production in human umbilical vein endothelial cells. *FASEB J* 17: 1003-14
235. Sauter RJ, Sauter M, Reis ES, Emschermann FN, Nording H, Ebenhoch S, Kraft P, Munzer P, Mauler M, Rheinlaender J, Madlung J, Edlich F, Schaffer TE, Meuth SG, Durschmied D, Geisler T, Borst O, Gawaz M, Kleinschnitz C, Lambris JD, Langer HF. 2018. Functional Relevance of the Anaphylatoxin Receptor C3aR for Platelet Function and Arterial Thrombus Formation Marks an Intersection Point Between Innate Immunity and Thrombosis. *Circulation* 138: 1720-35
236. Sauter RJ, Sauter M, Obrich M, Emschermann FN, Nording H, Patzelt J, Wendel HP, Reil JC, Edlich F, Langer HF. 2019. Anaphylatoxin Receptor C3aR Contributes to Platelet Function, Thrombus Formation and In Vivo Haemostasis. *Thromb Haemost* 119: 179-82
237. Guglietta S, Chiavelli A, Zagato E, Krieg C, Gandini S, Ravenda P, Bazolli B, Lu B, Penna G, Rescigno M. 2016. Coagulation induced by C3aR-dependent NETosis drives protumorigenic neutrophils during small intestinal tumorigenesis. *Nature Communications* 7: 11037
238. Boulay F, Mery L, Tardif M, Brouchon L, Vignais P. 1991. Expression cloning of a receptor for C5a anaphylatoxin on differentiated HL-60 cells. *Biochemistry* 30: 2993-9
239. Gerard NP, Gerard C. 1991. The chemotactic receptor for human C5a anaphylatoxin. *Nature* 349: 614-7
240. Reis ES, Chen H, Sfyroera G, Monk PN, Kohl J, Ricklin D, Lambris JD. 2012. C5a receptor-dependent cell activation by physiological concentrations of desarginated C5a: insights from a novel label-free cellular assay. *J Immunol* 189: 4797-805
241. Nishiura H, Zhao R, Yamamoto T. 2012. Dual functions of the C5a receptor as a connector for the K562 erythroblast-like cell-THP-1 macrophage-like cell island and as a sensor for the differentiation of the K562 erythroblast-like cell during haemin-induced erythropoiesis. *Clin Dev Immunol* 2012: 187080
242. Farzan M, Schnitzler CE, Vasilieva N, Leung D, Kuhn J, Gerard C, Gerard NP, Choe H. 2001. Sulfated tyrosines contribute to the formation of the C5a docking site of the human C5a anaphylatoxin receptor. *J Exp Med* 193: 1059-66
243. Monk PN, Scola AM, Madala P, Fairlie DP. 2007. Function, structure and therapeutic potential of complement C5a receptors. *Br J Pharmacol* 152: 429-48
244. Siciliano SJ, Rollins TE, Springer MS. 1990. Interaction between the C5a receptor and Gi in both the membrane-bound and detergent-solubilized states. *J Biol Chem* 265: 19568-74
245. Braun L, Christophe T, Boulay F. 2003. Phosphorylation of key serine residues is required for internalization of the complement 5a (C5a) anaphylatoxin receptor via a beta-arrestin, dynamin, and clathrin-dependent pathway. *J Biol Chem* 278: 4277-85
246. Perianayagam MC, Balakrishnan VS, King AJ, Pereira BJ, Jaber BL. 2002. C5a delays apoptosis of human neutrophils by a phosphatidylinositol 3-kinase-signaling pathway. *Kidney Int* 61: 456-63
247. Jiang H, Kuang Y, Wu Y, Smrcka A, Simon MI, Wu D. 1996. Pertussis toxin-sensitive activation of phospholipase C by the C5a and fMet-Leu-Phe receptors. *J Biol Chem* 271: 13430-4

248. Mullmann TJ, Siegel MI, Egan RW, Billah MM. 1990. Complement C5a activation of phospholipase D in human neutrophils. A major route to the production of phosphatidates and diglycerides. *J Immunol* 144: 1901-8
249. Karsten CM, Laumonnier Y, Eurich B, Ender F, Bröker K, Roy S, Czabanska A, Vollbrandt T, Figge J, Köhl J. 2015. Monitoring and cell-specific deletion of C5aR1 using a novel floxed GFP-C5aR1 reporter knock-in mouse. *Journal of immunology (Baltimore, Md. : 1950)* 194: 1841-55
250. Chiou WF, Tsai HR, Yang LM, Tsai WJ. 2004. C5a differentially stimulates the ERK1/2 and p38 MAPK phosphorylation through independent signaling pathways to induced chemotactic migration in RAW264.7 macrophages. *Int Immunopharmacol* 4: 1329-41
251. Riedemann NC, Guo RF, Hollmann TJ, Gao H, Neff TA, Reuben JS, Speyer CL, Sarma JV, Wetsel RA, Zetoune FS, Ward PA. 2004. Regulatory role of C5a in LPS-induced IL-6 production by neutrophils during sepsis. *FASEB J* 18: 370-2
252. Zaal A, Dieker M, Oudenampsen M, Turksma AW, Lissenberg-Thunnissen SN, Wouters D, van Ham SM, Ten Brinke A. 2017. Anaphylatoxin C5a Regulates 6-Sulfo-LacNAc Dendritic Cell Function in Human through Crosstalk with Toll-Like Receptor-Induced CREB Signaling. *Front Immunol* 8: 818
253. Solomkin JS, Jenkins MK, Nelson RD, Chenoweth D, Simmons RL. 1981. Neutrophil dysfunction in sepsis. II. Evidence for the role of complement activation products in cellular deactivation. *Surgery* 90: 319-27
254. Kurimoto Y, de Weck AL, Dahinden CA. 1989. Interleukin 3-dependent mediator release in basophils triggered by C5a. *J Exp Med* 170: 467-79
255. Bosmann M, Haggadone MD, Hemmila MR, Zetoune FS, Sarma JV, Ward PA. 2012. Complement activation product C5a is a selective suppressor of TLR4-induced, but not TLR3-induced, production of IL-27(p28) from macrophages. *J Immunol* 188: 5086-93
256. Werfel T, Oppermann M, Schulze M, Krieger G, Weber M, Gotze O. 1992. Binding of fluorescein-labeled anaphylatoxin C5a to human peripheral blood, spleen, and bone marrow leukocytes. *Blood* 79: 152-60
257. Werfel T, Oppermann M, Butterfield JH, Begemann G, Elsner J, Gotze O, Zwirner J. 1996. The human mast cell line HMC-1 expresses C5a receptors and responds to C5a but not to C5a(desArg). *Scand J Immunol* 44: 30-6
258. Dunkelberger J, Zhou L, Miwa T, Song WC. 2012. C5aR expression in a novel GFP reporter gene knockin mouse: implications for the mechanism of action of C5aR signaling in T cell immunity. *J Immunol* 188: 4032-42
259. Köhl J, Baelder R, Lewkowich IP, Pandey MK, Hawlisch H, Wang L, Best J, Herman NS, Sproles AA, Zwirner J, Whitsett JA, Gerard C, Sfyroera G, Lambris JD, Wills-Karp M. 2006. A regulatory role for the C5a anaphylatoxin in type 2 immunity in asthma. *Journal of Clinical Investigation* 116: 783-96
260. Soruri A, Kim S, Kiafard Z, Zwirner J. 2003. Characterization of C5aR expression on murine myeloid and lymphoid cells by the use of a novel monoclonal antibody. *Immunol Lett* 88: 47-52
261. Lalli PN, Strainic MG, Yang M, Lin F, Medof ME, Heeger PS. 2008. Locally produced C5a binds to T cell-expressed C5aR to enhance effector T-cell expansion by limiting antigen-induced apoptosis. *Blood* 112: 1759-66
262. Drouin SM, Kildsgaard J, Haviland J, Zabner J, Jia H, McCray PB, Tack BF, Wetsel RA. 2001. Expression of the Complement Anaphylatoxin C3a and C5a Receptors on Bronchial Epithelial and Smooth Muscle Cells in Models of Sepsis and Asthma. *The Journal of Immunology* 166: 2025-32

263. Fayyazi A, Sandau R, Duong LQ, Gotze O, Radzun HJ, Schweyer S, Soruri A, Zwirner J. 1999. C5a receptor and interleukin-6 are expressed in tissue macrophages and stimulated keratinocytes but not in pulmonary and intestinal epithelial cells. *Am J Pathol* 154: 495-501
264. Floreani AA, Heires AJ, Welniak LA, Miller-Lindholm A, Clark-Pierce L, Rennard SI, Morgan EL, Sanderson SD. 1998. Expression of receptors for C5a anaphylatoxin (CD88) on human bronchial epithelial cells: enhancement of C5a-mediated release of IL-8 upon exposure to cigarette smoke. *J Immunol* 160: 5073-81
265. Strunk RC, Eidlen DM, Mason RJ. 1988. Pulmonary alveolar type II epithelial cells synthesize and secrete proteins of the classical and alternative complement pathways. *J Clin Invest* 81: 1419-26
266. Foreman KE, Vaporciyan AA, Bonish BK, Jones ML, Johnson KJ, Glovsky MM, Eddy SM, Ward PA. 1994. C5a-induced expression of P-selectin in endothelial cells. *J Clin Invest* 94: 1147-55
267. Gasque P, Chan P, Fontaine M, Ischenko A, Lamacz M, Gotze O, Morgan BP. 1995. Identification and characterization of the complement C5a anaphylatoxin receptor on human astrocytes. *J Immunol* 155: 4882-9
268. Ohno M, Hirata T, Enomoto M, Araki T, Ishimaru H, Takahashi TA. 2000. A putative chemoattractant receptor, C5L2, is expressed in granulocyte and immature dendritic cells, but not in mature dendritic cells. *Mol Immunol* 37: 407-12
269. Kalant D, Cain SA, Maslowska M, Sniderman AD, Cianflone K, Monk PN. 2003. The chemoattractant receptor-like protein C5L2 binds the C3a des-Arg77/acylation-stimulating protein. *J Biol Chem* 278: 11123-9
270. Cui W, Lapointe M, Gauvreau D, Kalant D, Cianflone K. 2009. Recombinant C3adesArg/acylation stimulating protein (ASP) is highly bioactive: a critical evaluation of C5L2 binding and 3T3-L1 adipocyte activation. *Mol Immunol* 46: 3207-17
271. Johswich K, Martin M, Thalmann J, Rheinheimer C, Monk PN, Klos A. 2006. Ligand specificity of the anaphylatoxin C5L2 receptor and its regulation on myeloid and epithelial cell lines. *J Biol Chem* 281: 39088-95
272. Okinaga S, Slattery D, Humbles A, Zsengeller Z, Morteau O, Kinrade MB, Brodbeck RM, Krause JE, Choe HR, Gerard NP, Gerard C. 2003. C5L2, a nonsignaling C5A binding protein. *Biochemistry* 42: 9406-15
273. Cain SA, Monk PN. 2002. The orphan receptor C5L2 has high affinity binding sites for complement fragments C5a and C5a des-Arg(74). *J Biol Chem* 277: 7165-9
274. Hopken UE, Lu B, Gerard NP, Gerard C. 1996. The C5a chemoattractant receptor mediates mucosal defence to infection. *Nature* 383: 86-9
275. Bamberg CE, Mackay CR, Lee H, Zahra D, Jackson J, Lim YS, Whitfeld PL, Craig S, Corsini E, Lu B, Gerard C, Gerard NP. 2010. The C5a receptor (C5aR) C5L2 is a modulator of C5aR-mediated signal transduction. *J Biol Chem* 285: 7633-44
276. Gao H, Neff TA, Guo RF, Speyer CL, Sarma JV, Tomlins S, Man Y, Riedemann NC, Hoesel LM, Younkin E, Zetoune FS, Ward PA. 2005. Evidence for a functional role of the second C5a receptor C5L2. *FASEB J* 19: 1003-5
277. Chen NJ, Mirtsos C, Suh D, Lu YC, Lin WJ, McKerlie C, Lee T, Baribault H, Tian H, Yeh WC. 2007. C5L2 is critical for the biological activities of the anaphylatoxins C5a and C3a. *Nature* 446: 203-7
278. Zhang X, Schmudde I, Laumonnier Y, Pandey MK, Clark JR, Konig P, Gerard NP, Gerard C, Wills-Karp M, Kohl J. 2010. A critical role for C5L2 in the pathogenesis of experimental allergic asthma. *J Immunol* 185: 6741-52

279. Li R, Coulthard LG, Wu MC, Taylor SM, Woodruff TM. 2013. C5L2: a controversial receptor of complement anaphylatoxin, C5a. *FASEB J* 27: 855-64
280. Karsten CM, Wiese AV, Mey F, Figge J, Woodruff TM, Reuter T, Scurtu O, Kordowski A, Almeida LN, Briukhovetska D, Quell KM, Sun J, Ender F, Schmudde I, Vollbrandt T, Laumonnier Y, Kohl J. 2017. Monitoring C5aR2 Expression Using a Floxed tdTomato-C5aR2 Knock-In Mouse. *J Immunol* 199: 3234-48
281. Strainic MG, Shevach EM, An F, Lin F, Medof ME. 2013. Absence of signaling into CD4(+) cells via C3aR and C5aR enables autoinductive TGF-beta1 signaling and induction of Foxp3(+) regulatory T cells. *Nat Immunol* 14: 162-71
282. Traves SL, Culpitt SV, Russell RE, Barnes PJ, Donnelly LE. 2002. Increased levels of the chemokines GROalpha and MCP-1 in sputum samples from patients with COPD. *Thorax* 57: 590-5
283. Keatings VM, Collins PD, Scott DM, Barnes PJ. 1996. Differences in interleukin-8 and tumor necrosis factor-alpha in induced sputum from patients with chronic obstructive pulmonary disease or asthma. *Am J Respir Crit Care Med* 153: 530-4
284. Xiong Z, Leme AS, Ray P, Shapiro SD, Lee JS. 2011. CX3CR1+ lung mononuclear phagocytes spatially confined to the interstitium produce TNF-alpha and IL-6 and promote cigarette smoke-induced emphysema. *J Immunol* 186: 3206-14
285. Berenson CS, Kruzel RL, Eberhardt E, Dolnick R, Minderman H, Wallace PK, Sethi S. 2014. Impaired innate immune alveolar macrophage response and the predilection for COPD exacerbations. *Thorax* 69: 811-8
286. Hodge S, Hodge G, Scicchitano R, Reynolds PN, Holmes M. 2003. Alveolar macrophages from subjects with chronic obstructive pulmonary disease are deficient in their ability to phagocytose apoptotic airway epithelial cells. *Immunol Cell Biol* 81: 289-96
287. Eltboli O, Bafadhel M, Hollins F, Wright A, Hargadon B, Kulkarni N, Brightling C. 2014. COPD exacerbation severity and frequency is associated with impaired macrophage efferocytosis of eosinophils. *BMC Pulm Med* 14: 112
288. Taylor AE, Finney-Hayward TK, Quint JK, Thomas CM, Tudhope SJ, Wedzicha JA, Barnes PJ, Donnelly LE. 2010. Defective macrophage phagocytosis of bacteria in COPD. *Eur Respir J* 35: 1039-47
289. Grumelli S, Corry DB, Song LZ, Song L, Green L, Huh J, Hacken J, Espada R, Bag R, Lewis DE, Kheradmand F. 2004. An immune basis for lung parenchymal destruction in chronic obstructive pulmonary disease and emphysema. *PLoS Med* 1: e8
290. Kosmas EN, Zorpidou D, Vassilareas V, Roussou T, Michaelides S. 1997. Decreased C4 complement component serum levels correlate with the degree of emphysema in patients with chronic bronchitis. *Chest* 112: 341-7
291. Miller RD, Kueppers F, Offord KP. 1980. Serum concentrations of C3 and C4 of the complement system in patients with chronic obstructive pulmonary disease. *J Lab Clin Med* 95: 266-71
292. Marc MM, Korosec P, Kosnik M, Kern I, Flezar M, Suskovic S, Sorli J. 2004. Complement factors c3a, c4a, and c5a in chronic obstructive pulmonary disease and asthma. *Am J Respir Cell Mol Biol* 31: 216-9
293. Westwood JP, Mackay AJ, Donaldson G, Machin SJ, Wedzicha JA, Scully M. 2016. The role of complement activation in COPD exacerbation recovery. *ERJ Open Res* 2
294. Bonfield TL, Panuska JR, Konstan MW, Hilliard KA, Hilliard JB, Ghnaim H, Berger M. 1995. Inflammatory cytokines in cystic fibrosis lungs. *Am J Respir Crit Care Med* 152: 2111-8

295. Zhang Y, Li X, Grassme H, Doring G, Gulbins E. 2010. Alterations in ceramide concentration and pH determine the release of reactive oxygen species by Cftr-deficient macrophages on infection. *J Immunol* 184: 5104-11
296. Del Porto P, Cifani N, Guarnieri S, Di Domenico EG, Mariggio MA, Spadaro F, Guglietta S, Anile M, Venuta F, Quattrucci S, Ascenzioni F. 2011. Dysfunctional CFTR alters the bactericidal activity of human macrophages against Pseudomonas aeruginosa. *PLoS One* 6: e19970
297. Hair PS, Sass LA, Vazifedan T, Shah TA, Krishna NK, Cunnion KM. 2017. Complement effectors, C5a and C3a, in cystic fibrosis lung fluid correlate with disease severity. *PLoS One* 12: e0173257
298. Mueller-Ortiz SL, Drouin SM, Wetsel RA. 2004. The alternative activation pathway and complement component C3 are critical for a protective immune response against Pseudomonas aeruginosa in a murine model of pneumonia. *Infect Immun* 72: 2899-906
299. Matanic D, Beg-Zec Z, Stojanovic D, Matakoric N, Flego V, Milevoj-Ribic F. 2003. Cytokines in patients with lung cancer. *Scand J Immunol* 57: 173-8
300. Siziopikou KP, Harris JE, Casey L, Nawas Y, Braun DP. 1991. Impaired tumoricidal function of alveolar macrophages from patients with non-small cell lung cancer. *Cancer* 68: 1035-44
301. Ahn MC, Siziopikou KP, Plate JM, Casey L, Silver M, Harris JE, Braun DP. 1997. Modulation of tumoricidal function in alveolar macrophages from lung cancer patients by interleukin-6. *Cancer Immunol Immunother* 45: 37-44
302. Barthelemy-Brichant N, David JL, Bosquee L, Bury T, Seidel L, Albert A, Bartsch P, Baugnet-Mahieu L, Deneufbourg JM. 2002. Increased TGFbeta1 plasma level in patients with lung cancer: potential mechanisms. *Eur J Clin Invest* 32: 193-8
303. Yanagawa H, Takeuchi E, Suzuki Y, Hanibuchi M, Haku T, Ohmoto Y, Sone S. 1999. Production of interleukin-10 by alveolar macrophages from lung cancer patients. *Respir Med* 93: 666-71
304. Gorrin-Rivas MJ, Arii S, Mori A, Takeda Y, Mizumoto M, Furutani M, Imamura M. 2000. Implications of human macrophage metalloelastase and vascular endothelial growth factor gene expression in angiogenesis of hepatocellular carcinoma. *Ann Surg* 231: 67-73
305. Chen JJ, Yao PL, Yuan A, Hong TM, Shun CT, Kuo ML, Lee YC, Yang PC. 2003. Up-regulation of tumor interleukin-8 expression by infiltrating macrophages: its correlation with tumor angiogenesis and patient survival in non-small cell lung cancer. *Clin Cancer Res* 9: 729-37
306. Kwak JW, Laskowski J, Li HY, McSharry MV, Sippel TR, Bullock BL, Johnson AM, Poczobutt JM, Neuwelt AJ, Malkoski SP, Weiser-Evans MC, Lambris JD, Clambey ET, Thurman JM, Nemenoff RA. 2018. Complement Activation via a C3a Receptor Pathway Alters CD4(+) T Lymphocytes and Mediates Lung Cancer Progression. *Cancer Res* 78: 143-56
307. Nabizadeh JA, Manthey HD, Steyn FJ, Chen W, Widiapradja A, Md Akhir FN, Boyle GM, Taylor SM, Woodruff TM, Rolfe BE. 2016. The Complement C3a Receptor Contributes to Melanoma Tumorigenesis by Inhibiting Neutrophil and CD4+ T Cell Responses. *J Immunol* 196: 4783-92
308. Cohen SB, Gern BH, Delahaye JL, Adams KN, Plumlee CR, Winkler JK, Sherman DR, Gerner MY, Urdahl KB. 2018. Alveolar Macrophages Provide an Early Mycobacterium tuberculosis Niche and Initiate Dissemination. *Cell Host Microbe* 24: 439-46 e4

309. Jung JY, Madan-Lala R, Georgieva M, Rengarajan J, Sohaskey CD, Bange FC, Robinson CM. 2013. The intracellular environment of human macrophages that produce nitric oxide promotes growth of mycobacteria. *Infect Immun* 81: 3198-209
310. Delogu G, Sali M, Fadda G. 2013. The biology of mycobacterium tuberculosis infection. *Mediterr J Hematol Infect Dis* 5: e2013070
311. Goldmann O, von Kockritz-Blickwede M, Holtje C, Chhatwal GS, Geffers R, Medina E. 2007. Transcriptome analysis of murine macrophages in response to infection with Streptococcus pyogenes reveals an unusual activation program. *Infect Immun* 75: 4148-57
312. Medeiros AI, Serezani CH, Lee SP, Peters-Golden M. 2009. Efferocytosis impairs pulmonary macrophage and lung antibacterial function via PGE2/EP2 signaling. *J Exp Med* 206: 61-8
313. Stolberg VR, McCubbrey AL, Freeman CM, Brown JP, Crudgington SW, Taitano SH, Saxton BL, Mancuso P, Curtis JL. 2015. Glucocorticoid-Augmented Efferocytosis Inhibits Pulmonary Pneumococcal Clearance in Mice by Reducing Alveolar Macrophage Bactericidal Function. *J Immunol* 195: 174-84
314. M K, M A, J K, C H, K W, eds. 2015. *The role of complement in experimental infection with Mycobacterium tuberculosis*: Thieme
315. Dutow P, Fehlhaber B, Bode J, Laudeley R, Rheinheimer C, Glage S, Wetsel RA, Pabst O, Klos A. 2014. The complement C3a receptor is critical in defense against Chlamydia psittaci in mouse lung infection and required for antibody and optimal T cell response. *J Infect Dis* 209: 1269-78
316. Wynn TA, Chawla A, Pollard JW. 2013. Macrophage biology in development, homeostasis and disease. *Nature* 496: 445-55
317. Gu H, Fisher AJ, Mickler EA, Duerson F, 3rd, Cummings OW, Peters-Golden M, Twigg HL, 3rd, Woodruff TM, Wilkes DS, Vittal R. 2016. Contribution of the anaphylatoxin receptors, C3aR and C5aR, to the pathogenesis of pulmonary fibrosis. *FASEB J* 30: 2336-50
318. Huang X, Xiu H, Zhang S, Zhang G. 2018. The Role of Macrophages in the Pathogenesis of ALI/ARDS. *Mediators Inflamm* 2018: 1264913
319. Lomas-Neira J, Chung CS, Perl M, Gregory S, Biffl W, Ayala A. 2006. Role of alveolar macrophage and migrating neutrophils in hemorrhage-induced priming for ALI subsequent to septic challenge. *Am J Physiol Lung Cell Mol Physiol* 290: L51-8
320. Johnston LK, Rims CR, Gill SE, McGuire JK, Manicone AM. 2012. Pulmonary macrophage subpopulations in the induction and resolution of acute lung injury. *Am J Respir Cell Mol Biol* 47: 417-26
321. Wilson MR, Choudhury S, Goddard ME, O'Dea KP, Nicholson AG, Takata M. 2003. High tidal volume upregulates intrapulmonary cytokines in an in vivo mouse model of ventilator-induced lung injury. *J Appl Physiol (1985)* 95: 1385-93
322. Beck-Schimmer B, Schwendener R, Pasch T, Reyes L, Booy C, Schimmer RC. 2005. Alveolar macrophages regulate neutrophil recruitment in endotoxin-induced lung injury. *Respir Res* 6: 61
323. Bhatia M, Zemans RL, Jeyaseelan S. 2012. Role of chemokines in the pathogenesis of acute lung injury. *Am J Respir Cell Mol Biol* 46: 566-72
324. Pechkovsky DV, Prasse A, Kollert F, Engel KM, Dentler J, Luttmann W, Friedrich K, Muller-Quernheim J, Zissel G. 2010. Alternatively activated alveolar macrophages in pulmonary fibrosis-mediator production and intracellular signal transduction. *Clin Immunol* 137: 89-101

325. Sun S, Zhao G, Liu C, Wu X, Guo Y, Yu H, Song H, Du L, Jiang S, Guo R, Tomlinson S, Zhou Y. 2013. Inhibition of complement activation alleviates acute lung injury induced by highly pathogenic avian influenza H5N1 virus infection. *Am J Respir Cell Mol Biol* 49: 221-30
326. Sylvestre D, Clynes R, Ma M, Warren H, Carroll MC, Ravetch JV. 1996. Immunoglobulin G-mediated inflammatory responses develop normally in complement-deficient mice. *J Exp Med* 184: 2385-92
327. Amara U, Flierl MA, Rittirsch D, Klos A, Chen H, Acker B, Bruckner UB, Nilsson B, Gebhard F, Lambris JD, Huber-Lang M. 2010. Molecular intercommunication between the complement and coagulation systems. *J Immunol* 185: 5628-36
328. Nurmagambetov T, Kuwahara R, Garbe P. 2018. The Economic Burden of Asthma in the United States, 2008-2013. *Ann Am Thorac Soc* 15: 348-56
329. Nunes C, Pereira AM, Morais-Almeida M. 2017. Asthma costs and social impact. *Asthma Res Pract* 3: 1
330. Cezmi A. Akdis IA. 2013. Global Atlas of Asthma. *European Academy of Allergy and Clinical Immunology*
331. 2018. *The Global Asthma Report 2018*, The Global Asthma Network, Auckland, New Zealand
332. Lambrecht BN, Hammad H. 2015. The immunology of asthma. *Nat Immunol* 16: 45-56
333. Simpson A, Tan VY, Winn J, Svensen M, Bishop CM, Heckerman DE, Buchan I, Custovic A. 2010. Beyond atopy: multiple patterns of sensitization in relation to asthma in a birth cohort study. *Am J Respir Crit Care Med* 181: 1200-6
334. Anderson GP. 2008. Endotyping asthma: new insights into key pathogenic mechanisms in a complex, heterogeneous disease. *Lancet* 372: 1107-19
335. Wu W, Bleecker E, Moore W, Busse WW, Castro M, Chung KF, Calhoun WJ, Erzurum S, Gaston B, Israel E, Curran-Everett D, Wenzel SE. 2014. Unsupervised phenotyping of Severe Asthma Research Program participants using expanded lung data. *J Allergy Clin Immunol* 133: 1280-8
336. Ozdemir C, Kucuksezer UC, Akdis M, Akdis CA. 2018. The concepts of asthma endotypes and phenotypes to guide current and novel treatment strategies. *Expert Rev Respir Med* 12: 733-43
337. Vercelli D. 2008. Discovering susceptibility genes for asthma and allergy. *Nat Rev Immunol* 8: 169-82
338. Werner M, Topp R, Wimmer K, Richter K, Bischof W, Wjst M, Heinrich J. 2003. TLR4 gene variants modify endotoxin effects on asthma. *J Allergy Clin Immunol* 112: 323-30
339. Pykalainen M, Kinos R, Valkonen S, Rydman P, Kilpelainen M, Laitinen LA, Karjalainen J, Nieminen M, Hurme M, Kere J, Laitinen T, Lahesmaa R. 2005. Association analysis of common variants of STAT6, GATA3, and STAT4 to asthma and high serum IgE phenotypes. *J Allergy Clin Immunol* 115: 80-7
340. Kabesch M, Tzotcheva I, Carr D, Hofler C, Weiland SK, Fritzsch C, von Mutius E, Martinez FD. 2003. A complete screening of the IL4 gene: novel polymorphisms and their association with asthma and IgE in childhood. *J Allergy Clin Immunol* 112: 893-8
341. Vladich FD, Brazille SM, Stern D, Peck ML, Ghittoni R, Vercelli D. 2005. IL-13 R130Q, a common variant associated with allergy and asthma, enhances effector mechanisms essential for human allergic inflammation. *J Clin Invest* 115: 747-54
342. Levy H, Raby BA, Lake S, Tantisira KG, Kwiatkowski D, Lazarus R, Silverman EK, Richter B, Klimecki WT, Vercelli D, Martinez FD, Weiss ST. 2005. Association of defensin beta-1 gene polymorphisms with asthma. *J Allergy Clin Immunol* 115: 252-8

343. Moffatt MF, Cookson WO. 1997. Tumour necrosis factor haplotypes and asthma. *Hum Mol Genet* 6: 551-4
344. Silverman ES, Palmer LJ, Subramaniam V, Hallock A, Mathew S, Vallone J, Faffe DS, Shikanai T, Raby BA, Weiss ST, Shore SA. 2004. Transforming growth factor-beta1 promoter polymorphism C-509T is associated with asthma. *Am J Respir Crit Care Med* 169: 214-9
345. Strachan DP. 1989. Hay fever, hygiene, and household size. *BMJ* 299: 1259-60
346. Wills-Karp M, Santeliz J, Karp CL. 2001. The germless theory of allergic disease: revisiting the hygiene hypothesis. *Nat Rev Immunol* 1: 69-75
347. Bloomfield SF, Rook GA, Scott EA, Shanahan F, Stanwell-Smith R, Turner P. 2016. Time to abandon the hygiene hypothesis: new perspectives on allergic disease, the human microbiome, infectious disease prevention and the role of targeted hygiene. *Perspect Public Health* 136: 213-24
348. Scudellari M. 2017. News Feature: Cleaning up the hygiene hypothesis. *Proc Natl Acad Sci U S A* 114: 1433-6
349. Guarnieri M, Balmes JR. 2014. Outdoor air pollution and asthma. *Lancet* 383: 1581-92
350. Gilliland FD. 2009. Outdoor air pollution, genetic susceptibility, and asthma management: opportunities for intervention to reduce the burden of asthma. *Pediatrics* 123 Suppl 3: S168-73
351. Silverman RA, Ito K. 2010. Age-related association of fine particles and ozone with severe acute asthma in New York City. *J Allergy Clin Immunol* 125: 367-73 e5
352. Zacharasiewicz A. 2016. Maternal smoking in pregnancy and its influence on childhood asthma. *ERJ Open Res* 2
353. Thavagnanam S, Fleming J, Bromley A, Shields MD, Cardwell CR. 2008. A meta-analysis of the association between Caesarean section and childhood asthma. *Clin Exp Allergy* 38: 629-33
354. Miller RL. 2008. Prenatal maternal diet affects asthma risk in offspring. *J Clin Invest* 118: 3265-8
355. Loewen K, Monchka B, Mahmud SM, t Jong G, Azad MB. 2018. Prenatal antibiotic exposure and childhood asthma: a population-based study. *Eur Respir J* 52
356. Lapin B, Piorkowski J, Ownby D, Freels S, Chavez N, Hernandez E, Wagner-Cassanova C, Pelzel D, Vergara C, Persky V. 2015. Relationship between prenatal antibiotic use and asthma in at-risk children. *Ann Allergy Asthma Immunol* 114: 203-7
357. Douros K, Moustaki M, Tsabouri S, Papadopoulou A, Papadopoulos M, Priftis KN. 2017. Prenatal Maternal Stress and the Risk of Asthma in Children. *Front Pediatr* 5: 202
358. Subbarao P, Mandhane PJ, Sears MR. 2009. Asthma: epidemiology, etiology and risk factors. *CMAJ* 181: E181-90
359. Kozyrskyj AL, Ernst P, Becker AB. 2007. Increased risk of childhood asthma from antibiotic use in early life. *Chest* 131: 1753-9
360. Klopp A, Vehling L, Becker AB, Subbarao P, Mandhane PJ, Turvey SE, Lefebvre DL, Sears MR, Investigators CS, Azad MB. 2017. Modes of Infant Feeding and the Risk of Childhood Asthma: A Prospective Birth Cohort Study. *J Pediatr* 190: 192-9 e2
361. Ferrante G, Antona R, Malizia V, Montalbano L, Corsello G, La Grutta S. 2014. Smoke exposure as a risk factor for asthma in childhood: a review of current evidence. *Allergy Asthma Proc* 35: 454-61
362. Ahmadizar F, Vijverberg SJH, Arets HGM, de Boer A, Turner S, Devereux G, Arabkhazaeli A, Soares P, Mukhopadhyay S, Garssen J, Palmer CNA, de Jongste JC, Jaddoe VWV, Duijts L, van Meel ER, Kraneveld AD, Maitland-van der Zee AH. 2017.

Early life antibiotic use and the risk of asthma and asthma exacerbations in children. *Pediatr Allergy Immunol* 28: 430-7

363. Ahmadizar F, Vijverberg SJH, Arets HGM, de Boer A, Lang JE, Garssen J, Kraneveld A, Maitland-van der Zee AH. 2018. Early-life antibiotic exposure increases the risk of developing allergic symptoms later in life: A meta-analysis. *Allergy* 73: 971-86
364. Ahmadizar F, Vijverberg SJH, Arets HGM, de Boer A, Garssen J, Kraneveld AD, Maitland-van der Zee AH. 2017. Breastfeeding is associated with a decreased risk of childhood asthma exacerbations later in life. *Pediatr Allergy Immunol* 28: 649-54
365. Levitzky MG, ed. 2013. *Pulmonary Physiology*: The McGraw-Hill Companies
366. Chroneos ZC, Sever-Chroneos Z, Shepherd VL. 2010. Pulmonary surfactant: an immunological perspective. *Cell Physiol Biochem* 25: 13-26
367. Du X, Meng Q, Sharif A, Abdel-Razek OA, Zhang L, Wang G, Cooney RN. 2016. Surfactant Proteins SP-A and SP-D Ameliorate Pneumonia Severity and Intestinal Injury in a Murine Model of Staphylococcus Aureus Pneumonia. *Shock* 46: 164-72
368. Haczku A. 2008. Protective role of the lung collectins surfactant protein A and surfactant protein D in airway inflammation. *J Allergy Clin Immunol* 122: 861-79; quiz 80-1
369. McCormack FX, Whitsett JA. 2002. The pulmonary collectins, SP-A and SP-D, orchestrate innate immunity in the lung. *J Clin Invest* 109: 707-12
370. van Rozendaal BA, van Spriel AB, van De Winkel JG, Haagsman HP. 2000. Role of pulmonary surfactant protein D in innate defense against Candida albicans. *J Infect Dis* 182: 917-22
371. Ferguson JS, Voelker DR, McCormack FX, Schlesinger LS. 1999. Surfactant protein D binds to Mycobacterium tuberculosis bacilli and lipoarabinomannan via carbohydrate-lectin interactions resulting in reduced phagocytosis of the bacteria by macrophages. *J Immunol* 163: 312-21
372. Hartshorn KL, Crouch E, White MR, Colamussi ML, Kakkanatt A, Tauber B, Shepherd V, Sastry KN. 1998. Pulmonary surfactant proteins A and D enhance neutrophil uptake of bacteria. *Am J Physiol* 274: L958-69
373. Hartshorn KL, Reid KB, White MR, Jensenius JC, Morris SM, Tauber AI, Crouch E. 1996. Neutrophil deactivation by influenza A viruses: mechanisms of protection after viral opsonization with collectins and hemagglutination-inhibiting antibodies. *Blood* 87: 3450-61
374. Schelenz S, Malhotra R, Sim RB, Holmskov U, Bancroft GJ. 1995. Binding of host collectins to the pathogenic yeast Cryptococcus neoformans: human surfactant protein D acts as an agglutinin for acapsular yeast cells. *Infect Immun* 63: 3360-6
375. Todd DA, Marsh MJ, George A, Henderson NG, Barr H, Sebastian S, Clark GT, Koster G, Clark HW, Postle AD. 2010. Surfactant phospholipids, surfactant proteins, and inflammatory markers during acute lung injury in children. *Pediatr Crit Care Med* 11: 82-91
376. Ohlmeier S, Vuolanto M, Toljamo T, Vuopala K, Salmenkivi K, Myllarniemi M, Kinnula VL. 2008. Proteomics of human lung tissue identifies surfactant protein A as a marker of chronic obstructive pulmonary disease. *J Proteome Res* 7: 5125-32
377. Gunther A, Schmidt R, Nix F, Yabut-Perez M, Guth C, Rosseau S, Siebert C, Grimminger F, Morr H, Velcovsky HG, Seeger W. 1999. Surfactant abnormalities in idiopathic pulmonary fibrosis, hypersensitivity pneumonitis and sarcoidosis. *Eur Respir J* 14: 565-73

378. Guillot L, Epaud R, Thouvenin G, Jonard L, Mohsni A, Couderc R, Counil F, de Blic J, Taam RA, Le Bourgeois M, Reix P, Flamein F, Clement A, Feldmann D. 2009. New surfactant protein C gene mutations associated with diffuse lung disease. *J Med Genet* 46: 490-4
379. Griese M, Essl R, Schmidt R, Rietschel E, Ratjen F, Ballmann M, Paul K, Group BS. 2004. Pulmonary surfactant, lung function, and endobronchial inflammation in cystic fibrosis. *Am J Respir Crit Care Med* 170: 1000-5
380. Arizmendi NG, Abel M, Mihara K, Davidson C, Polley D, Nadeem A, El Mays T, Gilmore BF, Walker B, Gordon JR, Hollenberg MD, Vliagoftis H. 2011. Mucosal allergic sensitization to cockroach allergens is dependent on proteinase activity and proteinase-activated receptor-2 activation. *J Immunol* 186: 3164-72
381. Kheradmand F, Kiss A, Xu J, Lee SH, Kolattukudy PE, Corry DB. 2002. A protease-activated pathway underlying Th cell type 2 activation and allergic lung disease. *J Immunol* 169: 5904-11
382. Lambrecht BN, Hammad H. 2012. The airway epithelium in asthma. *Nat Med* 18: 684-92
383. Lambrecht BN, Hammad H. 2014. Allergens and the airway epithelium response: gateway to allergic sensitization. *J Allergy Clin Immunol* 134: 499-507
384. Ather JL, Hodgkins SR, Janssen-Heininger YM, Poynter ME. 2011. Airway epithelial NF-kappaB activation promotes allergic sensitization to an innocuous inhaled antigen. *Am J Respir Cell Mol Biol* 44: 631-8
385. Hammad H, Chieppa M, Perros F, Willart MA, Germain RN, Lambrecht BN. 2009. House dust mite allergen induces asthma via Toll-like receptor 4 triggering of airway structural cells. *Nat Med* 15: 410-6
386. Kouzaki H, O'Grady SM, Lawrence CB, Kita H. 2009. Proteases induce production of thymic stromal lymphopoietin by airway epithelial cells through protease-activated receptor-2. *J Immunol* 183: 1427-34
387. Hammad H, Lambrecht BN. 2008. Dendritic cells and epithelial cells: linking innate and adaptive immunity in asthma. *Nat Rev Immunol* 8: 193-204
388. Fahy JV. 2015. Type 2 inflammation in asthma--present in most, absent in many. *Nat Rev Immunol* 15: 57-65
389. Gold MJ, Antignano F, Halim TY, Hirota JA, Blanchet MR, Zaph C, Takei F, McNagny KM. 2014. Group 2 innate lymphoid cells facilitate sensitization to local, but not systemic, TH2-inducing allergen exposures. *J Allergy Clin Immunol* 133: 1142-8
390. Hosoki K, Itazawa T, Boldogh I, Sur S. 2016. Neutrophil recruitment by allergens contribute to allergic sensitization and allergic inflammation. *Curr Opin Allergy Clin Immunol* 16: 45-50
391. Park SJ, Wiekowski MT, Lira SA, Mehrad B. 2006. Neutrophils regulate airway responses in a model of fungal allergic airways disease. *J Immunol* 176: 2538-45
392. Sevin CM, Newcomb DC, Toki S, Han W, Sherrill TP, Boswell MG, Zhu Z, Collins RD, Boyd KL, Goleniewska K, Huckabee MM, Blackwell TS, Peebles RS, Jr. 2013. Deficiency of gp91phox inhibits allergic airway inflammation. *Am J Respir Cell Mol Biol* 49: 396-402
393. Sibille Y, Marchandise FX. 1993. Pulmonary immune cells in health and disease: polymorphonuclear neutrophils. *Eur Respir J* 6: 1529-43
394. Voynow JA, Young LR, Wang Y, Horger T, Rose MC, Fischer BM. 1999. Neutrophil elastase increases MUC5AC mRNA and protein expression in respiratory epithelial cells. *Am J Physiol* 276: L835-43

395. Jahnsen FL, Strickland DH, Thomas JA, Tobagus IT, Napoli S, Zosky GR, Turner DJ, Sly PD, Stumbles PA, Holt PG. 2006. Accelerated antigen sampling and transport by airway mucosal dendritic cells following inhalation of a bacterial stimulus. *J Immunol* 177: 5861-7
396. Veres TZ, Voedisch S, Spies E, Tschernig T, Braun A. 2011. Spatiotemporal and functional behavior of airway dendritic cells visualized by two-photon microscopy. *Am J Pathol* 179: 603-9
397. Ito T, Wang YH, Duramad O, Hori T, Delespesse GJ, Watanabe N, Qin FX, Yao Z, Cao W, Liu YJ. 2005. TSLP-activated dendritic cells induce an inflammatory T helper type 2 cell response through OX40 ligand. *J Exp Med* 202: 1213-23
398. Liu YJ. 2007. Thymic stromal lymphopoietin and OX40 ligand pathway in the initiation of dendritic cell-mediated allergic inflammation. *J Allergy Clin Immunol* 120: 238-44; quiz 45-6
399. Zhang F, Huang G, Hu B, Song Y, Shi Y. 2011. A soluble thymic stromal lymphopoietin (TSLP) antagonist, TSLPR-immunoglobulin, reduces the severity of allergic disease by regulating pulmonary dendritic cells. *Clin Exp Immunol* 164: 256-64
400. Le Gros G, Ben-Sasson SZ, Seder R, Finkelman FD, Paul WE. 1990. Generation of interleukin 4 (IL-4)-producing cells in vivo and in vitro: IL-2 and IL-4 are required for in vitro generation of IL-4-producing cells. *J Exp Med* 172: 921-9
401. Swain SL, Weinberg AD, English M, Huston G. 1990. IL-4 directs the development of Th2-like helper effectors. *J Immunol* 145: 3796-806
402. Shimoda K, van Deursen J, Sangster MY, Sarawar SR, Carson RT, Tripp RA, Chu C, Quelle FW, Nosaka T, Vignali DA, Doherty PC, Grosveld G, Paul WE, Ihle JN. 1996. Lack of IL-4-induced Th2 response and IgE class switching in mice with disrupted Stat6 gene. *Nature* 380: 630-3
403. Zheng W, Flavell RA. 1997. The transcription factor GATA-3 is necessary and sufficient for Th2 cytokine gene expression in CD4 T cells. *Cell* 89: 587-96
404. Pai SY, Truitt ML, Ho IC. 2004. GATA-3 deficiency abrogates the development and maintenance of T helper type 2 cells. *Proc Natl Acad Sci U S A* 101: 1993-8
405. Al-Ramli W, Prefontaine D, Chouiali F, Martin JG, Olivenstein R, Lemiere C, Hamid Q. 2009. T(H)17-associated cytokines (IL-17A and IL-17F) in severe asthma. *J Allergy Clin Immunol* 123: 1185-7
406. Manni ML, Trudeau JB, Scheller EV, Mandalapu S, Elloso MM, Kolls JK, Wenzel SE, Alcorn JF. 2014. The complex relationship between inflammation and lung function in severe asthma. *Mucosal Immunol* 7: 1186-98
407. Lajoie S, Lewkowich IP, Suzuki Y, Clark JR, Sproles AA, Dienger K, Budelsky AL, Wills-Karp M. 2010. Complement-mediated regulation of the IL-17A axis is a central genetic determinant of the severity of experimental allergic asthma. *Nature Immunology* 11: 928-35
408. Galli SJ, Tsai M. 2012. IgE and mast cells in allergic disease. *Nat Med* 18: 693-704
409. Bingham CO, 3rd, Austen KF. 2000. Mast-cell responses in the development of asthma. *J Allergy Clin Immunol* 105: S527-34
410. Ashina K, Tsubosaka Y, Nakamura T, Omori K, Kobayashi K, Hori M, Ozaki H, Murata T. 2015. Histamine Induces Vascular Hyperpermeability by Increasing Blood Flow and Endothelial Barrier Disruption In Vivo. *PLoS One* 10: e0132367
411. Hayashi D, Li D, Hayashi C, Shatos M, Hodges RR, Dartt DA. 2012. Role of histamine and its receptor subtypes in stimulation of conjunctival goblet cell secretion. *Invest Ophthalmol Vis Sci* 53: 2993-3003

412. Irvin CG, Tu YP, Sheller JR, Funk CD. 1997. 5-Lipoxygenase products are necessary for ovalbumin-induced airway responsiveness in mice. *Am J Physiol* 272: L1053-8
413. Suzuki H, Kou K. 1983. Direct and indirect effects of histamine on the smooth muscle cells of the guinea-pig main pulmonary artery. *Pflugers Arch* 399: 46-53
414. Williams CM, Galli SJ. 2000. Mast cells can amplify airway reactivity and features of chronic inflammation in an asthma model in mice. *J Exp Med* 192: 455-62
415. Lajoie S, Lewkowich IP, Suzuki Y, Clark JR, Sproles AA, Dienger K, Budelsky AL, Wills-Karp M. 2010. Complement-mediated regulation of the IL-17A axis is a central genetic determinant of the severity of experimental allergic asthma. *Nat Immunol* 11: 928-35
416. Wills-Karp M, Chiaramonte M. 2003. Interleukin-13 in asthma. *Curr Opin Pulm Med* 9: 21-7
417. Lewkowich IP, Lajoie S, Clark JR, Herman NS, Sproles AA, Wills-Karp M. 2008. Allergen uptake, activation, and IL-23 production by pulmonary myeloid DCs drives airway hyperresponsiveness in asthma-susceptible mice. *PLoS One* 3: e3879
418. Wills-Karp M. 2001. Asthma genetics: not for the TIMid? *Nat Immunol* 2: 1095-6
419. Wills-Karp M, Luyimbazi J, Xu X, Schofield B, Neben TY, Karp CL, Donaldson DD. 1998. Interleukin-13: central mediator of allergic asthma. *Science* 282: 2258-61
420. Galli SJ, Tsai M, Piliponsky AM. 2008. The development of allergic inflammation. *Nature* 454: 445-54
421. Kuperman DA, Huang X, Koth LL, Chang GH, Dolganov GM, Zhu Z, Elias JA, Sheppard D, Erle DJ. 2002. Direct effects of interleukin-13 on epithelial cells cause airway hyperreactivity and mucus overproduction in asthma. *Nat Med* 8: 885-9
422. Murphy K, Travers P, Walport M, Janeway C. 2012. *Janeway's immunobiology*. New York: Garland Science. xix, 868 p. pp.
423. Amin K, Janson C, Bystrom J. 2016. Role of Eosinophil Granulocytes in Allergic Airway Inflammation Endotypes. *Scand J Immunol* 84: 75-85
424. Blanchard C, Rothenberg ME. 2009. Biology of the eosinophil. *Adv Immunol* 101: 81-121
425. Dombrowicz D, Capron M. 2001. Eosinophils, allergy and parasites. *Curr Opin Immunol* 13: 716-20
426. Robinson DS, Kay AB, Wardlaw AJ. 2002. Eosinophils. *Clin Allergy Immunol* 16: 43-75
427. Yu M, Tsai M, Tam SY, Jones C, Zehnder J, Galli SJ. 2006. Mast cells can promote the development of multiple features of chronic asthma in mice. *J Clin Invest* 116: 1633-41
428. Yu M, Eckart MR, Morgan AA, Mukai K, Butte AJ, Tsai M, Galli SJ. 2011. Identification of an IFN-gamma/mast cell axis in a mouse model of chronic asthma. *J Clin Invest* 121: 3133-43
429. Cruse G, Bradding P. 2016. Mast cells in airway diseases and interstitial lung disease. *Eur J Pharmacol* 778: 125-38
430. Perros F, Hoogsteden HC, Coyle AJ, Lambrecht BN, Hammad H. 2009. Blockade of CCR4 in a humanized model of asthma reveals a critical role for DC-derived CCL17 and CCL22 in attracting Th2 cells and inducing airway inflammation. *Allergy* 64: 995-1002
431. Luo J, An X, Yao Y, Erb C, Ferguson A, Kolls JK, Fan S, Chen K. 2019. Epigenetic Regulation of IL-17-Induced Chemokines in Lung Epithelial Cells. *Mediators Inflamm* 2019: 9050965
432. Newcomb DC, Peebles RS, Jr. 2013. Th17-mediated inflammation in asthma. *Curr Opin Immunol* 25: 755-60
433. Serhan CN, Savill J. 2005. Resolution of inflammation: the beginning programs the end. *Nat Immunol* 6: 1191-7

434. Barnig C, Frossard N, Levy BD. 2018. Towards targeting resolution pathways of airway inflammation in asthma. *Pharmacol Ther* 186: 98-113
435. Woolley KL, Gibson PG, Carty K, Wilson AJ, Twaddell SH, Woolley MJ. 1996. Eosinophil apoptosis and the resolution of airway inflammation in asthma. *Am J Respir Crit Care Med* 154: 237-43
436. Vandivier RW, Henson PM, Douglas IS. 2006. Burying the dead: the impact of failed apoptotic cell removal (efferocytosis) on chronic inflammatory lung disease. *Chest* 129: 1673-82
437. Barnig C, Cernadas M, Dutile S, Liu X, Perrella MA, Kazani S, Wechsler ME, Israel E, Levy BD. 2013. Lipoxin A4 regulates natural killer cell and type 2 innate lymphoid cell activation in asthma. *Sci Transl Med* 5: 174ra26
438. Awad A, Yassine H, Barrier M, Vorng H, Marquillies P, Tsicopoulos A, Duez C. 2014. Natural killer cells induce eosinophil activation and apoptosis. *PLoS One* 9: e94492
439. D'Alessio FR, Tsushima K, Aggarwal NR, West EE, Willett MH, Britos MF, Pipeling MR, Brower RG, Tuder RM, McDyer JF, King LS. 2009. CD4+CD25+Foxp3+ Tregs resolve experimental lung injury in mice and are present in humans with acute lung injury. *J Clin Invest* 119: 2898-913
440. Szondy Z, Sarang Z, Kiss B, Garabuczi E, Koroskenyi K. 2017. Anti-inflammatory Mechanisms Triggered by Apoptotic Cells during Their Clearance. *Front Immunol* 8: 909
441. Allard B, Panariti A, Martin JG. 2018. Alveolar Macrophages in the Resolution of Inflammation, Tissue Repair, and Tolerance to Infection. *Front Immunol* 9: 1777
442. Krishnamoorthy N, Burkett PR, Dalli J, Abdulnour RE, Colas R, Ramon S, Phipps RP, Petasis NA, Kuchroo VK, Serhan CN, Levy BD. 2015. Cutting edge: maresin-1 engages regulatory T cells to limit type 2 innate lymphoid cell activation and promote resolution of lung inflammation. *J Immunol* 194: 863-7
443. Levy BD, Serhan CN. 2014. Resolution of acute inflammation in the lung. *Annu Rev Physiol* 76: 467-92
444. Serhan CN, Chiang N, Van Dyke TE. 2008. Resolving inflammation: dual anti-inflammatory and pro-resolution lipid mediators. *Nat Rev Immunol* 8: 349-61
445. Kazani S, Planaguma A, Ono E, Bonini M, Zahid M, Marigowda G, Wechsler ME, Levy BD, Israel E. 2013. Exhaled breath condensate eicosanoid levels associate with asthma and its severity. *J Allergy Clin Immunol* 132: 547-53
446. Levy BD, Bonnans C, Silverman ES, Palmer LJ, Marigowda G, Israel E, Severe Asthma Research Program NHL, Blood I. 2005. Diminished lipoxin biosynthesis in severe asthma. *Am J Respir Crit Care Med* 172: 824-30
447. Planaguma A, Pfeffer MA, Rubin G, Croze R, Uddin M, Serhan CN, Levy BD. 2010. Lovastatin decreases acute mucosal inflammation via 15-epi-lipoxin A4. *Mucosal Immunol* 3: 270-9
448. Duncan CJ, Lawrie A, Blaylock MG, Douglas JG, Walsh GM. 2003. Reduced eosinophil apoptosis in induced sputum correlates with asthma severity. *Eur Respir J* 22: 484-90
449. Lamb JP, James A, Carroll N, Siena L, Elliot J, Vignola AM. 2005. Reduced apoptosis of memory T-cells in the inner airway wall of mild and severe asthma. *Eur Respir J* 26: 265-70
450. Fitzpatrick AM, Holguin F, Teague WG, Brown LA. 2008. Alveolar macrophage phagocytosis is impaired in children with poorly controlled asthma. *J Allergy Clin Immunol* 121: 1372-8, 8 e1-3

451. Simpson JL, Gibson PG, Yang IA, Upham J, James A, Reynolds PN, Hodge S, Group ASR. 2013. Impaired macrophage phagocytosis in non-eosinophilic asthma. *Clin Exp Allergy* 43: 29-35
452. Huynh ML, Malcolm KC, Kotaru C, Tilstra JA, Westcott JY, Fadok VA, Wenzel SE. 2005. Defective apoptotic cell phagocytosis attenuates prostaglandin E2 and 15-hydroxyeicosatetraenoic acid in severe asthma alveolar macrophages. *Am J Respir Crit Care Med* 172: 972-9
453. Modena BD, Bleecker ER, Busse WW, Erzurum SC, Gaston BM, Jarjour NN, Meyers DA, Milosevic J, Tedrow JR, Wu W, Kaminski N, Wenzel SE. 2017. Gene Expression Correlated with Severe Asthma Characteristics Reveals Heterogeneous Mechanisms of Severe Disease. *Am J Respir Crit Care Med* 195: 1449-63
454. Mousli M, Hugli TE, Landry Y, Bronner C. 1992. A mechanism of action for anaphylatoxin C3a stimulation of mast cells. *J Immunol* 148: 2456-61
455. Takafuji S, Tadokoro K, Ito K, Dahinden CA. 1994. Degranulation from human eosinophils stimulated with C3a and C5a. *Int Arch Allergy Immunol* 104 Suppl 1: 27-9
456. Krug N, Tschernig T, Erpenbeck VJ, Hohlfeld JM, Kohl J. 2001. Complement factors C3a and C5a are increased in bronchoalveolar lavage fluid after segmental allergen provocation in subjects with asthma. *Am J Respir Crit Care Med* 164: 1841-3
457. Nakano Y, Morita S, Kawamoto A, Suda T, Chida K, Nakamura H. 2003. Elevated complement C3a in plasma from patients with severe acute asthma. *J Allergy Clin Immunol* 112: 525-30
458. Abdel Fattah M, El Baz M, Sherif A, Adel A. 2010. Complement components (C3, C4) as inflammatory markers in asthma. *Indian J Pediatr* 77: 771-3
459. Onyemelukwe GC. 1989. Complement components in Nigerians with bronchial asthma. *Ann Allergy* 63: 309-12
460. Humbles AA, Lu B, Nilsson CA, Lilly C, Israel E, Fujiwara Y, Gerard NP, Gerard C. 2000. A role for the C3a anaphylatoxin receptor in the effector phase of asthma. *Nature* 406: 998-1001
461. Lee SH, Rhim T, Choi YS, Min JW, Kim SH, Cho SY, Paik YK, Park CS. 2006. Complement C3a and C4a increased in plasma of patients with aspirin-induced asthma. *Am J Respir Crit Care Med* 173: 370-8
462. Park JW, Taube C, Joetham A, Takeda K, Kodama T, Dakhama A, McConville G, Allen CB, Sfyroera G, Shultz LD, Lambris JD, Giclas PC, Holers VM, Gelfand EW. 2004. Complement activation is critical to airway hyperresponsiveness after acute ozone exposure. *Am J Respir Crit Care Med* 169: 726-32
463. Polack FP, Teng MN, Collins PL, Prince GA, Exner M, Regele H, Lirman DD, Rabold R, Hoffman SJ, Karp CL, Kleeberger SR, Wills-Karp M, Karron RA. 2002. A role for immune complexes in enhanced respiratory syncytial virus disease. *J Exp Med* 196: 859-65
464. Shima M, Adachi M. 1996. Effects of environmental tobacco smoke on serum levels of acute phase proteins in schoolchildren. *Prev Med* 25: 617-24
465. Uguz A, Berber Z, Coskun M, Halide Akbas S, Yegin O. 2005. Mannose-binding lectin levels in children with asthma. *Pediatr Allergy Immunol* 16: 231-5
466. Kaur S, Gupta VK, Shah A, Thiel S, Sarma PU, Madan T. 2006. Elevated levels of mannan-binding lectin [corrected] (MBL) and eosinophilia in patients of bronchial asthma with allergic rhinitis and allergic bronchopulmonary aspergillosis associate with a novel intronic polymorphism in MBL. *Clin Exp Immunol* 143: 414-9

467. Staley KG, Stover C, Strippoli MP, Spycher BD, Silverman M, Kuehni CE. 2007. Mannan-binding lectin in young children with asthma differs by level of severity. *J Allergy Clin Immunol* 119: 503-5
468. Aittoniemi J, Soranummi H, Rovio AT, Hurme M, Pessi T, Nieminen M, Karjalainen J. 2005. Mannose-binding lectin 2 (MBL2) gene polymorphism in asthma and atopy among adults. *Clin Exp Immunol* 142: 120-4
469. Takeda K, Thurman JM, Tomlinson S, Okamoto M, Shiraishi Y, Ferreira VP, Cortes C, Pangburn MK, Holers VM, Gelfand EW. 2012. The critical role of complement alternative pathway regulator factor H in allergen-induced airway hyperresponsiveness and inflammation. *J Immunol* 188: 661-7
470. Taube C, Thurman JM, Takeda K, Joetham A, Miyahara N, Carroll MC, Dakhama A, Giclas PC, Holers VM, Gelfand EW. 2006. Factor B of the alternative complement pathway regulates development of airway hyperresponsiveness and inflammation. *Proc Natl Acad Sci U S A* 103: 8084-9
471. Mascarell L, Airouche S, Berjont N, Gary C, Gueguen C, Fourcade G, Bellier B, Togbe D, Ryffel B, Klatzmann D, Baron-Bodo V, Moingeon P. 2017. The regulatory dendritic cell marker C1q is a potent inhibitor of allergic inflammation. *Mucosal Immunol* 10: 695-704
472. Wills-Karp M. 2007. Complement activation pathways: a bridge between innate and adaptive immune responses in asthma. *Proc Am Thorac Soc* 4: 247-51
473. Maruo K, Akaike T, Ono T, Okamoto T, Maeda H. 1997. Generation of anaphylatoxins through proteolytic processing of C3 and C5 by house dust mite protease. *J Allergy Clin Immunol* 100: 253-60
474. Khirwadkar K, Zilow G, Oppermann M, Kabelitz D, Rother K. 1993. Interleukin-4 augments production of the third complement component by the alveolar epithelial cell line A549. *Int Arch Allergy Immunol* 100: 35-41
475. Wang Y, Miwa T, Ducka-Kokalari B, Redai IG, Sato S, Gullipalli D, Zangrilli JG, Haczku A, Song WC. 2015. Properdin Contributes to Allergic Airway Inflammation through Local C3a Generation. *J Immunol* 195: 1171-81
476. Drouin SM, Sinha M, Sfyroera G, Lambris JD, Wetsel RA. 2006. A protective role for the fifth complement component (c5) in allergic airway disease. *Am J Respir Crit Care Med* 173: 852-7
477. McKinley L, Kim J, Bolgos GL, Siddiqui J, Remick DG. 2006. Allergens induce enhanced bronchoconstriction and leukotriene production in C5 deficient mice. *Respir Res* 7: 129
478. Zhang X, Lewkowich IP, Kohl G, Clark JR, Wills-Karp M, Kohl J. 2009. A protective role for C5a in the development of allergic asthma associated with altered levels of B7-H1 and B7-DC on plasmacytoid dendritic cells. *J Immunol* 182: 5123-30
479. Schmudde I, Ströver HA, Vollbrandt T, König P, Karsten CM, Laumonnier Y, Köhl J. 2012. C5a receptor signalling in dendritic cells controls the development of maladaptive Th2 and Th17 immunity in experimental allergic asthma. *Mucosal Immunology* 6: 807-25
480. Engelke C, Wiese AV, Schmudde I, Ender F, Strover HA, Vollbrandt T, Konig P, Laumonnier Y, Kohl J. 2014. Distinct roles of the anaphylatoxins C3a and C5a in dendritic cell-mediated allergic asthma. *J Immunol* 193: 5387-401
481. Schmudde I, Strover HA, Vollbrandt T, Konig P, Karsten CM, Laumonnier Y, Kohl J. 2013. C5a receptor signalling in dendritic cells controls the development of maladaptive Th2 and Th17 immunity in experimental allergic asthma. *Mucosal Immunol* 6: 807-25
482. Helft J, Bottcher J, Chakravarty P, Zelenay S, Huotari J, Schraml BU, Goubau D, Reis e Sousa C. 2015. GM-CSF Mouse Bone Marrow Cultures Comprise a Heterogeneous

Population of CD11c(+)MHCII(+) Macrophages and Dendritic Cells. *Immunity* 42: 1197-211

483. Drouin SM, Corry DB, Kildsgaard J, Wetsel RA. 2001. Cutting edge: the absence of C3 demonstrates a role for complement in Th2 effector functions in a murine model of pulmonary allergy. *Journal of immunology (Baltimore, Md. : 1950)* 167: 4141-5
484. Bautsch W, Hoymann HG, Zhang Q, Meier-Wiedenbach I, Raschke U, Ames RS, Sohns B, Flemme N, Meyer zu Vilsendorf A, Grove M, Klos A, Kohl J. 2000. Cutting edge: guinea pigs with a natural C3a-receptor defect exhibit decreased bronchoconstriction in allergic airway disease: evidence for an involvement of the C3a anaphylatoxin in the pathogenesis of asthma. *J Immunol* 165: 5401-5
485. Drouin SM, Corry DB, Hollman TJ, Kildsgaard J, Wetsel RA. 2002. Absence of the complement anaphylatoxin C3a receptor suppresses Th2 effector functions in a murine model of pulmonary allergy. *J Immunol* 169: 5926-33
486. Li K, Anderson KJ, Peng Q, Noble A, Lu B, Kelly AP, Wang N, Sacks SH, Zhou W. 2008. Cyclic AMP plays a critical role in C3a-receptor-mediated regulation of dendritic cells in antigen uptake and T-cell stimulation. *Blood* 112: 5084-94
487. Kawamoto S, Yalcindag A, Laouini D, Brodeur S, Bryce P, Lu B, Humbles AA, Oettgen H, Gerard C, Geha RS. 2004. The anaphylatoxin C3a downregulates the Th2 response to epicutaneously introduced antigen. *J Clin Invest* 114: 399-407
488. Gerard NP, Lu B, Liu P, Craig S, Fujiwara Y, Okinaga S, Gerard C. 2005. An anti-inflammatory function for the complement anaphylatoxin C5a-binding protein, C5L2. *J Biol Chem* 280: 39677-80
489. Jiang Z, Zhu L. 2016. Update on the role of alternatively activated macrophages in asthma. *J Asthma Allergy* 9: 101-7
490. Kurowska-Stolarska M, Stolarski B, Kewin P, Murphy G, Corrigan CJ, Ying S, Pitman N, Mirchandani A, Rana B, van Rooijen N, Shepherd M, McSharry C, McInnes IB, Xu D, Liew FY. 2009. IL-33 amplifies the polarization of alternatively activated macrophages that contribute to airway inflammation. *J Immunol* 183: 6469-77
491. Draijer C, Boorsma CE, Robbe P, Timens W, Hylkema MN, Ten Hacken NH, van den Berge M, Postma DS, Melgert BN. 2017. Human asthma is characterized by more IRF5+ M1 and CD206+ M2 macrophages and less IL-10+ M2-like macrophages around airways compared with healthy airways. *J Allergy Clin Immunol* 140: 280-3 e3
492. Draijer C, Robbe P, Boorsma CE, Hylkema MN, Melgert BN. 2013. Characterization of macrophage phenotypes in three murine models of house-dust-mite-induced asthma. *Mediators Inflamm* 2013: 632049
493. Draijer C, Peters-Golden M. 2017. Alveolar Macrophages in Allergic Asthma: the Forgotten Cell Awakes. *Curr Allergy Asthma Rep* 17: 12
494. Richgels PK, Yamani A, Chougnet CA, Lewkowich IP. 2017. Maternal house dust mite exposure during pregnancy enhances severity of house dust mite-induced asthma in murine offspring. *J Allergy Clin Immunol* 140: 1404-15 e9
495. Kondo Y, Yoshimoto T, Yasuda K, Futatsugi-Yumikura S, Morimoto M, Hayashi N, Hoshino T, Fujimoto J, Nakanishi K. 2008. Administration of IL-33 induces airway hyperresponsiveness and goblet cell hyperplasia in the lungs in the absence of adaptive immune system. *Int Immunol* 20: 791-800
496. Berend N, Salome CM, King GG. 2008. Mechanisms of airway hyperresponsiveness in asthma. *Respirology* 13: 624-31
497. Sterk PJ, Bel EH. 1989. Bronchial hyperresponsiveness: the need for a distinction between hypersensitivity and excessive airway narrowing. *Eur Respir J* 2: 267-74

498. Karsten CM, Laumonnier Y, Kohl J. 2014. Functional analysis of C5a effector responses in vitro and in vivo. *Methods Mol Biol* 1100: 291-304
499. Weischenfeldt J, Porse B. 2008. Bone Marrow-Derived Macrophages (BMM): Isolation and Applications. *CSH Protoc* 2008: pdb prot5080
500. Chao TH, Ember JA, Wang M, Bayon Y, Hugli TE, Ye RD. 1999. Role of the second extracellular loop of human C3a receptor in agonist binding and receptor function. *J Biol Chem* 274: 9721-8
501. de Felipe P, Luke GA, Hughes LE, Gani D, Halpin C, Ryan MD. 2006. E unum pluribus: multiple proteins from a self-processing polyprotein. *Trends Biotechnol* 24: 68-75
502. Kim JH, Lee SR, Li LH, Park HJ, Park JH, Lee KY, Kim MK, Shin BA, Choi SY. 2011. High cleavage efficiency of a 2A peptide derived from porcine teschovirus-1 in human cell lines, zebrafish and mice. *PLoS One* 6: e18556
503. Liu Z, Chen O, Wall JBJ, Zheng M, Zhou Y, Wang L, Ruth Vaseghi H, Qian L, Liu J. 2017. Systematic comparison of 2A peptides for cloning multi-genes in a polycistronic vector. *Sci Rep* 7: 2193
504. Kuzmich AI, Vvedenskii AV, Kopantsev EP, Vinogradova TV. 2013. [Quantitative comparison of expression for genes linked in bicistronic vectors via ires or 2A-peptide of porcine teschovirus-1 sequence]. *Bioorg Khim* 39: 454-65
505. Misharin AV, Morales-Nebreda L, Mutlu GM, Budinger GR, Perlman H. 2013. Flow cytometric analysis of macrophages and dendritic cell subsets in the mouse lung. *Am J Respir Cell Mol Biol* 49: 503-10
506. Kiafard Z, Tschernig T, Schweyer S, Bley A, Neumann D, Zwirner J. 2007. Use of monoclonal antibodies to assess expression of anaphylatoxin receptors in tubular epithelial cells of human, murine and rat kidneys. *Immunobiology* 212: 129-39
507. Chairakaki AD, Saridaki MI, Pyrillou K, Mouratis MA, Koltsida O, Walton RP, Bartlett NW, Stavropoulos A, Boon L, Rovina N, Papadopoulos NG, Johnston SL, Andreakos E. 2018. Plasmacytoid dendritic cells drive acute asthma exacerbations. *J Allergy Clin Immunol* 142: 542-56 e12
508. Kwan WH, van der Touw W, Paz-Artal E, Li MO, Heeger PS. 2013. Signaling through C5a receptor and C3a receptor diminishes function of murine natural regulatory T cells. *J Exp Med* 210: 257-68
509. Strainic MG, Liu J, Huang D, An F, Lalli PN, Muqim N, Shapiro VS, Dubyak GR, Heeger PS, Medof ME. 2008. Locally produced complement fragments C5a and C3a provide both costimulatory and survival signals to naive CD4+ T cells. *Immunity* 28: 425-35
510. Walker JA, Barlow JL, McKenzie AN. 2013. Innate lymphoid cells--how did we miss them? *Nat Rev Immunol* 13: 75-87
511. Walker JA, McKenzie AN. 2013. Development and function of group 2 innate lymphoid cells. *Curr Opin Immunol* 25: 148-55
512. Wang J, Li F, Zheng M, Sun R, Wei H, Tian Z. 2012. Lung natural killer cells in mice: phenotype and response to respiratory infection. *Immunology* 137: 37-47
513. Ritter SL, Hall RA. 2009. Fine-tuning of GPCR activity by receptor-interacting proteins. *Nature reviews. Molecular cell biology* 10: 819-30
514. Petering H, Kohl J, Weyergraf A, Dulkys Y, Kimmig D, Smolarski R, Kapp A, Elsner J. 2000. Characterization of synthetic C3a analog peptides on human eosinophils in comparison to the native complement component C3a. *J Immunol* 164: 3783-9
515. Karsten CM, Pandey MK, Figge J, Kilchenstein R, Taylor PR, Rosas M, McDonald JU, Orr SJ, Berger M, Petzold D, Blanchard V, Winkler A, Hess C, Reid DM, Majoul IV, Strait RT, Harris NL, Köhl G, Wex E, Ludwig R, Zillikens D, Nimmerjahn F, Finkelman FD, Brown

GD, Ehlers M, Köhl J. 2012. Anti-inflammatory activity of IgG1 mediated by Fc galactosylation and association of FcγRIIB and dectin-1. *Nature medicine* 18: 1401-6

516. Coulthard LG, Woodruff TM. 2015. Is the complement activation product C3a a proinflammatory molecule? Re-evaluating the evidence and the myth. *J Immunol* 194: 3542-8
517. Tschernig T, Kiafard Z, Dibbert C, Neumann D, Zwirner J. 2007. Use of monoclonal antibodies to assess expression of anaphylatoxin receptors in rat and murine models of lung inflammation. *Exp Toxicol Pathol* 58: 419-25
518. Ender F, Wiese AV, Schmudde I, Sun J, Vollbrandt T, Konig P, Laumonnier Y, Kohl J. 2017. Differential regulation of C5a receptor 1 in innate immune cells during the allergic asthma effector phase. *PLoS One* 12: e0172446
519. Fujimori T, Grabiec AM, Kaur M, Bell TJ, Fujino N, Cook PC, Svedberg FR, MacDonald AS, Maciewicz RA, Singh D, Hussell T. 2015. The Axl receptor tyrosine kinase is a discriminator of macrophage function in the inflamed lung. *Mucosal Immunol* 8: 1021-30
520. Jakubzick C, Gautier EL, Gibbings SL, Sojka DK, Schlitzer A, Johnson TE, Ivanov S, Duan Q, Bala S, Condon T, van Rooijen N, Grainger JR, Belkaid Y, Ma'ayan A, Riches DW, Yokoyama WM, Ginhoux F, Henson PM, Randolph GJ. 2013. Minimal differentiation of classical monocytes as they survey steady-state tissues and transport antigen to lymph nodes. *Immunity* 39: 599-610
521. Saenz SA, Taylor BC, Artis D. 2008. Welcome to the neighborhood: epithelial cell-derived cytokines license innate and adaptive immune responses at mucosal sites. *Immunol Rev* 226: 172-90
522. Oyoshi MK, Larson RP, Ziegler SF, Geha RS. 2010. Mechanical injury polarizes skin dendritic cells to elicit a T(H)2 response by inducing cutaneous thymic stromal lymphopoietin expression. *J Allergy Clin Immunol* 126: 976-84, 84 e1-5
523. Oboki K, Nakae S, Matsumoto K, Saito H. 2011. IL-33 and Airway Inflammation. *Allergy Asthma Immunol Res* 3: 81-8
524. Willart MA, Deswarte K, Pouliot P, Braun H, Beyaert R, Lambrecht BN, Hammad H. 2012. Interleukin-1alpha controls allergic sensitization to inhaled house dust mite via the epithelial release of GM-CSF and IL-33. *J Exp Med* 209: 1505-17
525. Tominaga S. 1989. A putative protein of a growth specific cDNA from BALB/c-3T3 cells is highly similar to the extracellular portion of mouse interleukin 1 receptor. *FEBS Lett* 258: 301-4
526. Werenskiold AK, Hoffmann S, Klemenz R. 1989. Induction of a mitogen-responsive gene after expression of the Ha-ras oncogene in NIH 3T3 fibroblasts. *Mol Cell Biol* 9: 5207-14
527. Schmitz J, Owyang A, Oldham E, Song Y, Murphy E, McClanahan TK, Zurawski G, Moshrefi M, Qin J, Li X, Gorman DM, Bazan JF, Kastelein RA. 2005. IL-33, an interleukin-1-like cytokine that signals via the IL-1 receptor-related protein ST2 and induces T helper type 2-associated cytokines. *Immunity* 23: 479-90
528. Iwahana H, Yanagisawa K, Ito-Kosaka A, Kuroiwa K, Tago K, Komatsu N, Katashima R, Itakura M, Tominaga S. 1999. Different promoter usage and multiple transcription initiation sites of the interleukin-1 receptor-related human ST2 gene in UT-7 and TM12 cells. *Eur J Biochem* 264: 397-406
529. Kamijo S, Takeda H, Tokura T, Suzuki M, Inui K, Hara M, Matsuda H, Matsuda A, Oboki K, Ohno T, Saito H, Nakae S, Sudo K, Suto H, Ichikawa S, Ogawa H, Okumura K, Takai T. 2013. IL-33-mediated innate response and adaptive immune cells contribute to

maximum responses of protease allergen-induced allergic airway inflammation. *J Immunol* 190: 4489-99
530. McCormick SM, Heller NM. 2015. Commentary: IL-4 and IL-13 receptors and signaling. *Cytokine* 75: 38-50
531. Junttila IS. 2018. Tuning the Cytokine Responses: An Update on Interleukin (IL)-4 and IL-13 Receptor Complexes. *Front Immunol* 9: 888
532. Serbina NV, Jia T, Hohl TM, Pamer EG. 2008. Monocyte-mediated defense against microbial pathogens. *Annu Rev Immunol* 26: 421-52
533. Geissmann F, Jung S, Littman DR. 2003. Blood monocytes consist of two principal subsets with distinct migratory properties. *Immunity* 19: 71-82
534. Palframan RT, Jung S, Cheng G, Weninger W, Luo Y, Dorf M, Littman DR, Rollins BJ, Zweerink H, Rot A, von Andrian UH. 2001. Inflammatory chemokine transport and presentation in HEV: a remote control mechanism for monocyte recruitment to lymph nodes in inflamed tissues. *J Exp Med* 194: 1361-73
535. Shi C, Pamer EG. 2011. Monocyte recruitment during infection and inflammation. *Nat Rev Immunol* 11: 762-74
536. Auffray C, Fogg D, Garfa M, Elain G, Join-Lambert O, Kayal S, Sarnacki S, Cumano A, Lauvau G, Geissmann F. 2007. Monitoring of blood vessels and tissues by a population of monocytes with patrolling behavior. *Science* 317: 666-70
537. Nahrendorf M, Swirski FK, Aikawa E, Stangenberg L, Wurdinger T, Figueiredo JL, Libby P, Weissleder R, Pittet MJ. 2007. The healing myocardium sequentially mobilizes two monocyte subsets with divergent and complementary functions. *J Exp Med* 204: 3037-47
538. Tsou CL, Peters W, Si Y, Slaymaker S, Aslanian AM, Weisberg SP, Mack M, Charo IF. 2007. Critical roles for CCR2 and MCP-3 in monocyte mobilization from bone marrow and recruitment to inflammatory sites. *J Clin Invest* 117: 902-9
539. Doherty TA, Khorram N, Lund S, Mehta AK, Croft M, Broide DH. 2013. Lung type 2 innate lymphoid cells express cysteinyl leukotriene receptor 1, which regulates TH2 cytokine production. *J Allergy Clin Immunol* 132: 205-13
540. McNally AK, Anderson JM. 2011. Macrophage fusion and multinucleated giant cells of inflammation. *Adv Exp Med Biol* 713: 97-111
541. Milde R, Ritter J, Tennent GA, Loesch A, Martinez FO, Gordon S, Pepys MB, Verschoor A, Helming L. 2015. Multinucleated Giant Cells Are Specialized for Complement-Mediated Phagocytosis and Large Target Destruction. *Cell Rep* 13: 1937-48
542. Tornetta MA, Foley JJ, Sarau HM, Ames RS. 1997. The mouse anaphylatoxin C3a receptor: molecular cloning, genomic organization, and functional expression. *J Immunol* 158: 5277-82
543. Hsu MH, Ember JA, Wang M, Prossnitz ER, Hugli TE, Ye RD. 1997. Cloning and functional characterization of the mouse C3a anaphylatoxin receptor gene. *Immunogenetics* 47: 64-72
544. H.J. H, ed. 2012. *The Laboratory Mouse*: Elsevier Ltd. All
545. J.G. F, S.W. B, M.T. D, C.E. N, F.W. Q, A.L. S, eds. 2007. *The Mouse in Biomedical Research*: Elsevier, Inc.
546. Gerardy-Schahn R, Ambrosius D, Saunders D, Casaretto M, Mittler C, Karwarth G, Gorgen S, Bitter-Suermann D. 1989. Characterization of C3a receptor-proteins on guinea pig platelets and human polymorphonuclear leukocytes. *Eur J Immunol* 19: 1095-102

547. Zwirner J, Gotze O, Begemann G, Kapp A, Kirchhoff K, Werfel T. 1999. Evaluation of C3a receptor expression on human leucocytes by the use of novel monoclonal antibodies. *Immunology* 97: 166-72
548. Wu MC, Brennan FH, Lynch JP, Mantovani S, Phipps S, Wetsel RA, Ruitenberg MJ, Taylor SM, Woodruff TM. 2013. The receptor for complement component C3a mediates protection from intestinal ischemia-reperfusion injuries by inhibiting neutrophil mobilization. *Proc Natl Acad Sci U S A* 110: 9439-44
549. Daley JM, Thomay AA, Connolly MD, Reichner JS, Albina JE. 2008. Use of Ly6G-specific monoclonal antibody to deplete neutrophils in mice. *J Leukoc Biol* 83: 64-70
550. Cravedi P, Leventhal J, Lakhani P, Ward SC, Donovan MJ, Heeger PS. 2013. Immune cell-derived C3a and C5a costimulate human T cell alloimmunity. *Am J Transplant* 13: 2530-9
551. Melendi GA, Hoffman SJ, Karron RA, Irusta PM, Laham FR, Humbles A, Schofield B, Pan CH, Rabold R, Thumar B, Thumar A, Gerard NP, Mitzner W, Barnum SR, Gerard C, Kleeberger SR, Polack FP. 2007. C5 modulates airway hyperreactivity and pulmonary eosinophilia during enhanced respiratory syncytial virus disease by decreasing C3a receptor expression. *J Virol* 81: 991-9
552. Thangam EB, Venkatesha RT, Zaidi AK, Jordan-Sciutto KL, Goncharov DA, Krymskaya VP, Amrani Y, Panettieri RA, Jr., Ali H. 2005. Airway smooth muscle cells enhance C3a-induced mast cell degranulation following cell-cell contact. *FASEB J* 19: 798-800
553. Dillard P, Wetsel RA, Drouin SM. 2007. Complement C3a regulates Muc5ac expression by airway Clara cells independently of Th2 responses. *Am J Respir Crit Care Med* 175: 1250-8
554. Daffern PJ, Pfeifer PH, Ember JA, Hugli TE. 1995. C3a is a chemotaxin for human eosinophils but not for neutrophils. I. C3a stimulation of neutrophils is secondary to eosinophil activation. *J Exp Med* 181: 2119-27
555. DiScipio RG, Daffern PJ, Jagels MA, Broide DH, Sriramarao P. 1999. A comparison of C3a and C5a-mediated stable adhesion of rolling eosinophils in postcapillary venules and transendothelial migration in vitro and in vivo. *J Immunol* 162: 1127-36
556. Li K, Fazekasova H, Wang N, Peng Q, Sacks SH, Lombardi G, Zhou W. 2012. Functional modulation of human monocytes derived DCs by anaphylatoxins C3a and C5a. *Immunobiology* 217: 65-73
557. Li K, Fazekasova H, Wang N, Sagoo P, Peng Q, Khamri W, Gomes C, Sacks SH, Lombardi G, Zhou W. 2011. Expression of complement components, receptors and regulators by human dendritic cells. *Mol Immunol* 48: 1121-7
558. Gutzmer R, Lisewski M, Zwirner J, Mommert S, Diesel C, Wittmann M, Kapp A, Werfel T. 2004. Human monocyte-derived dendritic cells are chemoattracted to C3a after up-regulation of the C3a receptor with interferons. *Immunology* 111: 435-43
559. Kolev M, Kemper C. 2017. Keeping It All Going-Complement Meets Metabolism. *Front Immunol* 8: 1
560. Kobayashi T, Iijima K, Checkel JL, Kita H. 2013. IL-1 family cytokines drive Th2 and Th17 cells to innocuous airborne antigens. *Am J Respir Cell Mol Biol* 49: 989-98
561. Esnault S, Kelly EA, Nettenstrom LM, Cook EB, Seroogy CM, Jarjour NN. 2012. Human eosinophils release IL-1ss and increase expression of IL-17A in activated CD4+ T lymphocytes. *Clin Exp Allergy* 42: 1756-64
562. Krupnick JG, Benovic JL. 1998. The role of receptor kinases and arrestins in G protein-coupled receptor regulation. *Annu Rev Pharmacol Toxicol* 38: 289-319

563. Pitcher JA, Freedman NJ, Lefkowitz RJ. 1998. G protein-coupled receptor kinases. *Annu Rev Biochem* 67: 653-92
564. Krutzik PO, Hale MB, Nolan GP. 2005. Characterization of the murine immunological signaling network with phosphospecific flow cytometry. *J Immunol* 175: 2366-73
565. Krutzik PO, Clutter MR, Nolan GP. 2005. Coordinate analysis of murine immune cell surface markers and intracellular phosphoproteins by flow cytometry. *J Immunol* 175: 2357-65
566. Grammer AC, Fischer R, Lee O, Zhang X, Lipsky PE. 2004. Flow cytometric assessment of the signaling status of human B lymphocytes from normal and autoimmune individuals. *Arthritis Res Ther* 6: 28-38
567. Forment JV, Jackson SP. 2015. A flow cytometry-based method to simplify the analysis and quantification of protein association to chromatin in mammalian cells. *Nat Protoc* 10: 1297-307
568. Coppin E, Malergue F, Thibult ML, Scifo C, Favre C, Nunes JA. 2017. Flow cytometric analysis of intracellular phosphoproteins in human monocytes. *Cytometry B Clin Cytom* 92: 207-10
569. Woodruff PG. 2008. Gene expression in asthmatic airway smooth muscle. *Proc Am Thorac Soc* 5: 113-8
570. Gour N, Wills-Karp M. 2015. IL-4 and IL-13 signaling in allergic airway disease. *Cytokine* 75: 68-78
571. Tamaoki J, Sakai N, Kanemura T, Yamawaki I, Takizawa T. 1991. IgE-dependent activation of alveolar macrophages augments neurally mediated contraction of small airways. *Br J Pharmacol* 103: 1458-62
572. Rankin JA, Hitchcock M, Merrill W, Bach MK, Brashler JR, Askenase PW. 1982. IgE-dependent release of leukotriene C4 from alveolar macrophages. *Nature* 297: 329-31
573. Liravi B, Piedrafita D, Nguyen G, Bischof RJ. 2015. Dynamics of IL-4 and IL-13 expression in the airways of sheep following allergen challenge. *BMC Pulm Med* 15: 101
574. Kang CM, Jang AS, Ahn MH, Shin JA, Kim JH, Choi YS, Rhim TY, Park CS. 2005. Interleukin-25 and interleukin-13 production by alveolar macrophages in response to particles. *Am J Respir Cell Mol Biol* 33: 290-6
575. Hancock A, Armstrong L, Gama R, Millar A. 1998. Production of interleukin 13 by alveolar macrophages from normal and fibrotic lung. *Am J Respir Cell Mol Biol* 18: 60-5
576. Byers DE, Holtzman MJ. 2011. Alternatively activated macrophages and airway disease. *Chest* 140: 768-74
577. Byers DE, Holtzman MJ. 2010. Alternatively activated macrophages as cause or effect in airway disease. *Am J Respir Cell Mol Biol* 43: 1-4
578. Careau E, Turmel V, Lauzon-Joset JF, Bissonnette EY. 2010. Alveolar macrophages reduce airway hyperresponsiveness and modulate cytokine levels. *Exp Lung Res* 36: 255-61
579. Kim JY, Sohn JH, Choi JM, Lee JH, Hong CS, Lee JS, Park JW. 2012. Alveolar macrophages play a key role in cockroach-induced allergic inflammation via TNF-alpha pathway. *PLoS One* 7: e47971
580. Lee AM, Fryer AD, van Rooijen N, Jacoby DB. 2004. Role of macrophages in virus-induced airway hyperresponsiveness and neuronal M2 muscarinic receptor dysfunction. *Am J Physiol Lung Cell Mol Physiol* 286: L1255-9

581. Wiese AV, Ender F, Quell KM, Antoniou K, Vollbrandt T, Konig P, Kohl J, Laumonnier Y. 2017. The C5a/C5aR1 axis controls the development of experimental allergic asthma independent of LysM-expressing pulmonary immune cells. *PLoS One* 12: e0184956
582. Durrant WE, Dong X. 2004. Systemic acquired resistance. *Annu Rev Phytopathol* 42: 185-209
583. Cheng SC, Quintin J, Cramer RA, Shepardson KM, Saeed S, Kumar V, Giamarellos-Bourboulis EJ, Martens JH, Rao NA, Aghajanirefah A, Manjeri GR, Li Y, Ifrim DC, Arts RJ, van der Veer BM, Deen PM, Logie C, O'Neill LA, Willems P, van de Veerdonk FL, van der Meer JW, Ng A, Joosten LA, Wijmenga C, Stunnenberg HG, Xavier RJ, Netea MG. 2014. mTOR- and HIF-1alpha-mediated aerobic glycolysis as metabolic basis for trained immunity. *Science* 345: 1250684
584. Netea MG, Joosten LA, Latz E, Mills KH, Natoli G, Stunnenberg HG, O'Neill LA, Xavier RJ. 2016. Trained immunity: A program of innate immune memory in health and disease. *Science* 352: aaf1098
585. Mitroulis I, Ruppova K, Wang B, Chen LS, Grzybek M, Grinenko T, Eugster A, Troullinaki M, Palladini A, Kourtzelis I, Chatzigeorgiou A, Schlitzer A, Beyer M, Joosten LAB, Isermann B, Lesche M, Petzold A, Simons K, Henry I, Dahl A, Schultze JL, Wielockx B, Zamboni N, Mirtschink P, Coskun U, Hajishengallis G, Netea MG, Chavakis T. 2018. Modulation of Myelopoiesis Progenitors Is an Integral Component of Trained Immunity. *Cell* 172: 147-61 e12
586. Gourbal B, Pinaud S, Beckers GJM, Van Der Meer JWM, Conrath U, Netea MG. 2018. Innate immune memory: An evolutionary perspective. *Immunol Rev* 283: 21-40
587. Italiani P, Boraschi D. 2015. New Insights Into Tissue Macrophages: From Their Origin to the Development of Memory. *Immune Netw* 15: 167-76
588. Kaufmann E, Sanz J, Dunn JL, Khan N, Mendonca LE, Pacis A, Tzelepis F, Pernet E, Dumaine A, Grenier JC, Mailhot-Leonard F, Ahmed E, Belle J, Besla R, Mazer B, King IL, Nijnik A, Robbins CS, Barreiro LB, Divangahi M. 2018. BCG Educates Hematopoietic Stem Cells to Generate Protective Innate Immunity against Tuberculosis. *Cell* 172: 176-90 e19
589. Yao Y, Jeyanathan M, Haddadi S, Barra NG, Vaseghi-Shanjani M, Damjanovic D, Lai R, Afkhami S, Chen Y, Dvorkin-Gheva A, Robbins CS, Schertzer JD, Xing Z. 2018. Induction of Autonomous Memory Alveolar Macrophages Requires T Cell Help and Is Critical to Trained Immunity. *Cell* 175: 1634-50 e17
590. Davison AG, Haslam PL, Corrin B, Coutts, II, Dewar A, Riding WD, Studdy PR, Newman-Taylor AJ. 1983. Interstitial lung disease and asthma in hard-metal workers: bronchoalveolar lavage, ultrastructural, and analytical findings and results of bronchial provocation tests. *Thorax* 38: 119-28
591. Lay G, Poquet Y, Salek-Peyron P, Puissegur MP, Botanch C, Bon H, Levillain F, Duteyrat JL, Emile JF, Altare F. 2007. Langhans giant cells from M. tuberculosis-induced human granulomas cannot mediate mycobacterial uptake. *J Pathol* 211: 76-85
592. McNally AK, Anderson JM. 2002. Beta1 and beta2 integrins mediate adhesion during macrophage fusion and multinucleated foreign body giant cell formation. *Am J Pathol* 160: 621-30
593. Podolnikova NP, Kushchayeva YS, Wu Y, Faust J, Ugarova TP. 2016. The Role of Integrins alphaMbeta2 (Mac-1, CD11b/CD18) and alphaDbeta2 (CD11d/CD18) in Macrophage Fusion. *Am J Pathol* 186: 2105-16
594. Saginario C, Qian HY, Vignery A. 1995. Identification of an inducible surface molecule specific to fusing macrophages. *Proc Natl Acad Sci U S A* 92: 12210-4

595. Ushach I, Zlotnik A. 2016. Biological role of granulocyte macrophage colony-stimulating factor (GM-CSF) and macrophage colony-stimulating factor (M-CSF) on cells of the myeloid lineage. *J Leukoc Biol* 100: 481-9
596. Helming L, Gordon S. 2009. Molecular mediators of macrophage fusion. *Trends Cell Biol* 19: 514-22
597. Skubitz KM, Cheng EY, Clohisy DR, Thompson RC, Skubitz AP. 2004. Gene expression in giant-cell tumors. *J Lab Clin Med* 144: 193-200
598. Puissegur MP, Lay G, Gilleron M, Botella L, Nigou J, Marrakchi H, Mari B, Duteyrat JL, Guerardel Y, Kremer L, Barbry P, Puzo G, Altare F. 2007. Mycobacterial lipomannan induces granuloma macrophage fusion via a TLR2-dependent, ADAM9- and beta1 integrin-mediated pathway. *J Immunol* 178: 3161-9
599. Fenech M, Kirsch-Volders M, Natarajan AT, Surralles J, Crott JW, Parry J, Norppa H, Eastmond DA, Tucker JD, Thomas P. 2011. Molecular mechanisms of micronucleus, nucleoplasmic bridge and nuclear bud formation in mammalian and human cells. *Mutagenesis* 26: 125-32
600. Lacroix B, Maddox AS. 2012. Cytokinesis, ploidy and aneuploidy. *J Pathol* 226: 338-51
601. Prieditis H, Adamson IY. 1996. Alveolar macrophage kinetics and multinucleated giant cell formation after lung injury. *J Leukoc Biol* 59: 534-8
602. Anderson HC. 1997. An antagonist of osteoclast integrins prevents experimental osteoporosis. *J Clin Invest* 99: 2059
603. Herde K, Hartmann S, Brehm R, Kilian O, Heiss C, Hild A, Alt V, Bergmann M, Schnettler R, Wenisch S. 2007. Connexin 43 expression of foreign body giant cells after implantation of nanoparticulate hydroxyapatite. *Biomaterials* 28: 4912-21
604. Kern I, Kecelj P, Kosnik M, Mermolja M. 2003. Multinucleated giant cells in bronchoalveolar lavage. *Acta Cytol* 47: 426-30
605. Myers JL, Tazelaar HD. 2008. Challenges in pulmonary fibrosis: 6--Problematic granulomatous lung disease. *Thorax* 63: 78-84
606. Kumarguru BN, Natarajan M, Biligi DS, Raghupathi AR. 2015. Giant Cell Lesions of Lungs: A Histopathological and Morphometric Study of Seven Autopsy Cases. *J Clin Diagn Res* 9: EC12-6
607. Mustafa T, Wiker HG, Morkve O, Sviland L. 2008. Differential expression of mycobacterial antigen MPT64, apoptosis and inflammatory markers in multinucleated giant cells and epithelioid cells in granulomas caused by Mycobacterium tuberculosis. *Virchows Arch* 452: 449-56
608. Zhu XW, Friedland JS. 2006. Multinucleate giant cells and the control of chemokine secretion in response to Mycobacterium tuberculosis. *Clin Immunol* 120: 10-20
609. Mustafa T, Mogga SJ, Mfinanga SG, Morkve O, Sviland L. 2006. Immunohistochemical analysis of cytokines and apoptosis in tuberculous lymphadenitis. *Immunology* 117: 454-62
610. Hernandez-Pando R, Bornstein QL, Aguilar Leon D, Orozco EH, Madrigal VK, Martinez Cordero E. 2000. Inflammatory cytokine production by immunological and foreign body multinucleated giant cells. *Immunology* 100: 352-8
611. Becher B, Schlitzer A, Chen J, Mair F, Sumatoh HR, Teng K, Low D, Ruedl C, Riccardi-Castagnoli P, Poidinger M, Greter M, Ginhoux F, Newell EW. 2014. High-dimensional analysis of the murine myeloid cell system. *Nature Immunology* 15: 1181-9
612. Dos Anjos Cassado A. 2017. F4/80 as a Major Macrophage Marker: The Case of the Peritoneum and Spleen. *Results Probl Cell Differ* 62: 161-79
613. Anderson JM. 2000. Multinucleated giant cells. *Curr Opin Hematol* 7: 40-7

614. Solari F, Flamant F, Cherel Y, Wyers M, Jurdic P. 1996. The osteoclast generation: an in vitro and in vivo study with a genetically labelled avian monocytic cell line. *J Cell Sci* 109 (Pt 6): 1203-13

Abbreviations and symbols

-/-	knock-out
°C	degree Celsius
%	percent
Δ	delta
m^2	square meter
®	registered trademark
™	trademark
aAM	airway alveolar macrophage
AEC	airway epithelial cell
AGM	aorta-gonad-mesonephros
AHR	airway hyperresponsiveness
ALI	acute lung injury
AM	alveolar macrophage
APC	antigen-presenting cell
Arg1	Arginase-1
ASP	acylation-stimulating protein
AT	anaphylatoxin
ATM	adipose tissue macrophage
ATP	adenosine triphosphate
ATR	anaphylatoxin receptor
BAL	bronchoalveolar lavage
BiN	binucleated
BCR	B cell receptor
BM	bone marrow
BMDC	bone marrow-derived DC
BMM	bone marrw-derived macrophages
bp	base pair
BSA	bovine serum albumin
C1Inh	C1 Inhibitor
C3aR	C3a receptor
C5aR1	C5a receptor 1
C5aR2	C5a receptor 2
CCL	CC-chemokine ligand

CCR	C-C chemokine receptor
CD	cluster of differentiation
cDNA	complementary desoxyribonucleic acid
cDC	conventional dendritic cell
CDP	dendritic cell progenitor
CF	cystic fibrosis
CFSE	carboxyfluorescein succinimidyl ester
CFTR	cystic fibrosis transmembrane conductance regulator
Chi3l1	Chitinase 3-like 1
cMoP	common monocyte progenitor
CMP	common myeloid progenitor
CNS	central nervous system
Cnx	connexin
CO_2	carbon dioxide
COPD	chronic obstructive pulmonary disease
CR	complement receptor
CRP	C reactive protein
CSF-2	Colony Stimulating Factor 2 (also known as GM-CSF)
CTSL	cathepsin L
CXCL	chemokine C-X-C Motif ligand
CXCR	chemokine C-X-C Motif receptor
DAF	decay-accelerating factor
DAMP	damage-associated molecular pattern
DAPI	diamidino-phenylindole
DC	dendritic cell
DC-STAMP	dendritic cell-specific transmembrane protein
Der p	*Dermatophagoides*
dH_20	deionized water
DNA	deoxyribonucleic acid
DRA	dust mite, ragweed, and *Aspergillus* species
E	embryonic day
EAE	experimental autoimmune encephalomyelitis
EC	epithelial cell
ECM	extracellular matrix
EMP	erythro-myeloid progenitor

ER	endoplasmic reticulum
ERK	extracellular signal-regulated kinase
et al.	et alii
FACS	fluorescence activated cell sorting
FCS	fetal calf serum
FcεR1	Fc epsilon receptor 1
FDC	follicular dendritic cell
FL	fetal liver
FITC	fluorescein isothiocyanate
FoxP3	forkhead box P3
FSC	forward scatter
g	gram
GFP	green fluorescent protein
GM-CSF	granulocyte-macrophage colony-stimulating factor
GMP	granulocyte-macrophage progenitor
GPCR	guanine nucleotide-binding (G) protein-coupled receptor
GRK	G protein-coupled receptor kinase
H&E	hematoxylin/eosin
HBBS	Hank's balanced salt solution
hrs	hour
HE	hemogenic endothelium
HDM	house dust mite
HMC-1	human mast cell line-1
HMGB-1	high mibility groupbox 1 protein
HSC	hematopoietic stem cell
HSP	heat-shock protein
IC	immune complex
IFN	interferon
Ig	immunoglobulin
IM	interstitial macrophage
IL	interleukin
ILC	innate lymphoid cell
IL-1ra	interleukin-1 receptor antagonist
i.p.	intraperitoneal
i.t.	intratracheal

iTreg	induced regulatory T
JAK	Januskinase
kb	kilobase pair
KC	Kupffer cell
kDa	kilodalton
kg	kilogram
L	ligand
LC	Langerhans cell
LDL	low-density lipoprotein
LN	lymph node
LP	lamina propria
LPM	large peritoneal macrophage
LPS	lipopolysaccharide
LT	leukotriene
LTA	lipoteichoic acid
Ly	lymphocyte antigen
mAb	murine antibody
MAC	membrane attack complex
MAPK	mitogen activated protein kinase
MASP	mannose-binding lectin-associated serine protease
MBL	mannose-binding lectin
MCP	monocyte chemotactic protein
MDP	macrophage dendritic cell progenitor
MDSC	myeloid-derived supressor cell
MerTK	Mer tyrosine kinase
methacholine	Acetyl-β-Methyl-Choline
MFI	mean fluorescence intensity
MFR	macrophage fusion receptor
µg	microgram
mg	milligram
MHC	major histocompatibility complex
min	minute
µl	microliter
ml	milliliter
mLN	mediastinal lymph node

µM	micromole
mM	millimole
MMP	matrix metalloproteinase
MN	micronuclei
MNGC	multinucleated giant cell
moDC	monocyte-derived dendritic cell
MonoM	mononuclear
MPS	mononuclear phagocyte system
mRNA	messenger ribonucleic acid
Mtb	*Mycobacterium tuberculosis*
mTOR	mammalian target of rapamycin
MuN	multinucleated
nAb	natural antibody
NET	neutrophil extracellular trap
NFATc1	nuclear factor of activated T-cells 1
NF-κB	nuclear factor κB
ng	nanogram
NK	natural killer
NLR	nucleotide oligomerization domain-like receptor
nM	nanomole
NO	nitric oxide
NOD	nucleotide oligomerization domain
NOS	nitric oxide synthase
nTreg	natural regulatory T
OVA	ovalbumin
OXPHOS	oxidative phosphorylation
P	Properdin
PAF	platelet-activating factor
PAMP	pathogen-associated molecular pattern
PAR	protease-activated receptor
PBS	phosphate buffered saline
PCR	Polymerase Chain Reaction
pDC	plasmacytoid dendritic cell
PE	phycoerythrin
PerC	peritoneal cavity

PG	prostaglandin
PI3K-γ	phospatidylinositol 3-kinase gamma
PL	phospholipase
PM	peritoneal macrophage
PMA	phorbol myristate acetat
PMT	photomultiplying tube
Pnx	pannexin
PRR	pattern recognition receptor
PTX3	pentraxin 3
R	receptor
RALDH	retinal dehydrogenase
RANKL	receptor activator of nuclear factor κB ligand
RBC	red blood cell
RBCL	red blood cell lysis
rcf	relative centrifual force
RNA	ribonucleic acid
RNS	reactive nitrogen species
RORγT	retinoic acid-related orphan receptor gamma T
ROS	reactive oxygen species
rpm	rounds per minute
RT	room temperature
RTI	respiratory tract infection
RT-PCR	real-time Polymerase Chain Reaction
s	second
SAA	serum amyloid A
SAP	serum amyloid P
SEM	standard error of the mean
sp.	species
SP	surfactant protein
SPM	small peritoneal macrophage
SSC	side scatter
ssp.	several species
STAT	signal transducer and activator of transcription
sq	semi-quantitative
tAM	tissue-associated alveolar macrophage

TBS	Tris-buffered salin
TCR	T cell receptor
tdTomato	tandem-dye Tomato
Tfh	T follicular helper
TGF	tumor growth factor
Th	T helper
Treg	regulatory T
TLR	Toll-like receptor
TNF	tumor necrosis factor
TSLP	thymic stromal lymphopoeitin
VAT	visceral adipose tissue
vs.	versus
WB	western blot
WGA	Wheat Germ Agglutinin
WT	wild type
x g	gravity
YM1	chitinase-3-like protein 3
YS	yolk sac

List of figures

List of tables

Curriculum Vitae

Personal Details

Name	Katharina Maria Quell
Address	Grotenkamp 10 25421 Pinneberg
Date of Birth	26th January 1988 in Hünfeld, Germany

Professional Experience

04/2019 – present	PostDoctoral fellowship in the *International Research Training Group 1911* at the Institute for Systemic Inflammation Research, University of Lübeck
04/2016 – 03/2019	PhD student as member of the *International Research Training Group 1911* at Institute for Systemic Inflammation Research, University of Lübeck Project A1 "Regulation and function of the anaphylatoxin receptor C3aR during the development and severity of allergic asthma" Visiting researcher, Cincinnati Children's Hospital Medical Center, Cincinnati, USA (09/2017 – 03/2018)
01/2013 – present	Approbated pharmacist at the Privilegierte Adler Apotheke, Hamburg

Education

03/12/2012	Approbation – Pharmaceutical license (final grade: 1.8)
10/2007 – 11/2012	Pharmaceutical studies at the Philippe-Universität, Marburg
23/11/2012	Third state examination (2.0) Pharmacy practice, pharmacy law
27/09/2011	Second state examination (1.2) Pharmaceutical/medicinal chemistry, pharmaceutical biology, pharmaceutical technology/bio-pharmacy, pharmacology and toxicology, clinical pharmacy
21/08/2009	First state examination (2.5) Inorganic and organic chemistry, pharmaceutical biology and human biology, physics/physical chemistry and pharmaceutical technology, pharmaceutical analytics
08/1998 – 07/2007	Higher education entrance qualification (A-level), Wigbertschule, Hünfeld (2.2)

Methodological Competence

In vivo mouse models	Intraperitoneal injection
	Intratracheal application
Cell biology	Isolation and purification of various murine immune cells from lung tissue, bronchoalveolar lavage, bone marrow, peritoneum, spleen, visceral adipose tissue, small intestine and blood
	In vitro culture of murine alveolar macrophages
	In vitro differentiation of bone marrow-derived dendritic cells and macrophages
	In vitro co-culture system of alveolar macrophages and T cells
	In vitro generation of bone marrow-derived multinucleated giant cell
	In vitro generation of multinucleated alveolar macrophages
	Functional assays
Molecular biology	RNA extraction
	cDNA preparation
	Real-Time PCR
Protein biology	Cell lyisis
	SDS polyacrylamide gel electrophoresis (SDS-PAGE)
	Western immunoblot
	Flow cytometry
Microscopy	Transmitted-light micrscopy
	Confocal laser scanning microscopy

Additional Qualifications

Certificates	FELASA B
Internship	University internship (project group of Prof. Dr. Steinmetzer) Synthesis, purification and characterization of peptidomimetic furin-inhibitors
Languages	English (fluent), Frensh (basic), German (native)
IT	MS Office, Graph Pad Prism, FlowJo, Imaris, ImageJ

Congress Contributions

Poster

Quell KM, Wiese AV, Vollbrandt T, König P, Lewkowich IP, Köhl J, Laumonnier Y. C3aR is instrumental to the formation of multinucleated macrphages in experimental allergic asthma. DZL Annueal Meeting, Mannheim, Germany (2019)

Quell KM, Wiese AV, Almeida LN, Vollbrandt T, Verschoor A, König P, Deep G, Lewkowich IP, Köhl J, Laumonnier Y. C3aR contributes to the formation of multinucleated giant cells in experimental allergic asthma. Allergy meets infection, Lübeck, Germany (2018)

Quell KM, Wiese AV, Almeida LN, Vollbrandt T, Verschoor A, König P, Deep G, Lewkowich IP, Köhl J, Laumonnier Y. C3aR contributes to the formation of multinucleated giant cells in experimental allergic asthma. 27th International Complement Workshop, Santa Fe, USA (2018)

Quell KM, Wiese AV, Vollbrandt T, Köhl J, Laumonnier Y. C3aR allows the discrimination of three distinct pulmonary alveolar macrophage populations in an experimental allergic asthma model. Annual Immunology Retreat, Deer Creek, USA (2017)

Quell KM, Wiese AV, Vollbrandt T, Köhl J, Laumonnier Y. House dust mite exposure upregulates C3a receptor expression in pulmonary innate immune cells during the sensitization phase of allergic asthma by an IL-33-dependent mechanism. Annual meeting of the American Society of Immunologists, Washington DC, USA (2017)

Quell KM, Wiese AV, Almeida LN, Vollbrandt T, Köhl J, Laumonnier Y. House dust mite upregulates the expression of C3aR in alveolar macrophages during the sensitization phase of allergic asthma in an IL-33-IL-13 dependent mechanism. 13th Spring School on Immunology, Ettal, Germany (2017)

Quell KM, Lewkowich IP, Laumonnier Y. Role of microbiome in C3aR-dependent regulation of allergic asthma. On-site visit DFG, Lübeck, Germany (2017)

Talks

Quell KM, Wiese AV, Almeida LN, Vollbrandt T, Verschoor A, König P, Deep G, Lewkowich IP, Köhl J, Laumonnier Y. C3aR contributes io the formation of multinucleated giant cells in experimental allergic asthma. HOROS Retreat, Obergurgl, Austria (2018)

Quell KM, Karsten CM, Kordowski A, Almeida LN, Briukhovetska D, Wiese AV, Sun J, Ender F, Antoniou K, Schröder T, Schmudde I, Berger JL, König P, Vollbrandt T, Laumonnnier Y, Köhl J. Monitoring C3aR expression using a floxed tdTomato-C3aR reporter knock-in mouse. 47th Annual Meeting of the German Society for Immunology, Erlangen, Germany (2017)

Quell KM. Role of microbiome in C3aR-dependent regulation of allergic asthma. IRTG 1911 Retreat, Boltenhagen, Germany (2016)

Quell KM, Laumonnier L, Karsten CM, Czabanska A, Schmudde I, Ender F, Briukhovetska D, Wiese AV, Almeida LN, Antoniou K, Vollbrandt T, Schröder T, Köhl J. Characterization of C3aR expression under steady state and inflammatory conditions using a novel floxed Td-Tomato C3aR knockin mouse. 39th Symposium of the North German Immunologists, Borstel, Germany (2016)

Awards

Young Investigator Cover Image Award
Quell, K. M., Cover Image. Society IC. Focus on Complement. In *Issue 51*, ed. TM Woodruff (2018)

Poster Award Annual Immunology Retreat
Quell, K. M., Wiese A. V., Vollbrandt, T., Köhl, J., Laumonnier, Y. C3aR allows the discrimination of three distinct pulmonary alveolar macrophage populations in an experimental allergic asthma model. Annual Immunology Retreat, Deer Creek, USA (2017)

List of Publications

Schroder T, Wiese AV, Ender F, **Quell KM**, Vollbrandt T, Duhn J, Sunderhauf A, Kunstner A, Moreno Fernandez ME, Derer S, Aherrahrou Z, Lewkowich I, Divanovic S, Sina C, Kohl J, Laumonnier Y. Short-term high-fat diet feeding protects from the development of experimental allergic asthma in mice. *Clin Exp Allergy*. 2019

Karsten CM, Wiese AV, Mey F, Figge J, Woodruff TM, Reuter T, Scurtu O, Kordowski A, Almeida LN, Briukhovetska D, **Quell KM**, Sun J, Ender F, Schmudde I, Vollbrandt T, Laumonnier Y, Köhl J. Monitoring C5aR2 Expression Using a Floxed tdTomato-C5aR2 Knock-In Mouse. *J Immunol*. 2017

Wiese AV, Ender F, **Quell KM**, Antoniou K, Vollbrandt T, König P, Köhl J, Laumonnier Y. The C5a/C5aR1 axis controls the development of experimental allergic asthma independent of LysM-expressing pulmonary immune cells. *PLoS One*. 2017

Quell KM, Karsten CM, Kordowski A, Almeida LN, Briukhovetska D, Wiese AV, Sun J, Ender F, Antoniou K, Schröder T, Schmudde I, Berger JL, König P, Vollbrandt T, Laumonnier Y, Köhl J. Monitoring C3aR Expression Using a Floxed tdTomato-C3aR Reporter Knock-in Mouse. *J Immunol*. 2017

Acknowledgement

Finally, I would like to extend my sincere thanks to all people, who gave advice and support to my work described in this thesis.

Firstly, I would like to express my sincere gratitude to my enthusiastic supervisor Dr. Yves Laumonnier for his continuous support and encouragement during my PhD thesis, for his patience, motivation, and immense knowledge. His guidance and motivation helped me during the whole research time and the writing of this thesis. Without his constant feedback, this PhD would not have been achievable.

A very special thanks also to Prof. Jörg Köhl as the Head of the Institute of Systemic Inflammation Research (ISEF) and Head of the *International Research Training Group (IRTG) 1911*. He gave me the opportunity to be part of the IRTG 1911 and provided me extensive academic guidance. Without his dedication to establish the *IRTG 1911*, this PhD thesis would not have been existing.

I am exceptionally grateful for the support by Prof. Ian Lewkowich as my secondary supervisor from the *IRTG 1911*. With his continuous advices via video conference, his extensive personal and scientific support during my stay in the US at the Cincinnati Children's Hospital Medical Center, as well as the encouragement during the writing of this thesis, he contributed with considerable proportion to the work presented here.

Special mention goes to the allergic asthma group for supporting me in strenuous times in the lab. A special thanks to Anna Wiese, who provided me with a fantastic lab and mouse training in the beginning of my PhD. To Jonas Fellenberg, who helped me with the RT-PCR analysis of a huge number of cDNA samples I generated in the US. And to Konstantina Antoniou. We always exchanged scientific and general knowledge associated to our PhD program and we had a great time together in Cincinnati.

Many thanks to all our technicians, in particular Gabi Köhl from Lübeck and Julie Hargis from Cincinnati, who supported me in all technical questions in the lab and took care about all the mouse breeding and genotyping.

Similar, profound gratitude goes to Jaclyn Walisa McAlles from the Lewkowich Lab, who provided me with training in various new techniques in the lab during my stay in Cincinnati. She was always gladly answering scientific questions and gave me the great and unforgettable opportunity to celebrate Thanksgiving with her whole family.

Thanks also to Tillman Vollbrandt and the CANAcore for the training in flow cytometry and for performing an immense number of cell sortings. To Ania Kordowski, Larissa Almeida and Daria Briukhovetska from the Institute of Systemic Inflammation Research, who supported me with their specialized knowledge in the lab during the characterization of the tdTomato-C3aR reporter mouse.

I gratefully acknowledge Prof. Christian Sina as my mentor in the *IRTG 1911* and also Prof. Peter König, Christin Broadley and Kathy Budler from the Institute for Anatomy, for their support in

immunohistochemistry, 2-photon microscopy and histology embedding of lung lobes. To Imke Lingel, who was a fantastic teammate during the time we spend together in the Lewkowich Lab in Cincinnati. A dept of gratitude to my sisters Sonja, Beate and Verena for all their helpful advices in general questions about my PhD and my further future.

I would also like to say a heartfelt thanks to Max, who has been with me since the last year of my PhD and who has always been a valuable support to me.

Last, but not the least, my biggest thanks go to my parents for their unbelievable support during my whole life. They always believed in me and encouraged me to follow my intentions, heartened me in challenging times and rejoiced over reached objectives. They are one of the most important people in my life, and I dedicate this thesis to them.